Terms and Conditions of Use of Digitised Theses from Trinity College Library Dublin

Copyright statement

All material supplied by Trinity College Library is protected by copyright (under the Copyright and Related Rights Act, 2000 as amended) and other relevant Intellectual Property Rights. By accessing and using a Digitised Thesis from Trinity College Library you acknowledge that all Intellectual Property Rights in any Works supplied are the sole and exclusive property of the copyright and/or other IPR holder. Specific copyright holders may not be explicitly identified. Use of materials from other sources within a thesis should not be construed as a claim over them.

A non-exclusive, non-transferable licence is hereby granted to those using or reproducing, in whole or in part, the material for valid purposes, providing the copyright owners are acknowledged using the normal conventions. Where specific permission to use material is required, this is identified and such permission must be sought from the copyright holder or agency cited.

Liability statement

By using a Digitised Thesis, I accept that Trinity College Dublin bears no legal responsibility for the accuracy, legality or comprehensiveness of materials contained within the thesis, and that Trinity College Dublin accepts no liability for indirect, consequential, or incidental, damages or losses arising from use of the thesis for whatever reason. Information located in a thesis may be subject to specific use constraints, details of which may not be explicitly described. It is the responsibility of potential and actual users to be aware of such constraints and to abide by them. By making use of material from a digitised thesis, you accept these copyright and disclaimer provisions. Where it is brought to the attention of Trinity College Library that there may be a breach of copyright or other restraint, it is the policy to withdraw or take down access to a thesis while the issue is being resolved.

Access Agreement

By using a Digitised Thesis from Trinity College Library you are bound by the following Terms & Conditions. Please read them carefully.

I have read and I understand the following statement: All material supplied via a Digitised Thesis from Trinity College Library is protected by copyright and other intellectual property rights, and duplication or sale of all or part of any of a thesis is not permitted, except that material may be duplicated by you for your research use or for educational purposes in electronic or print form providing the copyright owners are acknowledged using the normal conventions. You must obtain permission for any other use. Electronic or print copies may not be offered, whether for sale or otherwise to anyone. This copy has been supplied on the understanding that it is copyright material and that no quotation from the thesis may be published without proper acknowledgement.

An investigation into the role of TLR4 interactor with leucine rich repeats (TRIL) in Toll-like receptor responses in brain

Thesis submitted to the
University of Dublin
For the
Degree of Doctor of Philosophy

By
Paulina Wochal

School of Biochemistry and Immunology
Trinity College
Dublin
Ireland

December 2013

I dedicate this thesis to my Mom & Dad

Marzena and Zdzislaw Wochal

I wouldn't be where I am today without you

MAMO, TATO, KOCHAM WAS!!!

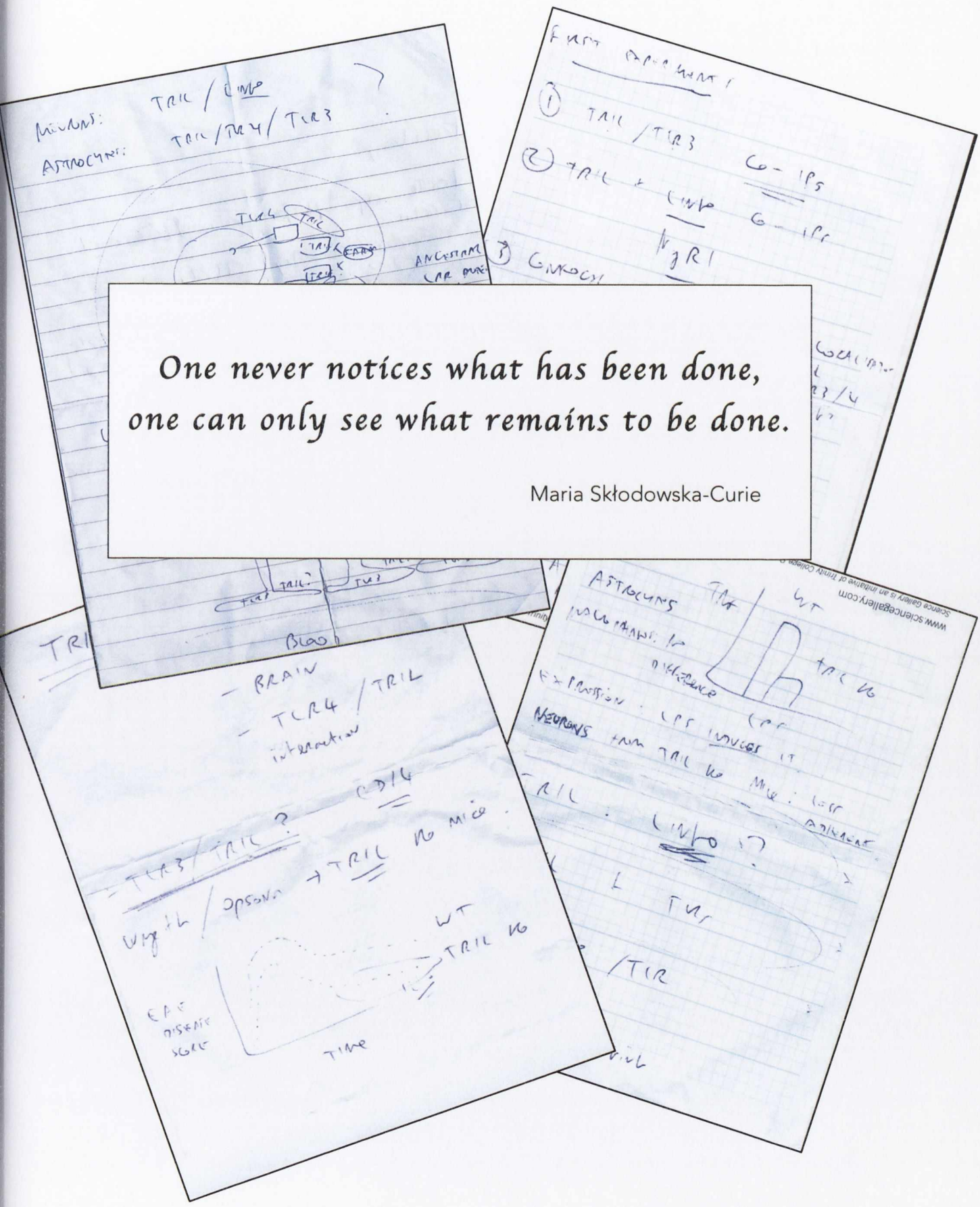

One never notices what has been done,
one can only see what remains to be done.

Maria Skłodowska-Curie

And so here I am, writing the very last page of my PhD thesis. I cannot believe it has been four years since I began my PhD. Undertaking this PhD has been a life-changing experience for me and it would not have been possible to do without the support and guidance that I received from many people.

First and foremost I would like to thank my supervisor Prof Luke O'Neill, for his continuous support, enthusiasm and patience. Luke you kept me motivated even in the 'darkest moments' of this PhD, boosting my scientific self-esteem and making me believe that it will all work out in the end. It has been a great pleasure and privilege to work for you. I could not have imagined a better advisor and mentor for my PhD.

Thanks to my co-supervisor Dr Susan Carpenter. Susan you have been a very important part of getting me here and I can never repay you for everything you have given me. In my eyes you are a role model for a scientists, kind of a Marie Curie of the 21st century. Thank you so much for taking such a good care of me, first early on in my PhD studies and then during my stay in Boston. I really feel like you have become like the older sister I always wanted to have.

Thanks also to all the past and present members of the LON lab, Fred, Kathy, Dympna, Moritz, Beth, Sarah J, Emer, Sarah D, Sue, Elaine, Jen, Annie, Eva, Anne, Sarah C, Gillian, Nick, Niamh, Mirjam, Mustafa, Danny, Liz, Christine, Sinead, Becca, Caio, Claire, Cait, Evanna, Silvia, Rachel and Seth. Thank you for the wonderful and friendly atmosphere in the lab. Thanks to you all, I felt like part of a big family, despite being so far away from home.

I would like to thank also Prof Kate Fitzgerald for giving me the opportunity to learn and work in her lab at the University of Massachusetts Medical School, USA. This has been such a valuable experience for me. Special thanks to an exquisite group of UMass PhD students: Jennie, John, Stefan, Mikayla, Sandhya and Sreya, you guys made me believe that Worcester is not that bad, as it is not about the place but about the people you are with. Thanks to Vijay Rathinam for all the help with the animal work and Shruti Sharma for all the stimulating scientific chats. The two of you have become a true scientific inspiration to me. Thanks also to all the members of the Fitzgerald lab for their help and never-ending patience with me, it was a great pleasure to work with

you all.

No words can ever express my gratitude for my family. Mom, Dad thanks for my roots and wings and a constant reminder that I can always come home whenever life is just too much to handle. Thanks to my older brother who I used to look after when he was a kid, and who is looking after me now. Thanks to my little sister Marcelina who made me love horses nearly as much as she does. Last but not least, a very special thank to my grandma Zosia, for all her prayers and eternal belief in me "Babciu dziękuję za wszytkie modlitwy I wiarę we mnie"

Thanks to my very best friends Kasia and Lolo who were always there for me through all the ups and downs...for better or for worse...until we all finish our PhDs. Thanks to my 'google girls' Adriana and Diana, you were the best housemates I've ever had, who have become my very dear friends. Thanks also to my Marie Curie Fellows; Tjerk, Karen, Joe, Mads, Mustafa, Mariana, Daniele, Dario, Virginie, Juha and Aurelien for all the meetings full of fun and inspiration.

I'm also grateful to the European Commission under the 7th Framework Programme of Marie Curie Action and Science Foundation Ireland for funding this project.

DECLARATION

This thesis is submitted by the undersigned to the University of Dublin for the examination of Doctorate in Philosophy. I declare, that the work herein is entirely my own with the exception of the following figures:

- Figure 3.3
- Figure 3.11
- Figure 3.12

This work was carried out by Dr Susan Carpenter at Trinity College Dublin.

- Figure 4.1 (part C)

This work was carried out by Dr Thaddeus Carlson at Pfizer.

This work has not been submitted as exercise for a degree to any other university. The library at Trinity College Dublin has my full permission to lend or copy this thesis upon request.

CONTENTS

List of figures

CHAPTER ONE

CHAPTER THREE

CHAPTER FOUR

List of Tables

CHAPTER ONE

CHAPTER TWO

5'ppp RNA	5'-triophosphate–containing dsRNA
Aβ	Amyloid β
AD	Alzheimer's disease
AIM2	Absent in melanoma 2
ALS	Amyotrophic lateral sclerosis
AP1	Activator protein 1
AMIGO	Amphoterin-induced gene and ORF
AMP	Adenosine monophosphate
APS	Ammonium persulphate
ARM	Heat armadillo repeat
ATP	Adenosine triphosphate
AWC	Asymmetrical olfactory receptor
BBB	Blood brain barrier
BCAP	B-cell adaptor for PI3K
BIR	Baculovirus inhibitor repeat domain
BMDC	Bone marrow dendritic cell
BMDM	Bone marrow derived macrophage
bp	Base pair
BSA	Bovine serum albumin
BTK	Bruton's tyrosine kinase
DAMP	Damage or danger associated molecular pattern
CARDIF	CARD adaptor inducing IFNβ
CARD	Caspase recruitment domain
CD14	Cluster of differentiation 14
CFP	Cyane fluorescent protein
CFU	Colony forming unit
cGAMP	Cyclic-GMP-AMP
cGAS	Cyclic GAMP synthase
CLR	C-type lectin receptor
CMV	Cytomegalovirus
CNS	Central nervous system
Co-IP	Co-immunoprecipitation
CpG	Cytosine phosphate guanine
CRD	Carbohydrate recognition domain

DAI	DNA-dependent activator of interferon (IFN)-regulatory factors
DAPI	4',6-Diamidino-2-phenylindole dihydrochloride
DCIR	DC-immunoreceptor
DC	Dendritic cell
DD	Death domain
DHX	DExD/H box helicase
DMEM	Dulbecco's modified eagles medium
DMSO	Dimethyl sulfoxide
DNA	Deoxyribonucleic acid
dsRNA/DNA	Double stranded RNA/DNA
DTT	Dithiothreitol
EAE	Experimental autoimmune encephalomyelitis
ECACC	European collection of animal cell cultures
ECD	Extracellular ectodomain
ECL	Enhanced chemiluminescence
ECM	Extracellular matrix
EEA1	Early endosome antigen 1
EDTA	Ethylendiaminetetraecetic acid
ELISA	Enzyme-linked immunosorbent assay
EMCV	Encephalomyocarditis virus
ER	Endoplasmic reticulum
EtBr	Ethidium Bromide
EV	Empty vector
FADD	FAS-associated death domain
FCS	Fetal calf serum
FLRT	Fibronectin leucine rich transmemebrane
FSL1	Pam2CGDPKHPKSF
HCMV	Human cytomegalovirus
GFP	Green fluorescent protein
GOLD	Golgi dynamics
GM-CSF	Granulocyte macrophage-colony stimulating factor
GPI	Glycosylphosphatidyl inositol
GRP94	Glucose-regulated protein 94
HA	Hyaluronic acid

HCV	Hepatitis C virus
HEK	Human embryonic kidney
HIV	Human Immunodeficiency Virus
HMGB	High mobility group box
HRP	Horseradish peroxidase
HS	Heparan sulphate
HSV	Herpes Simplex Virus
HSP	Heat shock protein
IAV	Influenza A virus
IFN	Interferon
Ig	Immunoglobulin
IFI16	IFN inducible protein 16
IκB	Inhibitor of κB
IKK	IκB kinase
IL	Interleukin
IL-1R	IL-1 receptor
IP	Immunoprecipitation
IPS 1	IFNβ promoter stimulator 1
IRAK	Interleukin-1 receptor-associated kinase
IRF	Interferon regulatory factor
ISRE	Interferon stimulated response element
ISG	Interferon stimulated gene
JAK	Janus kinase
JEV	Japanese encephalitis virus
JNK	c-jun-N-terminal kinase
kDa	Kilodalton
LACV	La Crosse virus
LB	Lauria-Bertani broth
LBP	LPS binding protein
LDL	Low density lipoprotein
LGP2	Laboratory of genetics and physiology 2
LINGO	LRR and Ig domain containing Nogo interacting protein
LPS	Lipopolysacharide
LRRFIP1	Leucine rich repeat flightless-interacting protein 1

LRR	Leucine rich repeat
LTA	Lipoteichoic acid
MALP2	Macrophage activating lipoprotein 2
MAPK	Mitogen activated protein kinase
MAPKK	Mitogen activated protein kinase kinase
MAL	MyD88 adaptor like
MCSF	Macrophage colony stimulating factor
MEF	Mouse embryonic fibroblast
MAVS	Mitochondrial antiviral signaling protein
MBL	Mannose binding lectin
MCMV	Murine cytomegalovirus
MDA5	Melanoma differentiation associated gene 5
MD2	Myeloid differentiation factor 2
MHC	Major histocompatibility complex
MMP9	Matrix metaloproteinase 9
MMR	Macrophage mannose receptor
MMTV	Mouse mammary tumor virus
MNDA	Myeloid cell nuclear differentiation antigen
mRNA	Messenger RNA
MyD88	Myeloid differentiation factor 88
MS	Multiple sclerosis
NAIP5	NLR apoptosis inhibitory protein 5
NAP1	NAK-associated protein 1
NEMO	NF-κB essential modulator
NET	Neutrophil extracellular trap
NF-κB	Nuclear factor-kappa B
NFT	Neurofibrillary tangle
NK	Natural killer
NOD	Nucleotide-binding domain
NLR	NOD-like receptor
NPC	Neural progenitor cell
OC	Overlap coefficient
OGD	Oxygen and glucose deprivation
ODN	Oligonucleotide

oxLDL	Oxidised low density lipoprotein
PAGE	Polyacrylamide gel electrophoresis
Pam3CSK4	Pam3Cys-Ser-(Lys)4
PAMP	Pathogen associated molecular pattern
PBMC	Peripheral blood mononuclear cell
PBS	Phosphate buffered saline
PCC	Pearson's correlation coefficient
PCR	Polymerase chain reaction
PD	Parkinson's disease
pDC	Plasmacytoid dendritic cell
PFU	Plaque forming unit
PGN	Peptidoglycan
PI3K	Phosphoinositide 3-kinase
PIP2	Phosphatidylinositol-4,5-bisphosphate
PKC	Protein kinase C
PMA	Phorbol 12-myristate 13-acetate
PMSF	Phenylmethylsulfonylfluoride
Pol III	RNA polymerase III
Poly(I:C)	Polyinosinic-polycytidylic acid
QPCR	Quantitative PCR
PRR	Pattern recognition receptor
PRAT4A	Protein associated with Toll-like receptor 4 (TLR4) A
PRRSV	Porcine reproductive and respiratory syndrome virus
P/S	Penicillin/Streptomycin
PVDF	Polyvinylidene fluoride
PYD	Pyrin domain
PYHIN	Pyrin and HIN domain
RAGE	Receptor for advanced glycation endproducts
RD	Repressor domain
RFP	Red fluorescent protein
RHIM	RIP homotypic interaction motif
RIG-I	Retinoic acid inducible gene I
RIP1	Receptor interacting kinase 1
RLR	RIG-I like receptor

RNA	Ribonucleic acid
RPMI	Roswell Park Memorial Institute
rRNA	Ribosomal RNA
RSV	Respiratory syncytial virus
RT-PCR	Reverse transcription PCR
R848	Resiquimod 848
SARM	Sterile alpha and HEAT-Armadillo motifs
SAM	Sterile α motif
SD	Standard deviation
SDS	Sodium dodecyl sulphate
SDS-PAGE	Sodium dodecyl sulphate-polyacrylamide gel electrophoresis
SEM	Standard error of the mean
SFM	Serum free media
siRNA	Small interfering RNA
SLE	Systemic lupus erythematosus
SOC1	Suppressor of cytokine signaling 1
STING	Stimulator of interferon genes
ssRNA	Single stranded RNA
TAB	TAK1 binding protein
TAE	Tris-acetate EDTA
TAK1	Transforming growth factor-β-activated kinase 1
TAG	TRAM adaptor with GOLD domain
TBK1	NF-κB activator binding kinase 1
TIG	Transcription factor-Ig
TIR	Toll-IL-1 receptor domain
TICAM	TIR domain-containing adaptor 1
TIRAP	TIR domain-containing adaptor protein
TK	Thymidine kinase
TLR	Toll-like receptor
TMB	3,3′,5,5′-Tetramethylbenzidine
TMED	N,N,N,N-Tetramethyllethylenediamine
TMED7	Transmembrane emp24 domain-containing protein 7
TMEV	Theiler's murine encephalomyelitis virus
TM	Transmembrane domain

TNFα	Tumor necrosis factor α
TNFR	Tumor necrosis factor receptor
TRIL	TLR4 interactor with leucine rich repeats
TRADD	Tumor necrosis factor receptor (TNFR) 1 associated death domain
TRAF6	TNF receptor associated factor 6
TRAM	TRIF related adaptor molecule
TRIF	TIR domain containing adaptor inducing interferon-β
UBC13	Ubiquitin conjugating enzyme E2 13
UEV1A	Ubiquitin conjugating enzyme variant 1A
UNC93B	Glycoprotein uncoordinated 93 homology B
VIPERIN	Virus inhibitory protein endoplasmic reticulum associated IFN-inducible
VISA	Virus induced signaling adaptor
VSV	Vesicular stomatitis virus
v/v	Volume per volume
WNV	West Nile Virus
WT	Wild-type
w/v	Weight per volume
YFP	Yellow fluorescent protein

Abstract

TLR4 interactor with leucine rich repeats (TRIL) was originally described as a protein required for Toll-like receptor 4 (TLR4) signalling. This thesis provides new insights into the function of TRIL within TLR signalling and uncovers the *in vivo* role of TRIL in bacterial and viral infection.

Initial localisation studies demonstrated that TRIL is differentially localised in a cell type specific manner. It is expressed intracellularly within human astrocytoma U373 and human monocytic THP-1 cell lines, whilst in HEK-293T cells it is found on the plasma membrane. Further investigation revealed that intracellular TRIL colocalises with the early endosome and the endoplasmic reticulum (ER), but not the mitochondria, or the Golgi structures. The endosomal localisation of TRIL can be further boosted by LPS stimulation.

TRIL is induced following stimulation with the TLR3 agonist Poly(I:C). When overexpressed TRIL positively regulates interferon stimulated response element (ISRE) and κB luciferase activation, as well as IL6 and RANTES production in response to Poly(I:C) in U373 cells. TRIL directly interacts with TLR3, but not with the plasma membrane associated TLR2. Stimulation with Poly(I:C) enhances the TRIL-TLR3 association, most probably via the increase in TRIL and/or TLR3 expression. TRIL is also capable of direct association with the TLR3 agonist Poly(I:C), pointing towards a function for TRIL in ligand delivery.

Silencing of TRIL using specific shRNA, led to impaired TLR3 responses, resulting in reduced ISRE luciferase activity, RANTES and type I interferons (IFNs) production. TRIL deficiency had no impact on TLR2 mediated responses, demonstrating the specificity of this protein in TLR3 signalling. Further studies into the role of TRIL using primary murine mixed glial cells confirmed that TRIL is induced by Poly(I:C) and LPS stimulation. Additionally, TRIL deficient primary mixed glial cells demonstrated diminished mRNA and protein levels for IL6, RANTES, TNFα and IFNβ in response to TLR4 and TLR3 ligand stimulation, with responses mediated by TLR7/8 and TLR2 remaining unaffected.

Examination of primary bone marrow derived macrophages and dendritic cells (BMDMs and BMDCs) derived from wild-type and TRIL deficient mice demonstrated no differences in response to LPS and Poly(I:C) stimulation consistent with the low expression of TRIL detected within these cells.

In vivo investigation into the function of TRIL further confirmed its importance in a TLR4 mediated response. TRIL deficient mice were found less susceptible to *E.coli* induced acute peritonitis. Decreased expression and production of proinflammatory cytokines was detected within the brain, peritoneal lavage and serum of TRIL deficient mice.

Additional *in vivo* studies revealed a role for TRIL in the antiviral response to neurotropic vesicular stomatitis virus infection. Mice lacking TRIL demonstrated reduced levels of antiviral mediators such as RANTES and VIPERIN largely in the brain.

This study therefore further characterises TRIL as a regulator of TLR signalling pathways. A new role for TRIL in TLR3 signalling has been uncovered and the *in vivo* function of TRIL in the fine-tuning of the innate immune response during bacterial and viral infection in the brain has been revealed.

CHAPTER ONE

Introduction

1. Innate immune system

The innate and adaptive immune systems are synergistic constituents of the immune system, which provide comprehensive protection against invading pathogens. The innate immune system is the first line of defence, whereas the adaptive immune system acts later on in an infection and leads to the formation of immunological memory (Janeway, 1992).

A key feature of the innate immune system is self/non-self discrimination, mediated by germ-line encoded pattern recognition receptors (PRRs). PRRs are expressed on the cell surface, within subcellular compartments or in a secreted form in both immune and non-immune cells (Kawai & Akira, 2008). PRRs are responsible for recognition of highly conserved microbial and viral components known as pathogen associated molecular patterns (PAMPs) (Janeway, 1992), as well as host derived danger and/or damaged associated molecular patterns (DAMPs), released in response to stress, tissue damage or upon necrotic cell death (Bianchi, 2007). Activated by PAMPs and/or DAMPs PRRs trigger an immediate inflammatory response, mediated by several conserved signalling pathways leading to production of proinflammatory mediators as well as subsequent priming of the adaptive immune system.

PRRs have been classified according to their subcellular localisation, molecular structure, and recognition repertoire into two main classes: the membrane bound receptors consisting of Toll-like receptors (TLRs) and C-type lectin receptors (CLRs), and the cytoplasmic sensors comprising retinoic inducible gene-I (RIG-I)-like receptors (RLRs), nucleotide oligomerisation domain (NOD)-like receptors (NLRs), and cytosolic nucleic acid sensors.

This project concerns the characterisation of the role of a protein termed TLR4 interactor with leucine rich repeats (TRIL). I will now describe the main receptors and signalling pathways in innate immunity and our current understanding of the role of TRIL as an accessory molecule in TLR4 signalling.

1.2 Pattern recognition receptors (PRRs)

1.2.1 NOD-like receptors (NLRs)

The NOD-like receptors (NLRs) represent a large family of cytosolic receptors. The first group of NLRs to be identified were NOD1 and NOD2 receptors responsible for the recognition of bacterial peptidoglycan and triggering of both nuclear factor-κB (NF-κB) activation and type I IFNs production (Strober et al, 2006). In addition, NOD2 has been linked with sensing viral RNA (Sabbah et al, 2009). The other NLRs comprise a large group implicated in the recognition of PAMPs and various DAMPs and leading to the assembly of multi-protein inflammasome complexes, mediating activation of caspase-1 and subsequent processing of pro-IL1β and pro-IL18 into their active forms (Franchi et al, 2012; Kanneganti, 2010; Schroder & Tschopp, 2010). Although the recognition of intracellular PAMPs/DAMPs and the regulation of IL1β and IL18 production are considered as primary functions of the NLRs, their contribution to innate immunity is far more complex as they have also been found to play a role in mediating the proinflammatory forms of cell death pyroptosis and pyronecrosis (Kroemer et al, 2009) and also in autophagy (Cooney et al, 2010).

1.2.2 C-type lectin receptors (CLRs)

The CLRs are a large family of transmembrane and soluble receptors characterised by the presence of one or more carbohydrate recognition domains (CRDs) and responsible for sensing of carbohydrate structures derived from pathogens, such as bacteria, viruses and fungi in a calcium dependent manner. The transmembrane CLRs can be divided into two groups, group I CLRs, which belong to the mannose receptor family, and group II CLRs comprising the asioaloglycoprotein receptor family and including the DC-associated C-type lectin 1 (dectin 1) and DC-immunoreceptor (DCIR) subfamilies (Geijtenbeek & Gringhuis, 2009). CLRs are widely expressed on different cell types such as macrophages and dendritic cells. Activation of CLRs leads to the internalisation of the pathogen, its degradation and subsequent antigen presentation. CLRs also trigger various signalling cascades depending primarily on NF-κB activation leading to the production of proinflammatory mediators and

involving crosstalk with other PRRs (Geijtenbeek & Gringhuis, 2009). CLRs can synergise with, antagonise, or modulate signals from other receptors, such as TLRs, thereby fine-tuning the response to infection or damage (Hardison & Brown, 2012). CLRs are also implicated in gene transcription regulation, activation of endo- and phagocytosis and modulation of cell adhesion and migration (Osorio & Reis e Sousa, 2011; Robinson et al, 2006).

1.2.3 RIG-I like receptors (RLRs)

The RLRs are a family of RNA helicases composed of three members: the retinoic acid inducible gene-I (RIG-I), melanoma differentiation associated gene 5 (MDA5), and laboratory of genetics and physiology 2 (LGP2), which are crucial for the antiviral response. RIG-I and MDA5 sense various forms of viral dsRNA and ssRNA, such as 5′ triphosphorylated, uncapped ssRNA, as well as short and long forms of dsRNA. MDA5 acts also as a primary sensor of synthetic dsRNA, Poly(I:C). Upon activation, residing in the cytoplasm in an inactive form RIG-I and MDA5 undergo conformational change. Generated multimeric forms of RIG-I or MDA5 subsequently interact with the adaptor molecule mitochondrial antiviral signalling protein (MAVS), which initiates signalling cascades leading to the activation of the transcription factors IRF3/7 and NF-κB and the production of proinflammatory and antiviral mediators. In contrast LGP2 was demonstrated to act as a regulator of both RIG-I and MDA5 (Bowie & Fitzgerald, 2007; Kawai et al, 2005; Meylan et al, 2005; Schlee et al, 2009). The RLRs are expressed in numerous cell types such as fibroblasts, epithelial cells, conventional dendritic cells, as well as microglia and astrocytes (Furr et al, 2008), where they are responsible for sensing of various groups of RNA viruses. RIG-I recognises the respiratory syncytial virus (RSV), vesicular stomatitis virus (VSV), Sendai virus (SeV), hepatitis C virus (HCV), Japanese encephalitis virus (JEV), and Influenza A and B virus. MDA5 detects picoranviruses and acts as sensor of encephalomyocarditis virus (EMCV) and Theiler's virus (Kato et al, 2006; Loo et al, 2008; Thompson et al, 2011).

1.2.4 Sensors of cytosolic DNA

The dsDNA sensors are PRRs implicated in the recognition of various forms of cytosolic DNA, including DNA derived from viruses, bacteria and apoptotic host cells. These include the DNA dependent activator of interferon (IFN) regulatory factors (DAI or ZBP1) (Takaoka et al, 2007); the RNA polymerase III (Pol III) (Ablasser et al, 2009), the leucine rich repeat in flightless I interacting protein 1 (LRRFIP1) (Yang et al, 2010b), the DExD/H box helicases (DHX9, DHX36, DDX41)(Kim et al, 2010; Zhang et al, 2011b), the recently identified Ku70 (Zhang et al, 2011a) and IFN inducible protein 16 (IFI16) (Unterholzner et al, 2010), which is a member of a larger family of proteins named the pyrin and HIN domain containing (PYHIN) family.

The cytosolic DNA sensors recognise various DNA structures such as Z and B-forms of dsDNA, detected by DAI and LRRFIP1 (Takaoka et al, 2007; Yang et al, 2010b), CpG-DNA sensed by DHX9 and DHX36 (Kim et al, 2010) and AT-rich dsDNA transcribed by the RNA polymerase III into 5' triphosphate dsRNA (5'ppp RNA), serving as a ligand for RIG-I (Ablasser et al, 2009). Additionally, recent studies have uncovered a new dsDNA sensor termed cGAS, which catalyses formation of cyclic dinucleotides (c-di-AMP/GMP) in response to dsDNA, which are subsequently recognised by DDX41 and adaptor molecule stimulator of IFN genes (STING) (Civril et al, 2013; Parvatiyar et al, 2012; Sun et al, 2013; Wu et al, 2013).

The majority of the DNA sensors trigger activation of the transcription factor IRF3 mediated by STING and leading to production of type I IFNs (Atianand & Fitzgerald, 2013; Paludan & Bowie, 2013). However, some of them trigger additional signalling pathways. DDX41 activates NF-κB and MAPK signalling cascades. LRRFIP1 triggers IFNβ production via the specific β-catenin dependent pathway (Yang et al, 2010b). Ku70 induces type III rather than type I IFNs through the activation of IRF1 and IRF7 (Zhang et al, 2011a). In addition the PYHIN family members AIM2 and IFI16 trigger formation of the inflammasome complex (Atianand & Fitzgerald, 2013). Recognition of DNA by cytosolic DNA sensors has been associated with a beneficial immune response to pathogenic infection as well as detrimental recognition of host DNA leading to

autoimmune diseases such as amyotrophic lateral sclerosis (ALS) (Atianand & Fitzgerald, 2013; Paludan & Bowie, 2013; Sharma & Fitzgerald, 2011).

1.3 Toll-like receptors (TLRs)

Toll-like receptors are probably the best-characterised and most extensively studied group of PRRs. TLRs were initially discovered in *Drosophila*, where the cell surface receptor Toll was recognised for its role in the regulation of dorsal-ventral polarity (Lemaitre et al, 1996). Later studies found it to be important also for the immune response, particularly against fungal and bacterial infection, which subsequently led to the search for mammalian homologues.

To date, 10 TLRs have been identified in humans, 13 in mice with TLRs 1–9 common to both species. Mouse TLR10 is not functional due to a retrovirus insertion, whereas TLR11, TLR12 and TLR13 have been lost from the human genome (Kawai & Akira, 2006).

TLRs are specialised in the recognition of a wide range of PAMPs such as lipids, lipoproteins, proteins and nucleic acids derived from bacteria, viruses, fungi and parasites. The recognition of PAMPs by TLRs occurs in different cellular compartments from the plasma membrane to intracellular vesicles. Upon activation, TLRs trigger signalling events leading to production of proinflammatory cytokines and chemokines as well as type I IFNs. Those, in turn, cause recruitment of neutrophils and activation of macrophages, which eliminate invading pathogens (Kawai & Akira, 2006).

1.3.1 Structure of TLRs

TLRs are type I transmembrane glycoproteins composed of three major domains. An extracellular ectodomain (ECD) consisting of varying numbers of leucine rich repeat (LRR) motifs, a single transmembrane (TM) helix and an intracellular Toll-IL-1 receptor resistance (TIR) domain required for downstream signal transduction (Hashimoto et al, 1988; Medzhitov & Janeway, 1997). The LRR domain, which is primarily responsible for mediating ligand recognition, is comprised of 19-25 tandem repeats each of which is 24-29 amino acids in length and contains consensus

LxxLxLxxNxL motif, where "X" is any amino acid, and an additional variable region (Figure 1.1).

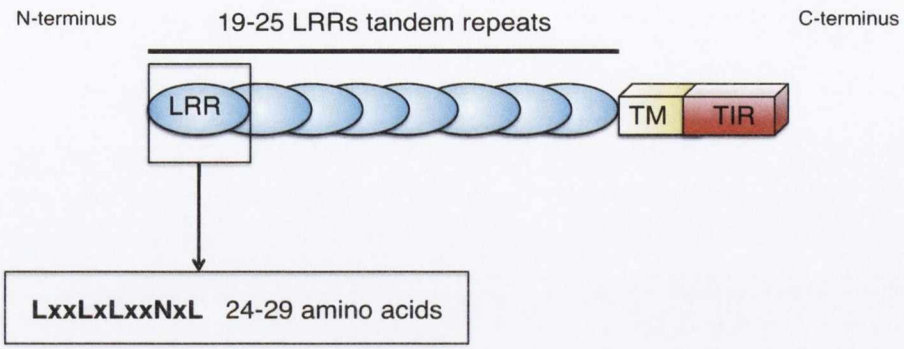

Figure 1.1 The structure of TLRs

The structure of TLRs is characterised by the presence of an extracellular leucine rich repeat (LRR) domain, a single transmembrane (TM) domain and an intracellular Toll-IL-1 receptor resistance (TIR) domain. The LRR domain comprises of 19-25 tandem LRRs, each of which contains the consensus LxxLxLxxNxL motif, in which X represents any amino acid.

1.3.2 Expression of TLRs

TLRs are widely expressed and can be found in numerous tissues and cell types. They can be found in various immune and non-immune cells, such as macrophages, conventional and plasmacytoid dendritic cells and B cells, as well as epithelial cells. Interestingly TLRs are also broadly expressed in neuronal and glial cells, like microglia and astrocytes.

1.3.3 TLR localisation and ligand recognition

TLRs can be classified into two distinct groups based on their cellular distribution and recognised ligands. The first group represents plasma membrane associated TLRs and comprises TLR1, TLR2, TLR4, TLR5, TLR6 and TLR10, which recognise primarily microbial membrane components such as lipids, lipoproteins and proteins. The second group consists of endosomal membrane associated TLRs, including TLR3, TLR7, TLR8 and TLR9, that are directed to the intracellular

compartments such as endosomes, lysosomes and endolysosomes, where they sense microbial nucleic acids (Akira et al, 2006).

Specific cellular localisation of TLRs is considered to be crucial for proper recognition of PAMPs (Takeda & Akira, 2005). Intracellularly localised TLRs are capable of sensing bacterial and viral nucleic acids only following their initial degradation within late endosomes and lysosomes of the cell. Moreover, it is now clear that distinct localisation of TLRs is an important mechanism of discrimination between self and non-self molecules (Kawai & Akira, 2010).

1.3.3.1 Ligands specific for cell surface TLRs

1.3.3.1.1 TLR4

TLR4 was the first human TLR to be identified and characterised (Medzhitov et al, 1997). It responds to bacterial lipopolysaccharide (LPS), a major component of the outer membrane of Gram-negative bacteria such as *Escherichia coli* (*E.coli*). The evidence that TLR4 is the receptor for LPS came from studies on the C3H/HeJ mouse strain. These mice, carrying a point mutation in the gene encoding TLR4, are hypo-responsive to LPS stimulation and are therefore highly susceptible to infection by Gram-negative bacteria (Poltorak et al, 1998).

The recognition of LPS by TLR4 requires several accessory molecules, including LPS binding protein (LBP), glycosylphosphatidyl inositol (GPI) anchored glycoprotein CD14 and glycoprotein MD2 (Lu et al, 2008). TLR4 and MD2 form a complex at the cell surface, serving as the LPS binding platform. LPS binds to LBP, which in turn interacts with CD14, allowing delivery of LPS-LBP to the TLR4-MD2 complex. This results in the formation of multiprotein TLR4-MD2-LPS complexes, which trigger downstream signalling pathways leading to the activation of the transcription factor NF-κB and production of proinflammatory cytokines such as IL6, IL8 and TNFα. Interestingly, structural analysis of the TLR4-MD2-LPS complex revealed that there is no direct association between TLR4 and LPS (Kim et al, 2007a; Park et al, 2009).

Apart from sensing LPS, TLR4 was shown to be involved in the recognition of fusion proteins derived from respiratory syncytial virus (RSV), envelope proteins from

mouse mammary tumor virus (MMTV), pneumolysin from *Streptococcus pneumoniae* and the plant derived cytostatic drug paclitaxel (Akira et al, 2006). Additionally, TLR4 can also recognise cell wall components of fungi such as *Sacharomyces cerevisiae* and *Candida albicans* (Netea et al, 2002) (Table 1.1.).

Notably, TLR4 has been also implicated in sensing of DAMPs, endogenous danger signals specifically generated upon tissue injury or damaged (Piccinini & Midwood, 2010). TLR4 has been reported to recognise endogenous fatty acids (Shi et al, 2006), as well as intracellular molecules released from necrotic cells such as the nuclear DNA binding protein high-mobility group box 1 (HMGB1) (Lotze & Tracey, 2005), heat-shock proteins HSP60, HSP70, HSP22 and gp96 (Asea et al, 2002; Vabulas et al, 2002) and neutrophil elastase (Tsujimoto et al, 2005) Additionally, TLR4 can be also activated by the extracellular matrix (ECM) structural components including oligosaccharides, hyaluronic acid (HA) (Taylor et al, 2004) and heparan sulfate (HS) (Johnson et al, 2002; Termeer et al, 2002) as well as ECM proteins, biglycan (Schaefer et al, 2005) and tenascin-C (Midwood et al, 2009). Sensing of HA by TLR4 is mediated by accessory molecules CD44 and MD2 and leads to dendritic cell maturation and production of proinflammatory cytokines (Taylor et al, 2004; Taylor et al, 2007). Similarly tenascin-C induces synthesis of proinflammatory cytokines via activation of TLR4 (Midwood et al, 2009). Interestingly, in a recent study Piccinini *et al.* demonstrated that tenascin-C is also required for an effective immune response to bacterial LPS during experimental sepsis *in vivo* (Piccinini & Midwood, 2012). In addition, TLR4 was also shown to mediate responses to low-density lipoprotein (LDL) and β-amyloid peptide though CD36-TLR4-TLR6 complex formation (Stewart et al, 2010). A more complete list of PAMPs and DAMPs sensed by TLR4 can be found in Table 1.1.

1.3.3.1.2 TLR1/2/6

TLR2 has been implicated in the recognition of a wide spectrum of PAMPs derived form bacteria, fungi, parasites and viruses (Akira et al, 2006). These include lipopeptides from various pathogens, peptidoglycan (PGN) and lipoteichoic acid (LTA)

from Gram-positive bacteria, lipoarabinomannan from mycobacteria, glycophoshatidyloinositol anchors, fungal zymosan, and hemagglutinin derived from measles virus (Takeda, 2005) (see Table 1.1). The ability of TLR2 to recognise such a broad array of microbial components has been attributed to its unique ability to heterodimerise with TLR1 and TLR6. The TLR2/TLR1 association specifically recognises triacyl lipopeptides from Gram-negative bacteria and mycobacteria, while the TLR2/TLR6 heterodimer allows the recognition of diacyl lipopeptides from Gram-positive bacteria and mycobacteria as well as fungal zymosan (Jin et al, 2007; Kang et al, 2009). The difference in binding of diacylated and triacylated lipoproteins by TLR2/6 and TLR2/1 respectively is determined by the structural features of these complexes. In addition, TLR2 is also capable of interaction with coreceptors involved in recognition of PAMPs such as CD14 and CD36 (Hoebe et al, 2005), and the C-type lectin receptor Dectin-1 (Goodridge & Underhill, 2008).

Similar to TLR4, TLR2 has been also shown to recognise endogenous DAMPs such as ECM constituents biglycan (Schaefer et al, 2005) and versican (Kim et al, 2009), as well as hyaluronic acid fragments (Johnson et al, 2002; Termeer et al, 2002).

Following recognition of PAMPs and DAMPs, TLR2 induces signalling pathways leading to the activation of NF-κB and production of inflammatory cytokines. Barbalat *et al.* have shown that TLR2 also triggers the production of type I IFNs by inflammatory monocytes in response to viral, but not bacterial infection, which suggests a cell type specific role for TLR2 in the antiviral response (Barbalat et al, 2009).

1.3.3.1.3 TLR5

Localised to plasma membrane TLR5 is responsible for the recognition of bacterial flagellin. Flagellin is a structural component of bacterial whip-like flagella used for locomotion (Hayashi et al, 2001). Recognition of flagellin by TLR5 induces a signalling cascade leading to the activation of NF-κB in epithelial cells, monocytes, and dendritic cells (Gewirtz et al, 2001; Hayashi et al, 2001).

Recent studies have demonstrated that bacterial flagellin is also sensed by the NLR family member, apoptosis inhibitory protein 5 (NAIP5) (Kofoed & Vance, 2011) and intracellular mouse TLR11 (Mathur et al, 2012).

A broad range of natural and synthetic ligands sensed by extracellular TLRs can be found in Table 1.1 below.

TLRs	Natural ligands	Synthetic ligands
TLR2	• Peptidoglycan (PGN) (Lien et al, 1999; Takeuchi et al, 1999; Yoshimura et al, 1999) • Haemagglutinin (Bieback et al, 2002) • HMGB1 (Park et al, 2006; Park et al, 2004) • Biglycan (Schaefer et al, 2005) • Hyaluronic acid (HA) (Termeer et al, 2002) • Heparan sulfate (HS) (Johnson et al, 2002) • Versican (Kim et al, 2009)	• Pam3CSK4
TLR1/2	• Triaclated lipopeptides (Jin et al, 2007(Jin et al, 2007; Takeda et al, 2002)	• Pam3CSK4
TLR2/6	• Diacyl lipopeptides (Kang et al, 2009; Ozinsky et al, 2000; Takeda et al, 2002) • Lipoteichoic acid (LTA) (Schroder et al, 2003) • Zymosan (Sato et al, 2003a)	• FSL1 • MALP2 • Pam2CSK4
TLR4	• LPS (Poltorak et al, 1998) • Mannan (Tada et al, 2002) • HSP60 (Ohashi et al, 2000) • HSP70 (Asea et al, 2002) • HSP22 (Roelofs et al, 2006) • gp96 (Vabulas et al, 2002) • Fibrinogen (Smiley et al, 2001) • HMGB1 (Park et al, 2006; Park et al, 2004) • Hyaluronic acid (HA) (Termeer et al, 2002) • Heparan sulfate (HS) (Johnson et al, 2002) • Bigyclan (Schaefer et al, 2005) • Tenanscin-C (Midwood et al, 2009) • *Streptococcus pneumoniae* (Pneumolysin) (Malley et al, 2003) • RSV (fusion protein) (Kurt-Jones et al, 2000) • VSV (glycoprotein) (Georgel et al, 2007) • MMTV (envelope protein) (Miller et al, 2003; Rassa et al, 2002)	• Lipid A derivatives
TLR4/6	• β amyloid (Stewart et al, 2010) • oxLDL (Rassa et al, 2002)	• ND
TLR5	• Flagellin (Hayashi et al, 2001)	• ND
TLR10	• ND	• ND

Table 1.1 Natural and synthetic ligands of extracellular TLRs

1.3.3.2 Ligands specific for intracellular TLRs

1.3.3.2.1 TLR3

Localised primarily in endosomes, TLR3 is capable of recognising double-stranded RNA (dsRNA) as well as its synthetic analogue polyinosinic-polycytidylic acid (Poly(I:C)). The structural analysis of TLR3 revealed that dsRNA recognition by TLR3 is not sequence specific (Choe et al, 2005). Upon binding of dsRNA, TLR3 undergoes dimerization, which in turn leads to ligand-receptor complex formation (Leonard et al, 2008; Liu et al, 2008; Wang et al, 2010). The affinity of ligand recognition by TLR3 increases with the acidic environment found in endosomes (de Bouteiller et al, 2005; Leonard et al, 2008). Initial studies on the TLR3 activation mechanism demonstrated, that enzymatic processing of TLR3 by endosomal cathepisns is essential for its activation and subsequent immune response (Ewald et al, 2011; Ewald et al, 2008; Garcia-Cattaneo et al, 2012). However, contrasting data presented by Qi *et al.* indicated that proteolytic cleavage modulates the degree of the TLR3 response but it is not critical for TLR3 signalling (Qi et al, 2012). Both the full-length and cleaved fragments of TLR3 can bind Poly(I:C) and both can be found in the endosome (Qi et al, 2012).

Although TLR3 primarily recognises viral dsRNA, it has also been implicated in the sensing of numerous ssRNA and DNA viruses. The basis of this recognition relies on the intermediate dsRNA form generated during replication of positive-strand ssRNA viruses and transcription of viral dsDNA (Weber et al, 2006). Studies using TLR3 deficient mice demonstrated that TLR3 mediates the innate immune response against RNA viruses, such as West Nile virus (WNV), RSV and EMCV as well as DNA viruses like HSV and mouse cytomegalovirus (Daffis et al, 2008; Tabeta et al, 2004; Wang et al, 2004; Zhang et al, 2007). Interestingly, recent studies by Tatematsu *et al.* demonstrated that TLR3 is also capable of recognising incomplete RNA stem structures derived from poliovirus (Tatematsu et al, 2013). This finding, together with studies by Bernard *et al.* who implicated TLR3 in the recognition of UV-damaged self-non coding RNA (Bernard et al, 2012), suggests that viral and host derived RNAs with stable stem structures, can serve as lignads for TLR3. In addition, small interfering RNA (siRNA) is

also capable of triggering TLR3 activation, depending on cell type and the structure of the siRNA (Reynolds et al, 2006).

Upon ligand recognition, TLR3 initiates signalling cascades leading to NF-κB and IRF3 activation, and production of proinflammatory cytokines and type I IFNs. In addition, dsRNA mediated TLR3 stimulation also has an effect on cell migration, adhesion and proliferation (Yamashita et al, 2012).

1.3.3.2.2 TLR7/8

TLR7 and TLR8 are both localised intracellularly and represent similar structural architecture. Studies using TLR7 deficint mice revealed that murine TLR7 respond to synthetic compounds, imidazoquinolines, imiquid and resiquimod (R848)(Hemmi et al, 2002). Similarly, human TLR7 and TLR8 are capable of sensing R848. TLR7 receptor demonstrates higher sensitivity to resiquimod at low concentrations, whereas TLR8 responds better to high doses of R848 (Jurk et al, 2002). Mouse TLR7 is also capable of sensing other synthetic coumpounds such as loxiribine (Heil et al, 2003; Lee et al, 2003). In contrast to TLR7, mouse TLR8 does not recognise imidazoquinolines like R848 (Hemmi et al, 2002; Jurk et al, 2002). Moreover, stimulation with a natural TLR7/8 ligand, viral ssRNA activates human TLR7 and TLR8 and mouse TLR7 but not mouse TLR8, leading to belief that TLR8 is biologically inactive in mice (Heil et al, 2004). However, studies by *Gorden et al.* demonstrated that stimulation of HEK-293 cells expressing murine TLR8, with a combination of TLR8 agonist and poly-T oligonucleotides leads to NF-κB activation (Gorden et al, 2006a; Gorden et al, 2006b). Interestingly, recent studies have also shown high expression level of TLR8 during mouse brain development, where TLR8 acts as a negative regulator of neurite outgrowth and an activator of neuronal cell death, suggesting that mouse TLR8 remains biologically functional (Ma et al, 2006). Apart from the synthetic guanine analogues imidazoquinoline and loxoribine, TLR7 and human TLR8 recognise RNA from *Borrelia burgdorferi* (Cervantes et al, 2012; Mancuso et al, 2009). TLR7 also detects poly(U) RNA, certain siRNA structures (Hornung et al, 2005) and guanosine/uridine (G/U) rich ssRNA, similar to that found in the human immunodeficiency virus (HIV-1)

(Heil et al, 2004) as well as ssRNA from VSV (Diebold et al, 2004) and Influenza virus (Lund et al, 2004). A more complete list of natural and synthetic ligands of TLR7 and TLR8 is presented in Table 1.2.

Recognition of nucleoside structures by TLR7 or TLR8 activates intracellular pathways that culminate in the induction of proinflammatory cytokines, chemokines, and type I IFNs, and in the upregulation of co-stimulatory molecules.

1.3.3.2.3 TLR9

Intracellularly localised TLR9 was initially described as a sensor of unmethylated CpG motifs of bacterial and viral DNA (Hemmi et al, 2000). It was shown however, that DNA recognition by TLR9 critically depends on the 2' deoxyribophosphate backbone and not on the CpG motifs (Haas et al, 2008). TLR9 has been implicated in the recognition of dsDNA from viruses such as MCMV and herpes simplex virus 1 and 2 (HSV-1 and HSV-2)(Krug et al, 2004; Lund et al, 2003), as well as sensing protozoa such as *Trypanosoma cruzi* (Bafica et al, 2006). TLR9 can also be triggered by hemozoin (Coban et al, 2005) and synthetic CpG oligonucleotides (ODNs).

TLRs	Natural ligands	Synthetic ligands
TLR3	• dsRNA (Alexopoulou et al, 2001b)	• Poly(I:C) • PolyU
TLR7	• G/U rich ssRNA (Diebold et al, 2004; Heil et al, 2004; Lund et al, 2004) • Short dsRNA (Hornung et al, 2005)	• Imiquimod • Resiquimod • Loxoribine • Gardiqimod • CL075 • CL097 • CL264 • CL307
TLR8	• G/U rich ssRNA (Diebold et al, 2004; Heil et al, 2004; Lund et al, 2004) • Short dsRNA (Hornung et al, 2005) • Bacterial RNA (Kariko et al, 2005)	• Resiquimod* • CL075 • CL097
TLR9	• CpG DNA (Haas et al, 2008; Hemmi et al, 2000) • Hemozoin (Coban et al, 2005)	• CpG • ODNs

Table 1.2 Natural and synthetic ligands of intracellular TLRs
*Synthetic ligand directly sensed by human TLR7/8 and mouse TLR7 but not TLR8

1.3.3.3 Ligands specific for mouse TLR11, TLR12 and TLR13

TLR11, TLR12 and TLR13 are endosomal TLRs functional in mouse but not human (Kawai & Akira, 2011). Mouse TLR11 responds to profilin-like proteins derived from the parasite *Toxoplasma gondii* (Yarovinsky et al, 2005; Zhang et al, 2004). TLR11 deficient mice are also highly susceptible to uropathogenic *E.coli* infection (Zhang et al, 2004). Further studies revealed that TLR11, similar to TLR5 (Hayashi et al, 2001), detects flagellin from uropathogenic *E.coli* and *Salmonella typhimurium* (Mathur et al, 2012), but most likely via a different mechanism due to diverse expression patterns of these TLRs. TLR12 recognises profilin from *Plasmodium falciparum* either on its own or as a heterodimer with TLR11 (Koblansky et al, 2013). However, unlike TLR11, TLR12 is incapable of sensing bacterial flagellin. TLR13, which is lost from the human genome, has been recently reported to engage with a large bacterial ribosomal RNA (rRNA), specifically the CGGAAAGACC motif of 23S rRNA of Gram-negative *E.coli*, which resulted in the induction of pro-IL1β (Oldenburg et al, 2012). Ligands specific for TLR11-13 are presented in Table 1.3 below.

TLRs	Natural ligands	Synthetic ligands
TLR11	• Profilin (Yarovinsky et al, 2005; Zhang et al, 2004) • Flagellin (Mathur et al, 2012)	• ND
TLR12	• Profilin (Koblansky et al, 2013)	• ND
TLR13	• CGGAAAGACC motif of bacterial 23S rRNA (Oldenburg et al, 2012)	• ND

Table 1.3 Natural and synthetic ligands of mouse TLR11, TLR12 and TLR13

1.3.4 TLR signalling

The engagement of TLRs by microbial PAMPs leads to the activation of downstream signalling events resulting in the production of proinflammatory mediators and type I IFNs. Upon ligand recognition, TLRs homo- or heterodimerise and undergo conformational changes in order to enable physical contact of two intracellular TIR domains (Zhu et al, 2009). This structural rearrangement initiates a signalling cascades mediated by different adaptor molecules: Myeloid differentiation

factor 88 (MyD88), MyD88 adaptor like (Mal), TIR domain containing adaptor inducing interferon β (TRIF), and TRIF related adaptor molecule (TRAM) (Kawai & Akira, 2010), all of which act as positive regulators of TLR signalling. There are also two TLR adaptor molecules, which have been demonstrated to function as negative regulators of TLRs, B-cell adaptor for PI3K (BCAP) (Ni et al, 2012; Troutman et al, 2012) and sterile alpha and HEAT-Armadillo motifs containing protein (SARM) (Carty et al, 2006).

All of the TLR adaptor proteins consist of a TIR domain, mediating TIR–TIR interactions between TLR receptors, receptor–adaptor, and adaptor–adaptor, that are crucial for signalling (O'Neill & Bowie, 2007; Palsson-McDermott & O'Neill, 2007). The structure of all TIR-domain containing TLR adaptor molecules is presented in Figure 1.2.

Selective usage of the adaptor molecules by different TLRs triggers two distinct signalling pathways. All TLRs, with the sole exception of TLR3, trigger their signalling via the adaptor protein MyD88, which in turn activates the transcription factor NF-κB and mitogen activated protein-kinases (MAPKs) to induce production of inflammatory cytokines (Akira et al, 2006). In contrast, TLR3 utilises the adaptor molecule TRIF, which initiates an alternative signalling pathway leading to activation of IRF3, 5 and 7 (Honda et al, 2005) and NF-κB, culminating in type I IFN and inflammatory cytokine production (Kawai et al, 2001; Toshchakov et al, 2002). Therefore, the TLR signalling pathways can be classified as either MyD88-dependent, or MyD88-independent (TRIF-dependent) leading to the production of proinflammatory cytokines and type I IFN, respectively.

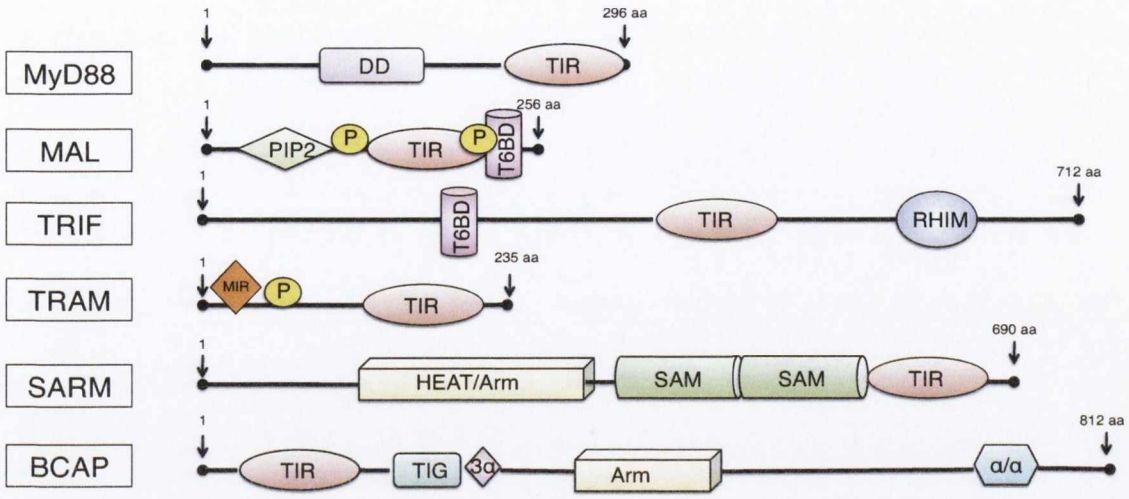

Figure 1.2 Domain architecture of TIR adaptor proteins

The figure represents the structure of all known TIR domain containing adaptor proteins. MyD88 consists of a N-terminal death domain (DD) and a C-terminal TIR domain. Mal consists of the TIR domain and also contains the PIP2 and TRAF6 (T6BD) binding domains. Tyrosines (Y) at positions 86 and 187 in the structure of Mal are phosphorylated by Bruton's tyrosine kinase (BTK). TRIF similarly to Mal has a TRAF6 binding motif, followed by the TIR domain and the RHIM region. TRAM consists of a TIR domain. TRAM undergoes phosphorylation by protein kinase C ε (PKCε) at the serine (S) 16 and post-translational myristolyation at its N-terminus. SARM consists of the HEAT and Armadillo-motifs (HEAT/ARM) present at the N-terminus, followed by the two SAM domains and the TIR domain localised on the C-terminal end. Expressed within B-cells and macrophages, BCAP consists of a cryptic N-terminal TIR domain, a transcription factor-Ig (TIG) and 3-α-helix (3α) structural unit, a short set of armadillo repeats (ARM), and a C-terminal helical (α/α) module.

1.3.4.1 MyD88-dependent TLR signalling pathway

MyD88 was the first TIR-domain containing adaptor molecule to be identified. It was initially shown to be involved in signalling by the type I IL-1 receptor (IL-1R), and later also in signalling mediated by various TLRs (Medzhitov et al, 1998; Wesche et al, 1997). All these findings were verified using MyD88 deficient mice, which failed to response to any of the TLR ligands, with the exception of TLR3 (Alexopoulou et al, 2001a; Kawai et al, 1999).

Following activation, MyD88 binds first to the cytoplasmic TIR domain of TLRs, and then recruits Interleukin 1 receptor associated kinase 4 (IRAK4) (Suzuki et al, 2002). Activated IRAK4 transduces inflammatory signals by a rapid phosphorylation of IRAK1 (Li et al, 2002; Suzuki et al, 2002). This is followed then by the activation of IRAK2, which has been shown to play a key role in sustaining proinflammatory cytokine production (Kawagoe et al, 2008). The IRAK complex activates TNF receptor-associated factor 6 (TRAF6) (Li et al, 2002), an E3 ubiquitin ligase, which is negatively regulated by another member of IRAK family, IRAK-M (Kobayashi et al, 2002). In addition, IRAK1 and/or IRAK4 phosphorylate the E3 ubiquitin ligases Pellino. Pellino can also directly bind to IRAKs, TRAF6 and transforming growth factor β activated protein kinase 1 (TAK1) triggering polyubiquitination of IRAK1 (Moynagh, 2009). Activated by the IRAK complex TRAF6 combines with an E2 ubiquitin-conjugating enzyme UBC13 and UEV1A and catalyse the synthesis of Lys63 (K63)-linked polyubiquitin chains, resulting in the autoubiquitination of TRAF6 (Chen, 2005; Yamamoto et al, 2006). Generated K63–polyubiquitin chains mediate TRAF6 binding of TAB2 and TAB3, which leads to the activation of TAK1, a MAP kinase kinase kinase (MAP3K) family member. Phosporylated TAK1 triggers activation of a cascade of mitogen activated protein kinases (MAPKs) (Sato et al, 2005; Wang et al, 2001; Yamamoto & Takeda, 2010). Starting from MAPKK3 and MAPKK6, through the phosphorylation of Jun kinases (JNKs) and p38, the MAPKK cascade results in the activation of transcription factor AP-1 (Kawai & Akira, 2006). Simulatneously, TAK1 activates the IKK complex comprised of catalytic subunits IKKα and IKKβ and regulatory IKKγ (NEMO) leading to phosphorylation of IκB proteins. Once phosphorylated, IκB proteins undergo degradation, which results in nuclear translocation of the transcription factor NF-κB and expression of various inflammatory cytokine genes (Bhoj & Chen, 2009; Takeuchi & Akira, 2010; Yamamoto & Takeda, 2010).

In addition, MyD88 activates certain members of the IRF family of transcription factors. IRF1 associates with MyD88 (Negishi et al, 2006), while IRF7 interacts with both MyD88 and TRAF6 (Takaoka et al, 2005). Ultimately, activation of IRFs, NF-κB and AP-1 in a MyD88-dependent manner induces a wide spectrum of inflammatory gene

transcription. The MyD88-dependent signalling pathway has been depicted in Figure 1.3.

Mal (also known as TIRAP) was the second adaptor protein to be discovered (Fitzgerald et al, 2001; Horng et al, 2001). First *in vitro* studies on Mal indicated its function in TLR4 signalling, as the overexpression of a dominant negative form of Mal led to inhibition of NF-κB following LPS stimulation but not upon stimulation with IL1 or IL18 (Fitzgerald et al, 2001). Further *in vitro* studies carried out using Mal deficient mice demonstrated a requirement for Mal in TLR4 and also TLR2 mediated signalling (Horng et al, 2001; Yamamoto et al, 2002). Mal deficient macrophages treated with LPS showed impaired inflammatory cytokine production and delayed NF-κB activation, however no change in IRF3 activation and expression of IFN inducible genes (Fitzgerald et al, 2001; Yamamoto et al, 2002). Mal/MyD88 double knockout mice also showed a normal expression of IFN inducible genes, thus Mal is essential for MyD88-dependent but not MyD88-independent signalling via TLR4. Mal acts as a bridging adaptor, facilitating the transfer of MyD88 to TLR4 at the plasma membrane (Kagan & Medzhitov, 2006). Additionally, studies by Kenny *et al.* demonstrated that Mal is required in TLR2 signalling, however only to sensitize the host to low levels of ligand, while it is dispensable for the TLR2 response to high ligand concentrations. Thus at high ligand concentrations signalling via TLR2 occurs exclusively through MyD88 and not Mal (Kenny et al, 2009).

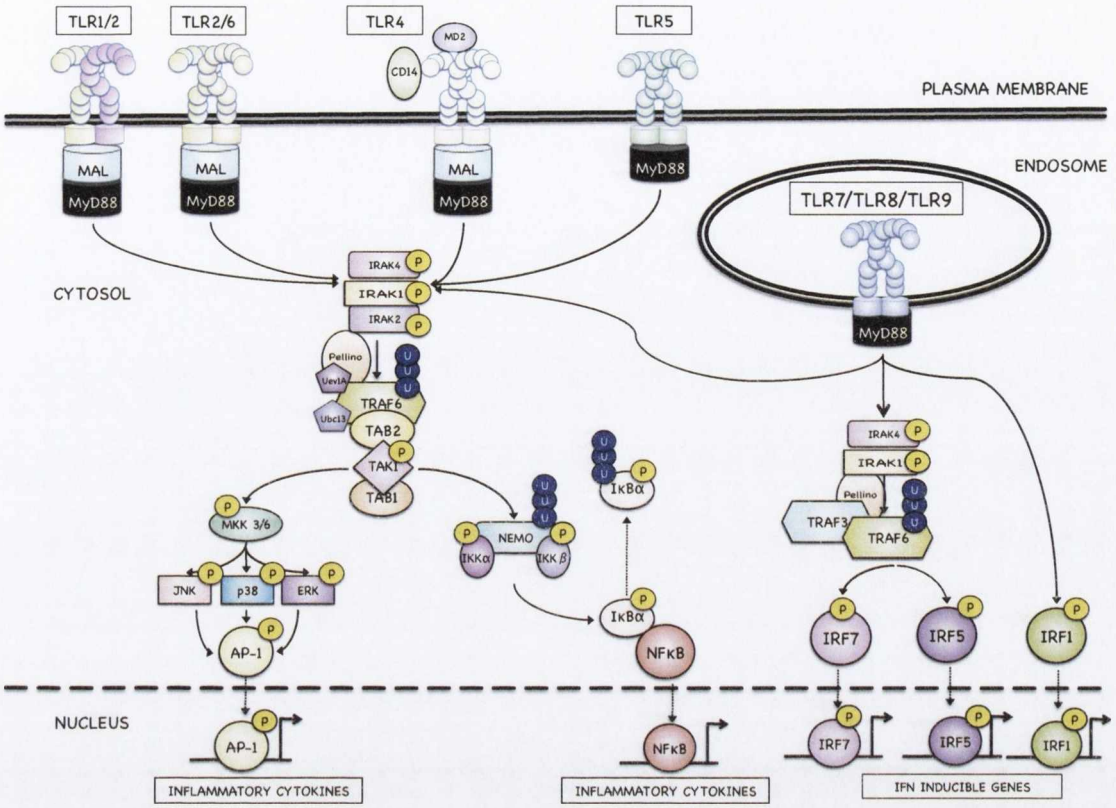

Figure 1.3 MyD88-dependent signalling pathways

The MyD88 signalling pathway is utilized by all TLRs except for TLR3. Signal transduction mediated by MyD88 leads to the activation of IRAKs 1, 2, and 4, which subsequently recruit TRAF6. In association with UBC13, UEV1A and Pellino, TRAF6 undergoes polyubiquitination. Activated TRAF6 recruits TAB2, followed by the recruitment of TAK1, TAB1 and TAB2. Phosphorylation of TAK1 leads to the activation of MAPKs, which in turn phosphorylate JNK, p38 and ERK, which results in translocation of AP1 into the nucleus and terminates in the production of proinflammatory cytokines. TAK1 also activates the IKK complex consisting of IKKγ (NEMO), IKKα and IKKβ. Phosphorylated IKKα and IKKβ targets IκBα for degradation through phosphorylation and polyubiquitination. This allows for nuclear translocation of NF-κB, which triggers expression of proinflammatory cytokines. MyD88 mediated signalling initiated by the endosomal TLRs leads to activation of IRAK4 and IRAK1. Phosphorylated IRAKs recruit TRAF6, which undergoes polyubiquitination and together with TRAF3 triggers phosphorylation of IRF5 and IRF7, leading to activation of IFNs. MyD88 dependent signal transduction from the endosomally localised TLRs, can also leads to phosphorylation of IRF1 resulting in IFN production.

1.3.4.2 MyD88-independent/TRIF-dependent TLR signalling pathway

TRIF (also known as TICAM1) was identified subsequently to MyD88 and Mal (Oshiumi et al, 2003a; Yamamoto et al, 2002). Examination of macrophages derived from MyD88/Mal double knockout mice demonstrated a normal response to both TLR3 and TLR4 stimulation, suggesting the existence of alternative signalling pathways. Further database searches using MyD88 and Mal sequences as templates, led to the discovery of TRIF (Yamamoto et al, 2002). The same molecule was also independently identified in a yeast two-hybrid screen as a TLR3 binding protein (Oshiumi et al, 2003a). Following on from *in vitro* studies, indicating involvement of TRIF in the MyD88-independent signalling, TRIF deficient mice were used to further determine the physiological role of TRIF. Mice lacking TRIF showed defective IRF3 activation and IFNβ production following LPS and Poly(I:C) stimulation (Hoebe et al, 2003; Yamamoto et al, 2003a). In contrast, the early phase of NF-κB and MAPK activation in response to LPS remained unaffected in the TRIF deficient mice.

Upon activation, TRIF recruits TRAF6 and RIP1 to its N- and C-terminal sites respectively. Direct interaction of TRIF with TRAF6 via its N-terminal TRAF6 binding domain activates TAK1 for NF-κB induction (Sato et al, 2003b). Mechanisms of TAK1 activation are not yet fully understood, but most probably resemble ubiquitination-dependent mechanisms found in the MyD88 dependent pathway. Recruitment of RIP1 to TRIF occurs through RIP homotypic interaction motif (RHIM) present in the C terminus of TRIF (Meylan et al, 2004). Following binding to TRIF, RIP1 undergoes K63-linked polyubiquitynation, and this modification was shown to be required for NF-κB activation. RIP1 also interacts with the adaptor Tumor Necrosis Factor Receptor (TNFR) 1-associated death domain (TRADD), and this multiprotein complex has been shown to be critical for activation of NF-κB and MAPK pathways (Chang et al, 2009; Ermolaeva et al, 2008). This signalling pathway has been represented in Figure 1.4 (shaded in grey).

Apart from NF-κB activation, TRIF-dependent signalling leads also to IRF3 activation and production of IFNβ. TRIF recruits non-canonical IKKs including TRAF family member associated NF-κB activator binding kinase 1 (TBK1) and IKKi (IKKε) to activate both IRF3 and IRF7 by phosphorylation, with the help of TRIF interacting

proteins TRAF3 and NAK-associated protein 1 (NAP1). Phosphorylated IRF3 and IRF7 homodimerise and translocate to the nucleus, where they initiate transcription of type I IFNs (Fitzgerald et al, 2003; Sharma et al, 2003).

Finally the TRIF-dependent pathway can culminate in cell apoptosis though activation of RIP1, FAS-associated death domain (FADD) and caspase-8 signal transduction (Kaiser & Offermann, 2005). Comprehensive TRIF-dependent signalling cascades are represented in Figure 1.4.

Notably, the role of TRIF is not exclusive to modulation of TLR responses. Recent studies by Rathinam *et al.* demonstrated that TRIF-dependent type I IFN production leads to subsequent caspase-11 mediated inflammasome activation (Rathinam et al, 2012).

TRAM (also known as TICAM2) was identified through sequence homology in database searches (Fitzgerald et al, 2003; Oshiumi et al, 2003b; Yamamoto et al, 2003b), followed by an *in vitro* study, which demonstrated that TRAM directly interacts with TRIF and TLR4, but not TLR3. In addition, TRAM overexpression and knockdown experiments further emphasized its exclusive role in TLR4 signalling pathway (Oshiumi et al, 2003b). Analysis of TRAM deficient mice established that TRAM acts to bridge TRIF to TLR4, and that it plays a critical role in the MyD88-independent TLR4 signalling cascade (Yamamoto et al, 2003b) (Figure 1.4). TRAM deficient mice, similar to TRIF knockouts, demonstrated impaired activation of IRF3 and production of IFN inducible genes. However, in contrast to TRIF deficient mice, those lacking TRAM were still capable of responding to TLR3 stimulation (Yamamoto et al, 2003b). TRIF is therefore the sole adaptor required for TLR3 signal activation. There is also a splice variant of TRAM, named TAG (TRAM adaptor with GOLD domain). TAG acts as a negative regulator of the TLR4/TRIF-dependent signalling pathway, by displacing the adaptor TRIF from TRAM (Palsson-McDermott et al, 2009), which is mediated by the GOLD domain-containing protein TMED7 (Doyle et al, 2012).

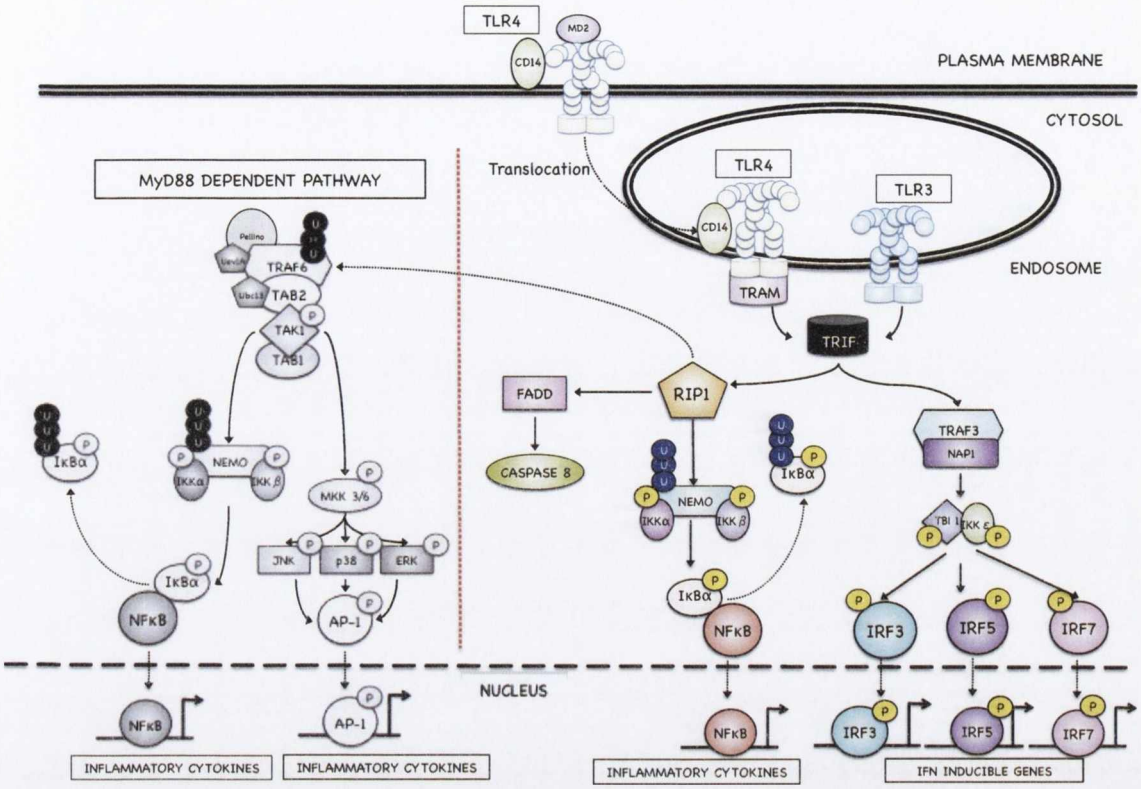

Figure 1.4 TRIF-dependent signalling pathways

The TRIF-dependent/MyD88-independent signalling pathway is used by the intracellularly localised TLR3, and by TLR4 following its internalisation into the endosomal compartments and binding of TRAM. TRIF recruits NAP1 and TRAF3 to activate TBK1 and IKKε, resulting in the phosphorylation of IRF3, IRF5 and IRF7, which then translocate into the nucleus activating the expression of IFN inducible genes. Alternatively TRIF associates with RIP1, which leads to the activation of the IKK complex, resulting in the nuclear translocation of NF-κB and induction of proinflammatory cytokine production. Signal transduction following recruitment of TRIF can also lead to MyD88-dependent signalling, through its association with TRAF6. Moreover, TRIF recruits FADD though its interaction with RIP1, resulting in apoptosis dependent on Caspase 8 activation.

1.3.4.3 TLR adaptor proteins BCAP and SARM

As mentioned above, apart from the TLR adaptor molecules: MyD88, Mal, TRIF and TRAM, which act as positive mediators of TLR signalling, there are also two TLR adaptor molecules named BCAP and SARM which have been shown to function as negative regulators of TLR responses (Carty et al, 2006; Ni et al, 2012; Peng et al, 2010; Troutman et al, 2012).

1.3.4.3.1 BCAP

B-cell adaptor for PI3K (BCAP) was initially identified as an adaptor protein mediating B-cell antigen receptor signalling to phosphoinositide 3-kinase (PI3K) activation (Okada et al, 2000). Further studies revealed that BCAP acts as a TLR adaptor protein linking, TLRs to PI3K/Akt activation and thereby modulating the innate immune response both *in vitro* and *in vivo*. Macrophages derived from BCAP deficient mice demonstrated a decrease in TLR mediated PI3K activity and Akt phosphorylation, when compared to wild-type cells. Additionally, BCAP knockout mice displayed an increased inflammatory response following bacterial infection *in vivo* (Ni et al, 2012; Troutman et al, 2012). Further studies are required in order to determine the exact mechanism by which BCAP negatively impacts on TLR mediated signalling.

1.3.4.3.2 SARM

SARM (also known as MyD88-5) is a fifth and most highly conserved member of the TIR adaptor family (O'Neill & Bowie, 2007). SARM homologues have been identified across many species including *Drosophila melanogaster*, *Caenorhabditis elegans*, zebrafish and horseshoe crab (Belinda et al, 2008; Couillault et al, 2004; Meijer et al, 2004; Mink et al, 2001), where SARM was found to execute multiple functions.

The *C.elegans* form of SARM (TIR-1) has been implicated in the regulation of the immune system and neuronal development. The knockdown of TIR-1, led to increased susceptibility and mortality to bacterial and fungal infections (Couillault et al, 2004). Additionally, TIR-1 has been found in olfactory neurons, and shown to be

involved in the regulation of the olfactory patterning (Chang et al, 2011). Interestingly, recent studies on TIR-1 in *C.elegans* have also linked the protein with a non-apoptotic cell death (Blum et al, 2012).

The initial studies into the role of SARM within mammals demonstrated its function as a negative regulator of TLR mediated signalling pathways (Carty et al, 2006; Peng et al, 2010). Carty *et al.* demonstrated the involvement of SARM in the direct interaction and inhibition of the adaptor TRIF (Carty et al, 2006), whereas Peng *et al.* revealed additional impact of SARM on MAPK phosphorylation leading to LPS and Poly(I:C) mediated AP-1 activation (Peng et al, 2010). In contrast to these findings, studies of mouse macrophages lacking SARM have demonstrated that cytokine production is unaltered after TLR stimulation (Kim et al, 2007b). Various expression patterns of human and mouse SARM could explain differences in the results obtained. The role of SARM as a negative modulator of TLR3 and TLR4 mediated signalling is presented in Figure 1.5.

Further *in vivo* studies on SARM revealed its role in innate immunity to neurotropic viral infections. WNV infection of SARM deficient mice led to reduced proinflammatory cytokine production and increased susceptibility to viral infection (Szretter et al, 2009). Additionally, recent studies by Zhou *et al.* showed that porcine SARM attenuates NF-κB activation following ligand stimulation, and that SARM might be involved in the pathogenicity of porcine reproductive and respiratory syndrome virus (PRRSV) infection (Zhou et al, 2012). Recent studies by Hou *et al.* uncovered a role for SARM in the regulation of immune response to neurotropic VSV infection (Hou et al, 2013). Mice lacking SARM demonstrated reduced inflammation and improved survival in response to VSV, pointing towards a negative role of SARM, acting as a mediator of immunopathology during the VSV infection (Hou et al, 2013).

Of note, a number of studies have identified SARM as a mediator of neuronal survival and degeneration. SARM was found to regulate neuronal cell death during oxygen and glucose deprivation (OGD) by targeting JNK3 to the mitochondria (Kim et al, 2007b), as well as neuronal morphology by controlling dendritic shape rearrangement through MKK4-JNK pathway (Chen et al, 2011). Moreover, SARM has

been found to regulate an active neuronal injury-induced axon degeneration programme, termed Wallerian degeneration, where SARM potently inhibits axon self destruction triggered by the injury (Osterloh et al, 2012b). Interestingly, a recent study reported that SARM also mediates neuronal apoptosis in response to a neurotropic La Crosse virus (LACV) (Mukherjee et al, 2013). SARM mediated cell death was associated with induced oxidative stress response and mitochondrial damage. Mukherjee *at al.* demonstrated that mice lacking SARM exhibited less neuronal damage following LACV infection (Mukherjee et al, 2013).

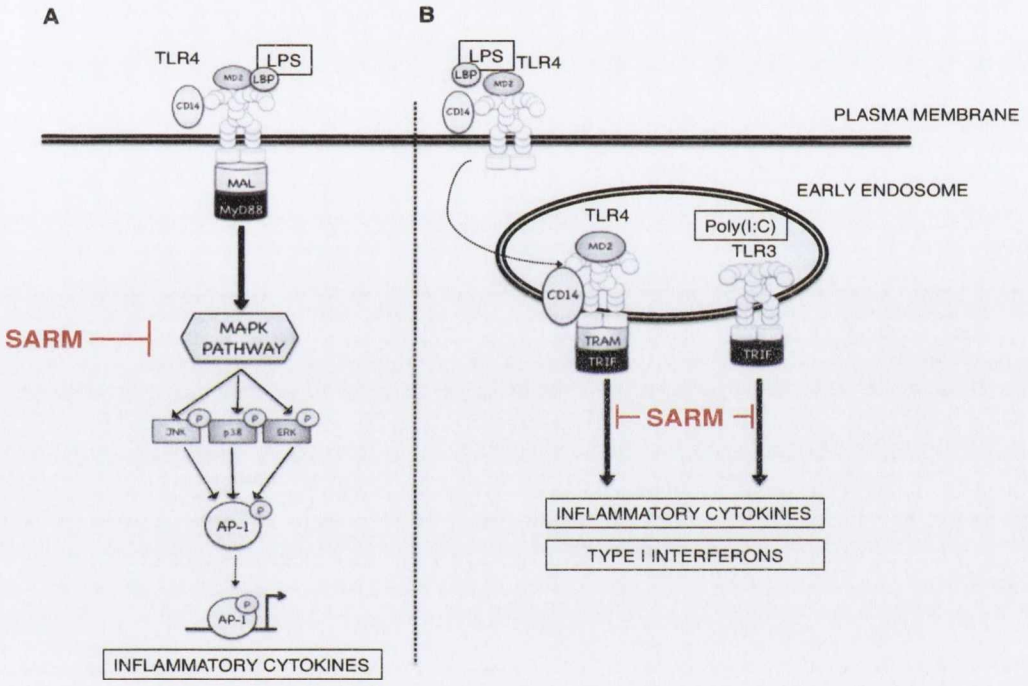

Figure 1.5 Role of SARM as negative modulator of TLR signalling

The TLR adaptor SARM negatively regulates TRIF- and MyD88-dependent signalling pathways. **A**, SARM mediates inhibition of MyD88-dependent signalling acting as an inhibitor of MAPK phosphorylation. **B**, SARM negatively regulates TRIF-dependent signalling triggered by TLR4 and TLR3 via direct interaction with TRIF.

1.4 Accessory molecules in TLR signalling

Mechanisms of microbial recognition, signalling and regulation of TLR responses require a number of specific accessory molecules. These molecules cooperate with TLRs ensuring proper detection of PAMPs/DAMPs, control of TLR folding in the ER and regulating of intracellular localisation and trafficking of TLRs. Similar to differentially localised TLRs, accessory proteins function at the level of the cell surface and from within intracellular compartments. Additionally, they can be involved in the regulation of TLRs via direct interaction with the receptor and/or its specific ligand (Lee et al, 2012). A wide spectrum of accessory molecules involved in modulation of TLRs is shown in Figure 1.6.

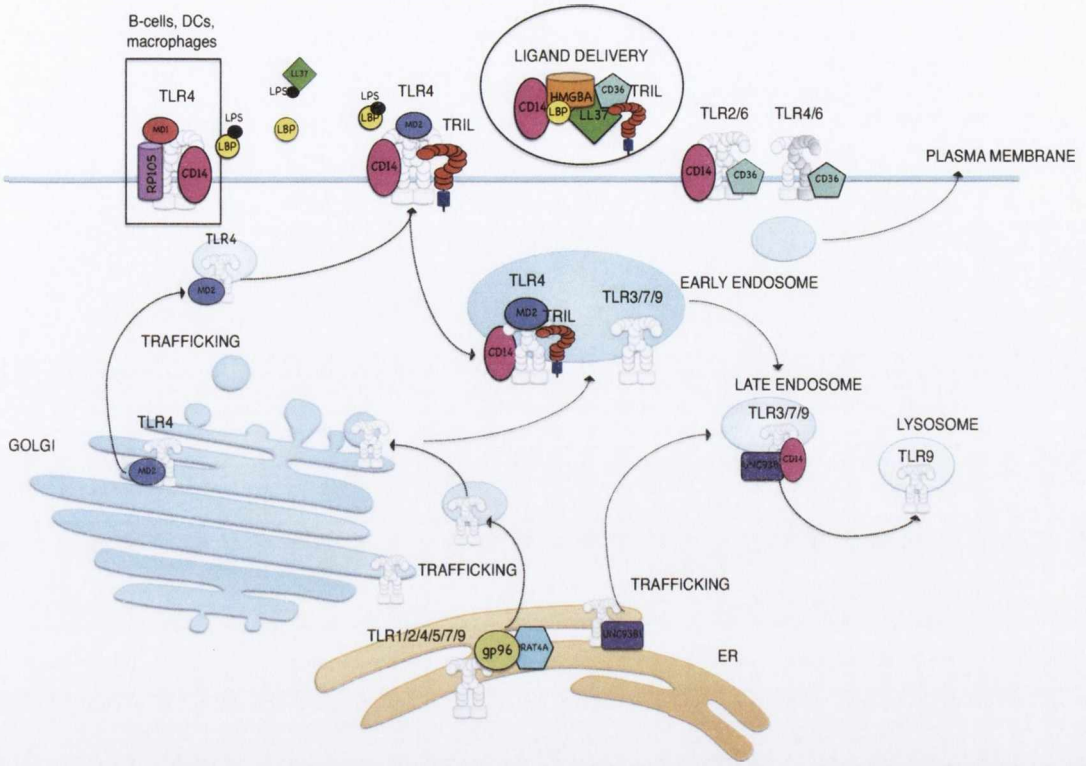

Figure 1.6 Accessory molecules involved in the regulation of TLRs signalling

Accessory proteins are essential components of the TLRs signalling network. They execute numerous functions and are involved in many aspects of TLR responses. MD2 regulates LPS recognition and the cell surface expression of TLR4. CD14 is implicated in ligand recognition and binding as well as trafficking of multiple TLRs, such as TLR2, TLR3, TLR4, TLR7 and TLR8. A novel accessory molecule TRIL has been shown to modulate TLR4 mediated response and it is also capable of binding TLR4 and its ligand LPS. Expressed in B cells RP105 and MD-1 act as positive regulators of TLR2 and TLR4 signalling. Simultaneously, RP105 found in dendritic cells and macrophages negatively modulates TLR4 responses. Accessory molecules gp96 and PRAT4A chaperon a number of cell surface and intracellular TLRs, including TLR1, TLR2, TLR4, TLR5, TLR7 and TLR9. Residing in the endoplasmic reticulum (ER), UNC93B function as a central regulator of the endosomal trafficking of the intracellular TLRs and has been shown to directly interact with TLR3, TLR7 and TLR9 as well as human TLR8. Finally, a group of accessory molecules comprising of CD14, HMGB1, CD36, LBP and LL37 are capable of direct binding and delivering TLR ligands to respective TLRs or to the endosomal compartments.

1.4.1 Accessory molecules acting at the cell surface

1.4.1.1 MD-2

Myeloid differentiation factor 2 (MD2 also known as LY96) is a small soluble glycoprotein associated with the extracellular domain of TLR4 and is critical for LPS recognition and subsequent signalling via TLR4 (Shimazu et al, 1999). MD2 deficient mice are incapable of sensing LPS, hence are resistant to LPS induced endotoxic shock but are concurrently more susceptible to *Salmonella typhimurium* (Nagai et al, 2005). Structural analysis of TLR4-MD2, revealed that upon binding LPS, two complexes of TLR4-MD2 dimerise crafting a multiprotein, symmetrical TLR4–MD2–LPS structure (Kim et al, 2007a; Ohto et al, 2007; Park et al, 2009). Apart from its role in ligand binding and TLR4 signalling, MD2 also regulates the trafficking and cell surface expression of this receptor. Confocal imaging revealed that complexes consisting of two TLR4-MD2-CD14 heterotrimers, continuously cycle between the plasma membrane and the Golgi (Latz et al, 2002) as also does the LPS (Thieblemont & Wright, 1999). Once it encounters LPS at the cell surface, TLR4-MD2 complex dimerises and initiates MyD88-dependent pathway followed by endosomal translocation and activation of TRIF-mediated signalling (McGettrick & O'Neill, 2010; Saitoh, 2009).

1.4.1.2 RP105

RP105 (also known as CD180) is a type I transmembrane protein modulating TLR4 signalling (Divanovic et al, 2005a). RP105 contains 22 LRRs in its extracellular domain and is expressed on the cell surface of B cells, dendritic cells (DCs) and macrophages. Cell surface expression of RP105 requires its association with MD1, a homologue of MD2 accessory molecule, and as a dimer RP105-MD1 directly binds to TLR4-MD2 (Divanovic et al, 2005a). RP105 functions in a cell type specific manner, acting as a positive regulator of TLR2 and TLR4 signalling in B cells (Nagai et al, 2002b) and as a negative modulator of TLR4 in DCs and macrophages (Divanovic et al, 2005a). A number of published studies link RP105 with systemic lupus erythematosus (SLE), where the RP105 deficient B cells demonstrated increased production of autoantibodies leading to SLE (Koarada et al, 2005; Koarada & Tada, 2012).

1.4.2 Intracellularly localised accessory molecules

1.4.2.1 UNC93B1

Uncoordinated 93 homolog B (UNC93B) is a multi membrane-spanning glycoprotein residing in the ER, which acts as a central regulator of intracellular TLRs (Tabeta et al, 2006). UNC93B knockout mice (also known as 'triple D' or 3d) carrying a missense allele of UNC93B showed impaired signalling via endosomal TLR3, TLR7 and TLR9 and not other TLRs (Tabeta et al, 2006). Moreover, UNC93B has been reported to directly interact with TLR3, TLR7 and TLR9 as well as human TLR8, through their transmembrane domains and this interaction was found critical for signalling mediated by these TLRs (Brinkmann et al, 2007; Itoh et al, 2011). Further studies on 3d knockouts by Kim *et al.* revealed another function of UNC93B, which has been shown to deliver nucleotide sensing TLR7 and TLR9 from the ER to the endolysosome, where they respond to their ligands (Kim et al, 2008). In addition, UNC93B fullfill the same role in the regulation of murine TLR11, TLR12 and TLR13 (Lee et al, 2013). UNC93B differentially associates with TLR9 and TLR7 in dendritic cells and was reported to be biased towards TLR9 sensing DNA (Fukui et al, 2009). This was also linked with the UNC93B regulation of excessive TLR7 activation by employing TLR9 to compete with TLR7 (Fukui et al, 2011b). UNC93B plays a central role in the regulation of endosomal TLR trafficking and 3d mutant mice have been shown to be highly susceptible to a number of pathogens including *Listeria monocytogenes*, *Staphylococcus aureus* and mouse cytomegalovirus (Tabeta et al, 2006). UNC93B deficiency has also been associated with the etiology of HSV-1 encephalitis in humans (Casrouge et al, 2006). Recent data demonstrating the involvement of both TLR7 and TLR9 in autoimmune diseases, such as SLE, points also towards the potential role of UNC93B in the pathogenicity of this disorder (Deane et al, 2007; Fukui et al, 2011a).

1.4.2.2 gp96

Glucose-regulated protein of 94 kDa (GRP94, also known as gp96 or endoplasmin) is an endoplasmic reticulum paralogue of the chaperone heat-shock protein 90 (HSP90), which mediates protein folding. gp96 is constitutively expressed in

various cell types, and can be found exclusively within the lumen of the ER and not the ER membrane fraction (Koch et al, 1988). gp96 chaperones a number of cell surface and intracellular TLRs, with the exception of TLR3. It is essential for the function of TLR1, TLR2, TLR4, TLR5, TLR7 and TLR9 and can directly interact with TLR1, TLR2, TLR4 and TLR9 through their ectodomains. In addition, gp96 was shown to regulate cell surface expression of TLR1, 2 and 4 as well as maturation and enzymatic processing of TLR9 (Liu & Li, 2008; Randow & Seed, 2001; Staron et al, 2011). Recent data demonstrated that the chaperone function of gp96 depends on another ER luminal protein, CNPY3 (also known as PRAT4A), which directly binds to gp96. Disruption of this interaction completely abolished the function of gp96 as a TLR chaperone (Liu et al, 2010a). Thus, gp96 ensures proper folding and maturation of TLRs in the ER. gp96 was also shown to promote infection by serving as a receptor for cell invasion of various pathogens, such as *Listeria monocytogenes* (Cabanes et al, 2005) and VSV (Bloor et al, 2010).

1.4.2.3 PRAT4A

PRAT4A was initially identified as a protein that directly binds to TLR4 and regulates its cell surface expression (Wakabayashi et al, 2006). PRAT4A is a highly conserved soluble protein residing in the lumen of the ER. It has been implicated in regulation of both cell surface and endosomally localised TLRs (Takahashi et al, 2007). PRAT4 regulates cell surface expression and trafficking of TLR1, TLR2 and TLR4, which in the absence of PRAT4 demonstrated significantly reduced cytokine production (Takahashi et al, 2007). Additionally, PRAT4A has been also implicated in the regulation of TLR5 cell surface expression in neutrophils, monocytes and DCs (Shibata et al, 2012). Mice lacking PRAT4A have shown impaired responses of multiple TLRs, with the exception of TLR3 (Takahashi et al, 2007). TLR9 mediated signalling was completely abolished in PRAT4A deficient BMDCs and macrophages. Residing in the ER in resting cells TLR9 was unable to traffic from the ER to endolysosomes following stimulation in the absence of PRAT4A (Takahashi et al, 2007). Thus, PRAT4A is indispensable for ligand-induced translocation of TLR9 from the ER to lysosomal compartments.

Additionally, similar to UNC93B, PRAT4A is crucial for enzymatic processing of TLR9 (Onji et al, 2013; Takahashi et al, 2007). PRAT4A has also been shown to directly interact with TLR9 as well as the other ER-residing accessory molecule, gp96, which is also capable of binding to TLR9 (Liu et al, 2010a). Knockdown of either PRAT4A or gp96 expression impaired their ability to associate with TLR9, indicating strong dependency of those two accessory molecules (Liu et al, 2010a).

1.4.3 Ligand binding accessory molecules

1.4.3.1 LBP

LPS-binding protein (LBP) is an acute phase protein synthesized in the liver and lung (Schumann et al, 1990). LBP is responsible for high affinity binding of LPS, which leads to its disaggregation and presentation to CD14, and subsequent delivery to the TLR4-MD2 signalling complex (Wright et al, 1990). LBP is also capable of binding other TLR ligands, such as lipoteichoic acid, peptidoglycan and lipopeptides (Schroder et al, 2004; Schroder et al, 2003). This suggests that LBP mediates not only the function of TLR4 but also TLR1, TLR2 and TLR6. Studies have shown that mice lacking LBP are more susceptible to infections with Gram-negative bacteria and the Gram-positive pneumococci strains, thus LBP plays a role in both Gram-positive and Gram-negative bacterial infections (Jack et al, 1997; Weber et al, 2003).

1.4.3.2 CD14

Cluster of differentiation 14 (CD14) is a LRR containing glycoprotein present in soluble form in the serum or as a GPI anchored cell surface protein in myeloid cells (Wright et al, 1990). CD14 was shown to interact with a variety of PAMPs and their synthetic analogues, including LPS, PGN, Pam3CSK4, Poly(I:C) and CpG DNA (Baumann et al, 2010; Dziarski et al, 1998; Dziarski et al, 2000; Lee et al, 2006). Structural analysis of CD14 revealed that its horseshoe-like homodimeric structure, common to both human and mouse CD14, is highly similar to that found in the ectodomains of TLRs (Kim et al, 2005). CD14 has been implicated in the regulation of multiple TLRs. CD14 is required for TLR4 signalling, where it binds to LPS and facilitates its translocation to

the TLR4-MD2 complex. Interestingly, CD14 was shown to be indispensable for the detection of smooth LPS, rather than its rough form or the lipid-A motif. In the absence of CD14 only MyD88-dependent signalling was activated following smooth and rough LPS stimulation, while its presence led to signal transduction via both MyD88- and TRIF-dependent TLR4 signalling (Jiang et al, 2005; Zanoni et al, 2012; Zanoni et al, 2011). Recent studies have demonstrated that CD14 also plays a role in LPS induced endocytosis and trafficking of TLR4, thus specifically regulating TRIF-dependent IFN production (Zanoni et al, 2012). Zanoni *et al.* examined CD14 deficient cells, which demonstrated significantly reduced TRIF-dependent IFN production, but not MyD88-mediated TNFα production. CD14 is a key component of TLR4 signalling, implicated in ligand delivery, recognition and binding, as well as trafficking of this receptor (Zanoni et al, 2011).

CD14 also plays a role in the function of other cell surface TLRs, including TLR2 and TLR6. Interacting with both TLR4 and TLR2, CD14 was shown to be important, but not essential, to TLR2/TLR6 signalling. CD14 knockout cells showed partially impaired sensing of all TLR2/TLR6 agonists (Hoebe et al, 2005). Interestingly, recent studies by Rabin *et al.* have demonstrated that CD14 positively impacts on TLR2-mediated response. CD14 is capable of binding to TLR2-derived peptides, which accelerates microbial ligand transfer from CD14 to TLR2 leading to enhanced TLR2 response, through increased and sustained ligand occupancy of TLR2 and receptor clustering (Raby et al, 2013).

CD14 also participates in responses mediated by intracellular TLRs. It was shown to bind directly to dsRNA and interact with endosomally localised TLR3, TLR7 and TLR9. Although the presence of CD14 enhances responses to these TLRs, its absence does not completely abolish Poly(I:C), imiquimod and CpG DNA mediated signalling, suggesting involvement of additional accessory molecules (Baumann et al, 2010; Lee et al, 2006). In addition, CD14 mediates sensing of various pathogens, mostly viruses, such as RSV, VSV, influenza virus and human cytomegalovirus (HCMV) (Compton et al, 2003; Georgel et al, 2007; Kurt-Jones et al, 2000).

1.4.3.3 CD36

CD36 is a double-spanning plasma membrane glycoprotein classified as a class B scavenger receptor family member (Calvo et al, 1995; Hoebe et al, 2005). CD36 was initially characterised as an accessory molecule implicated in enhancing TLR2/TLR6-mediated responses to LTA, MALP2 and diacylated lipopeptide. Deficiency of CD36 led to increased susceptibility to infection by the Gram-positive bacteria *Staphylococcus aureus* (Hoebe et al, 2005; Stewart et al, 2010).

CD36 associates with the heterodimer TLR2-TLR6 exclusively upon ligand stimulation. Following activation the TLR2/TLR6 complex aggregates within lipid rafts at the plasma membrane, where it associates with CD36 and then translocates to the Golgi apparatus (Triantafilou et al, 2006). Importantly, CD36 has been also linked with the immune response to oxidized low-density lipoprotein (oxLDL) and amyloid-β fibrils, via CD36-TLR4-TLR6 complex formation (Stewart et al, 2010). In recent studies Sheedy *et al.* demonstrated that CD36 coordinates conversion of soluble oxLDL and amyloid-β into crystals or fibrils, which subsequently leads to lysosomal disruption and NLRP3 inflammasome activation (Sheedy et al, 2013). This points towards a key regulatory role of CD36 and its potential as a therapeutic target in three major diseases namely atherosclerosis, Alzheimer's disease, and type 2 diabetes.

1.4.3.4 HMGB1

High-mobility group box (HMGB) proteins 1, 2 and 3 are nuclear proteins acting as universal sensors for nucleic acids. All three HMGB family members are capable of direct interaction with DNA and/or RNA and induction of type I IFN and proinflammatory cytokine production (Tian et al, 2007; Yanai et al, 2009). HMGB1 is the best characterised member of HMGB family and it has been shown to interact with TLR2 and TLR4, as well as receptor for advanced glycation endproducts (RAGE). The association of HMGB1 and TLR4 enhances the formation of neutrophil extracellular traps (NETs) (Tadie et al, 2012) as well as the production of TNFα in macrophages (Yang et al, 2010a). HMGB1 associates with both TLR9 and its ligand CpG DNA and mediates endosomal TLR9 trafficking. Absence of HMGB1 leads to impaired expression

of type I IFNs and proinflammatory cytokine production in response to CpG DNA. Thus, HMGB1 is required for TLR9 mediated responses to CpG DNA (Ivanov et al, 2007; Tian et al, 2007).

1.4.3.5 LL37

Endogenous antimicrobial peptide LL37 acts as a TLR9 accessory molecule, involved in binding and delivery of self-DNA to TLR9 in plasmacytoid dendritic cells (pDCs) (Filewod et al, 2009; Ganguly et al, 2009; Gilliet & Lande, 2008; Lande et al, 2007). In pDCs, LL37-DNA complexes are internalised and directed to the early endosomes where they regulate TLR9 dependent IFNα production. Enhanced expression of LL37 has been linked with the autoimmune skin disease termed psoriasis, where self-DNA coupled with LL37 activates pDCs (Filewod et al, 2009; Ganguly et al, 2009; Gilliet & Lande, 2008; Lande et al, 2007). LL37 has also been reported to associate with LPS and prevent LPS induced TNFα production (Brown et al, 2011), and with single stranded RNA (ssRNA) to boost signalling by TLR7 and TLR8 (Filewod et al, 2009; Ganguly et al, 2009; Gilliet & Lande, 2008; Lande et al, 2007). Interestingly, a recent study by Lai *et al.* demonstrated that LL37 functions as a positive regulator of the TLR3 signalling pathway in response to viral dsRNA. Thus, LL37 acts as an accessory molecule involved in binding and delivery of self-nucleic acids to endosomal TLRs (Lai et al, 2011).

1.4.4 TLR4 interactor with leucine rich repeats (TRIL)

The accessory molecule of particular interest in this project is TLR4 interactor with leucine rich repeats (TRIL). TRIL was initially identified in a search for novel LPS inducible genes in cells derived from wild-type and Mal deficient mice. TRIL is highly conserved and its homologues have been identified across many species including human, mouse, cow, chicken, rat and most recently zebrafish (Carpenter et al, 2009; Pietretti et al, 2013).

TRIL is highly expressed in a number of tissues such as spinal cord, lung, kidney and ovary, with the most elevated level reported in the brain, particularly

hippocampus, cortex and cerebellum and brain specific cells, astrocytes (Carpenter et al, 2009). In addition, Carpenter *et al.* have demonstrated that the high expression of TRIL reported in the brain can be further enhanced following LPS stimulation both *in vitro* and *in vivo* (Carpenter et al, 2009).

Structurally, TRIL consists of an N-terminal LRR domain, type III fibronectin domain and a transmembrane region localised at the C-terminal site. Additionally, a 23 aa signal sequence common for proteins directed to the ER has been reported at the N-terminal site of TRIL (Walter & Johnson, 1994). The structure of TRIL is illustrated in Figure 1.7. The LRR domain of TRIL, consisting of 13 LRR motifs, is highly similar to the LRRs present in the other accessory molecule CD14, as well as those found within the TLR family members (Palaniyar et al, 2002). Similarly, the predicted horseshoe shape structure of the LRR domain of TRIL exhibits high structural resemblance to the LRR domain of CD14 and other LRR proteins, such as brain-enriched; the LRR and Ig domain containing Nogo interacting protein (LINGO), the fibronectin-leucine-rich transmemebrane (FLRT), and the Amphoterin-induced gene and ORF (AMIGO) family of proteins (Carpenter et al, 2009), all of which have been shown to play a role in the neuronal system, primarily in neurite outgrowth and cell differentiation.

Functionally, TRIL has been identified as a component of the TLR4 signalling complex. TRIL is capable of direct interaction with TLR4 and its ligand LPS. Moreover, TRIL was found to enhance TLR4 mediated responses following LPS stimulation. Human astrocytoma cells stably overexpressing TRIL demonstrate enhanced cytokine production in response to LPS, whereas siRNA silencing of TRIL attenuates LPS induced signalling and cytokine production in various cell types such as peripheral blood mononuclear cells (PBMCs) and primary murine mixed glial cells. Therefore, TRIL represents an additional accessory molecule in the TLR signalling network, acting as a positive regulator of TLR4 mediated responses (Carpenter et al, 2009).

An increasing amount of data reports involvement of TLR mediated responses in the pathogenesis of neurodegenerative diseases within the central nervous system (CNS), such as Alzheimer's disease (AD), Parkinson's disease (PD) and multiple sclerosis (MS). Notably, the expression of TRIL is enhanced in brain samples from patients with

Alzheimer's disease (Carpenter et al, 2009). Additionally, a recent study by Rabin *et al.* has demonstrated elevated levels of TRIL in the CNS of patients suffering from amyotrophic lateral sclerosis (ALS), a fatal neurodegenerative disease characterised by weakness resulting from loss of motor neurons (Carpenter et al, 2009; Rabin et al, 2010). It is therefore possible that TRIL plays a role in the pathogenesis of neurodegenerative disorders.

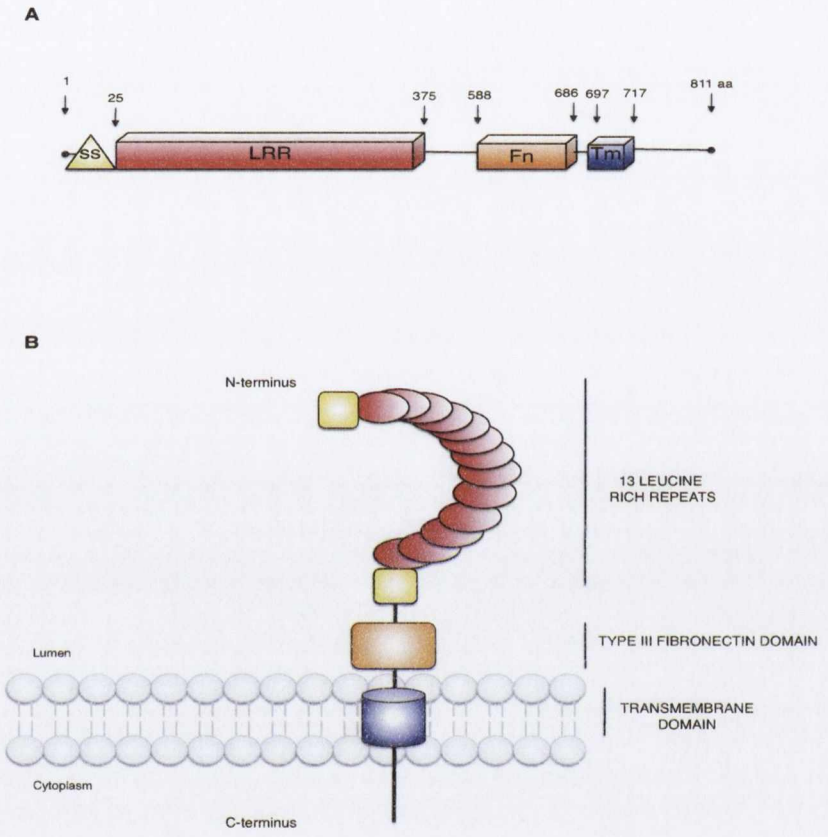

Figure 1.7 Domain structure and membrane topology of TRIL

Figure 1.7 represents domain structure and membrane topology of TRIL (**A** and **B**, respectively). **A**, The 811 amino acids protein consists of 13-leucine rich repeats (LRR) localised at the N-terminal end, followed by the type III fibronectin domain (Fn) and the transmembrane domain (Tm) present on its C-terminus. Additionally TRIL also contains a 23-aa signal sequence (ss) present on the N-terminal site. **B,** TRIL is a membrane bound protein. Present at the N-terminal site of TRIL 13 LRRs form the horseshoe-like shape with the N- and C-terminal capping structures (indicated by the yellow cubes). Most of the protein is localised in the lumen of some sort of intracellular organelle, while the short tail region is found in the cytoplasm.

1.5 TLRs and the central nervous system (CNS)

TRIL, which is the main focus of this project, has been identified as a brain enriched-protein implicated in the regulation of TLR4 signalling. I will now describe in more detail the expression pattern and function of TLRs within the CNS.

CNS inflammation largely depends on the brain resident cells, microglia and astrocytes constitutively expressing various PRRs, most predominantly TLRs. An active role of glial cells in the immune response is associated with both beneficial and detrimental effects. Acute inflammation of the brain is largely advantageous as it results in pathogen clearance and infection resolution. However, excessive or prolonged inflammation can lead to deleterious neurodegeneration.

1.5.1 Expression of TLRs in brain

TLRs are widely expressed in a number of tissues, including the brain. Highly vascularised sites of the brain, such as meninges, choroid plexus and circumventricular organs (CVOs) have been characterised as the main sites of TLR expression within the brain. The expression of TLRs was also reported in microglia and astrocytes, as well as neurons comprising the resident cells of the brain parenchyma (Kielian, 2009). Figure 1.8 represents the repertoire of TLRs expressed within glial cells and neurons.

1.5.1.1 Microglia

Microglia, similar to macrophages and dendritic cells, originate from the myeloid lineage and therefore are often referred to as 'resident macrophages' of the brain, acting as principle immune effector cells. Like other macrophage-like cells, microglia express a wide repertoire of PRRs, including all known TLR family members. Microglia constitutively express TLRs 1-9, with TLR3 and TLR4 at significantly higher levels, and TLR2 being the most highly expressed among all TLRs (Bsibsi et al, 2002; Laflamme et al, 2003; Zekki et al, 2002).

1.5.1.2 Astrocytes

Astrocytes are also major contributors to brain inflammation. Neuroectodermal-derived astrocytes constitutively express TLRs 1-5 and TLR9 (Bsibsi et al, 2006; Bsibsi et al, 2002; Carpentier et al, 2005; Jack et al, 2005), with particularly high levels of TLR3 in both human and mice (Carpentier et al, 2005; Farina et al, 2007; Jack et al, 2005). Moreover, high basal expression of TLR3 can be further enhanced following Poly(I:C) and LPS ligand stimulation as well as viral infection (Carpentier et al, 2005; Town et al, 2006). TLR3 is primarily directed to endosomal compartments, however in human astrocytes it was reported to be expressed both intracellularly and at the plasma membrane (Bsibsi et al, 2002; Jack et al, 2005). Apart from their role in inflammation, astrocytes provide nutrients for neuronal cells and mediate processes like formation of the blood brain barrier (BBB), tissue damage and neurotoxicity (Farina et al, 2007).

1.5.1.3 Oligodendrocytes and neurons

Increasing evidence indicates that neurons and oligodendrocytes also express TLRs (Hoffmann et al, 2007; Lehnardt, 2010; Lehnardt et al, 2003; Trudler et al, 2010). Oligodendrocytes express restricted number of TLRs and thus far have been reported to express TLR2, TLR3 and TLR4, which have been implicated in the regulation of repair and remyelination, following injury within the CNS (Kigerl et al, 2007).

In contrast neurons have been found to express a broader spectrum of TLRs, including all of the intracellular TLRs, TLR3, TLR7, TLR8 and TLR9, as well as extracellularly localised TLR2 and TLR4 (Kim et al, 2007b; Lehmann et al, 2012; Ma et al, 2007; Ma et al, 2006; Trudler et al, 2010; van Noort & Bsibsi, 2009). The main function of these receptors, apart from mediating the innate immune responses, appears to be the control of cellular migration and differentiation as well as processes of tissue development and repair (Trudler et al, 2010; van Noort & Bsibsi, 2009)

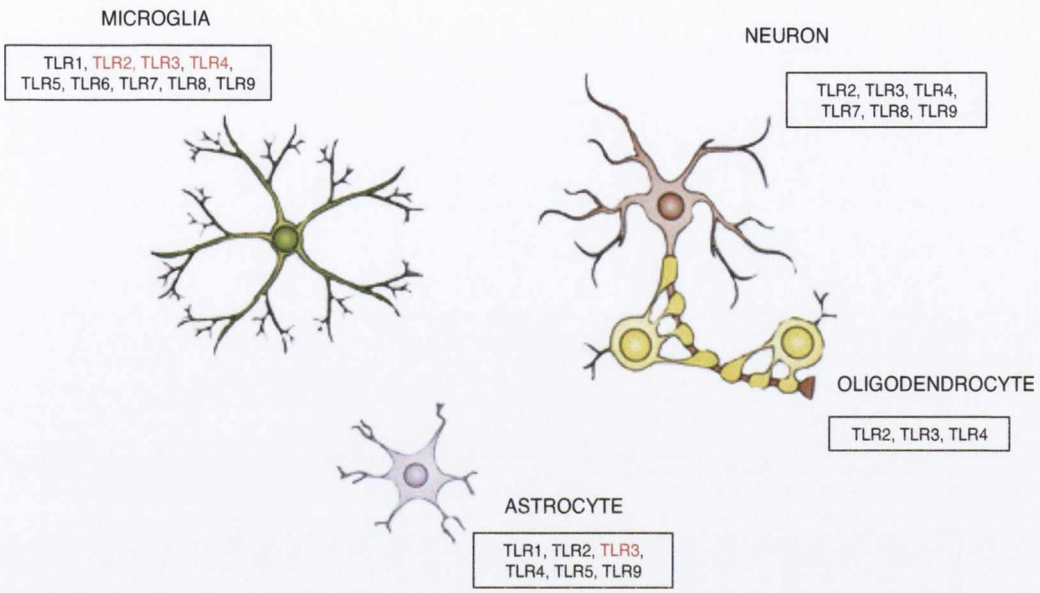

Figure 1.8 Expression patterns of TLRs in CNS cells

Microglia express a whole repertoire of TLRs, with high expression levels of TLR2-4 (marked in red). Astrocytes express TLRs 1-5, most prominently TLR3 (marked in red). Oligodendrocytes and neurons also express TLRs, oligodendrocytes were found to express TLR2, TLR3 and TLR4, while neurons express all of the intracellular TLRs (TLR7-9 and TLR3) and the membrane bound TLR2 and TLR4.

1.5.2 Function of TLRs in infection of the CNS

CNS infections can be divided into three main types based on the site where the infection occurs. These are meningitis, which affects the membranes surrounding the brain, encephalitis associated with the inflammation within the brain parenchyma and myelitis, which occurs in the spinal cord. Meningitis and encephalitis are the most common types of CNS infection, triggered primarily by bacterial and viral infections and mediated largely by TLRs governing production of proinflammatory mediators and type I IFNs, which have been associated with either beneficial or detrimental effects.

1.5.2.1 TLR function in bacterial CNS infection

A number of TLRs have been implicated in mediating the immune response to bacterial infections in glial cells. TLR2 and TLR4 are the main TLRs responsible for triggering the anti-bacterial immune response in the brain. Stimulation of microglia with LPS leads to production of proinflammatory cytokines mediated by TLR4 (Qin et al, 2005). Similarly, stimulation of glial cells with TLR2 ligands, bacterial PGN and LTA triggers their activation (Kielian et al, 2005b; Olson & Miller, 2004; Phulwani et al, 2008). Astrocytes expressing TLR2 are capable of sensing both PGN and as well as an intact *Staphylococcus aureus*, in contrast to microglia where the *S. aureus* response was found to be largely TLR2 independent (Esen et al, 2004; Kielian et al, 2005b). Combined action of multiple TLRs, including TLR2 and TLR4, was found to be essential for initiating the microglial immune response to a number of bacterial strains such as *Neisseria meningitides*, *Streptococcus pneumonia,* and *Lysteria monocytogenes*. Additionally, TLR9 expressed in microglial cells is capable of sensing bacterial DNA derived from live *S.pnaumoniae and N.meningiditis* and contributing to TLR2 and TLR4 dependent responses to these pathogens ((Carpentier et al, 2008; Hanke & Kielian, 2011; Koedel et al, 2003; Mogensen et al, 2006).

Interestingly TLR2 mediated immune responses to *Streptoccocus sp*. were found to be both beneficial and toxic to the cells of the CNS (Hoffmann et al, 2007; Lehnardt et al, 2006). Similarly, a direct injection of TLR2 agonist Pam3CSK4 into the CNS can lead to TLR2 dependent neurodegeneration (Hoffmann et al, 2007). TLR4-mediated signalling triggered by LPS has also been implicated in microglial activation leading to favourable pathogen elimination, as well as neuronal injury and oligodendrocyte death and demyelination (Lehnardt et al, 2003).

1.5.2.2 TLR function in viral CNS infection

TLR activation is also correlated with neurotropic viral infections, where TLRs were shown to mediate both protective and destructive innate immune reponse against CNS viruses. TLR3 is constitutively expressed in glial cells, most predominantly in astrocytes and microglia (Bsibsi et al, 2002; Carpentier et al, 2005; Farina et al, 2005;

Scumpia et al, 2005). Microglial cells expressing high levels of TLR3 are capable of responding to the TLR3 ligand Poly(I:C), and sensing of Theiler's murine encephalomyelitis virus (TMEV). TLR3 mediated activation of microglia leads to IFNβ, IL1β and IL6 production (Bsibsi et al, 2002; Kielian et al, 2005a; Olson & Miller, 2004). Similarly, astrocytes expressing substantial levels of TLR3 produce proinflammatory cytokines, when stimulated with Poly(I:C) (Bsibsi et al, 2002; Farina et al, 2005). TLR3 acts primarily as a sensor of viral dsRNA, however it has been also implicated in sensing of ssRNA and DNA neurotropic viruses, such as WNV, VSV and HSV-1, though an intermediate form of dsRNA generated during viral replication of ssRNA viruses and during the transcription of DNA viruses (Kawai & Akira, 2007; Wang et al, 2004). Most recent studies by Tatematsu *et al.* demonstrated that TLR3 acts also as a sensor of incomplete stem structures in viral RNA derived from poliovirus (Tatematsu et al, 2013).

TLR3 has been shown to provide a protective immunity to poliovirus, where following viral infection actived TLR3-TRIF signalling pathway limits viral replication in a number of organs, including brain and spinal cord (Oshiumi et al, 2011).

A study by Wang *et al.* reported a key role for TLR3 in the neurotropic ssRNA WNV infection in the brain (Wang et al, 2004). TLR3 was shown to contribute to viral lethality by enhancing peripheral cytokine production, leading to the BBB disruption and viral dissemination throughout the brain (Wang et al, 2004; Wilson et al, 2008). Thus, TLR3 deficient mice were more resistant to WNV infection compared to WT animals (Wang et al, 2004; Wilson et al, 2008). In subsequent studies however, TLR3 was demonstrated to have an opposite effect, contributing to protection against lethal WNV infection (Daffis et al, 2008). The exact role of TLR3 in WNV infection is therefore yet to be clarified. As previously mentioned, the TIR domain-containing adaptor SARM has been found to play a role in the lethal WNV infection. SARM is preferentially expressed in CNS resident cells, most prominently in neurons (Carty et al, 2006; Peng et al, 2010). *In vivo* studies on SARM deficient mice demonstrated increased viral replication and higher mortality following WNV infection when compared to WT mice (Szretter et al, 2009). Additionally, lack of SARM resulted in decreased TNFα

expression. Thus SARM was suggested to play a protective role in WNV infection and neuronal injury in brain. Interestingy, recent studies by Hou *et al.* revealed that SARM also plays a positive role in the antiviral response to neurotropic VSV infection, where SARM deficient mice demonstrated reduced CNS injury and cytokine production within the brain (Hou et al, 2013).

Expressed within microglia and astrocytes TLR2 also plays a role in the antiviral response within the brain. TLR2 deficient mice were found to be protected from lethal encephalitis mediated by the HSV-1 (Kurt-Jones et al, 2004). Following intracranial injection with HSV-1, TLR2 deficient mice demonstrated decreased inflammatory response within the brain, leading to an increase in the overall survival (Kurt-Jones et al, 2004). Similar to TLR2, TLR9 is also implicated in the immune response to HSV-1 infection of the brain. In fact both TLR2 and TLR9 were found to act synergistically during the HSV-1 encephalitis. Double TLR2/TLR9 knockout mice displayed significantly increased susceptibility to HSV-1 encephalitis compared to mice deficient in either TLR2 or TLR9 alone (Lima et al, 2010). Interestingly, genetic studies in children carrying an autosomal dominant mutation of TLR3 uncovered a protective role for TLR3 in HSV-1 encephalitis (Guo et al, 2011; Zhang et al, 2007).

1.5.2.3 TLRs in neuronal injury

TLR activation in the CNS has been associated with both positive and negative effects on the brain. TLRs mediate pathogens clearance and infection resolution, but can also cause irreversible neuronal damage. Stimulation with LPS both *in vitro* and *in vivo* leads to neuronal damage mediated primarily by TLR4 expressed in microglia (Lehnardt, 2010; Lehnardt et al, 2003). Similarly, TLR2 mediated immune responses to Streptoccocus sp. were found to be both beneficial and toxic to the cells of the CNS (Hoffmann et al, 2007; Lehnardt et al, 2006).

Ischaemic brain injury results from a loss in blood supply to a specific region of the brain that follows a stroke. Recent data established a role for TLRs in brain inflammation following stroke. While TLR activation after ischemia leads to tissue damage and neuronal death, their induction prior to stroke was associated with

neuroprotection (Abe et al, 2010). Many studies have reported important roles for TLR2 and TLR4 prior to and post the ischeamic brain injury. *In vivo* studies on TLR4 deficient mice revealed decreased infarct size, as well as lower expression of matrix metaloproteinase 9 (MMP9) and other proteins associated with brain damage following stroke in these animals (Qiu et al, 2010).

1.5.2.4 Role of TLRs in neurodegenerative diseases

A number of studies have revealed a functional implication of TLRs and also TLR accessory proteins such as CD14 and MD2 in the pathogenesis of neurodegenerative disorders such as Alzheimer's disease, Parkinson's disease and amyotropic lateral sclerosis.

1.5.2.4.1 TLRs in Alzheimer's disease

AD is a progressive neurodegenerative disease of which the etiology, despite intensive research remains unknown. The pathological signs of AD comprise of extracellular senile plaques and intracellular neurofibrillary tangles (NFTs), both resulting from the accumulation of β amyloid (Aβ). Both of them are also considered as activators of potentially pathological immune responses mediated by TLRs expressed primarily in microglia. Fibrillar Aβ directly induces microglial activation via TLR2, TLR4 and the accessory molecule CD14. Increased expression of TLR2, TLR4 and CD14 has also been demonstrated in the brain of AD patients (Fassbender et al, 2004; Liu et al, 2005). Additionally, the injection of Aβ into the hippocampus triggers an increase in TLR2 expression (Richard et al, 2008). The loss of function mutation in TLR4 was shown to inhibit the Aβ mediated activation of microglia, resulting in lower production of proinflammatory cytokines IL6 and TNFα (Walter et al, 2007). Additionally, the presence of the TLR4 accessory proteins MD2 and CD14, proved essential for sensing Aβ by microglia (Walter et al, 2007). Recent studies by Reed-Geaghan *et al.* also demonstrated a direct interaction between CD14 and the fibrillar form of Aβ, thus emphasizing even further the importance of this co-receptor in the TLR4 mediated response to Aβ (Reed-Geaghan et al, 2009). It is becoming clear that TLRs play an

important role in the pathogenesis of AD, nevertheless their exact role in this disease has yet to be clarified.

1.5.2.4.2 TLRs in Parkinson's disease

PD is a neurodegenerative disorder characterised by intracellular inclusions called Lewy bodies, comprised of the aggregated α-synuclein (α-syn)(Spillantini et al, 1998). α-syn, similarly to Aβ triggers activation of microglia through TLRs leading to increased proinflammatory cytokine production (Beraud et al, 2011). *In vivo* studies have revealed enhanced expression of TLR4 and CD14 in the animal model of PD (Panaro et al, 2008). Additionally, increased expression of TLR4 has been reported in the brains of patients suffering from a PD like neurodegenerative disease multiple system atrophy (MSA), characterised by oligodendrocytic accumulation of α-syn (Stefanova et al, 2007). Interestingly, recent studies by Kim *et al.* demonstrated that the extracellular oligomeric α-syn released from neuronal cells acts as an endogenous agonist of TLR2, triggering activation of microglia cells (Kim et al, 2013). Therefore similar to TLR4, TLR2 may also play a role in the pathogenesis of PD.

1.5.2.4.3 ALS and TLRs

ALS also known Lou Gehrig's disease leads to selective loss of motor neurons (Lomen-Hoerth, 2008). Recent studies have demonstrated increased expression of TLR2, TLR4 and RAGE in the spinal cord of sporadic ALS patients (Casula et al, 2011). TLR2 was predominantly detected in microglia, whereas the TLR4 and RAGE were strongly expressed in astrocytes (Casula et al, 2011). Activation of TLR2 and TLR4 may contribute to the progression of inflammation, resulting in motor neuron injury, however further studies are needed to evaluate the exact role of these receptors in the pathogenesis of ALS.

1.6 Project aims and objectives

TRIL is a novel LRR domain containing protein involved in the regulation of TLR4 mediated signalling. TRIL, which is highly expressed in the brain has been reported to enhance TLR4 responses via direct interaction with the receptor and its ligand LPS (Carpenter et al, 2009). Although TRIL has been characterised as a novel component and modulator of the TLR4 signalling complex, no further investigations were carried out into the function of TRIL in the regulation of other TLR signalling pathways. Additionally the role of TRIL in the *in vivo* setting has never been examined.

The main focus of this project is to further characterise TRIL, provide new insights into its function within the TLR signalling pathway, identify novel potential binding partners of TRIL and expand our understanding of TRIL's role in the TLR mediated response, particularly within the brain, using *in vivo* models of bacterial and viral infection. The specific aims are as follows:

1. Determine the exact location of TRIL within cellular compartments using different cell types
2. Identify novel binding partners of TRIL within the TLR family, and determine the functional outcome of the identified interactions
3. Examine the *in vivo* role of TRIL in TLR-mediated responses in bacterial and viral disease models
4. Provide new insights into the role of TRIL in the modulation of brain inflammation

Overall, I have uncovered a role for TRIL in TLR3 signalling and from *in vivo* studies revealed a role for TRIL in the regulation of the immune response to bacterial and viral infection in the brain.

CHAPTER TWO

Materials and Methods

2.1 Materials

Reagent	Source
Dulbecco's Modified Eagles Medium (DMEM)	Gibco® Biosciences
Roswell Park Memorial Institute (RPMI) medium	Gibco® Biosciences
Phosphate Buffered Saline (PBS)	Gibco® Biosciences
Trypsin-(Ethylenediaminetetraacetic acid) EDTA	Sigma®
α-thioglycerol	Sigma®
Trypan Blue	Sigma®
Fetal Calf Serum (FCS)	Biosera
Macrophage Colony-Stimulating Factor (MCSF)	obtained from L929 cells
Granulocyte-Macrophage Colony-Stimulating Factor (GM-CSF)	obtained from the J558 cells
Red Blood Cell Lysing buffer	Sigma®
Trypsin	Sigma®
Penicillin Streptomycin (PS)	Sigma®
Ciprofloxacin	Sigma®
G418	Sigma®
Puromycin	Sigma®

Table 2.1 Reagents used for tissue culture

Cell line	Description/Source
HEK-293T	Human embryonic kidney 293 cells European collection of animal cell cultures (ECACC)
U373	Human astrocytoma cell line European collection of animal cell cultures (ECACC)
U373 TRILV5	Human astrocytoma cell line stably overexpressing TRIL-V5 Generated in the lab by Dr. Susan Carpenter
THP-1	Human acute monocytic leukemia cell line European collection of animal cell cultures (ECACC)

Table 2.2 Cell lines

Name	Description	Source
LPS	Lipopolisacharide from *E.coli*, TLR4 ligand	Enzo Life Sciences
Poly(I:C)	Polyinosinic-polycytidylic acid (Poly(I:C)), synthetic analogue of double-stranded RNA (dsRNA), specific ligand for TLR3	InvivoGen
Pam3CSK4	Pam3Cys-Ser-(Lys)4, Hydrochloride, selective agonist of TLR2	InvivoGen
R848	Resiquimod 848, imidazoquinoline compound, ligand for TLR7/TLR8	InvivoGen
IL1β	Recombinant human IL1β	R&D Systems®
PMA	phorbol 12-myristate 13-acetate, used for monocytes differentiation (stock concentration 5 mg/ml)	Merck

Table 2.3 Ligands used for cell stimulation

Reagent	Source
Gene Juice®	Novagen
Lipofectamine™ 2000	Invitrogen
Opti-MEM® Reduced Serum Media	Life Technologies™

Table 2.4 Ligands used for cell tranfection

Name	Features	Source
pCMV6-AC-GFP TRIL-GFP	• TRIL in pCMV6-AC-GFP expressing vector • C-terminal GFP tag • ampicilin resistant	Origene Technologies®
pCMV6-AC-RFP TRIL-RFP	• TRIL in pCMV6-AC-RFP expressing vector • C-terminal RFP tag • ampicilin resistant	Origene Technologies®
pCMV6-AC-YFP TRIL-YFP	• TRIL in pCMV6-AC-GFP expressing vector • C-terminal YFP tag • ampicilin resistant	Origene Technologies®
pEGFP-N1 SARM-GFP	• SARM in pEGFP-N1 expressing vector • Under cytomegalovirus (CMV) promoter • N-terminal GFP tag • kanamycin resistant	Gift from Prof. A.Ding[1]
ER-CFP	• kanamycin resistant • KEDL motif of calreticulin (ER marker)	Clonetech
Golgi-CFP	• kanamycin resistant • β1,4- galactosyltransferase (Golgi marker)	Gift from Prof. H.Husebye[2]
EEA1-CFP	• kanamycin resistant • EEA1 (early endosome antigen 1)	Gift from Prof. H.Stanmark[2]
pcDNA 3.1	• ampicillin resistant	Strategene
pcDNA 3.1 TLR3-Flag	• TLR3 in pcDNA 3.1 expressing vector • under CMV promoter • ampicillin resistant	Gift from Prof. K.Fitzgerald[2]
pcDNA 3.1 TLR2-Flag	• TLR2, in pcDNA 3.1 expressing vector • under CMV promoter • ampicillin resistant	Gift from Prof. K.Fitzgerald[3]
pEF-Bos SARM-Flag	• SARM in expression vector pEF-Bos • C-terminal FLAG tag • ampicillin resistant	Gift from Dr. M.Carty[4]
pcDNA 3.1 TRIL-V5	• TRIL, in pcDNA 3.1 expressing vector • under CMV promoter • ampicillin resistant	Generated by Dr. S. Carpenter
pGL3-NF-κB luciferase	• Firefly luciferase reporter under NF-κB promoter • NF-κB-luciferase constructs contains 5κB sites upstream of the luciferase gene in the pGL3-NF-	Gift from Dr. R. Hofmeister[5]

[1] Department of Microbiology and Immunology, Weill Medical College of Cornell University, New York, NY 10021
[2] University of Massachusets Medical School, Worcester, MA, USA
[3] University of Massachusets Medical School, Worcester, MA, USA
[4] School of Biochemistry and Immunology, Trinity College, Dublin 2, Ireland
[5] Universitet Regensburg, Regensburg, Germany

	κB vector • ampicillin resistant	
pGL3-ISRE luciferase	• ISRE construct containing five repeats of the ISRE sequence from the ISG15 promoter in the pGL3-ISRE vector • ampicillin resistant	Clontech
pRL-TK-Renilla luciferase	• Renilla luciferase reporter in pRL-TK, • under HSV-TK promoter • ampicilin resistant	Promega
pMD2.G	• lentiviral packaging vector • ampicilin resistant	Gift from Prof. K Fitzgerald[4]
pCMV-dR8.74psPAX2	• lentiviral packaging vector • ampicilin resistant	Gift from Prof. K Fitzgerald[4]

Table 2.5 Expression vectors

Name	Source	Product code
Human pTRIPZ lentiviral inducible shRNAmir individual clone	Open Biosystems	V2THS_95531
Non-silencing TRIPZ Lentiviral shRNAmir Control	Open Biosystems	RHS4743
TRC mouse shRNA individual clone (pLKO.1 vector)	Open Biosystems	TRCN0000191275
TRC mouse shRNA individual clone 2 (pLKO.1 vector)	Open Biosystems	TRCN0000201250
pLKO.1 empty vector control	Open Biosystems	RHS4080
Doxycycline	Sigma®	-
Polybrene	Sigma®	-

Table 2.6 Lentiviral shRNA and control vectors and reagents

Reagent/Commercial kit	Source
DH5α™	Invitrogen™
EndoFree Plasmid Maxi Kit	Qiagen
Wizard® Plus SV Miniprep DNA Purification System Kit	Promega
RLT Buffer	Qiagen
Qiazol Buffer	Qiagen
RNeasy Mini Kit	Qiagen
High Capacity cDNA Reverse Transcription Kit	Applied Biosystems
iScript Select cDNA Synthesis Kit	Bio-Rad
TaqMan® Fast Universal PCR Master Mix (20x)	Applied Biosystems
iQ™ SYBR® Green Supermix	Bio-Rad
dNTP mix	Promega
DNA markers	New England Biolabs

Table 2.7 Reagents used for DNA and RNA purification

Reagent	Source
Protein A/G-plus agarose beads	Santa-Cruz Biotechnology®
Biotinylated Poly(I:C)	Invivogen
Phenylmethanesulfonyl fluoride (PMSF)	Sigma®
Sodium orthovanadate (Na_3VO_4),	Sigma®
Leupeptin	Sigma®

Aprotinin	Sigma®
20X LumiGLO® Reagent and 20X Peroxide Supersignal®	Cell Signaling Technology®
Coelentrazine	Calbiochem
Passive Lysis Buffer	Promega
Dithiothreitol (DTT)	Sigma®
N,N,N',N'-tetramethylethanediamine (TMED)	Sigma®
Amonium persulphate (APS)	Sigma®
30% Acrylamide/Bis-acrylamide solution	National Diagnostics
Pre-stained protein marker	New England Biolabs®
Polyvinylidene difloride (PVDF)	Millipore
Lumi-light western blotting substrate	Roche
Re-Blot Plus Solution	Millipore

Table 2.8 Reagents used for western blotting, co-immunoprecipitation and luciferase assays

Reagent	Source
Fibronectin	Sigma®
Poly-L-Lysine	Sigma®
Tx-100	Sigma®
Formaldehyde	Sigma®
ProLong® Gold Mounting Solution	Invitrogen
Fix&Perm® Cell Fixation and Permeabilization	AGD®
CellMask™ Plasmam Membrane Stain	Invitrogen
MitoTracker® Red CMXRos	Invitrogen
Hoechst	Sigma®
4',6-Diamidino-2-Phenylindole, Dihydrochloride DAPI	Invitrogen
Bovine Serum Albumin (BSA)	Sigma®

Table 2.9 Reagents used for confocal analysis

Name	Features	Source
Antibodies used for co-Immunoprecipitation and western blotting		
anti rabbit IgG	Rabbit polyclonal (whole molecule)	Jackson Immunoresearch
anti mouse IgG	Mouse polyclonal (whole molecule)	Jackson Immunoresearch
anti Flag	Mouse monoclonal anti-Flag antibody	Sigma®
anti TRIL	Rabbit polyclonal raised against a peptide sequence in the C terminus of TRIL (aa 797–811-SLRREDRLLQRFAD)	Eurogentic/21Century Biochemicals
anti TRIF	Rabbit polyclonal anti TRIF antibody	Cell signalling
anti V5	Mouse monoclonal anti V5 antibody	Sigma®
anti β-actin	Mouse monoclonal anti β-actin antibody	Abcam
anti SARM	Rabbit polyclonal anti SARM antibody	Sigma®

Horse radish peroxidase (HRP) conjugated secondary antibodies		Jackson Immunoresearch
Antibodies used for confocal microscopy studies		
anti Mouse IgG	Peroxidase-conjugated AffiPure Goat Anti-Mouse IgG	Jackson Immunoresearch
anti V5	Rabbit polyclonal to V5 tag (FITC conjugated)	Abcam
anti TLR3	Goat polyclonal anti TLR3 antibody	Santa Cruz
anti Flag	Mouse monoclonal anti-Flag antibody	Sigma®
anti mouse secondary antibody	Alexa 488 Secondary antibody	Invitrogen
anti goat secondary antibody	Alexa 647 Secondary antibody	Invitrogen

Table 2.10 Antibodies used for western blotting, co-Immunoprecipitation and confocal microscopy studies

Reagent	Source
DuoSet ELISA kits	R&D Systems®
3,3',5,5',-tetramethyl-benzidine (TMB)	Sigma®
Tween® 20	BD Biosciences

Table 2.11 Reagents used for ELISA assay

Name	Description
E.coli	BL21 strain
VSV	VSV Indina (IND) strain

Table 2.12 Bacterial and viral strains used for *in vivo* studies

2.2 Methods

2.2.2 Cell culture

2.2.2.1 Growth and maintenance of cell lines

All cell lines were stored in liquid nitrogen. Cells were stored in 80% (v/v) FCS and 10% (v/v) DMSO and 10 % DMEM in plastic cryovials placed in liquid nitrogen. Cells were thawed at 37°C, then removed from liquid nitrogen and immediately placed in 10 ml of warm DMEM media supplemented with 10% FCS and 1% PS. Cells were centrifuged at 290 x g for 5 min and the pellet was resuspended in 10 ml of appropriate media depending on the cell type. The human astrocytoma U373 and human embryonic kidney (HEK)-293T cells were resupsended in DMEM supplemented with 10% FCS and 1% PS. The human monocytic THP-1 cells was placed in RPMI media containing 10% FCS and 1% PS. Cell lines were maintained at 37°C with 5% CO_2 and

cultured when 80-90% confluent. Certain cell lines were also cultured in respective media supplemented with the additional antibiotics U373-TRIL-V5 with 300 μg/ml G418, U373 shRNA-TRIL-RFP and THP-1 shRNA-TRIL-RFP with 3 μg/ml and 2 μg/ml of puromycin, respectively.

For continuous cell culture, cells were maintained at 1 x 10^5 cells/ml and subcultured when 80-90% confluent. In order to subculture, adherent cell lines (U373, HEK-239T, U373 TRILV5, U373 shRNA-TRIL-RFP) cells were washed with 5 ml of PBS prior to addition of 3 ml of 0.25% trypsin/ EDTA for 5 min or until detachment occurred. 10 ml of complete media was added in order to terminate trypsinisation. Cells were centrifuged at 290 x g for 5 min. Suspension cell lines (THP-1, THP-1, shRNA-TRIL-RFP) were directly transferred to sterile 50 ml tube and centrifuged at 290 x g for 5 min In all cases, following centrifugation the supernatant was removed and the cell pellet suspended using 1 ml of appropriated media. 20 μl of cell suspension was removed and used to establish the cell number. In order to count cells, 20 μl of cell suspension was mixed with 180 μl of Trypan Blue solution (cell viability marker, excluded from healthy cells but taken up by non-viable cells), placed in a haemocytometer and counted following the calculation procedure: The cell number from 5 boxes (on grid) x 5 x 10,000 x 10 (dilution factor) = no of cells/ml .

2.2.2.2 Cryo-preservation of cells

Cells were cultured until 80-90% confluent and then harvested and counted as described above. Cells were centrifuged at 290 x g for 5 min and the pellet was resuspended in adequate media to obtain a final cell concentration of 10 x 10^6 cells/ml. 200 μl of the cell suspension was placed in a plastic cryovial with 800 μl of FCS and 100 μl of DMSO. Prepared aliquots were then incubated in a container filled with isopropanol and placed at -80°C overnight, prior to being placed in liquid nitrogen for long-term storage.

2.2.2.3 Primary cells generation

2.2.2.3.1 Generation of bone-marrow derived macrophages (BMDMs)

All utensils used for dissection were autoclaved prior to use and the bone marrow was harvested in a laminar flow hood. Mice were euthanized using a CO_2 chamber and cervical dislocation was performed to confirmed death. The abdomen and hind legs were sprayed with 70% ethanol. The incision was made in the midline of the abdomen and the skin pulled back to expose the hind legs. Muscle was removed from the femur and tibia. Legs were dissected away from the body by cutting at the ankle and the hip joint. Remaining tissue was removed from the pelvic and femoral bones that were separated at the knee joint. Both tibia and femur bones were transferred into a 10 cm dish containing PBS. Bones were cut off at each end. Using a 10 ml syringe filled with PBS and a 25-gauge needle, the bone marrow was flushed out into a 50 ml tube until bone appeared white. Bone marrow cells were resuspended by pipetting up and down using a 10 ml pipette. The obtained cell suspension was passed through a cell strainer and next centrifuged at 450 x g for 5 min at room temperature. The supernatant was removed and the cell pellet resuspended in 5ml of red blood cell lysis buffer for 5 min Cells were resuspended in 20 ml of PBS followed by another centrifugation (450 x g, 5 min). This step was repeated up to three times to ensure that all red blood cells were lysed. The cell pellet was resuspended in 5 ml of DMEM and counted as previously described (2.2.2.1). Cells were seeded at 1 x 10^6 cells/ml in 10cm dishes in DMEM supplemented with 10% of heat inactivated FCS, 1% PS, 0,1% ciprofloxacin (10 mg/ml) and 15% MCSF. Cells were left to grow for 8 days, prior to setting up for experiments. On day 8 cells cells were harvested and seeded at 1 x 10^6 cells/ml in 2 ml for a 6 well plate and at 0.1 x 10^6 cells/ml in 200 µl per well for a 96 well plate. Following the overnight incubation cells were left untreated or stimulated with various ligands and analysed for the expression and production of proinflammatory cytokines and chemokines.

2.2.2.3.2 Generation of bone-marrow derived dendritic cells (BMDCs)

Bone marrow cells were isolated as previously described (section 2.2.2.3.1). Cells were seeded at 2.5 x 10^6 cells/ml in 10 cm dishes in RPMI medium containing 10% FCS and 1% PS, 2mM L-glutamine, 50 μM βmercaptoethanol and 20 ng/ml GM-CSF. Cells were left to grow for 8 days, prior to setting up for experiments. On days 3 and 6 the non-adherent cells were removed. The media was removed and replaced with 5 ml of a fresh media. Collected media was centrifuged at 300 x g for 5 min and 5 ml of the supernatant was returned to the dish and the cell pellet discarded. On day 8 cells both the adherent and non-adherent cells were harvested and seeded at 1 x 10^6 cells/ml in 2 ml for a 6 well plate and at 0.1 x 10^6 cells/ml in 200 μl per well for a 96 well plate. Following the overnight incubation cells were left untreated or stimulated with various ligands and analysed for the expression and production of proinflammatory cytokines and chemokines.

2.2.2.3.3 Mixed glial cells generation

All instruments used for dissection were autoclaved prior to use. Within the laminar hood, 1-3 days old neonatal mice were anesthetised with isoflurane and beheaded using a sterile razor. Following the midline, skin on the skull was cut and the skull exposed. Small sharp scissors was inserted at the brain stem and the incisions were made along both sides of the head. The skull was then butterfly opened in order to expose the brain. Brain was scooped out and rolled on gauze in order to remove the meninges layer. Using syringe stopper and cell strainer, brain was carefully homogenised into the 10 cm dish containing 10 ml of DMEM. Mixed glial cells were resuspended by pipetting up and down using a 10 ml pipette and transferred into a falcon tube, followed by centrifugation at 300 x g for 3 min. The obtained supernatant was discarded. The cell pellet was resuspended in 15 ml of DMEM with 10% of heat inactivated FCS and 1% PS and transferred into a 75T flask. Cells were left to grow for 9-10 days prior to use for experiments. Media was replaced every 2-3 days. Following incubation cells were plated at 1 x 10^6 cells/ml in 2 ml for a 6 well plate and at 0.1 x 10^6 cells/ml in 200 μl per well for a 96 well plate. Following the overnight incubation cells

were left untreated or stimulated with various ligands and analysed for the expression and production of proinflammatory cytokines and chemokines.

2.2.2.3.4 Isolation of glial cells subpopulations

Primary mixed glial cells were isolated as previously described (section 2.2.2.3). On day 9-10 or when mixed glial cells became confluent the flask was secured by wrapping the neck and cap with parafilm and shook on orbital shaker at 110 rpm for 2 h at room temperature. Following shaking media containing microglia cells was transfered into a 50 ml tube and centrifuged at 300 x g for 5 min. The supernatant was discarded and cell pellet resuspended in 1 ml of DMEM containing 10% FCS and 1% PS. Cells were counted and plated at 1 x 10^6 cells/ml in 2 ml in a 6 well plate. Remaining in the flask astrocytes were trypsinised at previously described (section 2.2.2.1) and plated at 1 x 10^6 cells/ml in 2 ml in a 6 well plate. Hippocampal neurons were isolated and cultured as previously described (Kaech & Banker, 2006).

2.2.3 Plasmid DNA preparation

2.2.3.1 Plasmid transformation and purification

Chemically competent *E.Coli* (DH5α) cells were thawed on ice. 2 µl of plasmid DNA (1-3 µg) was added to 50 µl of competent cells and incubated on ice for 30 min. Following incubation cells were heat shocked treated for 2 min at 42°C and then placed on ice for 2 min. Sterile Lauria-Bertani (LB) broth without an antibiotic was then added to the cells, followed by 1 h incubation at 37°C with shaking (200 rpm). Next, samples were centrifuged at 15,000 x g, LB broth removed and pellets re-suspended in 200 µl of fresh broth without an antibiotic. The obtained bacterial cell suspension was then aseptically spread on sterile agar plates containing appropriate antibiotic and incubated upside down at 37°C overnight. A single bacterial colony was selected, transferred to 10 ml of LB broth and grown for 6 h at 37°C with shaking (200 rpm). After incubation 1 ml of bacterial cell suspension was then placed in 100 ml of LB broth with adequate antibiotic and incubated overnight at 37°C with shaking (200 rpm). Following incubation bacteria were centrifuged for 15 min at 3200 x g and the

plasmids were isolated using EndoFree Plasmid Maxi Kit according to the manufacturer's instructions. DNA concentration and purity was examined using NanoDrop ND-100 (Thermo Scientific). Isolated plasmid DNA was stored at -20 °C.

2.2.3.2 Transient transfection of plasmid DNA

2.2.3.2.1 Transfection using GeneJuice® reagent

Cells were seeded at a desired concentration and incubated for 24 h prior to transfection using GeneJuice® (liposomal based transfection reagent). 3 µl of GeneJuice® per 1 µg of DNA and 800 µl of serum-free media (SFM) (DMEM or RPMI) were mixed and incubated at room temperature for 5 min. Next, correct amount of the DNA of interest was added to the mixture and incubated for further 15 min at room temperature. The DNA/GeneJuice® mix was added to the cells drop-wise. Cells were incubated for 24-48 h at 37°C with 5% CO_2. Table 2.14 represents the amount of DNA, GeneJuice®, and SFM used for various experimental formats.

Dish/well format	Total amount of plasmid DNA	Serum free medium in transfection mix	Volume of GeneJuice® Transfection Reagent
10cm dish	5 µg	235 µl	15 µl
6 well plate	1 µg	100 µl	3 µl
12 well plate	0.5 µg	50 µl	1.5 µl
96 well plate	220 ng	9.2 µl	0.8 µl
35mm glass-bottomed dish	0.5-1 µg	100 µl	3 µl

Table 2.13 GeneJuice reagent transfection conditions

2.2.3.2.2. Transfection using Lipofectamine™ 2000 reagent

Cells were seeded at a desired concentration and incubated for 24 h prior to transfection using Lipofectamine™ 2000 transfection reagent. Two separate transfection mixtures were prepared, first one containing desired amount of DNA and second one containing Lipofectamine™ 2000 transfection reagent, both diluted in Opti-MEM® reduced serum medium. Mixtures were incubated separately at room temperature for 5 min and them mixed 1:1 followed by additional 20 min incubation also at room temperature. Media from the cells was removed and replaced with serum

free/low serum medium lacking antibiotics. The mix was then added drop-wise into cells. Cells were incubated for 4-6 h at 37°C with 5% CO_2. Following incubation media was change once again and replaced into complete respective growth medium. Cells were allowed to rest for another 12-24 h at 37°C with 5% CO_2 before continuing with the experiment. Table 2.15 represents the amount of DNA, Lipofectamine™ 2000 and Opti-MEM® medium used for various experimental formats.

Plate format	Volume of Plating Medium	Total amount of DNA	Lipofectamine	Lipofectamine/DNA Dilution Volume (µl)
96-well	100 µl	10-100 ng	0.2-0.5 µl	25 µl
24-well	500 µl	100-200 ng	0.5-1.5 µl	25 µl
6-well	2 ml	0.5-2 µg	2.5-6 µl	250 µl

Table 2.14 Lipofectamine™ 2000 Transfection conditions

2.2.4 Co-immunoprecipitation assay

HEK-239T or U373 cells were set up at 2 x 10^6 cells/ml in 10 cm dishes and incubated for 24 h at 37°C with 5% CO_2. For co-immunoprecipitation (Co-IP) of overexpressed proteins, cells were then transfected with plasmids of interest as outlined in Table 2.5 and incubated for a further 48 h. For an endogenous Co-IP assay the media was replaced 24 h following plating, and cells were then incubated for 48 h. Following incubation, media was removed and cells were washed once with an ice cold PBS. Cells were lysed in 0.5 ml of IP-lysis buffer (10% (v/v) glycerol, 50 mM NaF, 20 mM Tris-Cl pH 8.0, 2 mM EDTA, 137 mM NaCl, 1% (v/v) Nonidet P-40) or HSLB (10% (v/v) glycerol, 50 mM HEPES pH 7.5, 100 mM NaCl, 1 mM EDTA, 1% (v/v) Nonidet P-40), with freshly added protein inhibitors (1 mM orthovanadate (Na_3VO_4), 0.1 mM PMSF, 1 µg/ml aprotinin and 1 µg/ml leupeptin), transferred to a pre-cooled microcentrifuge tube and rolled at 4°C for 1 h to ensure that the lysis occurred. If the CoIPs were to be carried out at a later time samples were snap frozen using liquid nitrogen and placed at -80°C for a maximum time of 48 h, otherwise the following Co-IP protocol was carried out.

The freshly lysed or defrosted on ice samples were centrifuged at maximum speed for 5 min at 4°C to remove cell debris. 50 µl of the supernatants were mixed

with 15 µl of 5X Laemmli sample buffer (10% (v/v) glycerol, 2% (w/v) SDS, 200 µg/ml bromophenol blue, 125 mM Tris pH 6.8 and 5% β-mercaptoethanol, added just before use) boiled for 5 min and saved for further SDS-PAGE and western blot analysis as described in section 2.2.6 and 2.2.7, respectively. The remaining 450 µl of supernatant was used for immunoprecipitation, using the antibody-coupled beads. 40 µl of A/G-plus beads slurry (Santa-Cruz Biotechnology) was placed in pre-cooled microcentrifuge tubes. Desired concentration of the antibody against the protein of interest was added to A/G-plus beads and incubated overnight at 4°C with rolling. Beads were pelleted by centrifuging at 2200 x g, 3 min, 4°C and then washed three times using 0.5 ml of IP-wash buffer (0.5 mM EDTA, 10 mM Tris-Cl pH 7.5, 150 mM NaCl, containing freshly added protein inhibitors). The samples were centrifuged between each wash to pellet the antibody-coupled beads. 450 µl of the supernatant was added to prepared antibody pre-coupled beads and incubated for 3 h or overnight at 4°C with rolling to allow the antibody to bind the protein of interest. Samples were then washed three times (2200 x g, 3 min, 4°C) with 0.5 ml of IP-wash buffer and excess of wash buffer removed using gel loading tip. 50 µl of 5X Laemmli sample buffer was added, samples were boiled for 5 min and used for further SDS-PAGE and western blot analysis was carried out as described in section 2.2.6 and 2.2.7, respectively.

2.2.5 Biotynylated Poly(I:C)-streptavidin pull-down

U373 cells were set up at 1 x 10^6 cells/ml in 10 cm dishes and incubated for 48 h at 37°C with 5% CO_2. Following incubation, media was removed and cells were washed once with an ice cold PBS. Cells were lysed in 100 µl of lysis buffer (1X diluted from 2X prepared as follows: 20% (v/v) glycerol, 1 M Tris-Cl pH 7.9, 2.5 M NaCl, 0.5 mM EDTA, 0.1 M DTT and 20% (v/v) Nonidet P-40) containing freshly added protein inhibitors (1 mM orthovanadate (Na_3VO_4), 0.1 mM PMSF, 1 µg/ml aprotinin and 1 µg/ml leupeptin) Cells were vortexed and incubated for for 20 min at 4°C with rotation. Following incubation cells were short spinned and 900 µl of wash buffer (10 mM Tris-Cl pH 7.9, 0.5 mM EDTA, 1% NP40) was added to obtain a final volumne of 1 ml. 100 µl of whole cell lysate was mixed with 20 µl of 5X Laemmli sample buffer

boiled for 5 min and saved for further SDS-PAGE and western blot analysis as described in section 2.2.6 and 2.2.7, respectively. Cell debris was removed by centrifugation at maximum speed for 5 min at 4°C. The remaining 900 µl of cell lysate was then used for a pull-down using 1 µg of 5' biotinylated Poly(I:C) (10 µl of a 100 µg/ml stock) and 30 µl pre-washed streptavidin coupled agarose beads (50% w/v). Samples were incubated for 2 h at 4°C with rotation. Following incubation samples were then washed three times (2200 x g, 5 min, 4°C) with 0.5 ml of wash buffer and excess of wash buffer removed using gel loading tip. 30 µl of 5X Laemmli sample buffer boiled for 5 min and saved for further SDS-PAGE and western blot analysis as described in section 2.2.6 and 2.2.7, respectively. Blots were probed with the anti-TRIL and anti-TRIF antibody.

2.2.6 Sodium dodecyl sulphate-polyacrylamide gel electrophoresis (SDS-PAGE)

Samples were resolved using an SDS-PAGE gel consisting of a 5% stacking gel used to condense protein and a 10% resolving gel. Volumes for preparing two 10% resolving gels and two 5% stacking gels are represented in Table 2.16. Gels were prepared using Bio-Rad® apparatus. A 10% resolving gel was poured first. After the resolving gel was set, the 5% stacking gel was poured. The gels were run in a BioRad gel box filled with 1X WB running buffer (1X made from 10X stock, prepared as follows: 30.3g 25 mM Tris, 144g 192 mM glycine, 10g 0.1% SDS and made up to 1L with distilled H_2O) using a constant current 25/30 mA per gel. A pre-stained molecular marker (New England Biolabs) was run alongside the proteins as molecular weight standards.

10% Resolving gel		5% Stacking gel	
30% Acrylamide/Bis-acrylamide mix	5 ml	30% Acrylamide/Bis-acrylamide mix	1 ml
1.5 M Tris-HCl pH 8.8	3.8 ml	1 M Tris-HCl pH 6.8	0.75 ml
10% SDS (w/v)	150 µl	10% SDS (w/v)	60 µl
10% APS (w/v)	150 µl	10% APS (w/v)	60 µl
TMED	6 µl	TMED	6 µl
H_2O	5.9 ml	H_2O	4.1 ml

Table 2.15 Stacking and resolving gel composition

2.2.7 Western blot analysis

Electrophoresed on an SDS-gel proteins were then transferred to PVDF membrane and probed with antibodies in order to visualise protein of interest by enhanced chemiluminescence (ECL), following the method outlined below.

2.2.7.1 Electrophoretic transfer of proteins

The resolved proteins were transferred to PVDF membrane using a wet transfer system with all components soaked first in 1X transfer buffer (25 mM Tris pH 8.0, 0.2 M glycine, 20%, methanol. The PVDF membrane was activated with methanol prior to use. All components were assembled in the following order (bottom (-, cathode) to top (+, anode)): sponge, 3 layers of filter paper, gel immersed in 1X WB transfer buffer, methanol activated PVDF membrane, 3 layers of filter paper, sponge. Air bubbles were carefully removed before placing the assembly in the cassette. An ice pack was placed in the chamber filled with ice-cold 1X WB transfer buffer. A constant current of 150 mA/30 mA, was applied for 2 h/overnight, respectively.

2.2.7.2 Blocking of non-specific binding sites

Once the transfer of proteins to PVDF was terminated, the membrane was removed from the cassette and incubated at room temperature for 1 h or overnight at 4°C in a blocking solution of 5% non-fat dried milk powder (Marvel) or BSA (w/v) in 0.01% (v/v) TBS-Tween® with a gentle shaking. TBS-Tween® was made up from a 10X stock prepared as follows: 12.11g Tris, 87.6g NaCl, 10 ml Tween® and made up to 1L in distilled H_2O.

2.2.7.3 Probing with antibody

The membrane was placed in a 50 ml falcon tube containing 3 – 5 ml of 5% Marvel plus a 1:100 to 1:10000 dilution of the adequate primary antibody and incubated for 1 h at room temperature or overnight at 4°C with rolling. Next, the membranes were washed 3 times with the wash buffer (0.1% (v/v) TBS-Tween20®), for at least 5 min per wash. The membrane was then transferred into a 50 ml tube

containing 5 ml of 5% Marvel plus the appropriate horseradish peroxidase (HRP) conjugated secondary antibody at 1:1000 to 1:5000 dilutions, depending on the antibody. The membrane was incubated at room temperature with rolling for 1 h, followed by washing step performed as described above. Membranes were developed by enhanced chemiluminescence (20X LumiGLO® Reagent) according to the manufacturers instructions, using Fujifilm X-ray film.

2.2.7.4 Stripping and re-probing of PVDF membrane

The same membrane could be used to examine more than one protein if the membrane was stripped of the initial set of antibodies and re-probed with a second antibody of interest. The membrane was first reactivated using methanol (if left to dry) and washed using 1X WB wash buffer to remove ECL. Next, the membrane was stripped for 15 min by placing it in 10 ml 1X Re-Blot Plus solution (Millipore) with gentle shaking and washed again with 1X wash buffer. The stripped membrane was blocked, probed with primary and secondary antibodies and developed as described above.

2.2.8 Enzyme-Linked Immunosorbent Assay

Duo set ELISA kits (R&D Biosystems) were used in order to examine the levels of cytokines and chemokines produced by cells in response to different stimuli. Human cell lines U373, U373 TRIL-V5, U373 shRNA-TRIL-RFP, U373 non silencing control shRNA and primary murine mixed glial cells, BMDMs and BMDCs were seeded at 0.5-1 x 10^5 cells/ml and allow to rest for 24 h at 37°C with 5% CO_2. The following day media was replaced and cells were either left untreated or stimulated with the appropriate ligands for 24 h. The supernatants were then collected and analysed for human IL6, RANTES and TNFα (R&D Systems), murine RANTES (R&D Systems), IL6 and TNFα (eBIOSCIENCE) production using Enzyme-Linked Immunosorbent Assay (ELISA) kits according to the manufacturer's instruction. A sandwich ELISA for mouse IFNβ was used as previously described (Roberts et al, 2007). The optical density values were measured at 450 nm and concentrations were calculated using a standard curve.

2.2.9 Reporter gene assay

Cells were seeded in 24-well plates at 1×10^5 cells/ml and incubated for 24 h at 37°C with 5% CO_2. Cells were transfected using GeneJuice® transfection reagent (Novagen) as indicated in Table 2.13. A 160 ng of ISRE or NF-κB luciferase plasmid, together with 40 ng of TK Renilla luciferase and the indicated amount of plasmids encoding TRIL, TLR3 or both together were transfected into each well of a 24-well plate. The equivalent amount of empty vector was added as a control in addition to ensuring equal quantities of DNA in each well. Cells were allow to rest for 24 h and stimulated for desired amount of time. After 24 h incubation cells were lysed with 100 µl of passive lysis buffer (Promega) for 15 min with shaking. FireFly luciferase activity was assayed by the addition of 40 µl of luciferase assay mix (For 456 ml 2X solution: 20 mM Tricine, 2.67 mM $MgSO_47H_2O$, 0.1 mM EDTA, 33.3 mM DTT, 530 µm adenosine triphosphate (ATP), 270 µM Acetyl CoEnzyme A, 60 mg D-Luciferin madeup to 445.2 ml, add 1.14 ml 2M NaOH and 2.42 ml 50 mM Magnesium Carbonate Hydroxide) to 20 µl of the lysed sample. Renilla luciferase was read by the addition of 40 µl of Coelentrazine (diluted 1:1000 in PBS). The FireFly luciferase and TK Renilla luciferase values were measured using a Mediators PhL™ Luminometer. The Renilla luciferase plasmid was used to normalise for transfection efficiency in all experiments.

2.2.10 Confocal microscopy

2.2.10.1 Live cell imaging

THP-1 cells were cultured in RPMI media supplemented with 10% (v/v) FCS and 1% (v/v) PS solution. Cells were plated at 2.5 x 10^6 cells/ml using 35-mm glass-bottom tissue cell dishes (MatTek). Cells were treated with PMA (1:80 000, diluted from the 5mg/ml stock concentration) for 24 hours. Cells were transfected using Lipofectamine (Lipofectamine 2000 Invitrogen) with plasmid expressing TRIL-GFP and incubated for the following 24 h. Cells were treated with Hoechst 1:20 000 for 30 min and CellMask™ Plasma Membrane Stain, prior to viewing with a Point Scanning Confocal Microscope with a heated stage (Olympus FV1000 LSM Confocal Microscope).

U373 and HEK-239T cells were cultured in DMEM media supplemented with 10% FCS and 1% PS. Cells were set up at 0.05-0.1 x 10^6 cells/ml in 35 mm glass bottom dishes (MatTek) and left to rest for 24 hours at 37°C with 5% CO_2. Cells were then transfected using GeneJuice (Invitrogen) with plasmids encoding TRIL-GFP, TRIL-RFP, TRIL-YFP, SARM-GFP, Endoplasmic reticulum-cyan fluorescent protein (ER-CFP), Golgi-CFP, early endosome marker EEA1-CFP or combinations of each. Cells were then viewed with a Point Scanning Confocal Microscope with a heated stage (Olympus FV1000 LSM Confocal Microscope). DAPI or Hoechst were used to stain the nuclei, CellMask™ Plasma Membrane Stain and specific mitochodnria dye MITOTRACKER were used to visualise the plasma membrane and the mitochondria respectively.

2.2.10.2 Fixed cell imaging

2.2.10.2.1 Preparation of cover slips

Sterile cover slips were placed in 6-well plate and covered with poly-L-Lysine (1 mg/ml). After 2 min excess of poly-L-Lysine was aspirated and slides rinsed with a sterile PBS. Alternatively sterile cover slips were placed in 6-well plate and covered with fibronectin (1 μg/ml) followed by 2 h incubation at room temperature and rinsing with a sterile PBS. Following coating with poly-L-lysine or fibronectin cover slips were dried-out in the laminar flow hood prior to use.

2.2.10.2.2 Confocal imaging

THP-1 cells were maintained in RPMI media supplemented with 10% (v/v) FCS and 1% (v/v) PS. Cells were seeded at a concentration of a 1 x 10^6 cells/ml in 6 well plate. Cells were then transfected using Lipofectamine with 1 μg of plasmid encoding TLR2 Flag tagged and/or 1 μg of TRIL-RFP expressing plasmid. 24h following transfection cells were transferred into slides pre-treated with fibronectin and left to rest for another 24h. U373 cells were cultured in DMEM supplemented with 10% (v/v) FCS and 1% PS (v/v). Cells were seeded on cover slips coated with poly- L-lysine. Cells were transfected with 1 μg of expression plasmid TRIL/RFP using GeneJuice and after 24 h stimulated for 2 h with 25 μg/ml of Poly(I:C). U373-TRIL V5 stables were

maintained in DMEM supplemented with 10% (v/v) FCS and 1% PS (v/v) and 300 µg/ml of G418. Cells were seeded on poly-L-lysine coated slides 24h prior to stimulation at a concentration of 0.1×10^6 cells/ml. Cells were stimulated with 25 µg/ml PIC for 0 h, 1 h, 4 h, and 24 h, respectively.

Prior to antibody staining, media was removed, and cells carefully washed with PBS. Samples were fixed using 3.7% Formaldehyde at pH 7.0 for 10 min., at room temperature followed by washing three times with PBS. Cells were permeabilised using 0.2% (v/v) triton X-100 in PBS for 5min. at room temperature. Samples were washed once again using PBS before blocking for 1h with 2% (w/v) BSA in PBS. 100 µl of primary antibody diluted using 2% (w/v) BSA in PBS to a desired working concentration (Table 2.16) was added per cover slip and incubated for 1 h at room temperature. Following incubation slides were washed three times using PBS and next incubated with 100 µl per cover slip of adequate secondary antibody diluted to a desired working concentration (Table 2.16) using 2% (w/v) BSA in PBS for 1 h, and washed three times with PBS. Few drops of mounting solution Prolong Gold antifade reagent with DAPI were added onto each cover slip and they were mounted cell-side down onto glass microscope slides. Prepared slides were left to dry at room temperature in dark for 30 min. and then stored at 4°C in dark until viewed using a Point Scanning Confocal Microscope (Olympus FV1000 LSM Confocal Microscope).

Antibody	Stock concentration	Working concentration
Primary antobodies		
Mouse monoclonal anti-V5	1 mg/ml	10 µg/ml
Goat polyclonal anti-hTLR3	200 µg/ml	2 µg/ml
Mouse monoclonal anti-Flag	1 mg/ml	2 µg/ml
Secondary antobodies		
Anti-mouse Alexa 488 antibody	2 mg/ml	8 µg/ml
Anti-goat Alexa 647 antibody	2 mg/ml	8 µg/ml

Table 2.16 List of original stock and working concentrations of primary and secondary antibodies used for confocal staining

2.2.10.3 Quantitative colocalisation analysis

Confocal images were analyzed using FluoView FV1000 Confocal Microscope Software. Pearson's correlation coefficient (PCC), overlap coefficient (OC) and colocalization coefficient for each of analyzed channels were employed to evaluate colocalization. Pearson' s correlation coefficient (PCC) is one of the standard measures in pattern recognition. It is used to describe the correlation of the intensity distributions between channels. PCC estimates the correlation based on similarity between shapes and it ranges from value 1 to -1. A value of 1 represents perfect correlation; -1 represents perfect exclusion and zero random localization. Values close to 1 indicate there is reliable colocalization. Overlap coefficient (OC) represents an overlap of the signals from the 1st and 2nd channel. Values of OC are defined from zero to 1 with 1 being high- colocalization, zero being low.

2.2.11 RNA analysis

2.2.11.1 RNA extraction

2.2.11.1.1 RNA isolation from cells

Cells were rinsed in ice-cold PBS prior to lysis using RLT buffer (Qiagen) with 1% (v/v) β-mercaptoethanol. The cell lysates were then frozen and thawed prior to RNA extraction with an RNeasy Mini kit (Qiagen) in accordance with the manufacturer's instructions. The isolated RNA was quantified using a NanoDrop ND-1000 UV-vis spectrophotometer and normalised using nuclease free water

2.2.11.1.2 RNA isolation from animal brain and spleen tissues

Extracted brain and spleen tissues was placed in 500 µl of QIAzol lysis buffer and mechanistically homogenised. 100 µl of chloroform was added into each homogenate followed by 15 sec of vigorous shaking. Samples were incubated for 2-3 min at room temperature and next centrifuged at 12, 000 x g for 15 min at 4°C. The upper aqueous phase was transferred into a new tube containing 250 µl of isopropanol. Samples were then incubated for 10 min at room temperature. Following centrifugation at 12,000 x g for 10 min at room temperature, the supernatants were carefully aspirated and discarded. The remaining pellets were resuspended in 0.5 ml of

75% ethanol and centrifuged at 7500 x g for 5 min at 4°C. Following centrifugation, the obtained supernatants were removed completely and the RNA pellets were left to dry for few min, prior to resuspension in 100 µl of nuclease free water. The RNA was next cleaned up using an RNeasy® MinElute® Cleanup kit (Qiagen) according to the manufacturer's instructions. Purified RNA was quantified using a NanoDrop ND-1000 UV-vis spectrophotometer and normalised using nuclease free water

2.2.11.2 Reverse transcription PCR (RT-PCR)

RT-PCR was carried out on RNA in order to create cDNA using a High Capacity cDNA Reverse Transcription kit (Applied Biosystems) for human samples and iScript Select cDNA synthesis kit (BioRad) for mouse samples. The following reaction mix was prepared for each human (**A**), and mouse (**B**), samples dependent on the the cDNA synthesis kit used:

A High Capacity cDNA Reverse Transcription kit

- 2 µl 10X RT buffer
- 0.8 µl 100nM deoxyribonucleotide triphosphates (dNTPs)
- 2 µl 10X random primers
- 0.5 µl reverse transcriptase (MultiScribe™)
- 6.5 µl nuclease-free H_2O
- 8 µl RNA (100 ng/µl)

B iScript Select cDNA synthesis kit

- 4 µl 5X reaction mix (iScript)
- 1 µl reverse transcriptase (iScript)
- 5 µl nuclease-free H_2O
- 10 µl RNA (100 ng/µl)/per reaction

RT-PCR for human samples was performed using the Applied Biosystems Veriti 96-well fast thermal cycler (A) and Bio-Rad S1000™ Thermal Cycler (B). The following parameters were set up on the appropriate PCR machines.

A

- 25°C 10 min
- 37°C 60 min x2
- 85°C 15 min
- 4°C ∞

B

- 25°C 5 min
- 42°C 30 min x2
- 85°C 5 min
- 4°C ∞

Generated cDNA was either used directly for further experiments or stored for a later use at 4°C (short term).

2.2.11.3 Quantitative PCR (QPCR)

2.2.11.3.1 QPCR of human samples

In order to perform quantitative PCR (Q-PCR) isolated RNA was transcribed using the High Capacity cDNA Reverse Transcription kit (Applied Biosystems) as described in section 2.2.11.2. Following RT-PCR, generated cDNA was used for QPCR, using specific FAM labelled primers for TRIL (Hs00274460_s1) and TLR3 (Hs01551078_m1) and VIC labelled primers for GAPDH and β-actin purchased from Applied Biosystems. QPCR was carried out using TaqMan®Fast Universal PCR Master Mix (Applied Biosystems).

The following reaction mix was prepared for each sample:

- **5 µl TaqMan®Fast Universal PCR Master Mix 2x**
- **0.5 µl 20X FAM labelled TRIL or TLR3**
- **0.5 µl 20X VIC labelled GAPDH or β-actin**
- **1.6 µl nuclease free water**
- **2.4 µl cDNA**

The following parameters were used on Applied Biosystems 7900 Fast system: 45 cycles 95°C for 5 sec, followed by 60°C for 30 sec.

Relative quantification (RQ) values were calculated based on the ΔΔCt method. Data was analysed using the Applied Biosystems 7500 Fast System Sequence Detection Software v 1.3.1.21. The mRNA expression levels were normalised to human GAPDH mRNA level and represented as relative to control ± standard deviation (SD).

2.2.11.3.2 QPCR of murine samples

In order to perform Q-PCR, isolated RNA was transcribed using the iScript Select cDNA synthesis kit (Bio-Rad) as described in section 2.2.11.2. Following RT-PCR, generated cDNA was diluted 3X and used for QPCR. Primers specific for β-actin, TRIL, TLR3, TLR4 IL6, RANTES, TNFα, IFNβ and VIPERIN were purchased from Integrated DNA

Technologies and are listed in Table 2.16. Q-PCR reaction was performed in 96 well plate format using the DNA ENGINE OPTICON 2 CYCLER (Bio-Rad, Hercules CA).

The following reaction mix was prepared for each sample:

- **7.5 µl iQ SYBR Green Supermix**
- **1 µl forward primer**
- **1 µl reverse primer**
- **5.5 µl nuclease free water**
- **5 µl cDNA sample (diluted 10X)/cDNA standards (diluted as listed below)**

Standards cDNA dilutions were as follows:

- **5X**
- **50X**
- **500X**
- **5000X**

The following parameters were used on Bio-Rad CFX96 Touch™ Real-Time PCR Detection System: 45 cycles 95°C for 15 sec, followed by 60°C for 30 sec and 72°C for 45 sec.

RQ values were calculated based on the standard curve analysis. All gene expression were normalised with β-actin and represented in arbitrary units (A.U).

Primer	Sequence (5' -> 3')	
TRIL (set1)	Forward	ACG TGC TCA CCT ACA GCC TA
	Reverse	CAG ACG GTG GAA GTC GAA GG
TLR3	Forward	GTG AGA TAC AAC GTA GCT GAC TG
	Reverse	TCC TGC ATC CAA GAT AGC AAG T
TLR4	Forward	ATG GCA TGG CTT ACA CCA CC
	Reverse	GAG GCC AAT TTT GTC TCC ACA
IL6	Forward	AAC GAT GAT GCA CTT GCA GA
	Reverse	GAG CAT TGG AAA TTG GGG TA
RANTES	Forward	GCC CAC GTC AAG GAG TAT TTC TA
	Reverse	ACA CAC TTG GCG GTT CCT TC
TNFα	Forward	CAG TTC TAT GGC CCA GAC CCT
	Reverse	CGG ACT CCG CAA AGT CTA AG
IFNβ	Forward	ATA AGC AGC TCC AGC TCC AA
	Reverse	CTG TCT GCT GGT GGA GTT CA
VIPERIN	Forward	AAC CCC CGT GAG TGT CAA CTA
	Reverse	AAC CAG CCT GTT TGA GCA GAA

GAPDH	Forward	GAA CGG GAA GCT TGT CAT CAA
	Reverse	CTA AGC AGT TGG TGG TGC AG
βACTIN	Forward	TTG AAC ATG GCA TTG TTA CCA A
	Reverse	TGG CAT AGA GGT CTT TAC GGA

Table 2.17 List of primers

2.2.11.4 Nanostring analysis

Total RNA isolated from primary mixed glial cells untreated or stimulated for 5 h with LPS and Poly(I:C) was extracted as previously described in section 2.2.2. Similarly, total RNA isolated from brain tissue of WT and TRIL$^{-/-}$ following *E.coli* infection was extracted as previously described (section 2.2.11.1.1).

For RNA analysis 100 ng of total RNA used and hybridised to a custom designed gene expression CodeSet (non-enzimatic RNA profiling using bar-coded fluorescent probes) according to the manufacturer's inscructions (Nanostring technologies) and analysed on nCounter Digital Analyser. The nCounter® Analysis System is an automated, multi-application, digital detection and counting system which directly profiles up to 100 molecules simultaneously from a single sample using a novel barcoding technology. Counts were normalised to endogenous controls per Nanostring Technologies' specifications. Values were log-transformed and displayed as a heat map (Euclidean clustering) generated using the ggplot package within the open source R software environment.

2.2.11.5 Design and validation of murine TRIL primers

In order to examine the expression of TRIL across different murine cells and tissues, three different TRIL primers sets were designed:

TRIL (set1)	Forward	**5' ACG TGC TCA CCT ACA GCC TA 3'**
	Reverse	**5' CAG ACG GTG GAA GTC GAA GG 3'**
TRIL (set2)	Forward	**5' ACG TGC TCA CCT ACA GCC TA 3'**
	Reverse	**5' CA CCG TTG GCG TAA AGG ATG C 3'**
TRIL (set3)	Forward	**5' TCC TTT ACG CCA ACG GCA A 3'**
	Reverse	**5' CAG GTG TAG GTA GAG CAG GTT 3'**

Products of QPCR carried out using wild-type primary mixed glial cells were examined by the agarose gel electrophoresis (as described in section 2.2.11.6) and next confirmed by sequence analysis. Bioinformatics alignment of TRIL product (TRIL set1) and available murine mRNA sequence (NCBI Reference Sequence: NM_025817.4) revealed a 100% identity within the range of 103 nucleotides highlighted in yellow. The selected set of primers (set1) was then used for subsequent TRIL expression studies.

```
CLUSTAL 2.1 multiple sequence alignment

NM_025817.4             AGAAGCTCTCACGACTAGAGGAGCTGTACCTGGGGAACAACCTCTTGCAGGCGCTCGTTC 960
TRIL PRIMER SET1        NNNNNCTCTCACGACTAGAGGAGCTGTACCTGGGGAACAACCTCTTGCAGGCGCTCGTTC  60
                             ************************************************************

NM_025817.4             CTGGCACGTTGGCTCCGCTGCGCAAGTTGCGCATCCTTTACGCCAACGGCAACGAGATTG 1120
TRIL PRIMER SET1        CTGGCACGTTGGCTCCGCTGCGCAAGTTGCGCATCCTTTACGCCAACGGNNTTN---TTT  120
                        ********************************************
```

2.2.11.6 Agarose gel electrophoresis

In order to visualise the QPCR/PCR products a 1-2% (w/v) agarose gel was used. 1% (w/v) agarose gel was prepared as follows:

- **2 g ultrapure agarose**
- **100 ml Tris-Acetate EDTA (TAE)**
- **2-3 µl of Ethidium Bromide (EtBr)**

Agarose added to TAE buffer and heated up until completely dissolved, then allowed to cool, before adding EtBr. Prepared mixture was poured into gel rack and allowed to set with a comb in place. The comb was then removed and a gel placed in a ring with 1 x TAE buffer. DNA loading buffer (50% (v/v) sterile glycerol in sterile H_2O_2 and 10 mg bromophenol blue) was added to 20 µl of PCR product. A total volume of 15

µl was loaded into the gel. A 1kB molecular weight marker (New England Biolabs) was run alongside the samples. The gel was connected to power supply and run at 100 V for approximately 1-1.5 h or until sufficient separation of molecular marker bands had occured. Gel was then visualised using UV gel docking system.

2.2.12 Genotyping of TRIL deficient mice

The genotypes of TRIL deficient mice were determined by PCR analysis of genomic DNA, from tail biopsies. The genomic DNA was isolated using the Genomic DNA Isolation Kit (Lamda Biotech) according to the manufacturer's instructions. Isolated genomic DNA was next diluted 20x and used for genotyping by PCR with specific oligonucleotide primers for the TRIL wild-type and targeted allele (TRIL-F, 5'-TTC ACT TAC CAC CCT GCC AGG TTC -3', TRIL-R1, 5'-GTC TGT ATG GGA AGA GAG GCA CAC TG -3', TRL-R2, 5'-CAC CAG AGC GTT CTG GTC ATG C -3'). Primers F and R1 amplified wild-type allele and F and R2 targeted one. The three primers were used in a PCR reaction using GoTaq (Promega).

The following reaction mix was prepared for each sample:

- **12.5 µl GoTaq Promega Master Mix**
- **0.25 µl 100 µM primer F**
- **0.25 µl 100 µM primer R1**
- **0.25 µl 100 µM primer R2**
- **10.75 nuclease free water**
- **1 µl tail digest**

PCR reaction was carried out using the following amplification conditions: 95°C for 5 min and 30 cycles of 95°C for 30 s, 58°C for 30 s, and a 5 min incubation at 72°C at the end of the run. Amplification products were resolved on a 2% agarose gel.

2.2.13 Generation of cell lines stably expressing shRNA

In order to generate stable knock down of TRIL in various cell lines a set of three shRNAmir individual clones were purchased from Open Biosystems together with corresponding non-silencing control (Table 2.6).

2.2.13.1 Transfection and lentiviral production

HEK-239T cells were set up at 2 x 10^5 cells/ml in 10 cm dishes and incubated for 24 h at 37 °C with 5% CO_2. The following day 4 µg of plasmids encoding shRNA specific to TRIL or Non Silencing control together with 3 µg of the pCMV-dR8.74psPAX2 packaging plasmid and 1 µg of pMD2.G envelope plasmid were transfected using GeneJuice® as previously described (section 2.2.3.2.1). 48 h following transfection (day 3) the supernatant was harvested and replaced with fresh DMEM supplemented with 10% FCS and 1% PS. Collected supernatants were centrifuged at 400 x g, 5 min and filtered through a 0.45 µm membrane and stored at 4°C for 24 h. Harvesting step was repeated once again 24 h later (day 4). The supernatants were centrifuged at 400 x g, 5 min and filtered through a 0.45 µm membrane. Supernatants collected on day 3 and 4 were mixed together.

2.2.13.2 Lentiviral transduction

U373 or THP-1 target cells were plated at 2 x 10^5 cells/ml in 10 cm dishes in DMEM or RPMI containing 10% FCS and 1% PS. The following day, cells were re-plated with medium consisting of: 50% HEK-293T supernatant (mixed day 3 and 4), 50% DMEM (U373) or RPMI (THP-1) culture media containing 10% FCS and 1% PS and 4 µg of hexadimethrine bromide (Polybrene®). Cells were cultured for 24 h at 37 °C with 5% CO_2. Following 24 h of incubation media was aspirated and replaced with 50% HEK-239T supernatant (mixed day 3 and 4), 50% DMEM (U373) or RPMI (THP-1) culture media containing 10% FCS and 1% PS. 48 h after the second transduction media was removed from U373 and THP-1 cells and replaced with DMEM (U373) or RPMI (THP-1) supplemented with 10% FCS and 1% PS. Cells were allowed to rest for 48 h before Puromycin selection (2-3 µg/ml) was initiated.

U373 and THP-1 shRNA-TRIL stable knockdown cells and the non-silencing control cell line were maintained in DMEM (U373) containing 10% FCS and 1% PS and 3 μg/ml of puromycin or or RPMI (THP-1) containing 10% FCS and 1% PS and 2 μg/ml of puromycin. In order to activate shRNA expression, cells were stimulated with 1 μg or 2 μg of doxycycline for 48 h prior to performing an experiment.

2.2.14 The *in vivo* studies

2.2.14.1 Mice

C57Bl/6 mice from The Jackson Laboratory (Bar Harbor, ME) and TRIL$^{-/-}$, TRIF$^{-/-}$, TLR3$^{-/-}$, TLR4$^{-/-}$ all on the C57Bl/6 background were bred at UMASS Medical School. Mouse strain were maintained in specific pathogen-free conditions in UMASS Medical School, and the animal protocols were carried out in accordance with the guidelines set forth by UMASS Medical School Institutional Animal Care and Use Committee.

2.2.14.2 The *In vivo* model of *E.coli*-induced acute peritonitis

Day prior to the experiment the *E.coli* B21 strain was inoculated in 25 ml of antibiotic free LB broth and grown overnight at 37°C with shaking (200 rpm). The following day bacterial suspension was centrifuged at 3200 x g for 15 min. Obtained bacterial pellet was resuspened in 2.5 ml of sterile PBS.

10 weeks old age- and sex-matched C57Bl/6 wild-type (WT) and TRIL$^{-/-}$, TRIF$^{-/-}$, TLR3$^{-/-}$, TLR4$^{-/-}$ mice were infected with 100 μl 10^9 CFU of *E.coli* BL21 strain via the intraperitoneal route in order to induce acute peritonitis and shock. Following 5-6h of incubation mice were sacrificed and specimens collected. Samples were processed according to respective protocols described below.

2.2.14.2.1 Peritoneal Lavage (PL) and cells processing

The PL volumes were equalised with PBS and centrifuged at 400 x g for 5 min at 4°C. Cell pellet was resuspended in 100 μl of the NP-40 lysis buffer (10% (v/v) glycerol, 20 mM Tris-Cl pH 8.0, 137 mM NaCl, 1% NP-40) and transferred to -80°C. The cell pellet was subsequently thawed, followed by the RNA extraction (as described in

section 2.2.11.1.1) and QPCR analysis (as described in section 2.2.11.3.2). Supernatant was transferred into filter/concentrator device (Millipore) and centrifuged at 5000 x g for 1 h 4°C. Following centrifugation, 200-300 µl of concentrates were immediately transferred into a 96-deep well plate and kept at -80°C, prior to analysis by ELISA.

2.2.14.2.2 Serum processing

Blood obtained through the cardiac puncture was transferred into the blood collection tubes placed on ice. Tubes were next centrifuged at maximum speed for 5 min at 4°C. Obtained supernatants were immediately transferred into 96-well plate and kept in -80°C, prior to analysis by ELISA.

2.2.14.2.3 Spleen and brain tissue processing

Each tube containing 500 µl of PBS or QIAzol lysis reagent (Qiagen) was weight prior and after the collection of the organs. Following isolation, the spleen and the brain were divided into two parts and each of them was placed in PBS or QIAzol lysis reagent and kept on ice. Samples containing brain and spleen tissues in QIAzol lysis reagent were processed as previously described (section 2.2.11.1.2)

Samples containing PBS were then mechanistically homogenised, followed by centrifugation at 400 x g at 4°C. 100 ul of spleen or brain lysates were plated onto antibiotic free agar plates (in order to establish the amount of bacteria following infection). 400 µl of NP-40 lysis buffer was added into each sample following 30 min of incubation with at 4°C with rotation. Next samples were centrifuged at the maximum speed for 5 min. Obtained supernatants were next transferred into the 96 well plate and kept in -80°C, prior to examination by ELISA.

2.2.14.3 The *In vivo* VSV infection

6-8 weeks old age- and sex-matched C57Bl/6 WT and $TRIL^{-/-}$ or $TLR3^{-/-}$ mice were anesthetized with isoflurane prior to infection with 5 x 10^5 PFU of VSV. 30 µl of viral suspension in PBS was administered equally to both nostrils using pipette with and a protein gel loading tip. Following 24-48 h of infection mice were sacrificed and

blood spleen and brain were collected and processed as previously described (section 2.2.14.2.2, 2.2.14.2.3 and 2.2.11.1.2)

2.2.15 Statistical analysis

All the graphs were made using GraphPad Prism v 5.02 software. Two tailed unpaired student t test in Prism software was used to perform statistical analysis. *P* values of < 0.05 were considered significant. ***, ** and * represents p values of <0.001, <0.01 and <0.05, respectively.

CHAPTER THREE

Investigation into the role of TRIL in TLR-mediated signalling pathways

3.1 Introduction

As mentioned in chapter 1, TRIL is a novel accessory molecule involved in the regulation of TLR4 signalling pathway (Carpenter et al, 2009). Initial studies characterise TRIL as a positive modulator of TLR4 response, highly expressed in the brain. TRIL directly interacts with both TLR4 and its ligand LPS. Overexpression of TRIL in the human astrocytoma cell line U373 leads to enhanced cytokine production following LPS stimulation, while knockdown of TRIL attenuates TLR4 response in various cell lines (Carpenter et al, 2009). TRIL is therefore a component of the TLR4 signalling complex, which may have a particular relevance for the regulation of the innate immune response in the brain due to the high levels of expression of TRIL found there.

Apart from this initial study, TRIL has not yet been thoroughly investigated. A number of questions regarding TRIL remain to be answered in order to fully characterise this accessory molecule. Therefore the main goal of this study is to carry out a further investigation into TRIL, resulting in a comprehensive characterisation of this novel protein.

Similar to differentially localised TLRs, accessory molecules can be found in various cell compartments. MD2 and RP105 function at the level of the plasma membrane, while others such as UNC93B, PRAT4A and gp96 regulate TLRs at the level of the endoplasmic reticulum. In addition, a group of accessory molecules including CD14, HMGB1, CD36 and LL37 directly bind to TLR ligands and modulate TLR responses (Akashi-Takamura & Miyake, 2008; Lee et al, 2012). The cellular localisation of an accessory molecule is often strictly correlated with its function.

TLR4 utilizes a vast array of accessory molecules, which are implicated in various aspects of TLR4 signalling. Accompanied by the accessory molecules MD2 and CD14, TLR4 perpetually cycles between the plasma membrane and the Golgi structures (Latz et al, 2002). Once engaged at the cell surface by LPS, the TLR4-MD2-CD14 complex initiates the MyD88/Mal-dependent signalling pathway followed by translocation into the endosomal compartment where it triggers the TRIF/TRAM-mediated response. Therefore TLR4 can be found both at the plasma membrane and

intracellularly, where it initiates two distinct signalling pathways.

TRIL has been demonstrated to impact on TLR4 activity via direct interaction with the receptor and its ligand LPS (Carpenter et al, 2009), however the exact localisation of TRIL within the cell remains unknown. This study aims to uncover the subcellular localisation of TRIL, by a comprehensive confocal microscopy and plasma membrane fractionation analysis.

It is common for accessory molecules to execute multiple roles and participate in the regulation of more than one TLR. RP105 regulates responses of TLR2 and TLR4 (Liu et al, 2013). UNC93B is indispensible for TLR3, TLR7 and TLR9 (Brinkmann et al, 2007), whereas CD14 functions by modulating TLR4 (Haziot et al, 1996), TLR3 (Lee et al, 2006), and more recently TLR7 and TLR9 (Baumann et al, 2010) as well as TLR2 (Raby et al, 2013) mediated responses. TRIL has been associated thus far with the regulation of TLR4 signalling complex. Its role in the other TLR signalling pathways however has not yet been examined. Therefore this study explores in greater detail a role for TRIL in the regulation of TLR mediated signalling pathways. Examination of direct interaction of TRIL with other TLRs is addressed by co-immunoprecipitation (Co-IP) assay and confocal microscopy analysis, whereas the functional implication of TRIL in the regulation of TLR signalling is assessed by overexpression and gene silencing studies.

3.2 Results

3.2.1 TRIL localisation studies

Preliminary flow cytometry studies carried out on TRIL localisation demonstrated a cell specific expression pattern of this protein (Carpenter et al, 2011). Antibodies raised to the C-terminal site and mid region of TRIL revealed that in U373/TRIL cell line the protein can not be detected on the cell surface and is localised only intracellularly. In contrast, in HEK-293T/TRIL cell line the protein was found exclusively on the cell surface (as indicated by use of the mid-region TRIL antibody) (Carpenter et al, 2011).

In order to further verify preliminary findings on TRIL localisation, I carried out confocal microscopy studies using various cell types. Unfortunately, the anti-TRIL antibody generated to the N-terminus, C-terminus and mid region of the protein were not sensitive enough for confocal analysis. Three different variants of TRIL plasmid, tagged with GFP, RFP and YFP respectively, were therefore obtained for the purpose of these studies.

Plasmids were transiently overexpressed in three distinct human cell lines: U373, THP-1 and HEK-293T. Confocal imaging analysis clearly demonstrated an intracellular localisation of TRIL-YFP in U373 cell line (Fig. 3.1 panel B). Different expression patterns were seen with HEK-293T cells, where an overexpressed protein was associated with the plasma membrane, as indicated by co-localisation with a specific plasma membrane dye (CellMask) (Fig 3.1 panel C). Interestingly, in human THP-1 cell line GFP tagged TRIL was localised in a similar fashion as seen in the U373s and was found to be expressed intracellularly (Fig. 3.1 panel A), no co-localisation with CellMask was observed. To validate the specificity of TRIL expression and CellMask/Hoechst staining, appropriate controls were generated for each cell line, THP-1 (A), U373 (B) and HEK-293T (C) demonstrated in Fig. 3.2 (Fig. 3.2, panel A-C).

In addition, the expression pattern of TRIL was also assessed by membrane fractionation studies using U373 cell line stably overexpressing TRIL with a V5 tag. Western blot analysis carried out using U373/WT and U373/TRIL-V5 cells following

membrane fractionation revealed, that overexpressed TRIL is exclusively found in the membrane and not cytosolic fraction (Fig. 3.3, top panel, lane 3 and 4).

Given the fact that both confocal microscopy imaging and flow cytometry analysis clearly demonstrated an intracellular expression pattern of TRIL in U373 cells, I sought to characterise in depth its subcellular localisation within this cell line. As shown in Figure 3.4, upon stimulation with Poly(I:C), overexpressed TRIL co-localises (yellow) with the endoplasmic reticulum marker (KEDL motif of calreticulin) (Fig. 3.4 panel B), as well as the early endosome marker EEA1 (Fig. 3.4, panel A) in the U373s. TRIL did not co-localise with the Golgi apparatus (Fig. 3.4, panel C), nor with mitochondria (Fig. 3.6) in the Poly(I:C) stimulated U373 cell line. The specificity of plasmid expression (Fig. 3.5, panel A-D) and mitochondrial staining (Fig. 3.7, panel A-B) was verified by adequate controls.

Having established the localisation of TRIL to early endosomes, I next investigated whether stimulation with LPS impacts on this localisation. U373 cells were transiently transfected with plasmids encoding TRIL-GFP and the early endosome marker EEA1-CFP and following 24 h of incubation were stimulated with LPS. Single live cell microscope imaging revealed increased localised expression of both proteins following LPS stimulation. Additionally, the co-localisation of TRIL-GFP with the endosomal marker EEA1-CFP (indicated by arrows) was clearly enhanced upon LPS challenge in a time dependent manner (Fig. 3.8). Supplementary controls were generated in order to ensure the specificity of plasmid expression (Fig. 3.9).

Overall these studies demonstrate the intracellular localisation pattern of TRIL in the human astrocytoma cell line U373 and monocytic THP-1. Expressed intracellulary TRIL localises to the ER and early endosome structures, but not to mitochondria and the Golgi apparatus. In addition, the endosomal localisation of TRIL in the resting U373 cells is further enhanced by LPS stimulation in a time-dependent fashion.

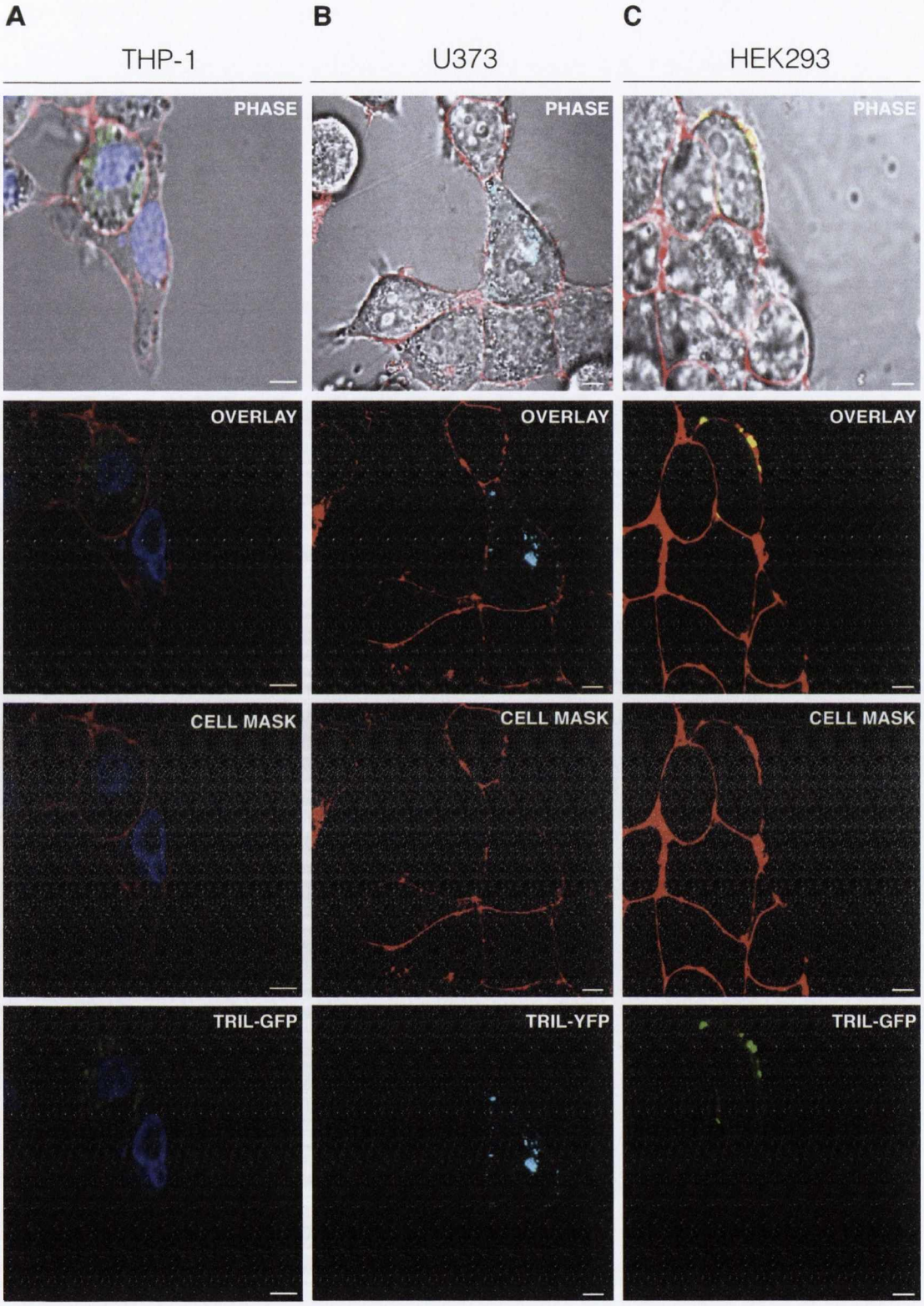

Figure 3.1 Localisation of TRIL in different cell types

Figure 3.1 Localisation of TRIL in different cell types

A, THP-1 cells were plated at 2.5 x 10^6 cells/ml using 35-mm glass-bottomed tissue cell dishes (MatTek). Cells were treated with PMA (1:80 000/stock concentration 5mg/ml) for 24 hours. Next, cells were transfected with plasmid encoding 1 μg of TRIL-GFP (green) and incubated for another 24 h. Prior to viewing with a Point Scanning Confocal Microscope with a heated stage (Olympus FV1000 LSM Confocal Microscope, (NA, 1.4; 60x), cells were treated with the nuclei dye, Hoechst (dark blue) and the plasma membrane marker CellMask (red). **B** and **C**, HEK-293T and U373 cells (0.05 x 10^6 cells/ml) respectively, were seeded on 35-mm MatTek dishes. 24 hours later cells were transfected with expression plasmids, HEK-239T with 1 μg of TRIL-GFP (**C**, green) and U373 with 1 μg of TRIL-YFP (**B**, bright blue). 48 hours following transfection cells were treated with CellMask (red). Live cell imaging was assessed using a Point Scanning Confocal Microscope with a heated stage (Olympus FV1000 LSM Confocal Microscope, (NA, 1.4; 60x)). Results are representative of three independent experiments. Scale bars indicate 5 μM.

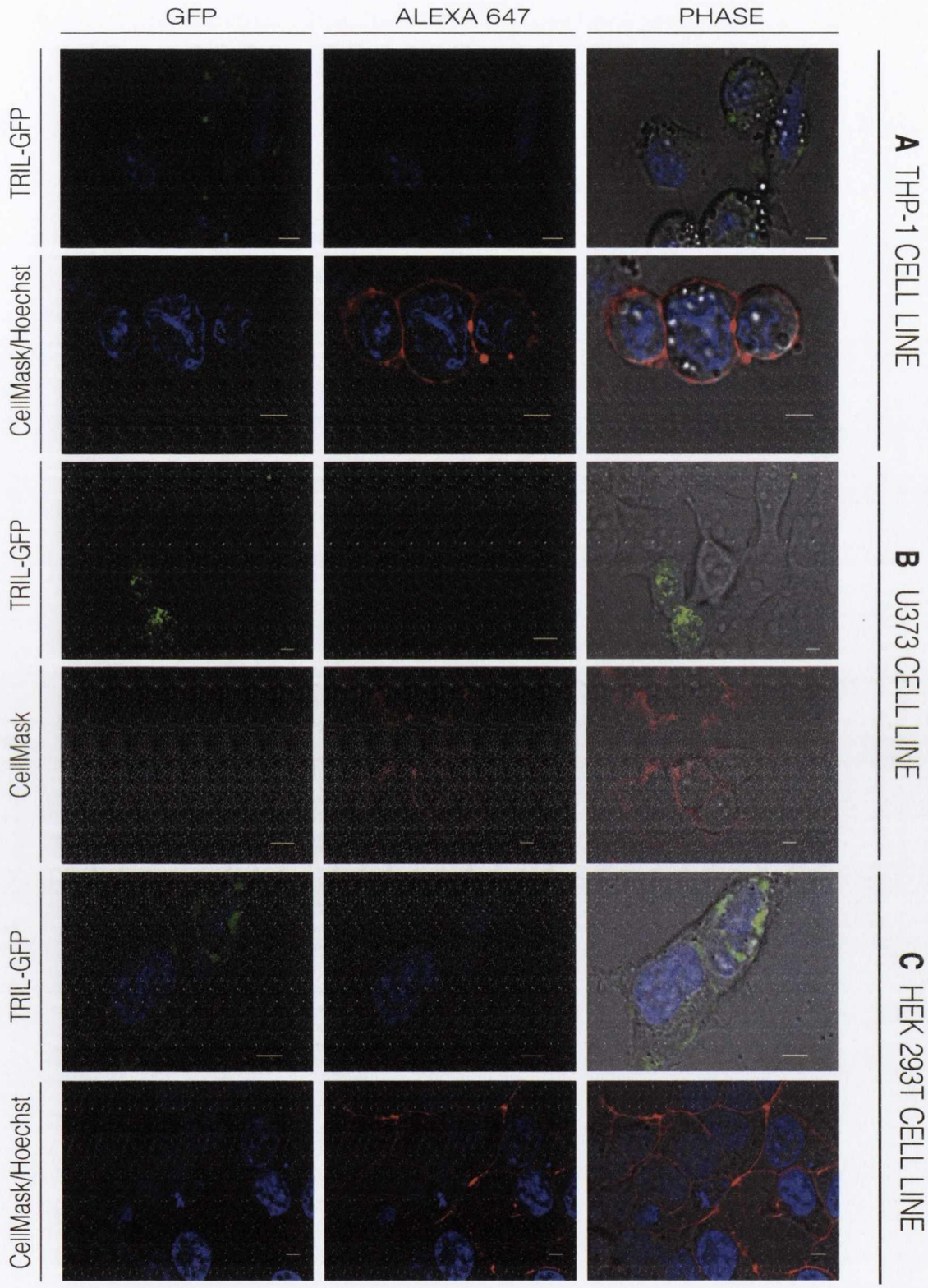

Figure 3.2 TRIL-GFP expression and CellMask staining specificity controls in THP-1, U373 and 293T cell lines

Figure 3.2 TRIL-GFP expression and CellMask staining specificity controls in THP-1, U373 and 293T cell lines

A, THP-1 cells were cultured at 2.5 x 10^6 cells/ml in 35-mm glass-bottomed tissue cell dishes (MatTek). After 24 h cells were treated with PMA (1:80 000/stock concentration 5mg/ml) for 24 h. Cells were transfected with 1 μg of TRIL-GFP expressing plasmid (green). 24 h following transfection cells were treated with Hoechst (blue) to stain the nuclei and the specific cell membrane marker, CellMask (red) to visualise plasma membrane. A Point Scanning Confocal Microscope with a heated stage (Olympus FV1000 LSM Confocal Microscope, (NA, 1.4; 60x), was used for viewing. **B** and **C**, U373 and 293T cells (0.05 x 10^6 cells/ml) respectively, were seeded on 35-mm glass-bottomed tissue cell dishes (MatTek). After 24 h 1 μg of plasmid encoding TRIL-GFP (green) was transfected into the cells. 24 h following transfection both U373 (**B**) and HEK-293T (**C**) cells were stained using CellMask (red). 293T cells were additionally stained with Hoechst (blue), to highlight the nucleus. A Point Scanning Confocal Microscope with a heated stage (Olympus FV1000 LSM Confocal Microscope, (NA, 1.4; 60x), was used to examine prepared samples. Scale bars indicate 5 μM.

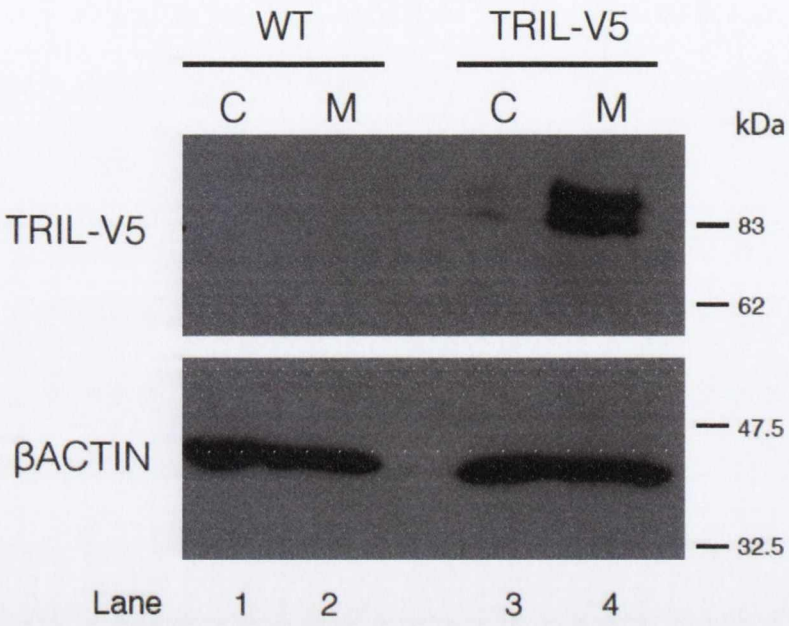

Figure 3.3 TRIL expression pattern in a membrane fractionation study carried out on U373/TRIL-V5 cells

Using membrane fractionation kit (ThermoScientific), cytosolic (C) and membrane (M) fractions were separated in wild-type (WT) and TRIL-V5 overexpressing U373 cells. Lysates were then analysed by Western blotting for TRIL and β-actin expression using an anti-V5 and anti-β-actin antibodies. The result shown is representative of three independent experiments.

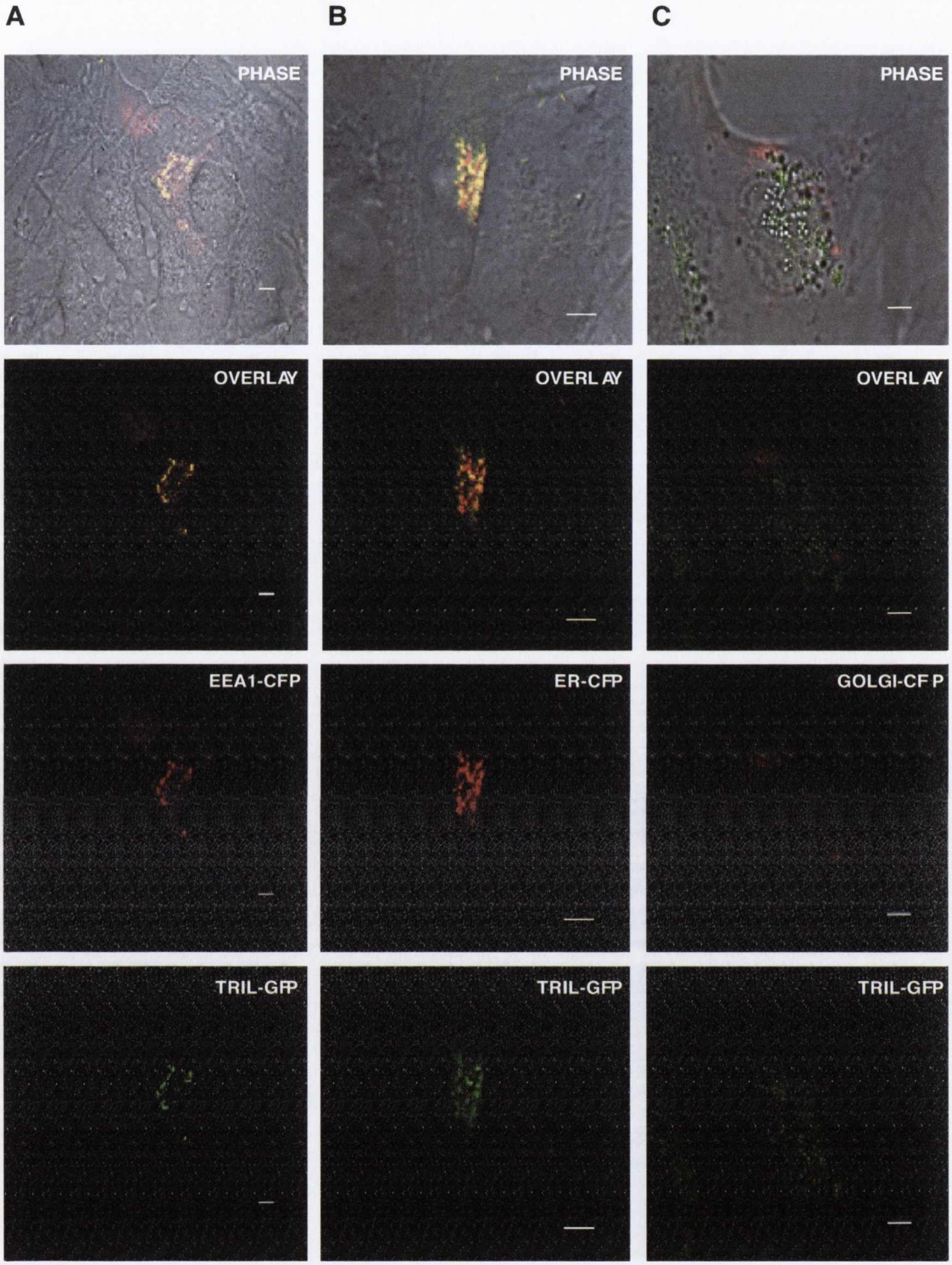

Figure 3.4 Analysis of TRIL localisation in the endoplasmic reticulum, early endosomes and Golgi apparatus in the U373 cell line following Poly(I:C) stimulation

Figure 3.4 Analysis of TRIL localisation in the endoplasmic reticulum, early endosomes and Golgi apparatus in the U373 cell line following Poly(I:C) stimulation

U373 cells (0.1 x 10^6 cells/ml) were seeded on 35-mm glass-bottomed tissue cell dishes (MatTek). Following 24 h incubation cells were transfected with 0.5 μg of plasmids encoding EEA1-CFP (an early endosome marker, panel **A**, red), ER-CFP (endoplasmic reticulum marker, panel **B**, red), Golgi-CFP (panel **C**, red) and/or 1 μg of plasmid encoding TRIL-GFP (green). After 48 hours live cell imaging was performed using a Point Scanning Confocal Microscope with a heated stage (Olympus FV1000 LSM Confocal Microscope, (NA, 1.4; 60x)), following 2 h of stimulation with 25 μg/ml of Poly(I:C). Results are representative of three independent experiments. Scale bars indicate 5 μM.

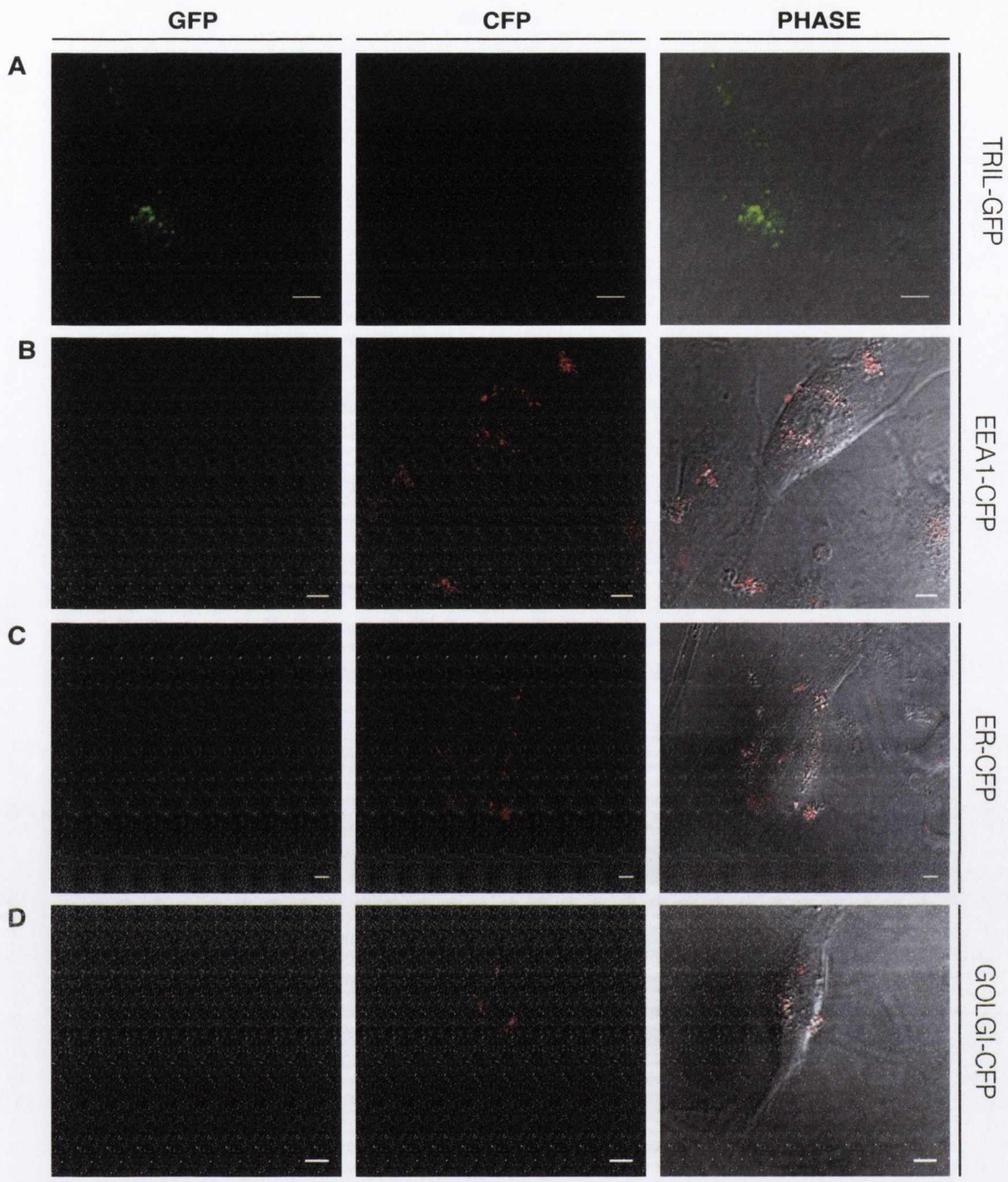

Figure 3.5 GFP-TRIL, EEA1-CFP, ER-CFP and GOLGI-CFP expression controls in U373 cells

U373 cells were cultured at 0.1 x 10^6 cells/ml in 35-mm glass-bottomed tissue cell dishes (MatTek). After 24 h cells were transfected with plasmids encoding 1 µg of TRIL-GFP (panel **A**, green) or 0.5 µg of EEA1-CFP (an early endosome maker), (panel **B**, red), ER-CFP (panel **C**, red) or Golgi-CFP (panel **D**, red), respectively. Cells were left to rest for 48 h prior to live cell viewing using a Point Scanning Confocal Microscope with a heated stage (Olympus FV1000 LSM Confocal Microscope, (NA, 1.4; 60x)), following 2 hours of stimulation with 25 µg/ml of Poly(I:C). Scale bars indicate 5 µM.

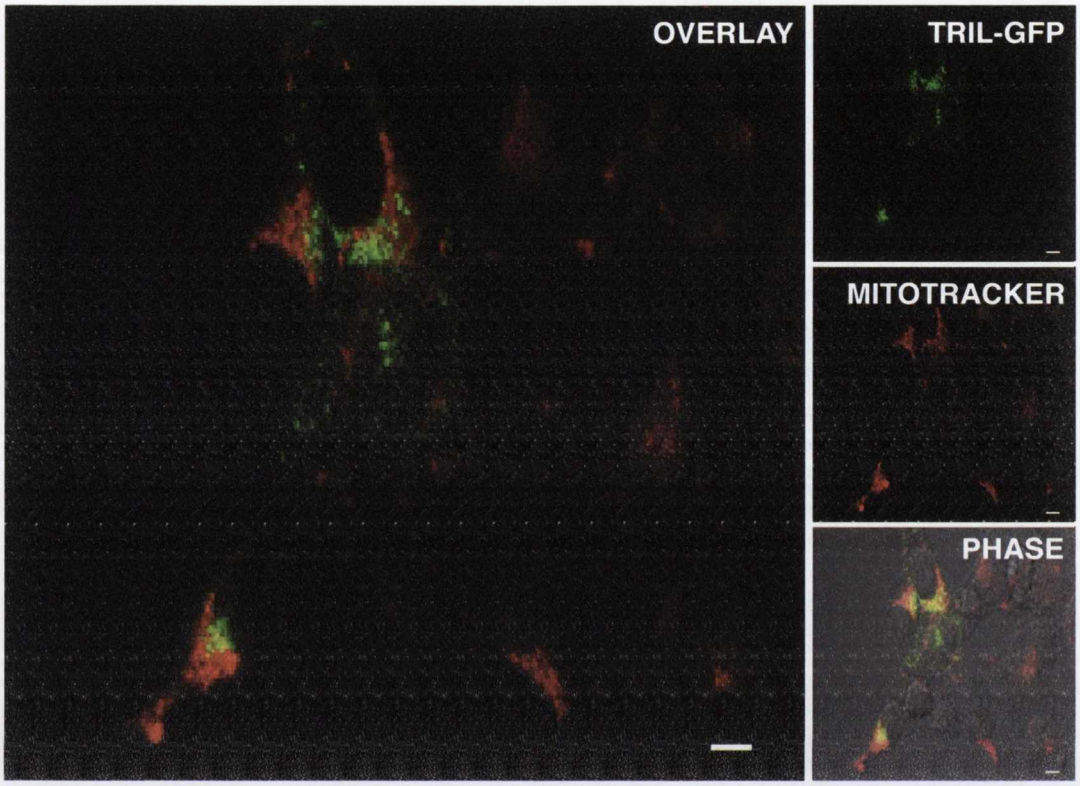

Figure 3.6 TRIL mitochondrial localisation studies in the U373 cell line

U373 cells were seeded at 0.1 x 10^6 cells/ml on 35-mm glass-bottomed tissue cell dishes (MatTek). 24 hours later cells were transfected with 1 µg of plasmid encoding TRIL-GFP (green) and incubated for the following 48 hours. Cells were treated for 2 h with 25 µg/ml of Poly(I:C) prior to staining with a specific mitochondrial marker (Mitotracker, red). Samples were analysed using a Point Scanning Confocal Microscope with a heated stage (Olympus FV1000 LSM Confocal Microscope, (NA, 1.4; 60x)). Results are representative of three independent experiments. Scale bars indicate 5 µM.

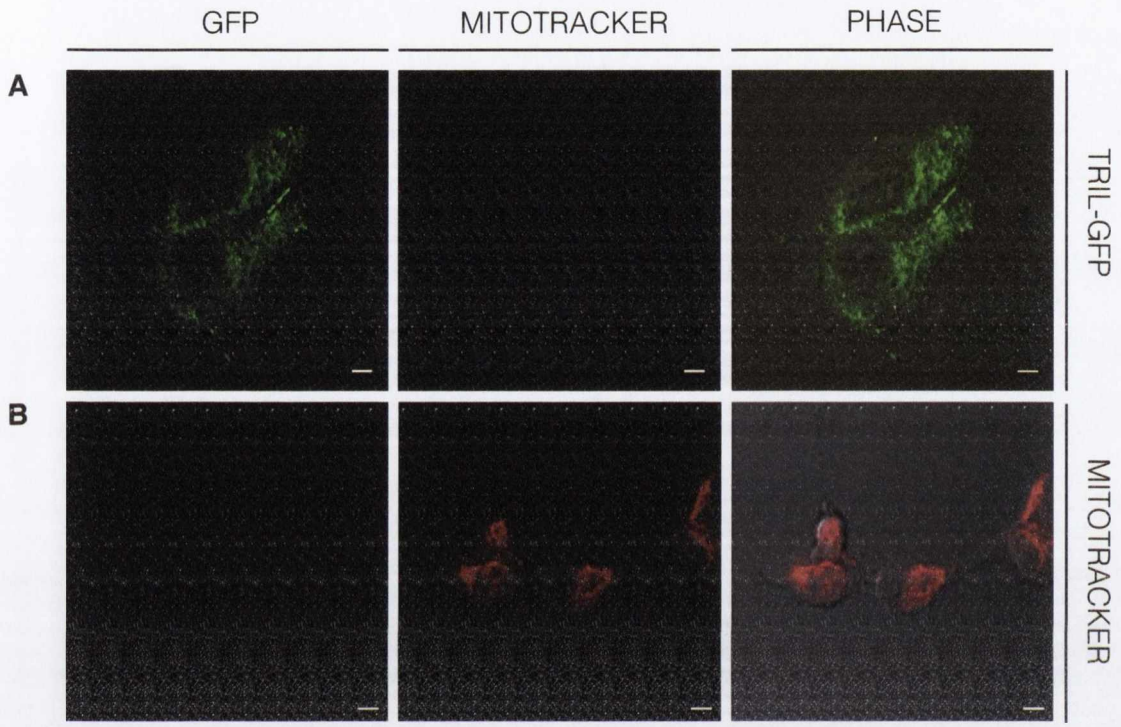

Figure 3.7 TRIL-GFP expression and mitochondrial staining specificity (MITOTRACKER) controls in the U373 cell line

U373 cells (0.1 x 10^6 cells/ml) were seeded on 35-mm glass-bottomed tissue cell dishes (MatTek). After 24 h 1 µg of plasmid encoding TRIL-GFP (**A**, green) was transfected into cells. 24 h following transfection cells were stimulated for two hours using Poly(I:C) (25 µg/ml) prior to staining with the specific mitochondrial dye, MITOTRACKER (**B**, red). A Point Scanning Confocal Microscope with a heated stage (Olympus FV1000 LSM Confocal Microscope, (NA, 1.4; 60x), was used to examine prepared samples. Scale bars indicate 5 µM.

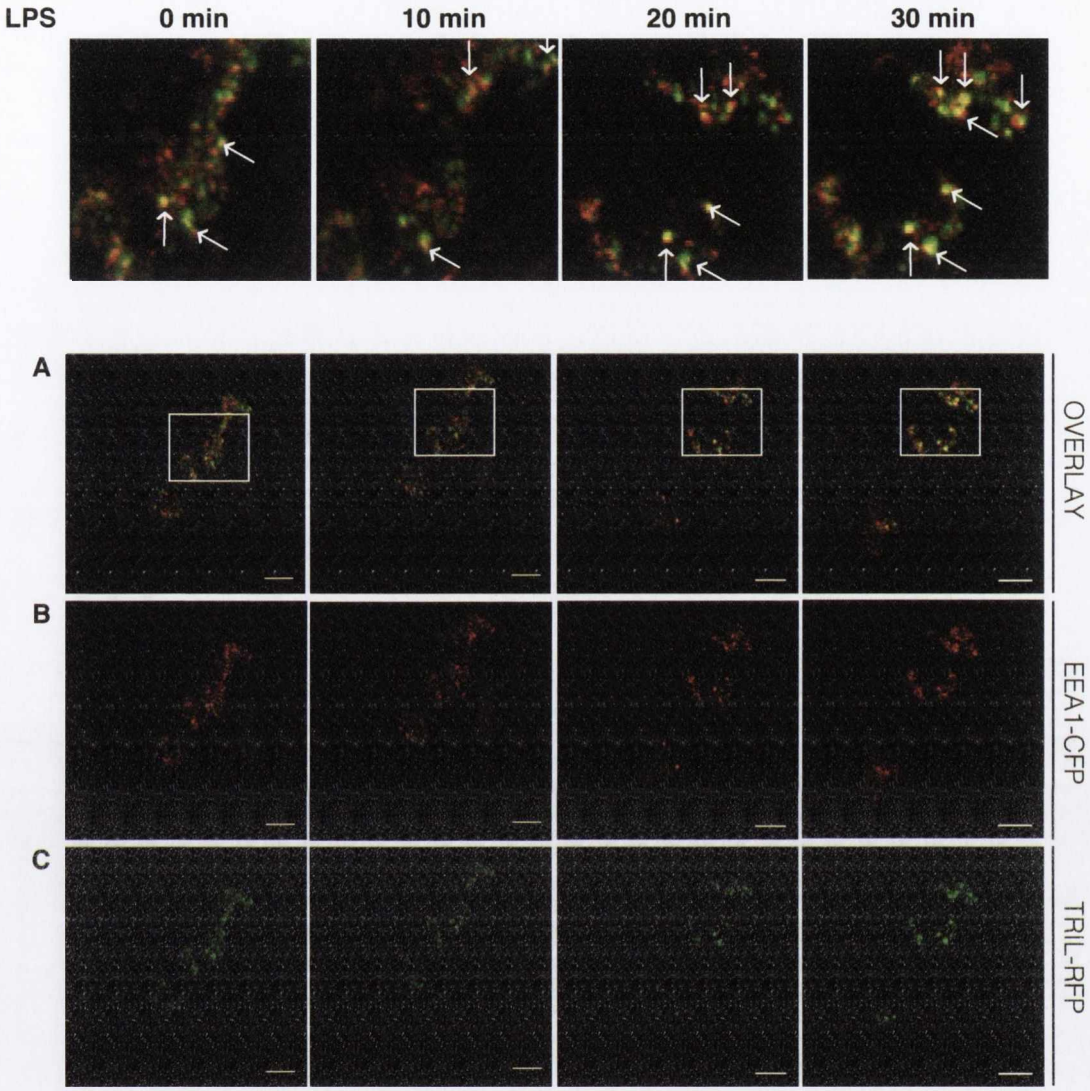

Figure 3.8 Co-localisation of TRIL with the early endosome marker EEA1 increases following LPS stimulation in the U373 cells

U373 cells (0.1 x 10^6 cells/ml) were seeded on 35-mm glass-bottomed tissue cell dishes (MatTek). Following 24 h incubation cells were transfected with 1 μg and 0.5 μg of plasmids encoding EEA1-CFP (an early endosome marker, **B** red) and TRIL-RFP (**C**, green). After 24 hours single live cell imaging was performed prior to and following stimulation with 100 ng/ml of LPS for indicated times, using a Point Scanning Confocal Microscope with a heated stage (Olympus FV1000 LSM Confocal Microscope, (NA, 1.4; 60x)). Data are representative of three independent experiments. Scale bars indicate 5 μM.

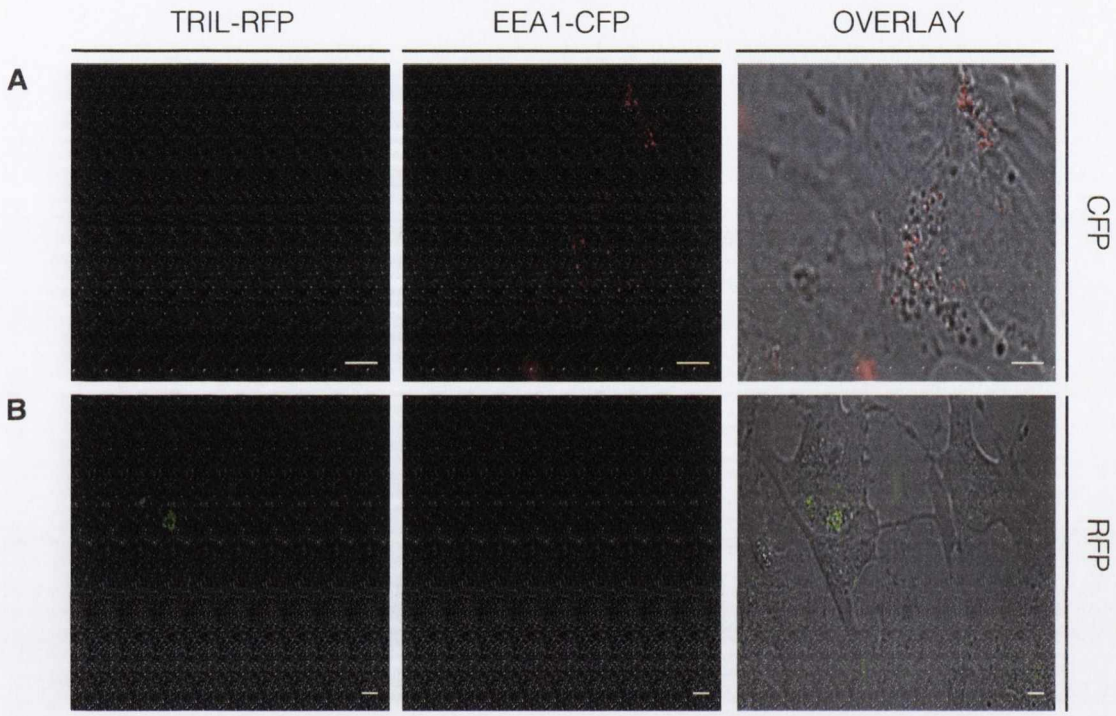

Figure 3.9 TRIL-RFP and EEA1-CFP expression controls in U373 cells

U373 cells (0.1 x 10^6 cells/ml) were seeded on 35-mm glass-bottomed tissue cell dishes (MatTek). Following 24 h incubation cells were transfected with 1 µg or 0.5 µg of plasmids encoding EEA1-CFP (**A**, red) and TRIL-RFP (**B**, green), respectively. After 24 hours live cell imaging was performed using a Point Scanning Confocal Microscope with a heated stage (Olympus FV1000 LSM Confocal Microscope, (NA, 1.4; 60x)). Data are representative of three independent experiments. Scale bars indicate 5 µM.

3.2.2 Expression of TRIL is induced by Poly(I:C) stimulation in various cell types

Previously published data described TRIL as a novel functional component of the TLR4 signalling pathway (Carpenter et al, 2009). This earlier finding, together with a strong indication of the endosomal localisation of the protein in U373 cells, suggested a potential additional role for TRIL in the endosomal TLR3-mediated signalling pathway.

In order to test this hypothesis, I set out to examine the induction of TRIL following stimulation with a TLR3 agonist Poly(I:C). Increased expression of TRIL upon Poly(I:C) stimulation was detected both at the mRNA and the protein levels. Quantitative PCR (QPCR) carried out using the U373 cells demonstrated a significant increase in TRIL expression following 24 h of Poly(I:C) stimulation (Fig. 3.10). The examination of the protein level by Western blot assay using the anti-TRIL antibody revealed a time-dependent induction of TRIL by Poly(I:C) in both U373 (Fig. 3.11 A) and rat mixed glial cells (Fig. 3.11 B). A visually detectable increase in TRIL expression was observed at the early stage of stimulation, from only 1 h in U373 and 2 h in rat mixed glial cells. In the previous studies, TRIL was demonstrated to migrate as a doublet due to posttranslational glycosylation (Carpenter et al, 2009). Interestingly, in both cell types, U373 and rat mixed glial cells, one out of two different forms of TRIL was expressed at the higher level during the time course. A slower migrating form was enhanced in U373, whereas in rat mixed glial cells stronger expression of the faster migrating form of TRIL was observed.

These data clearly indicate that the expression of TRIL is enhanced both at the mRNA and protein level following stimulation with Poly(I:C) in rat mixed glial cells and U373s.

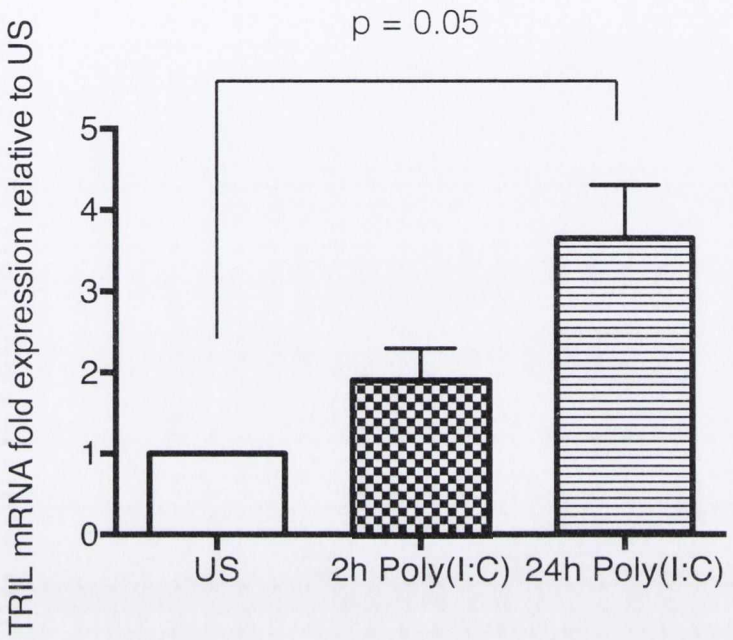

Figure 3.10 TRIL expression is induced following Poly(I:C) stimulation in U373 cells

U373 cells (0.1 x 10^6 cells/ml) were seeded in 6-well plates. After 24 h cells were stimulated with 25 μg/ml of Poly(I:C) for the indicated time points. Following stimulation TRIL expression was examined by QPCR analysis. TRIL mRNA levels were normalised against GAPDH and expressed relative to unstimulated cells. Data are represented as the mean ± SEM of three independent experiments, all carried out in triplicate. p = 0.05.

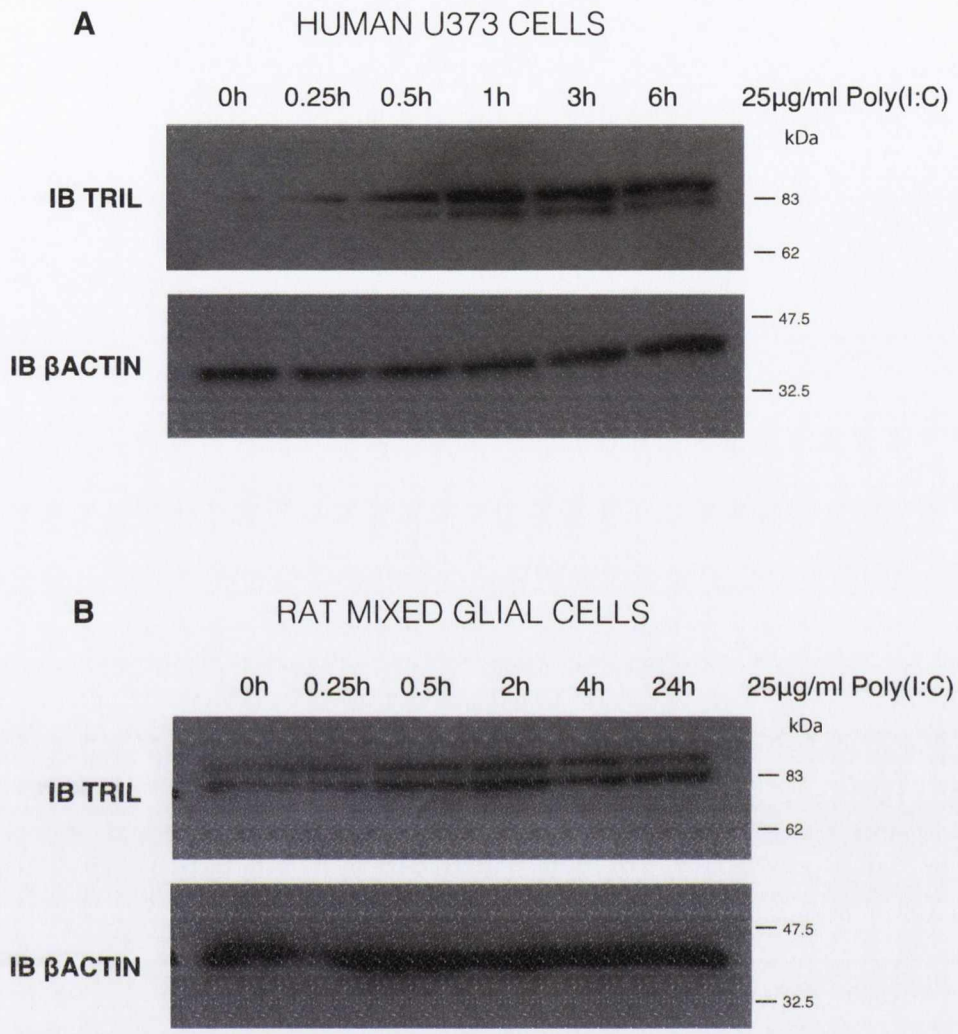

Figure 3.11 TRIL protein expression increases following Poly(I:C) stimulation in various cell types

Human U373 cells **A**, and rat mixed glial cells **B**, were stimulated with 25 µg/ml of Poly(I:C) for the indicated times. Following stimulation TRIL and β-actin expression levels were examined by Western blot analysis using either anti-TRIL or anti-β-actin antibodies. Results are representative of three independent experiments.

3.2.3 Investigation into the effect of TRIL on TLR3 signalling following Poly(I:C) stimulation

The human astrocytoma cell line U373, which endogenously expresses TLR3, was capable of only a moderate response to Poly(I:C) stimulation. Therefore, in an attempt to determine the effect of increased TLR3 or TRIL expression on U373 responsiveness to TLR3 stimulation, cells were transiently transfected with 1 ng of plasmid encoding either TLR3 or TRIL, prior to treatment with Poly(I:C). A slight increase in ISRE luciferase activity was observed when either TLR3 or TRIL were overexpressed in U373 cells upon Poly(I:C) stimulation (Fig. 3.12 A).

A similar impact of an overexpressed TLR3 and TRIL on the U373 response to Poly(I:C) led to a hypothesis of a functional link between these proteins. In order to address this a transient transfection of low levels (10 pg) of plasmid encoding TLR3 and/or TRIL was performed, followed by Poly(I:C) stimulation. Figure 3.12 clearly demonstrates that when transiently overexpressed, neither TLR3 nor TRIL alone has a major effect on Poly(I:C) induced ISRE activation and RANTES production at this low concentration (Fig. 3.12 B and C, respectively). However, when proteins were co-expressed together using the same low plasmid concentrations, a robust increase in the activation of ISRE and RANTES production was detected (Fig. 3.12 B and C, respectively).

In order to further confirm the potential impact of TRIL on TLR3 mediated signalling, I next examined U373 cells stably overexpressing TRIL (U373/TRIL). ISRE and κB luciferase assays were carried out using U373/TRIL and WT cells following treatment with Poly(I:C). As shown in Figure 3.13 a significant increase in ISRE (Fig. 3.13 A) and less marked in case of κB (Fig. 3.13 B) luciferase activity was detected in the U373/TRIL stable cell line upon stimulation with Poly(I:C). Similarly, enhanced IL6 and RANTES production was observed in Poly(I:C) stimulated U373/TRIL compared to U373/WT cells (Fig. 3.14 A and B).

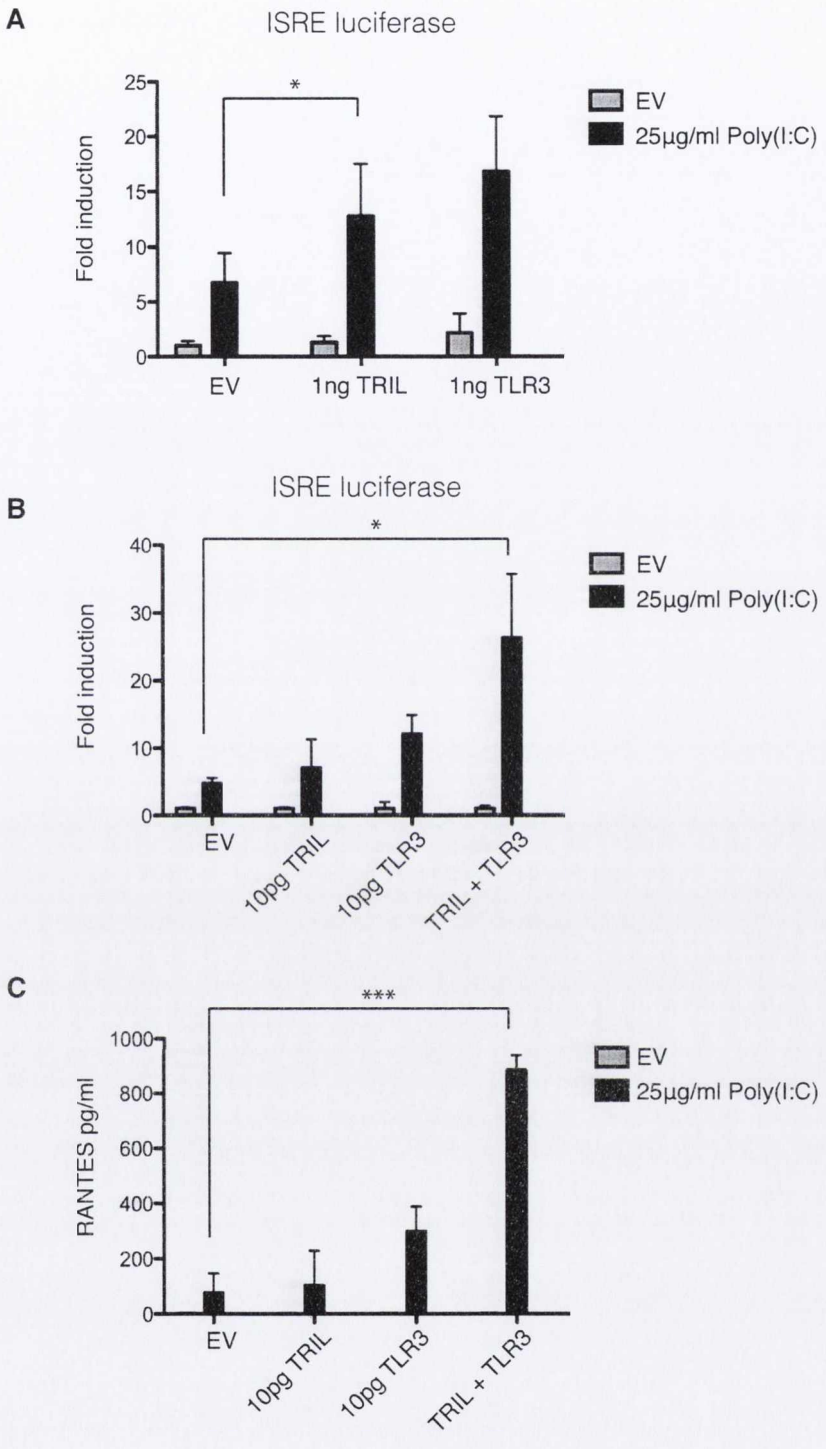

Figure 3.12 Overexpression of TRIL enhances ISRE luciferase activity and RANTES production following Poly(I:C) stimulation

Figure 3.12 Overexpression of TRIL enhances ISRE luciferase activity and RANTES production following Poly(I:C) stimulation

(**A** and **B**) U373 cells (0.1 x 10^6 cells/ml) were transiently transfected with plasmids encoding 80 ng of TK *Renilla* and 160 ng of ISRE luciferase along with plasmids expressing empty vector (EV), TRIL and/or TLR3. 24 h following transfection, cells were stimulated with 25 μg/ml of Poly(I:C) for 24 h. Cells were harvested and analysed for reporter gene activity. Results were normalised for *Renilla* luciferase activity and represented as fold stimulation over non-stimulated controls. Results are expressed as mean ± SD for triplicate determinants and representative of three independent experiments, each carried out in triplicate. *, $p < 0.05$. **C**, U373 cells (0.1 x 10^6 cells/ml) were transiently transfected with EV, TRIL and/or TLR3 expressing plasmids. 24 h following transfection cells were treated with 25 μg/ml of Poly(I:C). Supernatants were collected and assayed by ELISA for RANTES production. Results are expressed as mean ± SD for triplicate determinations and representative of three independent experiments, each carried out in triplicate. ***, $p < 0.001$.

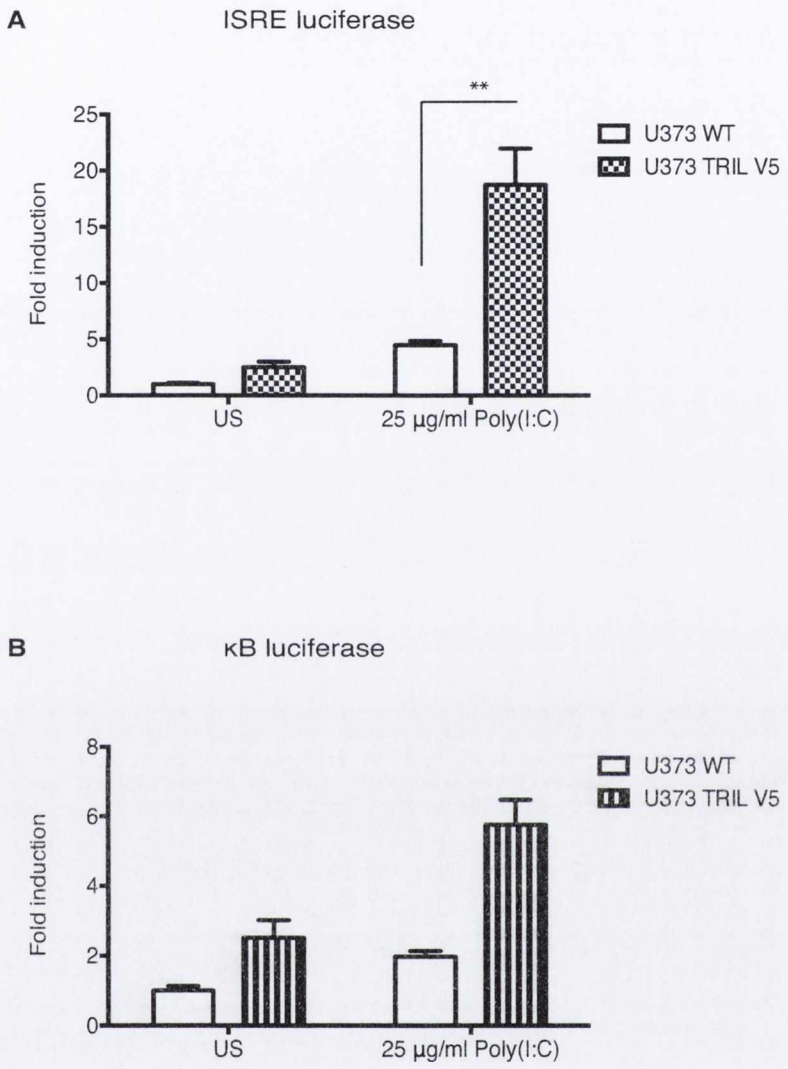

Figure 3.13 Stably overexpressed TRIL in the U373 cell line enhances Poly(I:C) induced κB and ISRE luciferase activity

U373 TRIL-V5 stable cells were plated in 24 well plates (0.1 x 10^6 cells/ml) and upon 24 h of incubation transiently transfected with plasmids encoding 80 ng of TK *Renilla* and 160 ng of ISRE **A**, or κB **B**, luciferase. 24 h following transfection cells were stimulated with 25 µg/ml of Poly(I:C) for 24 h. Lysates were analysed for luciferase activity. Results were normalised to *Renilla* luciferase and represented as fold stimulation over non-stimulated controls. Data are represented as the mean ± SD of one experiment representative of three independent experiments, each carried out in triplicate **, $p<0.01$.

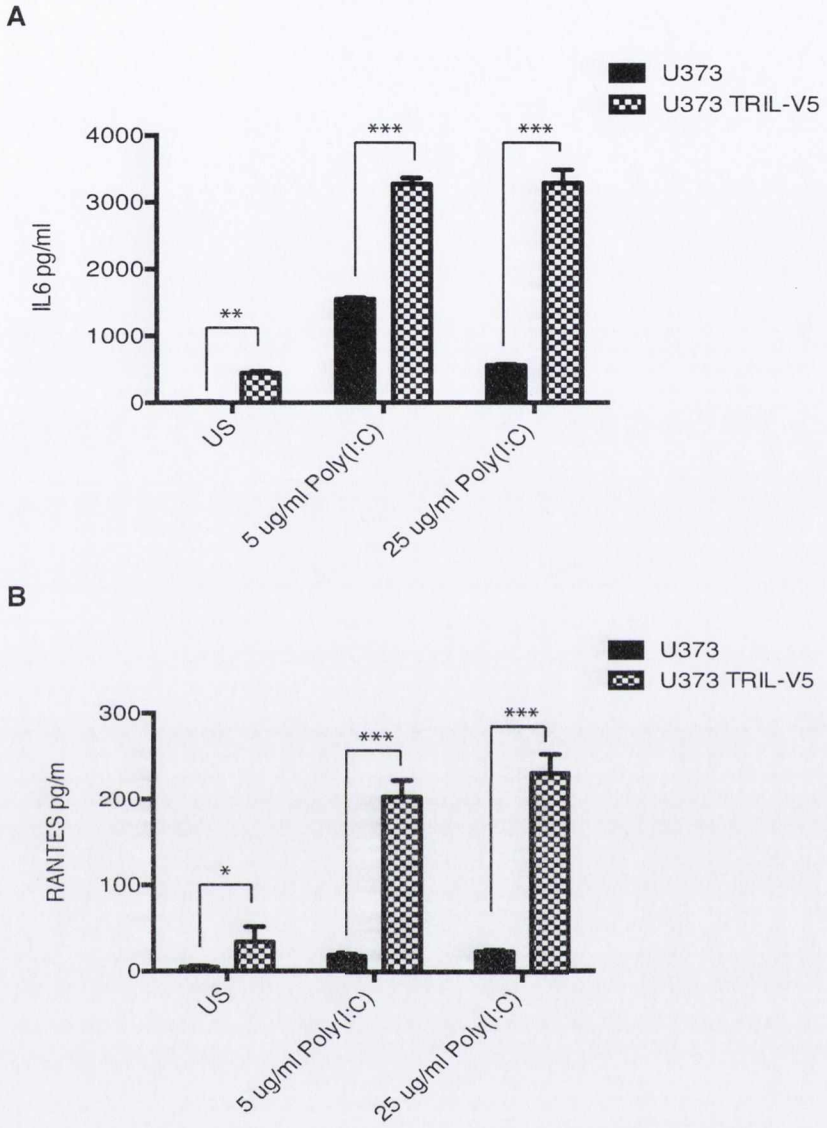

Figure 3.14 U373/TRIL enhanced IL6 and RANTES production in response to Poly(I:C) stimulation

U373 WT and U373 cells stably expressing TRIL-V5 (U373 TRIL-V5) were seeded in 24 well plates at 0.1 x 10^6 cells/ml. 24 h later cells were stimulated using various concentrations of Poly(I:C) as indicated above. 24 h following stimulation supernatants were removed and assayed by ELISA for IL6 **A**, or RANTES **B**, production. Results are expressed as mean ± SD for triplicate determinants and representative of three independent experiments, each carried out in triplicate. ***, $p<0.001$, **, $p<0.01$, *,$p<0.05$.

3.2.4 TRIL-TLR3 interaction studies

Following on from the data demonstrating the impact of TRIL on the TLR3 signalling pathway, I next aimed to establish if TRIL could also associate with TLR3.

In order to address this, I carried out a coimmunoprecipitation (co-IP) study using U373 cells endogenously expressing TRIL, transfected with plasmid encoding Flag-tagged TLR3. As indicated in Figure 3.15 endogenous TRIL was capable of binding with an overexpressed Flag-tagged TLR3 in the human astrocytoma cell line U373 (Fig. 3.15 top panel, indicated by a frame). The control examination of both endogenous TRIL and transiently transfected TLR3-Flag expression levels was performed by immunoblotting for TRIL (Fig. 3.15 middle panel) and Flag (Fig. 3.15 bottom panel), respectively.

As it was shown earlier, TRIL is localised intracellularly in the U373 cells. In order to evaluate the specificity of demonstrated TLR3-TRIL association, I next decided to examine the possible TRIL-TLR2 interaction using the human U373 cell line, as in contrast to expressed in the endosomal compartments TLR3, TLR2 can be exclusively found at the plasma membrane. As it can be seen from the Figure 3.16, endogenous TRIL can be detected when immunoblotted for TRIL, both after pulling down itself as well as directly in the lysates (Fig. 3.16 bottom left and right panel). The expression level of transiently transfected TLR2-Flag encoding plasmid was also examined (Fig. 3.16 top left panel, lane 6). Figure 3.16 clearly demonstrates that TRIL does not co-immunoprecipitate with TLR2-Flag in the U373 cells. No band was detected when blotting for Flag following co-IP using anti-TRIL antibody (Fig. 3.16 top panel, lane 4).

An additional confocal analysis was carried out to further corroborate the lack of an interaction between TRIL and TLR2. THP-1 cells, which similarly to U373s demonstrated earlier an intracellular localisation of TRIL, were transiently transfected with plasmids encoding RFP tagged TRIL and Flag tagged TLR2. Figure 3.17 demonstrates that when co-expressed TRIL-RFP and TLR2-Flag do not co-localise in THP-1 cells, which further verifies that TRIL is incapable of direct interaction with TLR2. A control staining was performed in order to confirm the specificity of both primary

and secondary antibodies used for TLR2 visualisation (Fig. 3.18, panel A-C). TRIL-RFP expression was also examined prior to use (Fig. 3.18, panel D).

In addition to co-IP experiments, interaction of TRIL and TLR3 was also investigated by confocal microscopy imaging. Based on preliminary experiments showing very strong TRIL-TLR3 association in the human astrocytoma cell line following immunoprecipitation with TRIL, I decided to carry out further microscopy studies using U373 cells. The presence of basally expressed TLR3 in those cells allowed me to investigate an interaction between endogenous TLR3 with over-expressed TRIL-RFP. A plasmid encoding TRIL with a C-terminal RFP tag was transiently transfected into the U373 cells. Co-localisation (marked in yellow) of TRIL and TLR3 was detected in most of the regions, where both of these proteins were strongly expressed (Fig. 3.19). The specificity of both primary and secondary antibody used for detection of endogenous TLR3 was examined by performing appropriate control staining (Fig. 3.20, panel A-C). The TRIL-RFP expression was also validated by generation of an adequate control (Fig. 3.20, panel D).

Overall these data conclusively demonstrate that TRIL is capable of direct interaction with endosomal TLR3 but it does not bind to TLR2 present at the plasma membrane in the examined human U373 and THP-1 cell line.

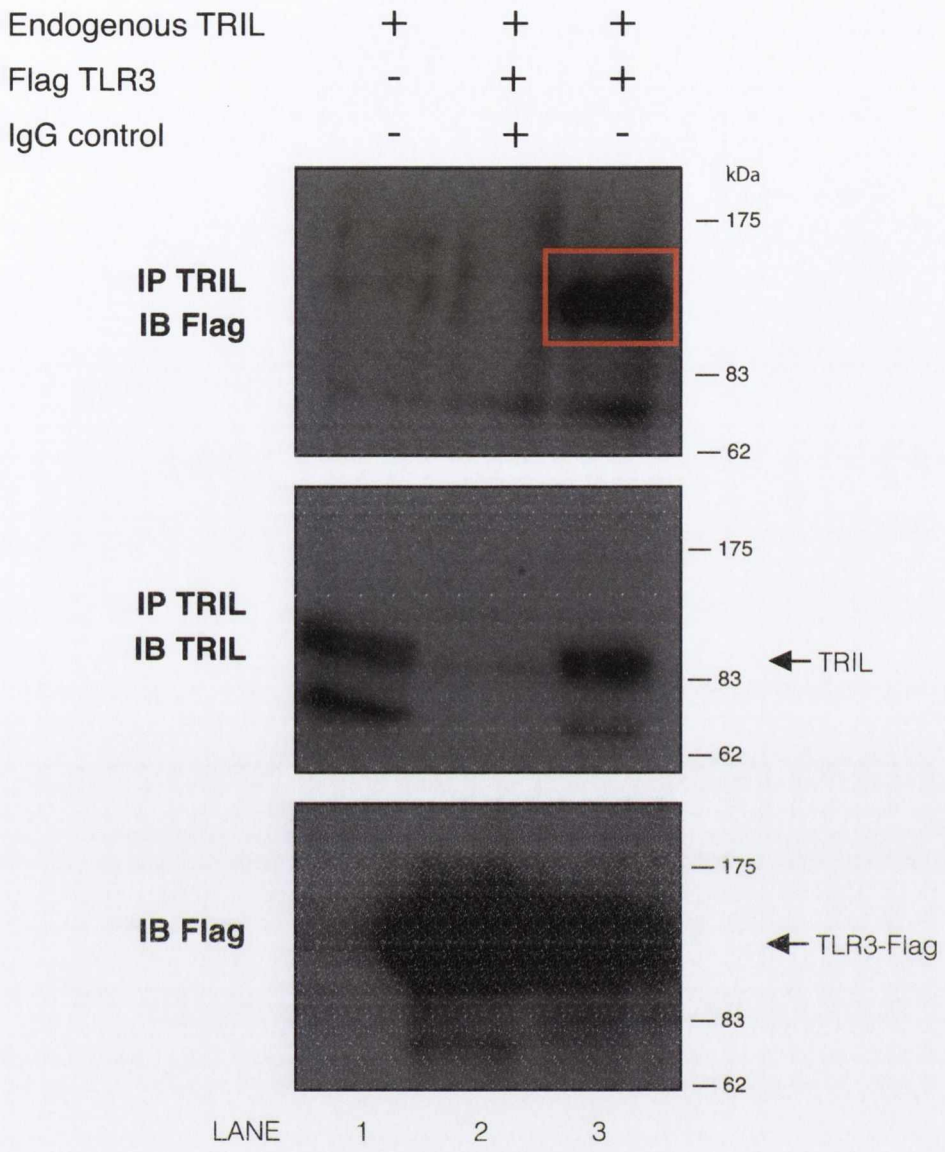

Figure 3.15 TRIL interacts with TLR3

U373 cells seeded at 0.2 x 10^6 cells/ml in 10 cm dishes were transiently transfected with plasmid encoding Flag-tagged TLR3 (3 µg). 48 hours following transfection cells were lysed. Samples of cell lysates were used to determine the endogenous TRIL and TLR3 expression levels (middle and lower panel, TRIL and TLR3 bands are indicated by arrows). The remainder was immunoprecipitated for 24 h at 4 °C with agarose beads pre-coupled either with anti-TRIL (lanes 1 and 3) or with an IgG control antibody (lane 2). This result represents four independent experiments.

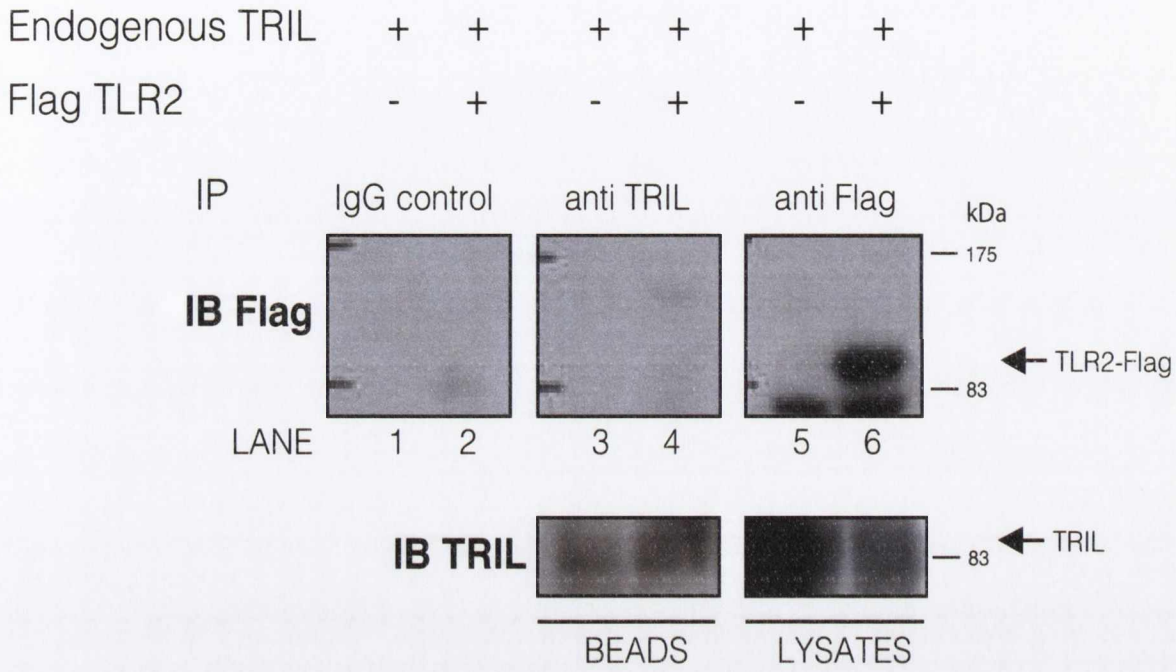

Figure 3.16 Endogenous TRIL does not co-immunoprecipitate with TLR2-Flag

U373 cells cells seeded in 10 cm dishes (0.2 x 10^6 cells/ml) were transiently transfected with 3 µg of TLR2-Flag expressing plasmid. 48 h following transfection cells were lysed. A portion of whole cell lysate from each sample was removed and blotted for endogenous TRIL (bottom, right panel). The remainder was co-immunoprecipited for 24 h at 4 °C with anti-Flag (top, right panel), anti-TRIL (top, middle panel) or an IgG control (top, left panel) pre-coupled to agarose beads. Beads were then washed three times and analysed by Western blotting using either anti-Flag or anti-TRIL antibodies respectively. This result represents three independent experiments.

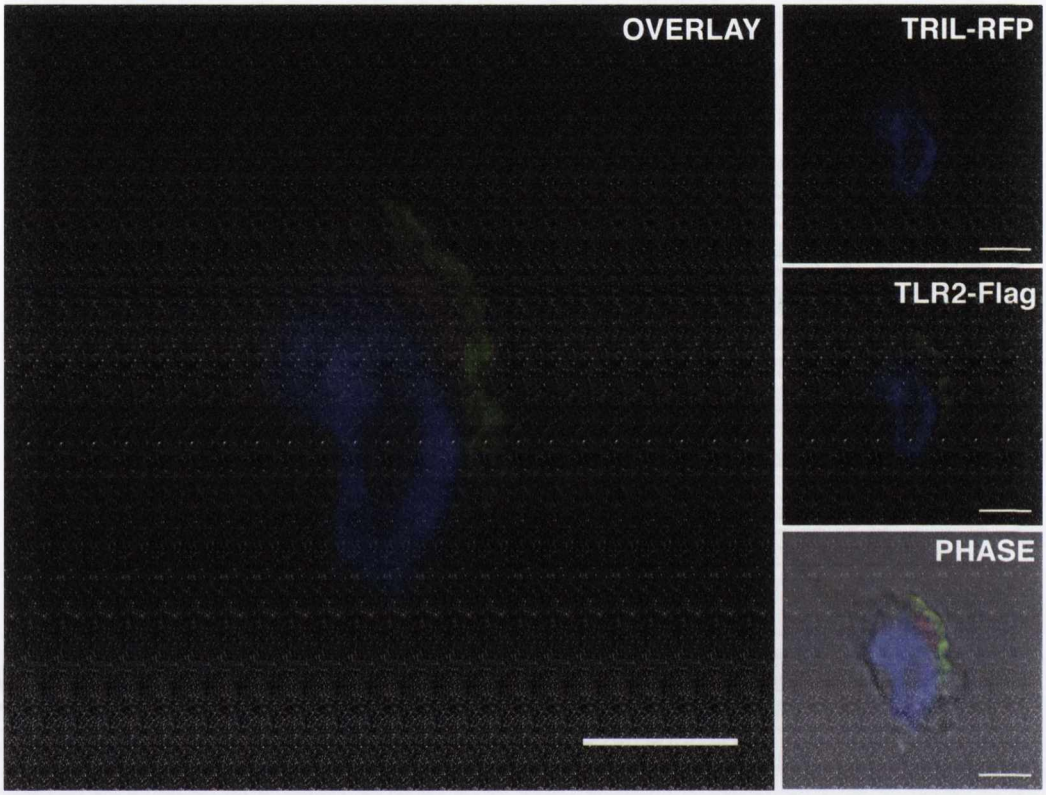

Figure 3.17 TRIL does not co-localise with TLR2 in the THP-1 cell line

THP-1 cells were cultured at 1 x 10^6 cells/ml in 6-well plates. Cells were transfected with 1 µg of TLR2-Flag and/or 1 µg of TRIL-RFP (red) respectively. 24 h later cells were transferred to slides pre-treated with fibronectin. Cells were then fixed, permeabilised and stained using primary anti-Flag and secondary Alexa-488 (green) antibodies. Mounting solution with nuclei dye DAPI (blue) was used prior to viewing with a Point Scanning Confocal Microscope with a heated stage (Olympus FV1000 LSM Confocal Microscope, (NA, 1.4; 60x)). Results are representative of four separate experiments. Scale bars indicate 5 µM.

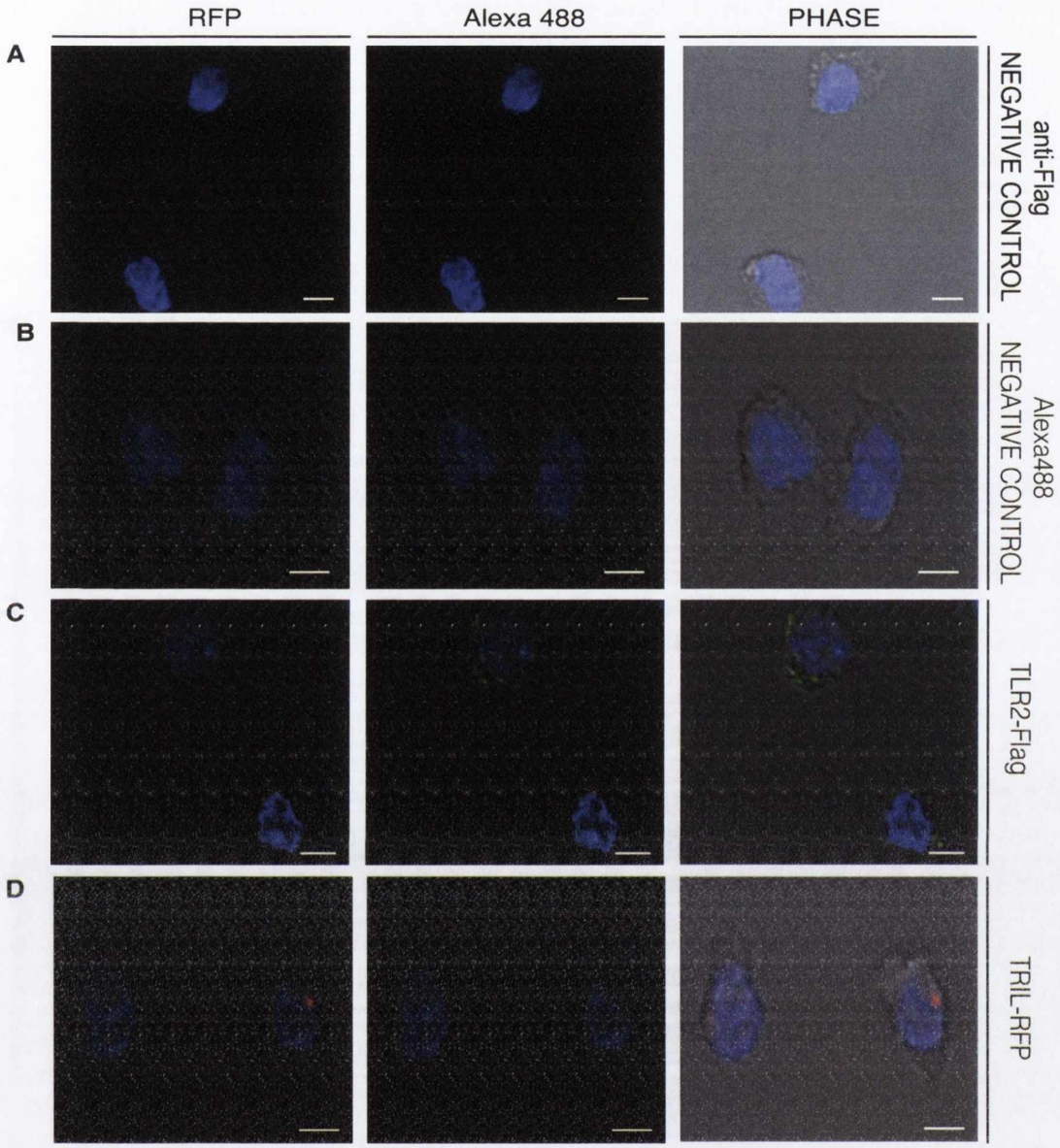

Figure 3.18 TRIL-RFP and TLR2-Flag expression and specificity of anti-Flag antibody staining controls in THP-1 cells

THP-1 cells were cultured at 1 x 10^6 cells/ml in 6-well plates. Cells were transfected with 1 µg of TLR2-Flag (**C**, green) or 1 µg of TRIL-RFP (**D**, red) expressing plasmid respectively. 24 h later cells were transferred to slides pre-treated with fibronectin. Cells were then fixed, permeabilised and stained using primary anti-Flag and secondary Alexa-488 (green) antibodies. Specificity of primary and secondary antibody was examined by staining with ether primary anti-Flag (panel **A**) or secondary Alexa-488 (panel **B**) antibody alone. Mounting solution with DAPI was used prior to taking images with a Point Scanning Confocal Microscope (Olympus FV1000 LSM Confocal Microscope, (NA, 1.4; 60x). Scale bars indicate 5 µM.

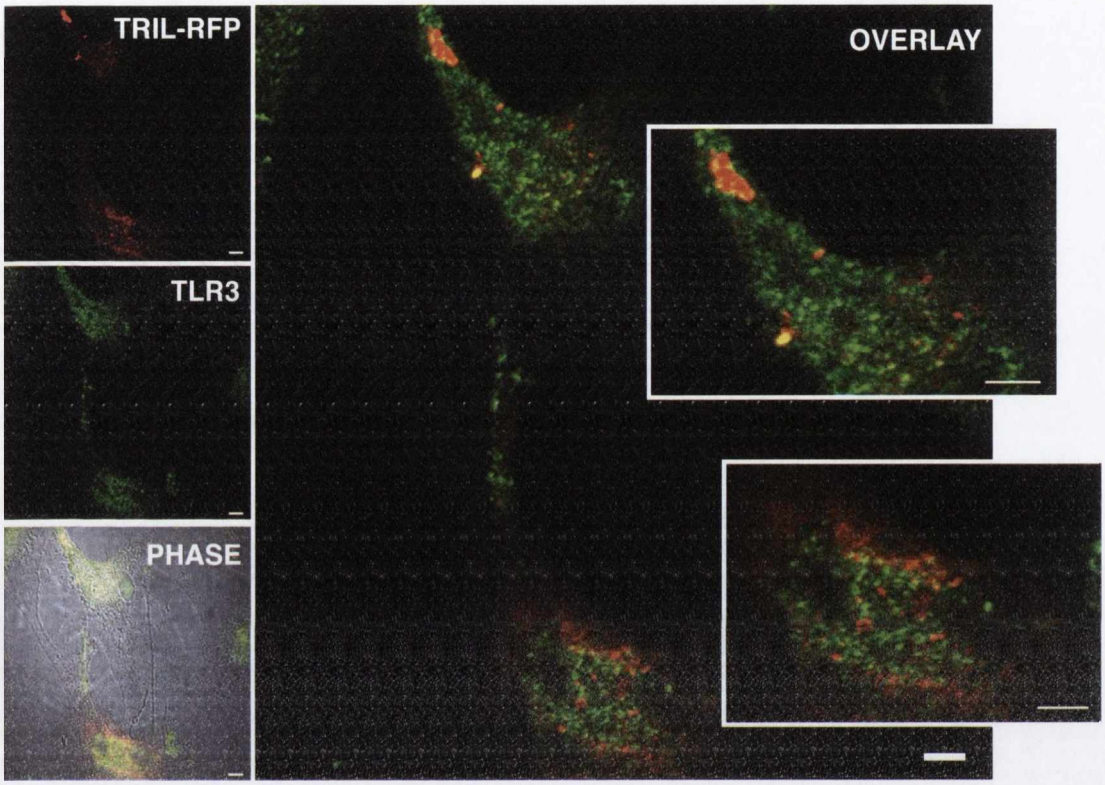

Figure 3.19 TRIL-RFP co-localises with endogenous TLR3 in U373 cell line

U373 cells (0.1 x 10^6 cells/ml) were plated on Poly-L-Lysine treated cover slips. 24 h later cells were transfected with 1 μg of TRIL-RFP (red) expression plasmid and incubated for another 24 h. U373 cell were then stimulated using 25 μg/ml of Poly(I:C) for 2 h, permeabilised and fixed prior to staining with primary goat anti-human TLR3 antibody followed by Alexa-488 secondary antibody (green). Slides were mounted and the Olympus FV1000 LSM Confocal Microscope, (NA, 1.4, 60x) was used to take images. Results are representative of five independent experiments. Scale bars indicate 5 μM.

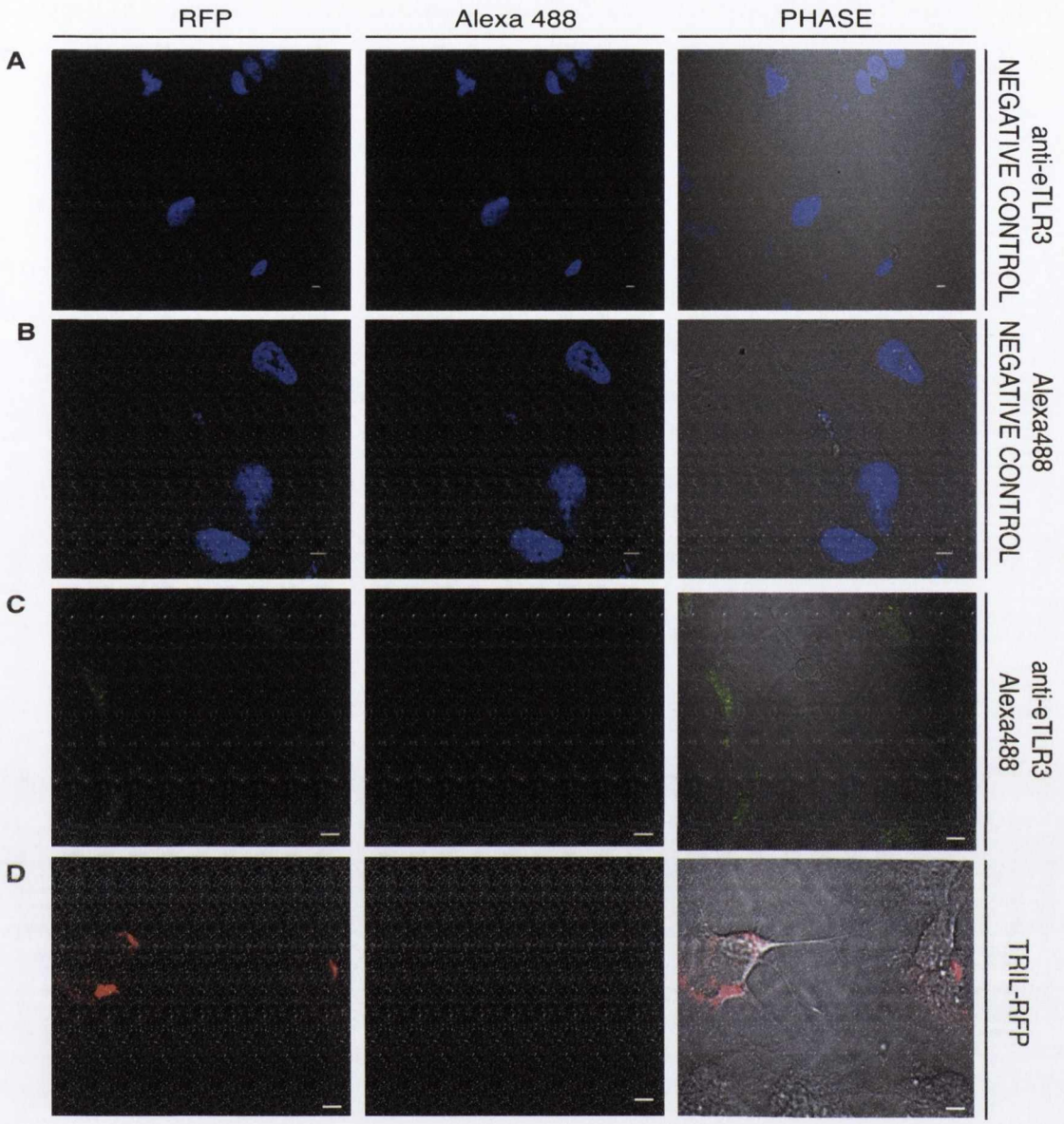

Figure 3.20 TRIL-RFP expression and specificity of anti-TLR3 antibody staining in the U373 cell line

U373 cells (0.1 x 10^6 cells/ml) were plated on 6 well plates containing Poly-L-Lysine treated cover slips. 24 h later cells were transfected with 1 µg of TRIL-RFP expression plasmid (**D**, red) and incubated for another 24 h. U373 cells were then stimulated using 25 µg/ml of Poly(I:C) for 2 h, permeabilised and fixed prior to staining with primary goat anti-human TLR3 antibody and Alexa 488 secondary antibody (**C**, green). The specificity of primary and secondary antibody was examined by staining with ether primary anti-TLR3 or secondary Alexa-488 antibody alone (panel **A** and **B**, respectively). Slides were mounted and then analysed using a Point Scanning Confocal Microscope Olympus FV1000 LSM Confocal Microscope, (NA, 1.4; 60x). Scale bars indicate 5 µM.

3.2.5 Examining the TRIL-TLR3 interaction following stimulation with Poly (I:C)

Co-IP studies and confocal analysis revealed direct association of TRIL with TLR3. I next aimed to determine if stimulation with Poly(I:C) impacts on this interaction.

A Co-IP assay with anti-TRIL antibody followed by Western blot analysis indicated positive expression of TRIL, which was slightly increased upon Poly(I:C) stimulation (Fig. 3.21 A, bottom panel, lane 2 and 4). When blotted with anti-Flag antibody, corresponding lysates showed similar amounts of TLR3 expressed in each of the samples, prior and post stimulation (Fig. 3.21 A, middle panel, lane 3 and 4). The top panel in Figure 3.21 A, representing a pull down using anti-TRIL antibody followed by detection with anti-Flag antibody, indicates that a fairly strong interaction between TRIL and TLR3 observed at the basal level (Fig. 3.21 A, lane 2), can be further enhanced by stimulation with Poly(I:C) (Fig. 3.21 A, lane 4).

In order to confirm the co-IP analysis showing an increase in TRIL-TLR3 interaction upon stimulation with Poly(I:C), an additional densitometry analysis was carried out using ImageJ software. Generated relative intensity values were consistent with the previous observation and further supported enhancement in TRIL-TLR3 complex formation following stimulation with Poly(I:C) (Fig. 3.21 B).

A time-dependent increase in TRIL-TLR3 interaction was also investigated by qualitative and quantitative confocal microscopy studies. U373 cells stably expressing TRIL-V5 were stimulated using Poly(I:C) for the indicated times, ranging from 1 h to 24 h. Cells were next fixed, permeabilised and stained using primary anti-TLR3 and/or anti V5-FITC antibody followed by a secondary Alexa-647 antibody for TLR3 visualisation. Qualitative analysis of generated images indicated an increase in TRIL-TLR3 co-localisation (circled) during the time course (Fig. 3.22 A, small images). In order to obtain a better quantification of the association between TRIL and TLR3, an additional more rigorous quantitative study was carried out. An average of 18 images were generated for each time point, in three independent experiments, and individually analysed using the FluoView software. Background noise can be misleading and result in false-positive co-localisation events, therefore prior to quantitative analysis a background-correction was conducted (Fig. 3.22 A, large images). Generated images

were further examined in order to establish average values for Pearson's Correlation Coefficient (PCC) and Overlap Coefficient (OC). PCC is a commonly used measure for the correlation between two variables, in this case separate signals generated from two channels, CH1 and CH2 corresponding to Alexa-647 and FITC, respectively. Values assigned to correlation range from -1, indicating absolute exclusion, to +1 representing perfect co-localisation, with 0 signifying random correlation. An Overlap Coefficient, similarly to PCC, also quantifies correlation, but in contrast to Person's Correlation Coefficient it is strongly influenced by the ratio of CH1 to CH2 signals. Therefore OC incorporate and analyse both the correlation and proportion between channels and value them from 0, for low co-localisation to +1, for a strong interaction. Figure 3.22 B representing average values of Pearson's Correlation Coefficient and Overlap Coefficient for each time point, demonstrates quite strong interaction between TRIL and TLR3 at the basal level (both PCC and OC are close to 1) which is further enhanced by Poly(I:C) stimulation in a time dependent manner, reaching statistical significance at the 24 h time point, when compared to unstimulated cells.

In order to additionally characterise the extent to which the two signals (CH1 and CH2) overlap each other, an additional Overlap Coefficient (OC) value was generated separately for both CH1 and CH2 channels. OC values ranging from 0 to 1 represent the ratio of CH1/CH2 and CH2/CH1 co-localisation for the CH1 and CH2 channels, respectively. As can be seen in Figure 3.22 C, the Overlap Coefficient for both channels increases during the time course, reaching a value close to 1 upon 24 h stimulation with Poly(I:C). This demonstrated that at the 24 h time point the ratios between CH1/CH2 and CH2/CH1 were nearly equal, indicating that nearly all of the TRIL and TLR3 positive signals were co-localised. All values generated by quantity confocal analysis are presented in frames next to corresponding images (Fig. 3.22 A).

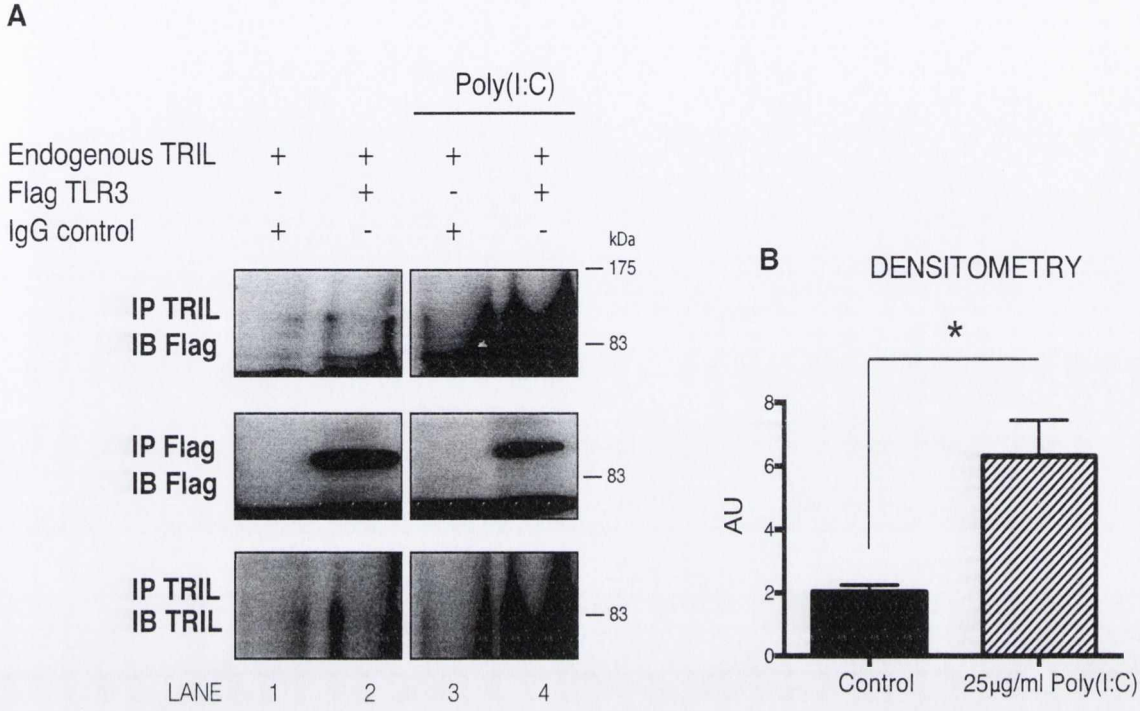

Figure 3.21 Interaction between TRIL and TLR3 increases following Poly(I:C) stimulation

A, U373 cells (0.2 x 10^6 cells/ml) were seeded in 10 cm dishes and left to rest for 24 h. Cells were transfected with 3 µg of plasmid encoding TLR3-Flag. 48 h following transfection cells were stimulated with 25 µg/ml Poly(I:C) prior to lysis. A portion of whole cell lysates was removed from each sample and blotted for Flag-TLR3 (middle panel). The remainder was co-immunoprecipitated for 24 h at 4°C with agarose beads pre-coupled with anti-TRIL antibody 24 h prior to use. Beads were washed three times and analysed by Western blot using either anti-Flag (top panel) or anti-TRIL (bottom panel) antibody. **B**, An additional densitometry analysis was carried out using ImageJ software to establish the intensity of bands indicating endogenous TRIL-TLR3 Flag interaction prior to and following stimulation with 25 µg/ml of Poly(I:C). Relative intensity values (arbitrary units) were calculated relative to time 0. Results are representative of three separate experiments **A**, or represent as the mean value ± SEM generated from three independent exepriments **B**. *, $p < 0.05$.

A

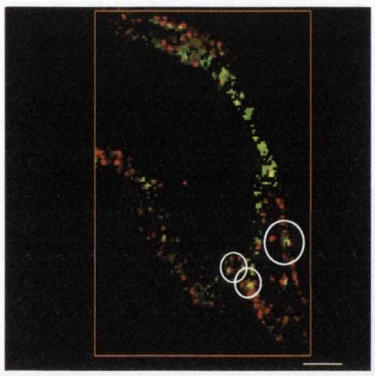

Pearson's Correlation Coefficient (PCC)	**0.794**
Overlap Coefficient (OC)	**0.795**
Corelation Coefficient for chanel 1 (CO1)	**1.0**
Corelation Coefficient for chanel 2 (CO2)	**0.935**

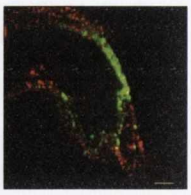

UNSTIMULATED

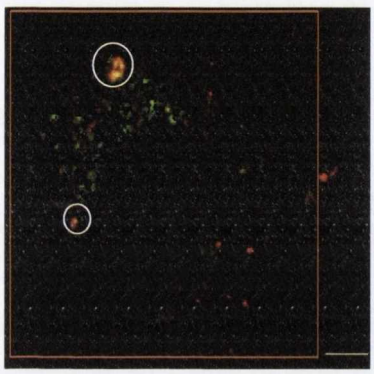

Pearson's Correlation Coefficient (PCC)	**0.761**
Overlap Coefficient (OC)	**0.762**
Corelation Coefficient for chanel 1 (CO1)	**0.824**
Corelation Coefficient for chanel 2 (CO2)	**0.415**

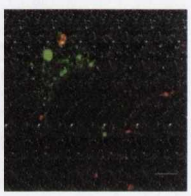

1 HOUR
25 µg/ml Poly(I:C)

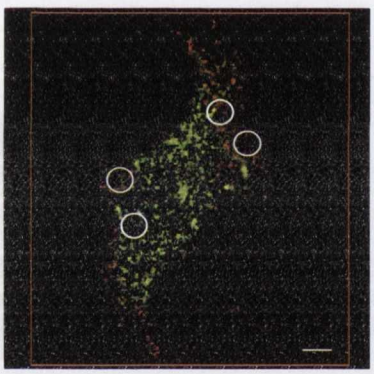

Pearson's Correlation Coefficient (PCC)	**0.891**
Overlap Coefficient (OC)	**0.892**
Corelation Coefficient for chanel 1 (CO1)	**1.0**
Corelation Coefficient for chanel 2 (CO2)	**1.0**

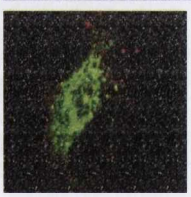

4 HOURS
25 µg/ml Poly(I:C)

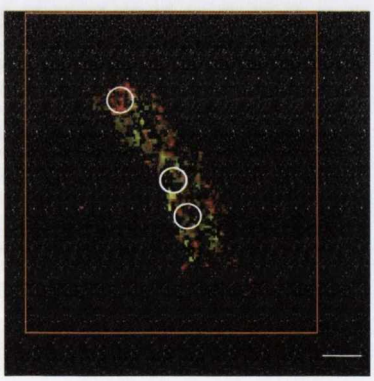

Pearson's Correlation Coefficient (PCC)	**0.798**
Overlap Coefficient (OC)	**0.798**
Corelation Coefficient for chanel 1 (CO1)	**0.809**
Corelation Coefficient for chanel 2 (CO2)	**0.985**

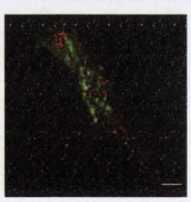

24 HOURS
25 µg/ml Poly(I:C)

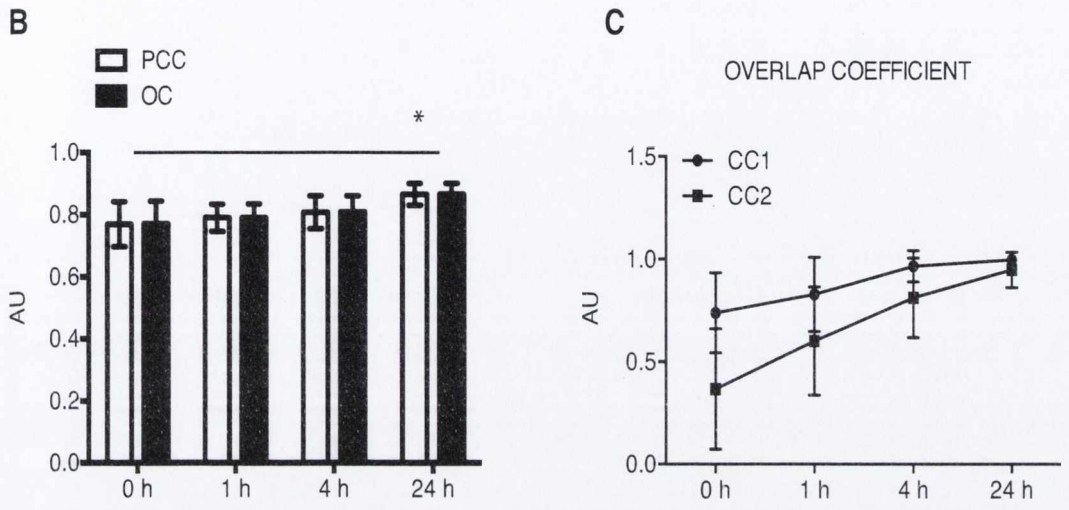

Figure 3.22 TRIL co-localisation with TLR3 is enhanced by Poly(I:C) stimulation in the U373 cell line

U373 cells stably expressing TRIL-V5 (0.1 x 10^6 cells/ml) were plated on Poly-L-lysine treated cover slips and left to rest for 24 h. Cells were stimulated with 25 μg/ml Poly(I:C) for the indicated time points (form 1 h to 24 h) fixed and permeabilised prior to staining with primary anti-TLR3 and/or anti-V5-FITC antibody followed by secondary Alexa-647. A Point Scanning Confocal Microscope (Olympus FV1000 LSM Confocal Microscope, (NA, 1.4; 60x) was used to analyse samples. Using the FluoView Olympus FV1000 LSM Confocal Microscope software, background noise was reduced (large images) and an average of 18 images generated in three independent experiments was further analysed for each time point separately in order to establish average values for Pearson's Correlation Coefficient (PCC), Overlap Coefficient (OC) and additional Correlation Coefficient (CO) for each channel individually (CH1 and CH2, respectively). An average values for each time points were represented in frames **A**, and next plotted on graphs (**B**, PCC and OC); (**C**, CO for channels 1 (CH1) and 2 (CH2) respectively). Values represent an average of 18 images generated for each time point in three independent experiments. The value for 24 h Poly(I:C) stimulation time point was compared with unstimulated cells (0 hours Poly(I:C) time point) and the increase in both PCC and OC was found statistically significant at 24 h ($p<0.02$, Mann-Whitney U test).

3.2.6 TRIL-Poly(I:C) interaction studies

In the initial studies on TRIL, the protein was demonstrated to directly interact with both TLR4 and its ligand LPS (Carpenter et al, 2009). Further analysis revealed that TRIL is also capable of binding with the TLR3, which is further enhanced by the Poly(I:C) stimulation. Based on that, I decided to test if similar to TLR4 and LPS, TRIL is also capable of association with TLR3 agonist, Poly(I:C). Potential interaction of TRIL with Poly(I:C) was examined by co-IP studies using the U373 cell line, constitutively expressing TRIL and the TLR3 adaptor protein TRIF. TRIF was shown to mediate recognition of Poly(I:C) in complex with the cytosolic helicases DDX1-DDX21-DHX36 (Zhang et al, 2011b). As the use of the anti-TLR3 antibody turned out to be challenging, due to the limitation of the antibody, I decided to use TRIF as a control for the purpouse of this study instead. Whole cell lysates obtained from the U373 cells were centrifuged and cell debris was removed. As can be seen from Fig. 3.23 pull-down with the streptavidin coated beads followed by immunoblotting with anti-TRIL antibody resulted in a band representing potential Poly(I:C)-TRIL association (Fig. 3.23, top panel, lane 1, marked with a red frame). Similarly, the co-IP followed by immunoblotting with anti-TRIF antibody resulted in a band indicating interaction of biotin labelled Poly(I:C) and TRIF (Fig. 3.23, bottom panel, lane 1, indicated by a yellow frame). Both endogenous TRIL and TRIF were detected in lysates devoid of cell debris used subsequently for pull-down, as well as in the whole cell lysates (WCL), when probed using anti-TRIL and anti-TRIF antibodies (Fig. 3.23 lane 2 and 3, top and bottom panel, respectively). An additional co-IP control using uncoated agarose beads and biotin labelled Poly(I:C) demonstrated an absence of any unspecific bands following immunoblotting with anti-TRIL antibody (Fig. 3.23, top panel, lane 4) and anti-TRIF antibody (Fig. 3.23, bottom panel, lane 4), emphasizing the specificity of detected bands indicating the Poly(I:C)-TRIL and Poly(I:C)-TRIF interaction.

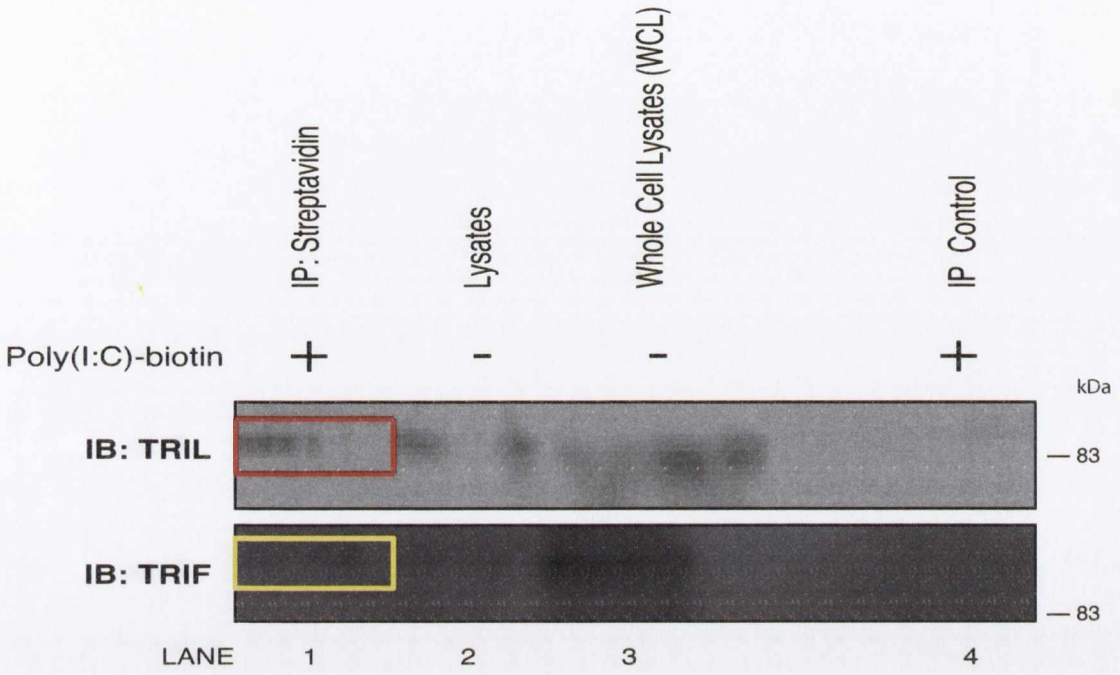

Figure 3.23 Endogenous TRIL co-immunoprecipitates with biotinylated Poly(I:C) in U373 cells

U373 cells were plated at concentration of 0.2 x 10^6 cells/ml in 10 cm dishes and left to rest for 24 hours. Following incubation, supernatants were removed and cells lysed in an ice-cold salt lysis buffer. A portion of a whole cell lysate from each sample was removed and blotted for endogenous TRIL or TRIF (lane 3 top and bottom panel, respectively). The cell debris was next discarded following centrifugation and lysate samples were blotted for endogenous TRIL and TRIF (lane 2 top and bottom panel, respectively). The remaining cell lysates were incubated with 1 μg of 5'-biotinylated Poly(I:C) and pre-washed agarose beads coated with streptavidin (50% (w/v)) for 2 h at 4°C. Beads were then analysed by Western blot using either anti-TRIL or anti-TRIF antibodies, lane 1 top and bottom panel, respectively. Uncoated agarose beads (50% (w/v)) incubated for 2 h at 4°C with 1 μg of 5'-biotinylated Poly(I:C) served as a negative control, lane 4. This result represents two independent experiments.

3.2.7 Investigating how loss of TRIL impacts TLR3 signalling in U373 cell line

The initial overexpression studies demonstrated that TRIL enhances ISRE and κB luciferase activity as well as cytokine production following stimulation with Poly(I:C). I decided to investigate that further and examine if knockdown of endogenous TRIL would cause an opposite effect. To this end, three distinct shRNA specific to TRIL were obtained and used to generate stable U373/TRIL knockdown cell lines. One shRNA was a TET-inducible TRIL shRNA, whereas the remaining two expressed shRNA TRIL in a constant manner. QPCR analysis of TRIL expression following induction of the TET-inducible shRNA specific to TRIL with doxycycline demonstrated a clear reduction of TRIL mRNA level compare to untreated control cells (Fig. 3.24). Unfortunattly, observed reduction in TRIL expression did not reach statistical significance. In order to further optimise the use of the selected shRNA, U373 cells stably expressing TET-inducible shRNA-TRIL-RFP were treated with two different concentrations of doxycycline, 1 μg/ml and 2 μg/ml. The higher concentration of doxycycline provided a better knockdown effect in U373/shRNA-TRIL-RFP cells when examined by Western blot (Fig. 3.25) and confocal microscopy (Fig. 3.26) assays, therefore these conditions were selected as optimal and used in further experiments.

U373/shRNA-TRIL-RFP cells were plated in 24-well plates and treated with 2 μg/ml of doxycycline to induce the expression of shRNA-TRIL. 48 h later both control and doxycycline treated U373 cells were transfected with luciferase constructs expressing an empty vector (pcDNA) or 10 pg/ml of TLR3, prior to 24 h stimulation with Poly(I:C). As shown in Figure 3.27 silencing of TRIL results in a significant reduction of both ISRE luciferase activation (Fig. 3.27 A) and production of RANTES (Fig. 3.27 B). In the stimulated control cells (transfected with an empty vector) a modest inhibitory effect can be seen, which then dramatically increases in cells transiently expressing TLR3.

To confirm that the observed effect is a direct result of TRIL silencing and not an off target effect of shRNA-TRIL-RFP, the mRNA levels of both TRIL and TLR3 proteins were examined in the doxycycline activated U373/shRNA-TRIL-RFP stable cell line. As expected knockdown of TRIL had a dramatic effect on TRIL but not TLR3 expression

levels when examined by QPCR (Fig. 3.28 A and B, respectively). To test whether the presence of doxycycline itself affects the U373/shRNA-TRIL-RFP cells response, an additional U373 cell line stably expressing the non-silencing shRNA encoded by pTRIPZ vector was generated. As shown in Figure 3.29 in which both U373 cells expressing either shRNA specific to TRIL or non-silencing control were treated with doxycycline prior to stimulation with Poly(I:C), addition of the antibiotic does not affect cell response (Fig. 3.29)

To further investigate the specificity of the TRIL silencing effect on the TLR3 mediated pathway, I carried out a luciferase activation assay following stimulation with a wide range of ligands. U373 cells stably expressing TET-inducible shRNA specific to TRIL were transiently transfected with ISRE or κB luciferase constructs following doxycycline treatment. Cells were stimulated with a number of ligands and examined for luciferase activity. Unfortunately U373 shRNA-TRIL cells do not respond to the human TLR7/8 agonist (R848) nor IL1β stimulation when examined for ISRE and κB luciferase activity and the TRIL knockdown effect could only be observed upon Poly(I:C) stimulation (Fig. 3.30 A and B).

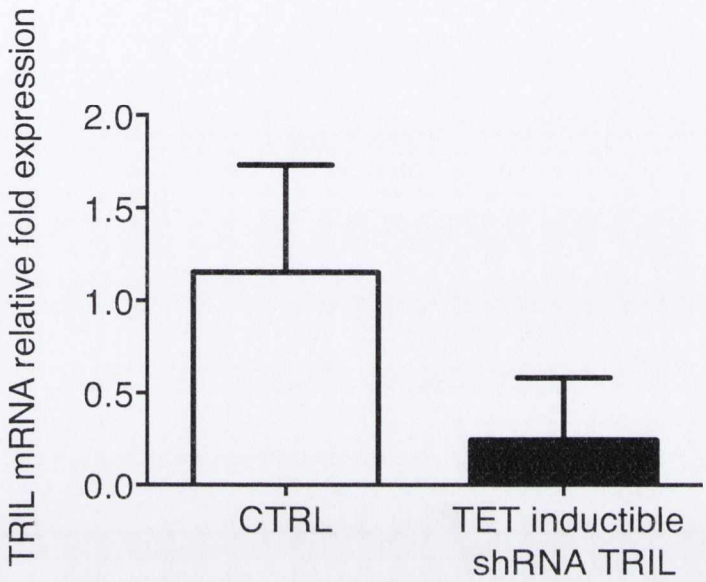

Figure 3.24 Optimisation of stable shRNA TRIL knockdown in U373

U373 cells were transduced using TET-inducible shRNA specific to TRIL. Following transduction step, positive antibiotic selection was performed using puromycin. shRNA-TRIL positive cells (0.1 x 10^6 cells/ml) were seeded in 6 well plates. Cells were next treated with 1 µg/ml of doxycycline for 48 h or left untreated (CTRL), prior to plating. Cells were incubated for additional 24 h followed by isolation of RNA and QPCR analysis for TRIL expression. TRIL mRNA levels were normalised against GAPDH and expressed relative to CTRL (untreated with doxycycline). Data are represented as the mean ± SEM of three independent experiments, all carried out in triplicate.

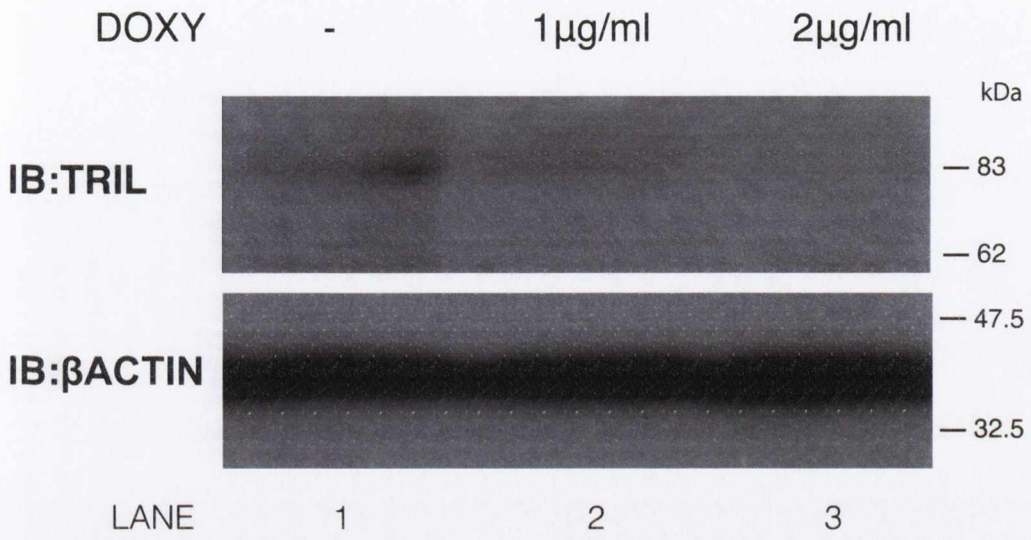

Figure 3.25 Dose dependent doxycycline induced knockdown of TRIL in U373 cells stably expressing TET inducible shRNA specific to TRIL

U373 cells stably expressing an inducible shRNA specific to TRIL were plated at 0.2 x 10^6 cells/ml on 10 cm dishes. Cells were treated with 1 µg/ml or 2 µg/ml of doxycycline for 48 h in order to activate shRNA-TRIL. Cells were lysed and Western blot was carried out using anti-TRIL or anti-β-actin antibodies. Results are representative of two separate experiments.

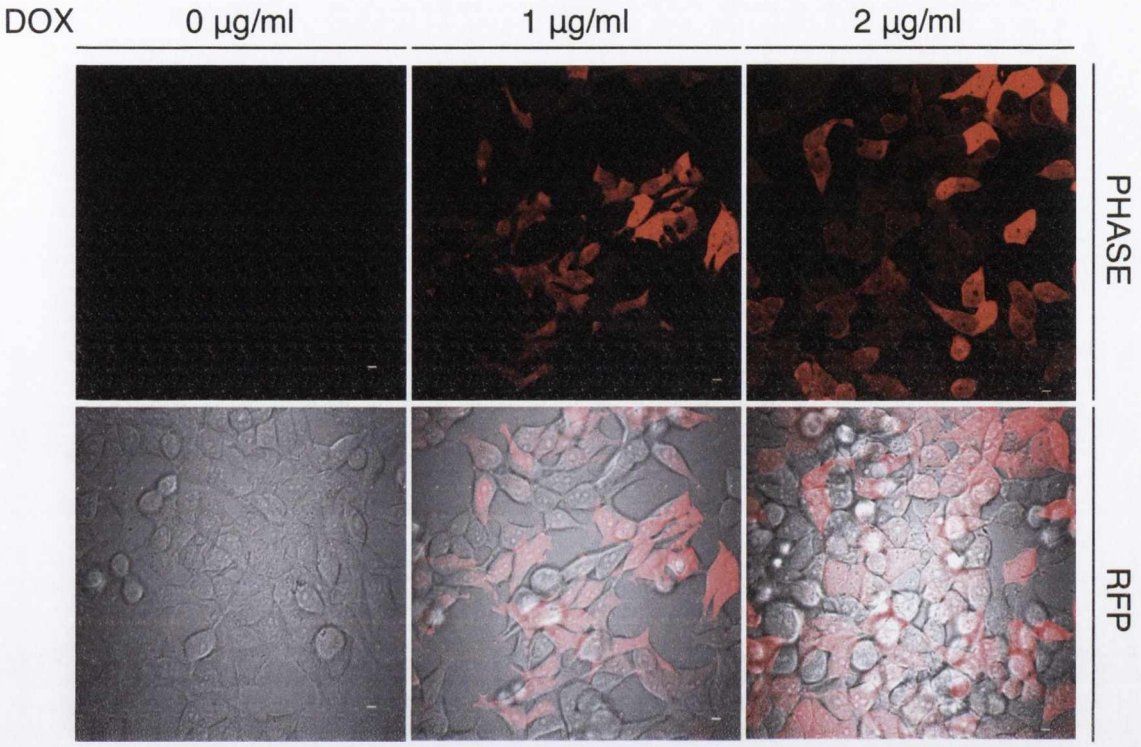

Figure 3.26 Control for doxycycline induced expression of shRNA-TRIL-RFP in U373 cells

U373 cells stably expressing doxycycline-induced RFP tagged shRNA specific to TRIL (0.05 x 10^6 cells/ml) were plated on 35-mm MatTek dishes and left to rest for 24 h. Cells were stimulated with 1 µg/ml or 2 µg/ml of doxycycline for 48 h in order to induce the expression of shRNA-TRIL-RFP. The efficiency of induction was examined by a Point Scanning Confocal Microscope with a heated stage (Olympus FV1000 LSM Confocal Microscope, (NA, 1.4; 60x))

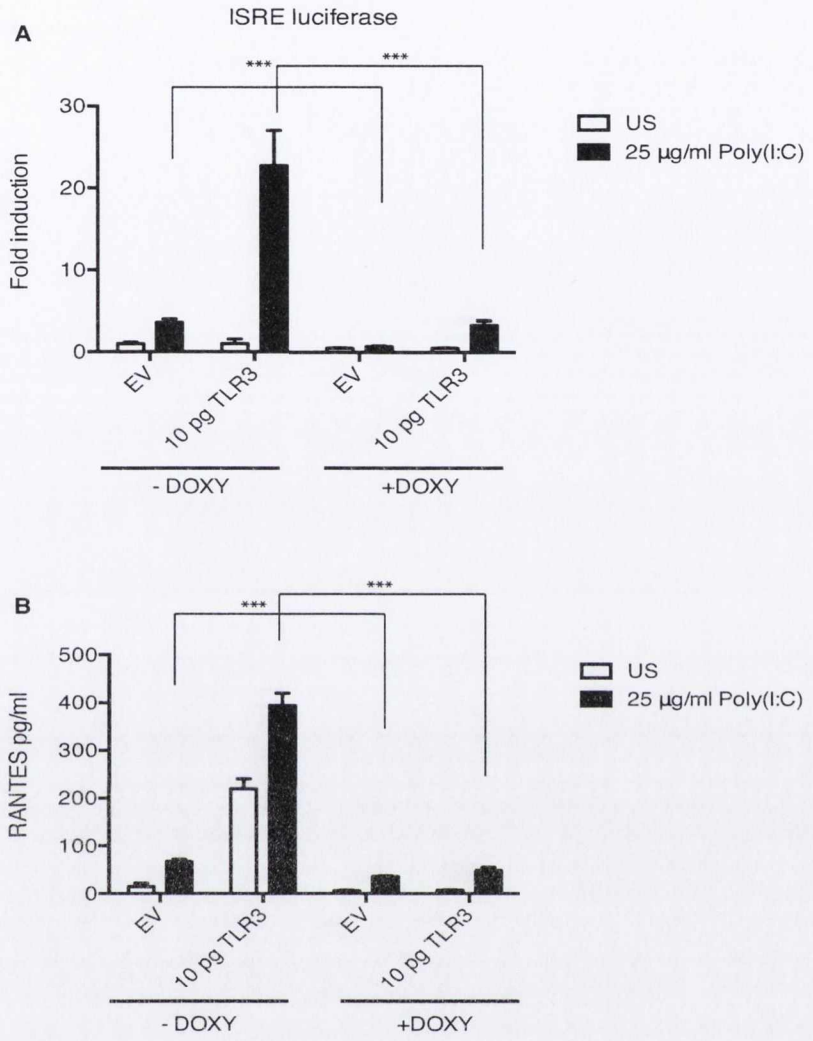

Figure 3.27 Knockdown of TRIL affects ISRE luciferase activity and RANTES production following Poly(I:C) stimulation

U373 cells stably expressing TET inducible shRNA specific to TRIL (0.1 x 10^6 cells/ml) were plated in 24 well plates. shRNA-TRIL was activated using 2 µg/ml of doxycycline. Cells were then transiently transfected with plasmids encoding 80 ng of TK *Renilla* and 160 ng of ISRE luciferase along with plasmids expressing 10 pg of empty vector (EV) or TLR3. 24 h following transfection cells were stimulated with 25 µg/ml of Poly(I:C) for 24 h. Cells were harvested and analysed for reporter gene activity, **A**. Supernatants were collected and examined for RANTES production, **B**. Results were normalised for *Renilla* luciferase activity and represented as fold stimulation over non-stimulated controls. Results are expressed as mean ± SD for triplicate determinants and representative of three independent experiments, each carried out in triplicate. ***, $p < 0.001$; *, $p < 0.05$.

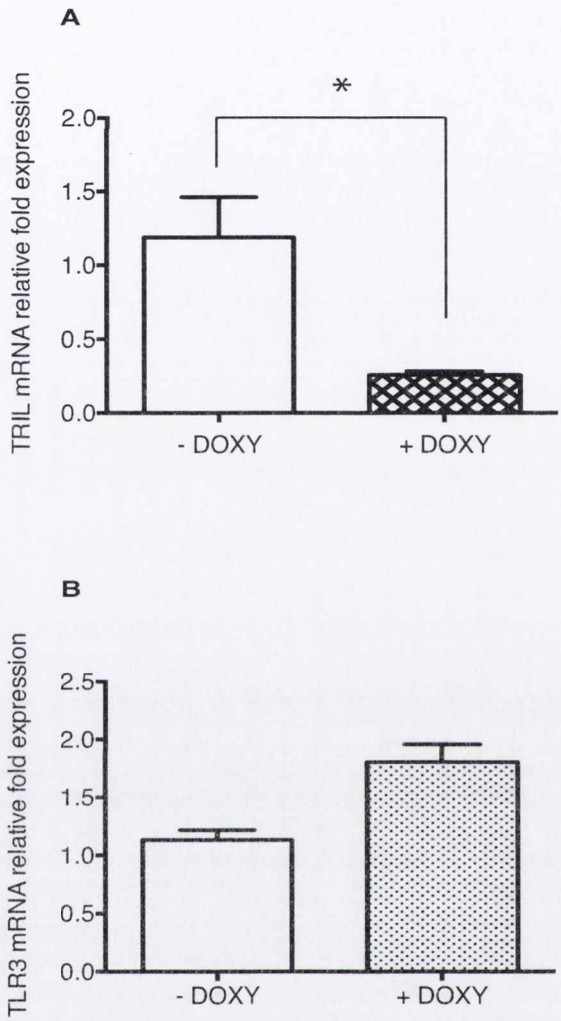

Figure 3.28 TET inducible shRNA specific to TRIL abolishes TRIL but not TLR3 expression in the U373/shRNA-TRIL stable cell line

U373 cells stably expressing TET inducible shRNA-TRIL (0.1 x 10^6 cells/ml) were plated in 12 well plates. Cells were treated with 2 μg/ml of doxycycline for 48 h in order to induce expression of shRNA specific to TRIL. Cells were lysed, followed by RNA extraction. Samples were analysed by QPCR for TRIL **A**, and TLR3 **B**, expression. mRNA levels were normalised against GAPDH and presented relative to CTRL (non doxycycline-treated samples). Results are expressed as mean ± SEM of three **A** or two **B** independent experiments, each carried out in triplicate. *, $p < 0.05$.

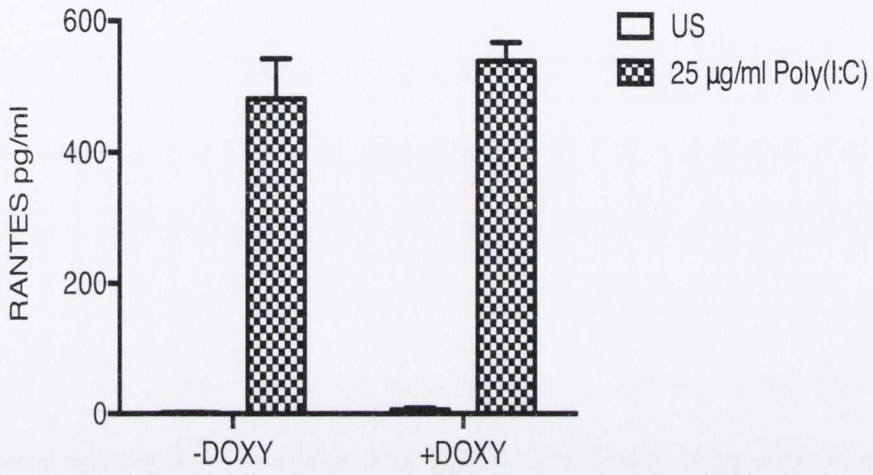

Figure 3.29 Doxycycline does not impact the ability of cells to respond to Poly(I:C) stimulation

U373 cells stably expressing the non-silencing control in pTRIPZ vector were cultured for 48 h, with or without addition of 2 µg/ml of doxycycline. Cells were stimulated for 24 h with 25 µg/ml of Poly(I:C). Supernatants were collected and assayed by ELISA for RANTES production. Results are expressed as mean ± SD for triplicate determinants and representative of three independent experiments, each carried out in triplicate.

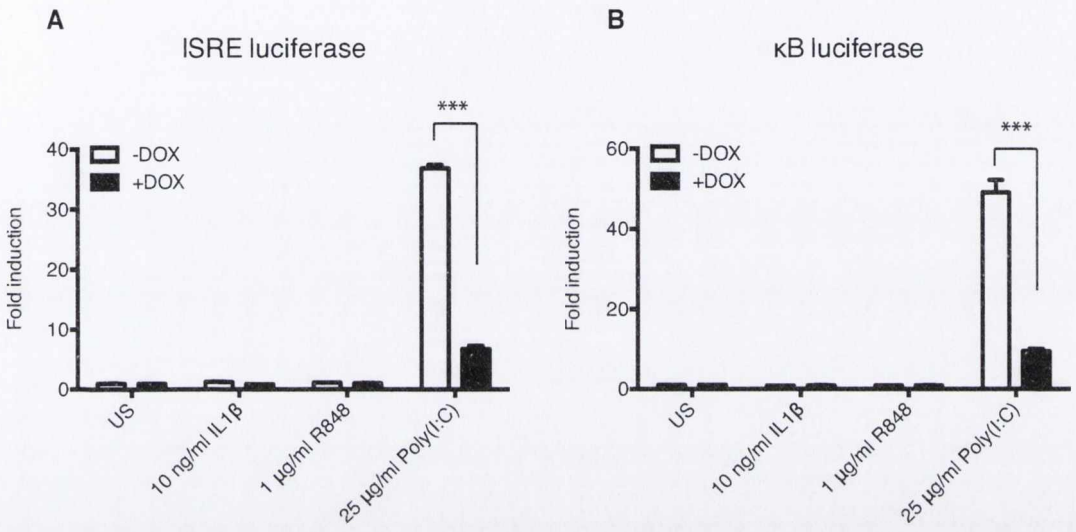

Figure 3.30 Knockdown of TRIL affects ISRE and κb luciferase activity following stimulation with Poly(I:C)

U373 cells stably expressing an inducible shRNA specific to TRIL were plated at 0.1 x 10^6 cells/ml in 24 well plates and were left untreated or stimulated with 2 μg/ml of doxycycline. 24 h later cells were transiently transfected with plasmids encoding 80 ng of TK *Renilla* and 160 ng of ISRE **A**, or κB **B**, luciferase. 24 h following transfection, cells were stimulated for another 24 h with a wide rage of ligands: 25 μg/ml of Poly(I:C), 10 ng/ml of IL1β or 1 μg/ml of R848 or remained unstimulated (US). Following stimulation cells were harvested and analysed for reporter gene activity. Results were normalised for *Renilla* luciferase activity and represented as fold stimulation over non-stimulated controls. Results are expressed as mean ± SD for triplicate determinants and representative of three independent experiments, each carried out in triplicate.

3.2.8 Investigation into the effect of silencing TRIL on TLR1/2 signalling in THP-1 cells

As my attempt to prove the specificity of silencing of TRIL on TLR3 signalling pathway failed in U373 cells due to their restricted responsiveness to TLR ligands, I decided to screen for other way to demonstrate this specificity. Based on previous data indicating a moderate effect of TRIL on the TLR2 response in PBMCs (Carpenter et al, 2009), I decided to further explore these findings. Given the very poor responsiveness of U373 cells to ligands other than Poly(I:C) and LPS and their lack of endogenous TLR2 expression, I decided to use the human THP-1 monocytic cell line to carry out further experiments. Using TET-inducible shRNA specific to TRIL I generated a THP-1/shRNA-TRIL-RFP stable cell line. Reduction of TRIL expression and induction of shRNA-TRIL-RFP following doxycycline treatment was then confirmed in these cells by QPCR (Fig. 3.31) and confocal microscopy analysis (Fig. 3.32), respectively.

In contrast to U373 cells, THP-1 cells express TLR2 but not TLR3, so I investigated cytokine production following Pam3CSK4 and LPS stimulation. TRIL is known to be involved in the TLR4 mediated signalling pathway, therefore stimulation of TLR4 was used as a positive control for the TRIL silencing effect. As shown in Figure 3.33 A, TRIL silencing impacts TLR4 responses to LPS stimulation by reducing TNFα (Fig. 3.33 A) and RANTES (Fig. 3.33 B) production in the THP-1/shRNA-TRIL stable cell line following 3 h and 24 h of stimulation with LPS, respectively (Fig. 3.33 A and B). In contrast, when cells were stimulated with a TLR2 specific agonist Pam3CSK4, no difference in cytokine production was reported following activation of shRNA specific to TRIL (Fig. 3.34 A-C). The level of TNFα production after short (3 h) and long (24 h) Pam3CSK4 stimulation (Fig. 3.34 A and C, respectively) as well the level of RANTES (Fig. 3.34 C) upon 24 h Pam3CSK4 challenge remained the same after TRIL shRNA induction when compared to the corresponding control.

Figure 3.31 TET inducible shRNA specific to TRIL reduces TRIL mRNA level in THP-1/shRNA-TRIL stable cells

THP-1 cells stably expressing TET inducible shRNA-TRIL (0.1 x 10^6 cells/ml) were plated in 12 well plates. Cells were treated with 2 µg/ml of doxycycline for 48 h in order to induce expression of shRNA specific to TRIL. Cells were lysed followed by RNA extraction. Samples were analysed by QPCR for TRIL expression. The mRNA levels were normalized against GAPDH and presented relative to CTRL (non doxycycline treated samples). Results are expressed as mean ± SEM of three independent experiments, each carried out in triplicate.

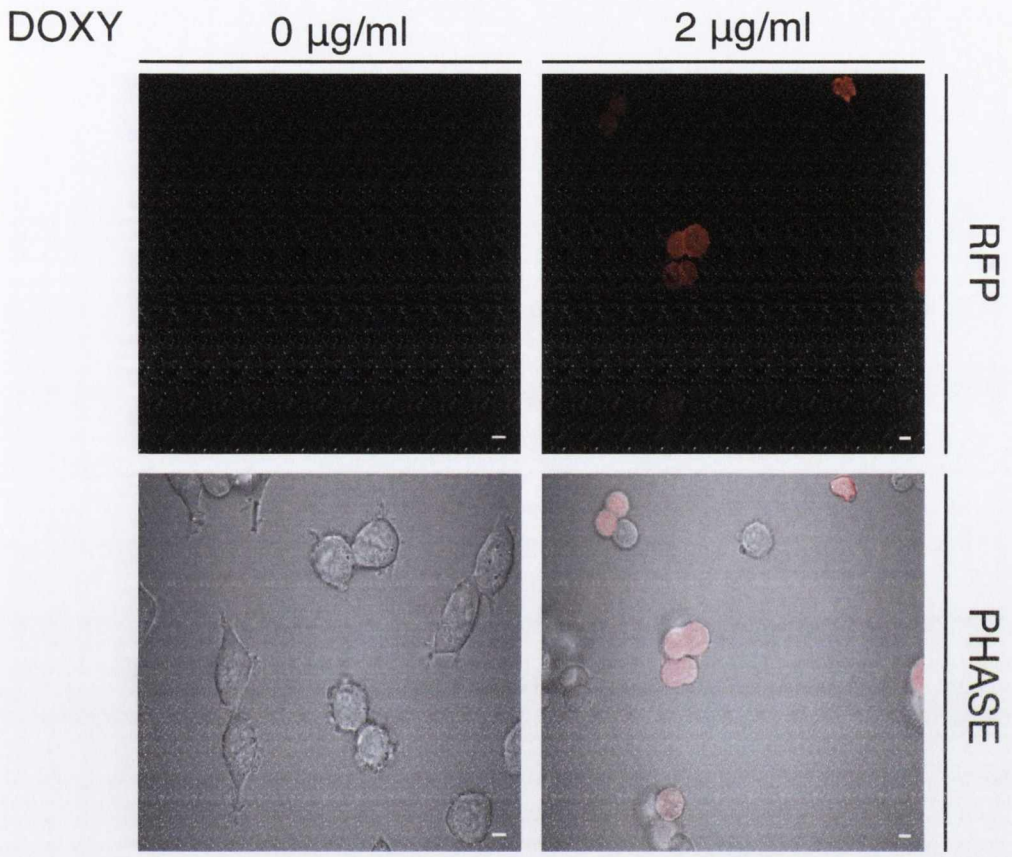

Figure 3.32 Control for doxycycline induced expression of shRNA-TRIL-RFP in THP-1 cells

THP-1 cells stably expressing doxycycline induced RFP-tagged shRNA specific to TRIL (1 x 10^6 cells/ml) were cultured in 35-mm glass-bottomed tissue cell dishes (MatTek) for 48 h with 2 µg/ml of doxycycline. Cells were then treated with PMA (1:80 000) for 24 h, prior to viewing with a Point Scanning Confocal Microscope (Olympus FV1000 LSM Confocal Microscope, (NA, 1.4; 60x). Results are representative of four independent experiments.

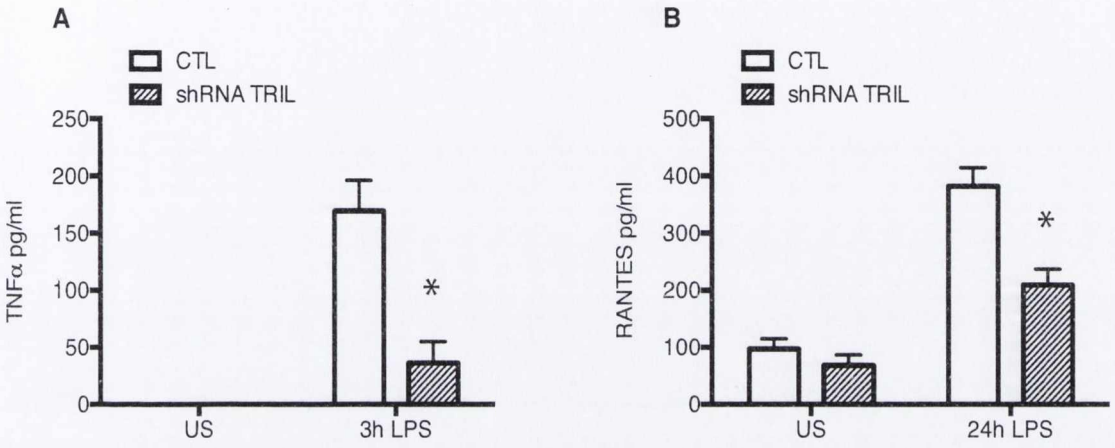

Figure 3.33 Knockdown of TRIL impacts TNFα and RANTES production in THP-1 cells following LPS stimulation

THP-1 cells stably expressing TET inducible shRNA specific to TRIL were plated at 0.1 x 10^6 cells/ml in 96-well plates. The shRNA specific to TRIL was induced by the addition of 2 μg/ml of doxycycline. Cells were then stimulated with 100 ng/ml of LPS for 3 h or 24 h. Supernatants were collected and assayed by ELISA for TNFα **A**, and RANTES **B**, production. Results are expressed as mean ± SD for triplicate determinations. *, $p < 0.05$. Results are representative of three individual experiments, each carried out in triplicate.

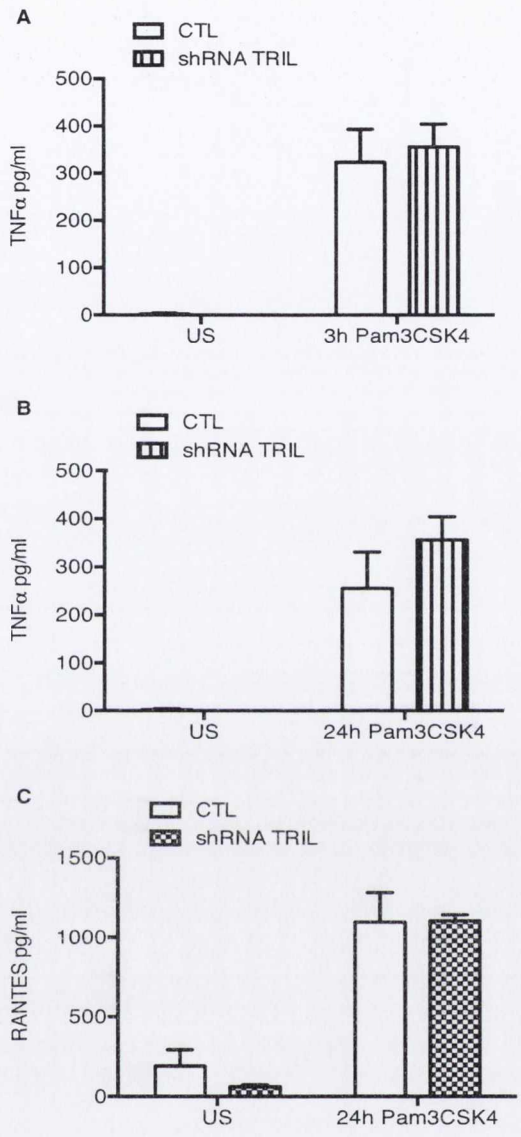

Figure 3.34 Knockdown of TRIL does not affect cytokine induction following Pam3CSK4 stimulation

THP-1 cells stably expressing TET inducible shRNA specific to TRIL were plated at 0.1 x 10^6 cells/ml in 96-well plates. shRNA specific to TRIL was induced by the addition of 2 μg/ml of doxycycline. Cells were then stimulated with 1 μg/ml of Pam3CSK4 for 3 h **A** and 24 h (**C** and **D**). Supernatants were collected and assayed for TNFα (A and B) and RANTES C, production. Results are expressed as mean ± SD for triplicate determinations. Results are representative of three individual experiments, each carried out in triplicate.

5.2.9 Investigation into association of TRIL with the TLR adaptor protein SARM

Some of the features assigned to TRIL such as high expression in the CNS and functional impact on both TLR3 and TLR4 signalling, suggest its similarity to another member of the TLR signalling network, SARM. SARM is a fifth and the most highly conserved TIR adaptor protein. Initial studies on SARM demonstrated that the protein acts as a negative regulator of TLR3 and TLR4 signalling pathway (Carty et al, 2006; Peng et al, 2010). Given the functional similarities and high expression within the CNS of TRIL and SARM, I hypothesized that the proteins may be somehow associated with each other. In order to test this hypothesis I set out to determine if there is a direct interaction between TRIL and SARM, by carrying out a co-IP and confocal microscopy imaging studies.

In the co-IP assay, HEK-239T cells were transiently transfected with a plasmid encoding Flag tagged SARM followed by an immunoprecipitation using the anti-TRIL antibody. As can be seen from the Figure 3.35, the Western blot analysis using the anti-Flag antibody reveals potential interaction of endogenous TRIL with an overexpressed SARM (Figure 3.35, lane 4, top panel, indicated by a frame). The expression of both proteins was examined by IP with anti-TRIL and anti-Flag followed by immunobloting with the corresponding antibodies (Figure 3.35, bottom and middle panel, respectively). The co-IP with anti-TRIL antibodies demonstrated quite strong interaction between TRIL and SARM, however given the different expression pattern of TRIL in HEK-239T cells and the fact that SARM was transiently overexpressed, further validation of this interaction was required.

I next investigated a potential TRIL-SARM interaction by performing confocal studies using the U373 cell line. GFP tagged SARM and RFP tagged TRIL were transiently transfected into U373 cells following stimulation with Poly(I:C). Figure 3.36 indicates that proteins of interest are capable of co-localising in the U373 cells (indicated in yellow, marked by white arrows). The specificity of both TRIL and SARM expression in U373 cells was examined by appropriate controls (Fig. 3.37, panel A and B).

Preliminary co-IP studies as well as confocal analysis indicated a possible interaction between TRIL and SARM. To further determine whether this observed interaction is not a false-positive effect of an overexpression of SARM, I performed a co-IP with endogenously expressed TRIL and SARM in U373 cells. TRIL-SARM interaction can be observed when immunoprecipitated with TRIL and immunoblotted for SARM (Fig. 3.38 lane 4, bottom panel). Examination of the endogenous expression levels of TRIL and SARM showed detectable amount of protein both in the lysates (Fig. 3.38 right top and bottom panels, lanes 5-8) and following IP with adequate antibodies. (Fig. 3.38 TRIL; top left panel lane 2 and 4, SARM; bottom left panel, lane 2). At least two isoforms of SARM (75 kDa and 80 kDa) are known to be expressed at the protein level (Mink et al, 2001). Interestingly, two bands corresponding to the sizes of two different isoforms of SARM were detected when SARM was immunoprecipitated using both anti-TRIL and anti-SARM antibodies followed by immunobloting for SARM (Fig. 3.38 bottom left panel, lane 2 and 4, indicated by frames). The faster migrating form in contrast to the slower migrating one was also present in the lysates, while the latter was not detected, most probably due to a limitation of the antibody.

Overall these data indicated clearly that TRIL and SARM are capable of direct interaction. Whether this association has a functional implication remains to be determined.

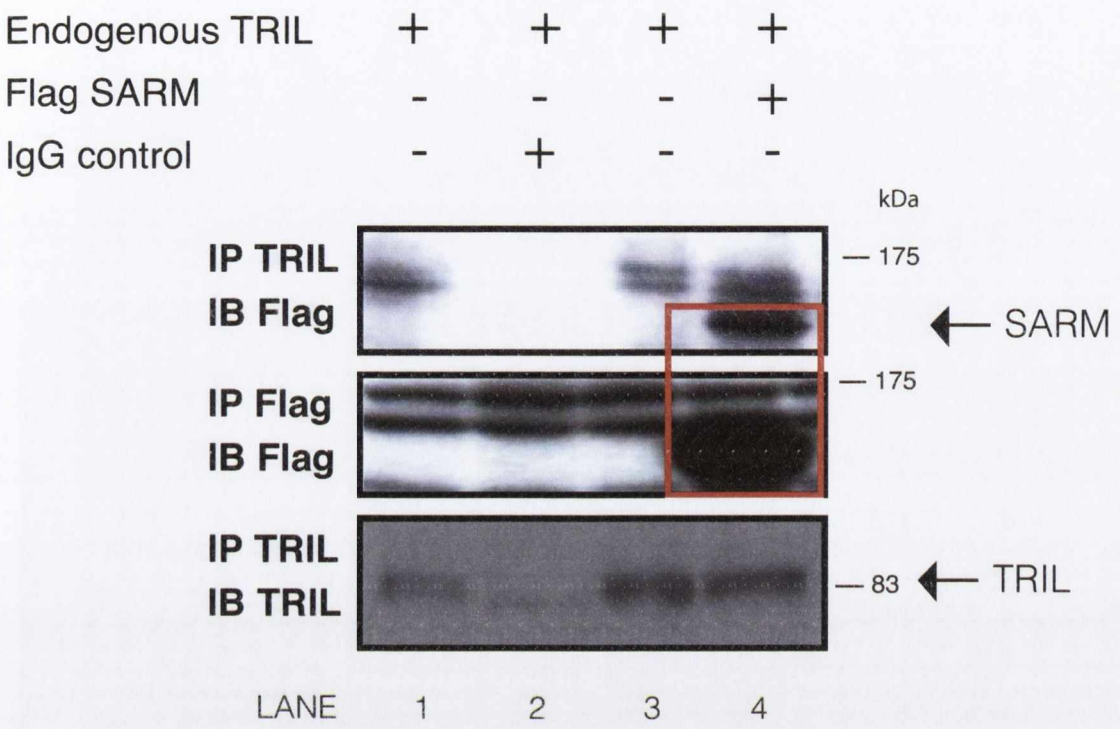

Figure 3.35 Co-immunoprecipitation of endogenous TRIL with SARM-Flag in HEK-239T cells

293T cells seeded at 0.2 x 10^6 cells/ml in 10cm dishes were transiently transfected with a plasmid encoding Flag tagged SARM (5 μg). 48 h following transfection cells were lysed. Whole cell lysates were then immunoprecipitated for 24 h at 4°C with agarose beads pre-coupled either with anti-TRIL, anti-Flag or with an IgG control antibody. Beads were washed three times followed by Western blot analysis with an anti-TRIL (top and bottom panel) or anti-Flag antibody (middle panel). This result represents one out of four independent experiments.

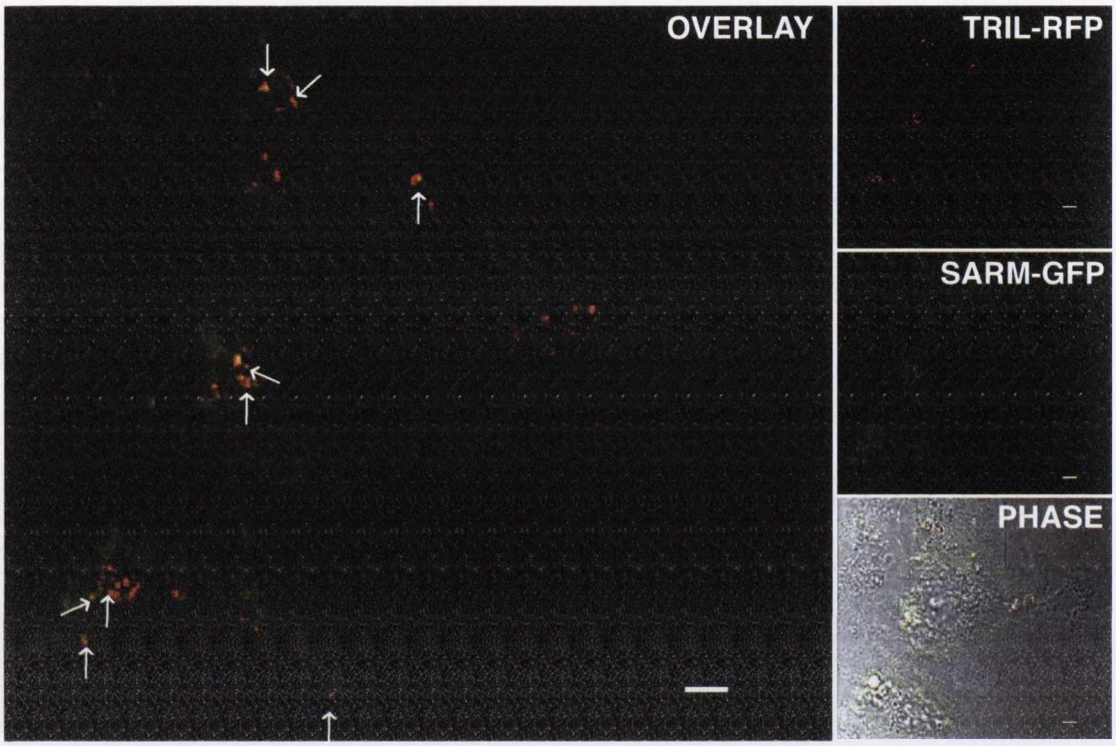

Figure 3.36 Co-localisation of TRIL-RFP and SARM-GFP in U373 cells following Poly(I:C) stimulation

U373 cells (0.1 x 10^6 cells/ml) were seeded on 35-mm glass-bottomed tissue cell dishes (MatTek). After 24 h cells were transfected with 1 mg of plasmid encoding SARM-GFP (green) and 1 mg of TRIL-RFP expression plasmid (red). 24 h following transfection cells were treated with 25 mg /ml of Poly(I:C) and incubated for another 24 h prior to viewing with a Point Scanning Confocal Microscope with a heated stage (Olympus FV1000 LSM Confocal Microscope, (NA, 1.4; 60x). Results are representative of three independent experiments.

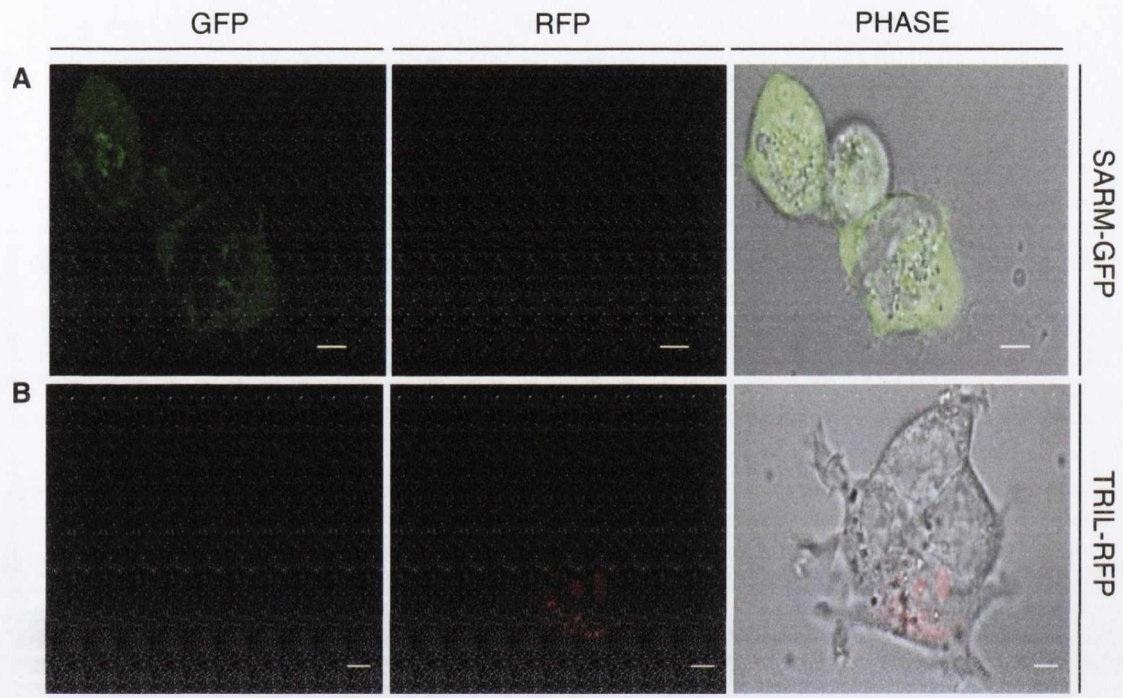

Figure 3.37 SARM-GFP and TRIL-RFP expression controls in the U373 cell line

U373 cells (0.05 x 10^6 cells/ml) were seeded on 35-mm glass-bottomed tissue cell dishes (MatTek). After 24 h cells were transfected with 1 μg of plasmid encoding SARM-GFP (green, panel **A**) or 1 μg of TRIL-RFP expression plasmid (red, panel **B**). 24 h following transfection cells were stimulated for 24 h using Poly(I:C) (25 μg/ml). A Point Scanning Confocal Microscope with a heated stage (Olympus FV1000 LSM Confocal Microscope, (NA, 1.4; 60x), was used to examine prepared samples.

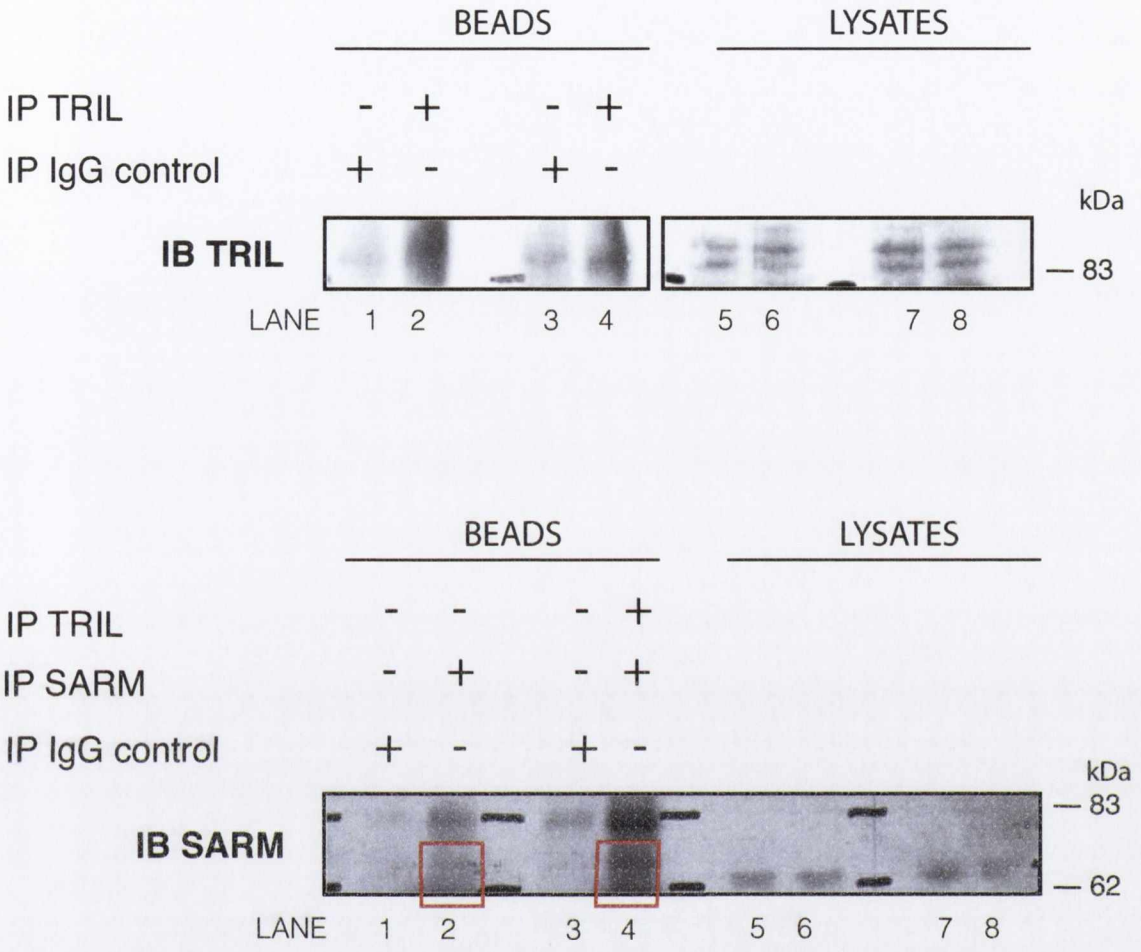

Figure 3.38 Endogenous IP between TRIL and SARM in U373 cells

U373 cells (0.2 x 10^6 cells/ml) were plated on 10 cm dishes. 48 h following plating cells were lysed. A portion of whole cell lysate from each sample was removed and blotted for endogenous TRIL (top, right panel, lanes 5-8) and SARM expression (bottom, right panel, lanes 5-8). The remainder was co-immunoprecipited for 24 h at 4°C with either anti-TRIL (left top panel lane 2 and 4) or an IgG control (left top panel lane 1 and 3) and for 4 h at 4 °C with either anti-SARM (left bottom panel, lane 2) or an IgG control (left bottom panel, lane 1) pre-coupled to agarose beads. Beads were then washed three times and analysed by Western blotting using antibodies against SARM and TRIL, respectively. Results are representative of two independent experiments.

3.4 Discussion

The inspiration for this project came about following the earlier work of Carpenter *et al.,* who first identified a novel protein TRIL (Carpenter et al, 2009). Structurally, TRIL consists of 13 leucine-rich repeats, a signal sequence, a fibronectin domain and a single transmembrane spanning region. TRIL is expressed in a number of tissues, largely within the brain but also in the spinal cord, lung, kidney and ovary. Functionally, TRIL acts as a positive regulator of TLR4 mediated responses. Carpenter at al., demonstrated that endogenous TRIL directly interacts with TLR4 and that this interaction is further boosted by stimulation with LPS. TRIL is also capable of binding with the TLR4 agonist LPS. Overall, TRIL is a novel component of the TLR4 complex highly expressed in the brain. Given the fact that TRIL has been discovered only recently, a number of questions regarding this protein remain to be addressed.

Accessory molecules are vital components of TLR signalling pathways implicated in numerous aspects of the TLR response, such as ligand binding and delivery, TLR trafficking and modulation of TLR signalling (Akashi-Takamura & Miyake, 2008; Lee et al, 2012; McGettrick & O'Neill, 2010). The function executed by an accessory molecule is usually correlated with its localisation and this in turn often reflects the expression pattern of the regulated TLR. Present at the plasma membrane MD2 regulates the cell surface expression of TLR4 and as a TLR4-MD2 heterodimer participates in the recognition and binding of LPS (Nagai et al, 2002a; Shimazu et al, 1999). RP105, which is also present at the cell surface, regulates responses of plasma membrane associated TLR2 and TLR4 in a cell type specific manner. In B cells RP105 acts as a positive regulator of TLR2 and TLR4 signalling (Nagai et al, 2005), whereas in macrophages and dendritic cells it negatively regulates LPS induced responses (Divanovic et al, 2005b). Expressed intracellularly UNC93B, PRAT4A and gp96 are all involved in the regulation of endosomal TLRs. UNC93B controls the intracellular trafficking of TLR3, TLR7 and TLR9 (Brinkmann et al, 2007; Tabeta et al, 2006) and it is also responsible for delivery of the nucleotide sensing TLRs, TLR7 and TLR9, into the endolysosomal compartments, where they can bind with their respective ligands (Kim et al, 2008). PRAT4A and gp96 both regulate the intracellular trafficking of TLRs and

also act as chaperone proteins ensuring proper folding of TLRs in the ER (Liu et al, 2010b; Randow & Seed, 2001; Takahashi et al, 2007; Wakabayashi et al, 2006; Yang et al, 2007).

Aside from studies by Carpenter at al., TRIL has not been characterised and studied. Therefore, a more in depth analysis into the characteristics of TRIL was undertaken. As previously mentioned the subcellular localisation of an accessory molecule is often correlated with its function. Therefore the exact subcellular localisation of TRIL was examined by confocal analysis and membrane fractionation studies. The comprehensive investigation into the involvement of TRIL in the TLR-mediated signalling pathways was carried out by co-immunoprecipitation and confocal microscopy analysis, as well as overexpression and shRNA-mediated gene silencing studies.

Initial flow cytometry studies by Carpenter at al., suggested a cell type specific expression pattern of TRIL, however they did not demonstrate the exact subcellular localisation of TRIL. To investigate this in more detail, confocal imaging studies were carried out using three different cell types; the human embryonic kidney cells (HEK-293T), the monocytic cell line (THP-1) and brain derived cells, the human astrocytoma cell line U373. Confocal studies clearly demonstrated an intracellular localisation of TRIL in two out of three tested cell lines: U373 and THP-1. In contrast, when TRIL was overexpressed in the HEK-293T cells, the protein was detected at the cell surface. It is possible that TRIL is mislocalised when overexpressed in HEK-293T cells. The other explanation could be that TRIL is differentially localised in epithelial cells. Some TLRs also demonstrate a cell type-specific expression pattern. Expressed largely at the cell surface, TLR2 is localised intracellularly in human dendritic cells, where it co-localises with microtubules and Golgi (Uronen-Hansson et al, 2004). TLR3, which has an intracellular expression pattern in macrophages and dendritic cells (Lee et al, 2006; Matsumoto et al, 2003; Nishiya & DeFranco, 2004), was also found at the plasma membrane level in fibroblasts (Matsumoto et al, 2002) and epithelial cells (Jorgenson et al, 2005). Thus it is possible that similar to differentially expressed TLRs, TRIL also has a cell-type specific expression pattern.

TRIL regulates signalling of TLR4, thus the cell type specific expression pattern might be also correlated with different functions of TRIL in the regulation of TLR4 signalling. In resting cells, TLR4 is found in Golgi and at the plasma membrane of human monocytes (Husebye et al, 2006; Latz et al, 2002). The multiprotein complex composed of TLR4 accompanied by accessory molecules MD2 and CD14, shuttles between the Golgi and the plasma membrane until engaged by LPS at the cell surface. Recognition of LPS initiates the MyD88-dependent signalling cascade and subsequent translocation of the TLR4 receptor complex from the plasma membrane to the endosome (Tanimura et al, 2008). Differentially localised TRIL may therefore execute multiple roles in the regulation of TLR4 signalling. Cell surface expressed TRIL may participate in the process of ligand binding, while intracellular TRIL may be implicated in the regulation of intracellular trafficking of TLR4.

Further membrane fractionation studies revealed that TRIL is exclusively found in a membrane fraction of U373 cells. This was a rather anticipated result given the presence of the transmembrane domain in the structure of TRIL (Carpenter et al, 2009). The intracellular localisation of TRIL in the U373 and THP-1 cells prompted further experiments, which aimed to determine the specific subcellular compartment of TRIL localisation.

Additional confocal microscopy analysis demonstrated that TRIL co-localises with the ER and the early endosomes, but does not associate with the Golgi and the mitochondrial structures, when overexpressed in U373 cells stimulated with Poly(I:C). These results are consistent with the earlier bioinformatics studies, which revealed the presence of a signal sequence on the N-terminal site of TRIL (Carpenter et al, 2009). This motif is a common feature of proteins directed to the ER, and subsequently translocated to the endosomal compartments of the cell (Walter & Johnson, 1994). TLR4, similarly to TRIL, is a transmembrane protein, which following translation resides in the ER where it associates with MD2, implicated in the regulation of intracellular TLR4 trafficking (Nagai et al, 2002a) and indispensable for the recognition of LPS at the plasma membrane (Shimazu et al, 1999). Association of TLR4-MD2 within the ER and subsequent translocation to the plasma membrane is regulated by the ER-resident

accessory molecules gp96 and PRAT4A (Randow & Seed, 2001; Wakabayashi et al, 2006). The expression of TRIL in the ER could suggest that the protein, similar to MD2, associates with TLR4 in the ER before translocation to plasma membrane and early endosome structures. However, the absence of TRIL in the Golgi excludes TRIL from previously described trafficking of TLR4-MD2-CD14 complex between the Golgi and the plasma membrane. Therefore, it is most likely that TLR4-TRIL interaction occurs either at the level of the plasma membrane or within the early endosomes, rather than in the ER.

LPS binding by the TLR4-MD2 complex at the plasma membrane initiates the MyD88/Mal-dependent signalling pathway (Lu et al, 2008) followed by the translocation of the complex to the endosomal compartments where TLR4 triggers the TRIF/TRAM mediated response (Kagan et al, 2008). Interestingly, the endosomal localisation of TRIL was also enhanced upon LPS challenge. Live cell imaging demonstrated a noticeable change in the expression pattern of overexpressed TRIL-RFP prior to and following LPS stimulation in the U373 cells. Expressed intracellularly in a diffuse, spot-like pattern TRIL provided a more concentrated localisation following LPS challenge. The co-localisation with the early endosomal marker EEA1 is also visibly enhanced following stimulation. As mentioned earlier, upon recognition of LPS, TLR4 triggers the MyD88/Mal-dependent signalling pathway and subsequently translocates to early endosomes where it activates the TRIF/TRAM mediated response. The adaptor proteins TRIF and TRAM similar to TLR4, relocate to early endosomes following LPS stimulation (Tanimura et al, 2008). Increased co-localisation of TRIL with the endosomal marker following LPS stimulation suggests that the role of TRIL in TLR4 signalling relies on the regulation of the plasma membrane TLR4/MyD88-dependent and the endosomal TLR4/TRIF mediated signalling pathways.

The strong evidence of the endosomal expression pattern of TRIL was further enhanced following LPS stimulation. This suggested that apart from its role in the endosomal TLR4 signalling pathway, TRIL might also function to regulate the intracellularly localised TLRs. The literature gives many examples of accessory proteins, such as gp96, PRAT4A, UNC93B or CD14, which modulate function of multiple

extracellular and endosomal TLRs (Latz et al, 2002; Takahashi et al, 2007). I therefore aimed to determine whether this might be also the case for TRIL. Since it has been previously shown that TRIL does not affect TLR9-mediated signalling (Carpenter et al, 2009), I investigated a possible role for TRIL in the TLR3 response, which similar to endosomal TLR4 signalling, depends on the adaptor protein TRIF.

Expression studies demonstrated that at both the mRNA and protein level, TRIL was induced by stimulation with the TLR3 agonist, Poly(I:C), in primary mixed glial cells and/or U373 cells. Transient overexpression of 1 ng of TRIL enhanced Poly(I:C) induced ISRE activation to the same extent as overexpression of 1 ng of TLR3 alone. Overexpression of a lower concentration of TRIL or TLR3 alone did not significantly alter responses to Poly(I:C), but co-expression of the same low concentration of TRIL and TLR3 together led to a tremendous enhancement in ISRE activation and RANTES production following stimulation with Poly(I:C). These results suggest that at high concentrations both TRIL and TLR3 enhance the response to Poly(I:C), while when expressed at lower concentrations, the proteins collaborate to provide an increased response to stimulation. Thus, TRIL positively modulates TLR3 mediated signalling. Further studies carried out using a stable U373 cell line expressing TRIL (U373/TRIL) also demonstrated a robust increase in ISRE and NF-κB activity in response to Poly(I:C). Interestingly, enhancement in ISRE activation was substantially higher than that observed in the case of the NF-κB based assay. This suggests that TRIL is a more potent modulator of the interferon inducible genes, rather than proinflammatory cytokine production in response to TLR3 stimulation. This observation further emphasizes that the role for TRIL is focused primarily on modulation of the TRIF-mediated response.

In addition, Poly(I:C) induced cytokine production was also enhanced in U373/TRIL cells, when compared with matching controls. Although these results clearly demonstrated that TRIL is involved in TLR3 mediated signalling, the exact mechanism by which TRIL impacts the TLR3 pathway remains elusive. The expression and cellular localisation of TLR3 is regulated in a cell-type specific manner and strongly depends on the cell activation status. TLR3 is found both intracellularly and on the cell surface of fibroblasts and epithelial cells, but is localised solely to the endosomal

compartment of myeloid DCs (Lundberg et al, 2007; Matsumoto et al, 2003). The activation of TLR3 is strongly dependent on pH and occurs exclusively in the acidified endosome (de Bouteiller et al, 2005). It is possible that TRIL functions to regulate the translocation of the TLR3 receptor from the plasma membrane to cellular vesicles, or the trafficking of TLR3 from the ER to endosomes, where the receptor undergoes enzymatic processing prior to bind with its agonist (Ewald et al, 2008; Garcia-Cattaneo et al, 2012).

Given the fact that TRIL is a membrane bound protein found within the early endosome I decided to examine, whether TRIL is capable of direct binding with TLR3. The coimmunoprecipitation studies using U373 and THP-1 cells, respectively demonstrated the association between TLR3 and TRIL and excluded binding of TRIL with TLR2.

Furthermore, direct interaction between TRIL and TLR3 was further enhanced following stimulation with Poly(I:C). Western blot analysis as well as confocal studies demonstrated a strong basal interaction between TRIL and TLR3, which was further increased following stimulation with the TLR3 agonist. Given the fact that TRIL is localised to the early endosomes, the observed co-localisation with TLR3 most likely occurs in the endosomal compartment of the cell. TRIL might be therefore involved in the regulation of endosomal expression and trafficking of the TLR3 receptor, as well as ligand binding and delivery.

TRIL is capable of direct interaction with TLR4 as well as LPS. Thus, similar to CD14, TRIL might be implicated in delivery of LPS to the TLR4-MD2 complex at the plasma membrane. Association of TRIL with TLR3 led me to investigate if TRIL is also capable of binding with the TLR3 ligand Poly(I:C). Co-IP studies using biotinylated Poly(I:C) and streptavidin coated beads, followed by immunoblotting with endogenous anti-TRIL antibody demonstrated that TRIL is capable of binding to Poly(I:C), thus it might be involved in the endosomal ligand delivery. However, it is also possible that the TRIL-Poly(I:C) interaction was not direct, but rather mediated by TLR3 endogenously expressed by U373 cells, as TLR3 is known to directly bind to Poly(I:C) and was shown to also interact with TRIL. An additional investigation, such as

immunoprecipitation using increasing concentration of Poly(I:C), IP carried out in TLR3 knockout cells or confocal studies, is needed to fully confirm direct association of TRIL with Poly(I:C).

The endosomal localisation of TRIL was greatly enhanced following LPS stimulation. This observation, together with the earlier finding demonstrating direct interaction of TRIL with TLR4, points towards a possible role for TRIL in the endosomal trafficking of the TLR4-MD2 complex. The majority of accessory molecules regulate multiple TLRs. One such example is CD14, which apart from its well established role in the modulation of TLR4 signalling, has been shown to modulate the response of TLR3 as well as TLR7 and TLR9 (Baumann et al, 2010; Lee et al, 2006). TRIL resembles CD14 in many ways, both proteins are implicated in TLR4 signalling and both of them also regulate TLR3 response. Interestingly, it has been demonstrated that CD14 directly binds to dsRNA and mediates its cellular uptake (Lee et al, 2006). TRIL may be also involved in the ligand delivery as it interacts with LPS and also possibly with Poly(I:C). It is plausible that while CD14 determines the uptake of dsRNA, TRIL is responsible for its translocation to TLR3 in the endosome. It is very intriguing that both CD14 and TRIL carry out similar functions. It is possible that CD14 and TRIL complement each other function in various cell types, as TRIL is largely expressed in various cell populations of the brain, in contrast to CD14 which is primarily expressed in the myeloid cell types. Additional studies are however needed to fully verify this hypothesis.

Having ascertained the association of TRIL with TLR3 I next investigated if this interaction impacts on the TLR3 mediated response. As I demonstrated earlier, the overexpression of TRIL boosts TLR3 mediated signalling following Poly(I:C) stimulation. I next examined the TLR3 mediated response in the absence of TRIL using shRNA-mediated gene silencing. Studies using a stable U373 cell line expressing shRNA specific to TRIL, revealed that the knockdown of TRIL led to a significant decrease in the induction of ISRE activity and cytokine production in response to Poly(I:C). Additional studies carried out using the THP-1 stable cell line expressing the shRNA-TRIL-RFP excluded the TLR2 mediated signalling pathway as a potential target of TRIL. In the previous studies Carpenter et al., demonstrated possible implication of TRIL in

the regulation of TLR2 mediated response, where transint knockdown of TRIL led to a reduction in TNFα production in response to TLR1/2 agonist Pam3CSK4 (Carpenter et al, 2009). However, this effect was demonstrated exclusively within the human PBMCs and not glial cells, where TRIL is primarily expressed.

Having established the association of TRIL with TLR3 and the implication of this interaction for the regulation of the TLR3 mediated response I next searched for other potential binding partners of TRIL within the TLR signalling pathways. Due to a number of similarities, including the high expression within the brain and involvement in the regulation of both TLR4 and TLR3 signalling pathways, my attention was drawn to a highly conserved and the least well characterised TIR adaptor protein SARM (O'Neill & Bowie, 2007). I decided to investigate whether TRIL might be correlated somehow with this TIR adaptor molecule.

Interaction studies carried out using HEK-293T and U373 cells demonstrated that TRIL and SARM are capable of direct interaction both when overexpressed and endogenously. Moreover, the co-IP experiment revealed that endogenous TRIL is capable of binding with the two known isoforms of SARM (Mink et al, 2001). Surprisingly, when I examined the lysates only one isofom of SARM was detected, which in addition was of a slightly lower size than the band detected in the immunoprecipitation study. This could be due to differences in the migration of the proteins during the electrophoresis. The other explanation could be that SARM is being immunoprecipitated in a complex with some other small protein. The observed association of TRIL and SARM suggest that these proteins could impact each other's function and act in synergistic or antagonistic fashion. However, additional work is needed to fully characterise the nature of this interaction.

There are many possible mechanisms that might be influenced by the correlation between TRIL and SARM. As both of these proteins were assigned contradictory functions in the regulation of TLR signalling, SARM as a negative, while TRIL as a positive modulator of TLR3 and TLR4 responses, their interaction might be yet another way of fine-tuning these signalling pathways. Of interest is also the high expression of TRIL and SARM within the brain, where both proteins might play a role in

the innate immunity of the CNS and also processes like neurogenesis and neurodegeneration. Expressed predominantly in neurons SARM has been demonstrated to execute a number of functions within the CNS. It has been implicated in the antiviral response to neurotropic WNV infection in the brain. Mice lacking SARM demonstrated decreased TNFα production and microglia activation, while brainstem-specific neuronal cell death was significantly enhanced (Szretter et al, 2009). Interestingly the latest work by Hou *et al.* implicated SARM in the immune response to neurotropic VSV infection, demonstrating reduced levels of proinflammatory cytokines in the brain of SARM deficient mice, which was also correlated with increased survival of these animals, compared to WT controls (Hou et al, 2013). Of note, most recent studies by Mukherjee at al., carried out both *in vitro* using primary neurons and *in vivo*, revealed an increased levels of SARM expression upon LACV infection mediated by the the RIG-I and mitochondrial antiviral signaling protein (MAVS) signaling pathway (Mukherjee et al, 2013). Enhanced expression of SARM was correlated with neuronal apoptotic cell death resulting from induced oxidative stress response and mitochondrial damage (Mukherjee et al, 2013).

It will be very exciting to test whether TRIL is also implicated in this antiviral immune response and if so, whether it is by modulating TLR signalling or maybe by the interaction with SARM. As mentioned before, apart from its role in modulating TLR response, SARM has been also shown to play a protective role in neuronal survival during oxygen and glucose deprivation-induced cell death (Szretter et al, 2009), and to participate in an active axonal destruction program called Wallerian degeneration (Osterloh et al, 2012a; Szretter et al, 2009). As I described above, most recently SARM has been also implicated in the regulation of neuronal apoptotic cell death in response to LACV (Mukherjee et al, 2013). It is therefore possible that TRIL, which is highly expressed in the brain, plays a considerably broader role in the CNS and is also involved in the regulation of such processes as neuronal survival and degeneration.

Overall this more in-depth analysis of TRIL uncovered a novel role for TRIL in the TLR3 signalling pathway. TRIL is expressed in a cell type specific fashion and was detected both at the plasma membrane and intracellularly in the HEK-293T and human

astrocytoma cell line, respectively. The identified endosomal localisation of intracellular TRIL is in agreement with the role for TRIL in the TLR3 and endosomal TLR4 signalling pathway. The implication of TRIL in the endosomal TLR4 signalling pathway is further supported by the enhanced endosomal localisation of TRIL upon LPS stimulation. TRIL was found to associate with TLR3 and might be also capable of binding with Poly(I:C) suggesting its role in ligand delivery. Series of overexpression and silencing studies demonstrated a positive functional implication of TLR3-TRIL interaction on TLR3 but not TLR2 signalling pathways, thus emphasizing even further the importance and specificity of TLR3-TRIL interaction. All in all, this study uncovered a new role of TRIL as a positive regulator of TLR3 signalling pathway. Figure 3.1 represents the potential function of TRIL as an accessory protein involved in regulation of TLR signalling

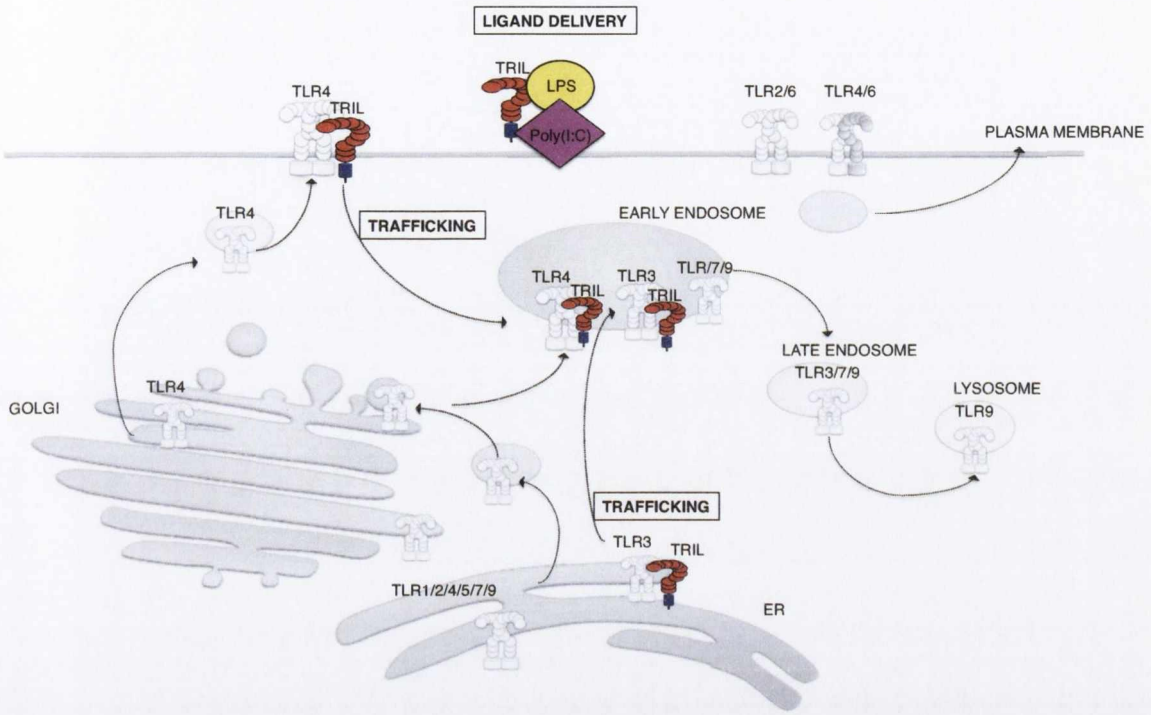

Figure 3.40 Potential role of TRIL as an accessory molecule involved in the TLR3 and TLR4-mediated signalling pathways

The figure represents the potential function of TRIL in the regulation of TLR signalling pathways. TRIL can be found at the plasma membrane where it binds to LPS and TLR4 and most likely regulates trafficking of TLR4-MD2 complex into the endosomal compartment. TRIL is also localised intracellularly in the early endosomes where it directly interacts with TLR3 and impacts on TLR3 and endosomal TLR4/TRIF-dependent signalling. Additionally, TRIL associates with the TLR ligands LPS and Poly(I:C) therefore plays a role in the ligand delivery. The expression of TRIL has been also reported in the endoplasmic reticulum (ER), where TRIL may execute a role in the intracellular TLR3 trafficking from the ER to early/late endosome.

CHAPTER FOUR

Investigation into the *in vitro* and *in vivo* role of TRIL is TLR–mediated responses to bacterial and viral infections

4.1 Introduction

Results from the previous chapter revealed the involvement of TRIL in the regulation of TLR3 and endosomal TLR4 signalling, particularly in the astrocytoma cell line U373. The functional implication of TRIL in the modulation of TLR response together with its high expression in the brain, strongly point towards the importance of TRIL in the immune response within the CNS.

As mentioned previously, TLRs are widely expressed within immune and non-immune cells of the CNS (Carpentier et al, 2008). Brain resident cells act as the key immune sentinels of the brain. Both microglia and astrocytes constitutively express a wide range of TLRs (Carpentier et al, 2008; Kielian, 2009). Under resting conditions *in vivo*, the expression of TLRs 1-9 with particularly high levels of TLR3 has been reported in the murine brain (McKimmie et al, 2005). Constitutive expression of TLRs is associated primarily with microglia and limited to meninges and circumventricular organs (CVOs) of the brain. These highly vascularised structures lack the BBB therefore are capable of sensing pathogens present in the periphery, as well as ones directly invading the CNS (Chakravarty & Herkenham, 2005; Laflamme et al, 2003; Laflamme et al, 2001). Interestingly, upon viral and bacterial infection, ligand stimulation or CNS immunity, enhanced expression of TLRs has been reported in both microglia as well as astrocytes (Bsibsi et al, 2002; Carpentier et al, 2005; Laflamme et al, 2001; Zekki et al, 2002). Systemic LPS injection leads to enhanced expression of TLR4 and TLR2 in microglial cells, whereas treatment of astrocytes with the TLR3 agonist Poly(I:C) upregulates the expression of TLR3 and also TLR2 and TLR4 (Carpentier et al, 2005). Similarly infection of mice with the neurotropic rabies virus is associated with increased expression of multiple TLRs within the brain resident cells (McKimmie & Fazakerley, 2005; McKimmie et al, 2005). In humans, cultured microglial cells express TLRs 1-9, whereas astrocytes have been shown to express TLRs 1-5 and TLR9 (Bsibsi et al, 2006; Bsibsi et al, 2002; Jack et al, 2005). Both human and murine astrocytes express exceptionally high levels of TLR3, (Carpentier et al, 2005; Farina et al, 2005; McKimmie & Fazakerley, 2005), which suggests the importance of these cells in the antiviral response in the CNS.

TRIL has been initially characterised as a novel regulator of TLR4 signalling highly expressed in the brain (Carpenter et al, 2009). This study has identified a new role for TRIL as a regulator of TLR3 responses. This chapter provides further insights into the function of TRIL using TRIL deficient mice. The results confirm a role for TRIL in the TLR3 and TLR4 responses within primary mixed glial cells and also indicate a function for TRIL *in vivo* within the CNS in controlling the immune response to to *E.coli* and vesicular stomatitis virus (VSV) infections.

4.2 Results

4.2.1 Examination of TRIL deficient mice

TRIL deficient mice were generated by our collaborators at Pfizer. A targeting vector to generate TRIL deficient mice was constructed to encode an FRT-neomycin resistance cassette and a mouse genomic TRIL DNA, flanked by two *LoxP* sites (Fig. 4.1 A). Conditional TRIL deficient female founders were next crossed with C57BL/6 males expressing Protamine-Cre resulting in permanent deletion of *LoxP*-flanked TRIL alleles. Prior to carrying further *in vitro* and *in vitro* experiments using the TRIL deficient mice ($TRIL^{-/-}$), the genotype of generated mice was evaluated by QPCR analysis.

I set out to examine mice homozygous for the targeted allele by carrying out PCR analysis of genomic DNA isolated from tail biopsies. As expected the wild-type (WT) (179 bp) and mutant (415 bp) alleles were detected in corresponding samples, confirming the genotype of WT and TRIL deficient mice (Fig. 4.1 B). TRIL was characterised as a brain-enriched protein, thus an additional QPCR study of TRIL expression in total brain lysates was carried out in the wild-type (+/+), heterozygous (+/-) and homozygous (-/-) TRIL deficient mice. As expected, TRIL expression was absent in $TRIL^{-/-}$ mice, whereas moderate to high levels of TRIL mRNA were detected in heterozygous and WT mice, respectively (Fig. 4.1 C).

Altogether, these data confirmed successful deletion of TRIL in knockout mice, which were subsequently used to carry out further *in vitro* and *in vivo* studies of TRIL function.

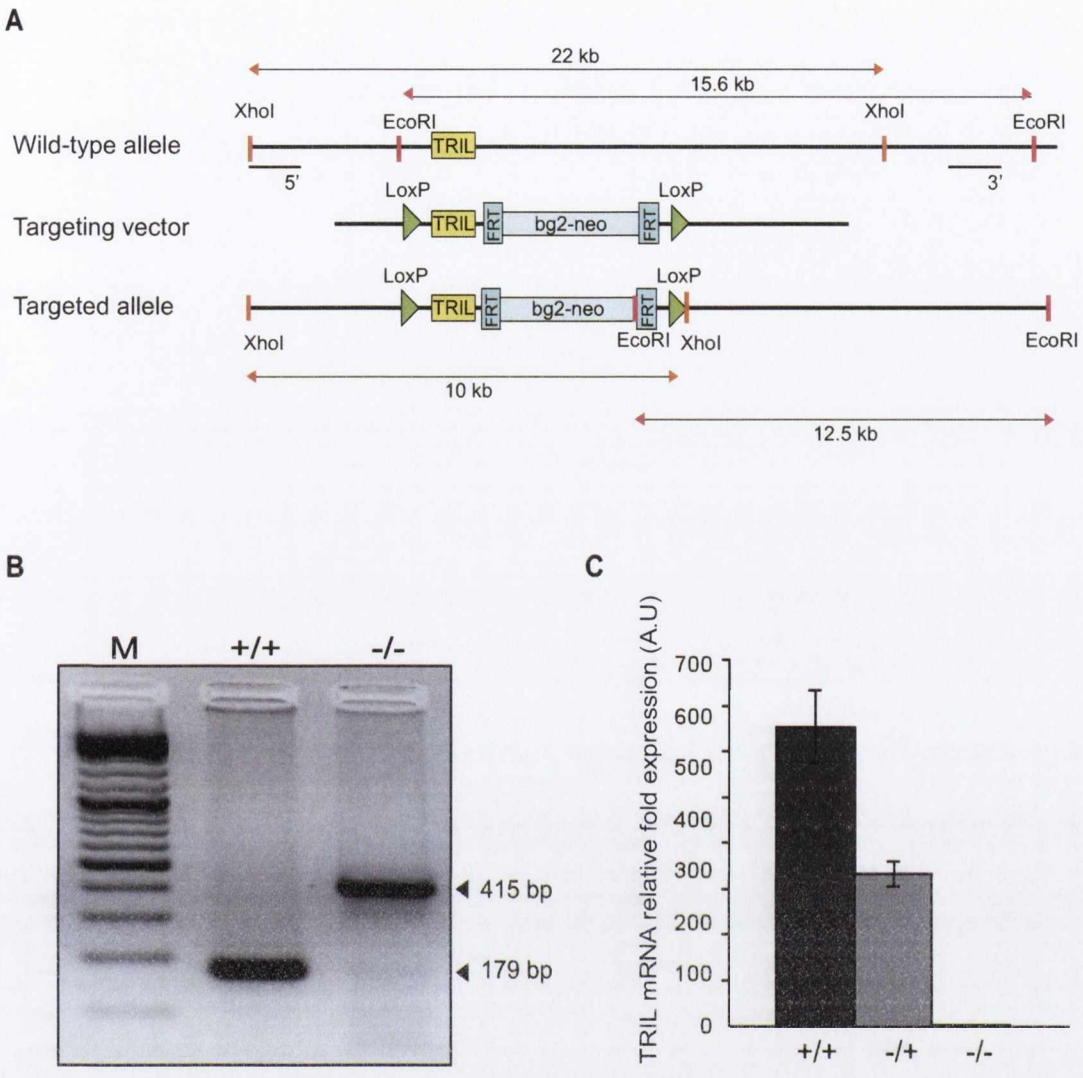

Figure 4.1 Generation of TRIL deficient mice

A, Gene targeting strategy for generation of TRIL deficient mice based on the principle of homologous recombination. The structures of WT allele, targeting vector and targeted allele are represented. **B,** Genomic DNA prepared from tail biopsies was used to carry out PCR using primers TRIL-F1, TRIL-R1 and TRIL-R2, detecting both wild-type (179 bp) and mutant (415 bp) alleles (indicated by arrow heads). PCR products were analysed by gel electrophoresis. Results are representative of three independent experiments. **C,** RT-PCR analysis of TRIL expression in the brain of wild-type (+/+), heterozygous (+/-) and mutant (-/-) mice. TRIL mRNA levels were normalised against GAPDH and expressed relative to the lowest detectable sample. Data are presented as the mean ± SD of one experiment representative of three independent experiments.

4.2.2 TRIL does not impact TLR4 and TLR3-mediated responses in primary bone marrow derived macrophages and dendritic cells (BMDMs and BMDCs)

Data available from BioGPS (Fig. 4.2) shows the expression pattern of murine TRIL. These data further support the earlier findings and demonstrate high levels of TRIL mRNA across the brain tissue (Fig. 4.2 blue bars). Interestingly, the analysis revealed only moderate to low levels of TRIL expression within myeloid cells, such as macrophages and dendritic cells.

Carrying on from this observation, I next examined the impact of TRIL on TLR-mediated responses in primary BMDMs and BMDCs derived from WT and $TRIL^{-/-}$ mice. LPS caused an increase in the mRNA level of IL6 (Fig. 4.3 A and C) and RANTES (Fig. 4.3 B and D) in the WT BMDMs and BMDCs and TRIL deficiency had no major effect on these responses. Poly(I:C) was a poor inducer of IL6 (Fig. 4.2 A and C), however the increase in mRNA level of RANTES (Fig. 4.3 B and D) was also unaffected by the absence of TRIL in both BMDMs and BMDCs. In order to further confirm these findings, an additional analysis of cytokine production in WT and TRIL deficient BMDMs and BMDCs was carried out by ELISA (Fig. 4.4). Cells were stimulated for 24 h with two different concentrations of LPS (10 and 100 ng/ml) and Poly(I:C) (25 and 50 μg/ml), as well as ligands specific for TLR2 and TLR7/8, Pam3CSK4 and R848, respectively. Similarly to mRNA levels, production of proinflammatory cytokines was unaffected by TRIL deficiency, as both WT and $TRIL^{-/-}$ primary BMDCs (top panel) and BMDMs (bottom panel) demonstrated the same level of IL6 (A and D), TNFα (B and E) and RANTES (C and F) production (Fig. 4.4). TRIL deficiency also had no effect on the induction of IL6, TNFα and RANTES by the TLR2 ligand Pam3CSK4 and TLR7 ligand R848, in either BMDCs (top panel) or BMDMs (bottom panel) (Fig. 4.4).

Overall these data demonstrated that TRIL does not impact on TLR-mediated responses in primary macrophages and dendritic cells, consistent with the low expression levels of TRIL detected within these cells.

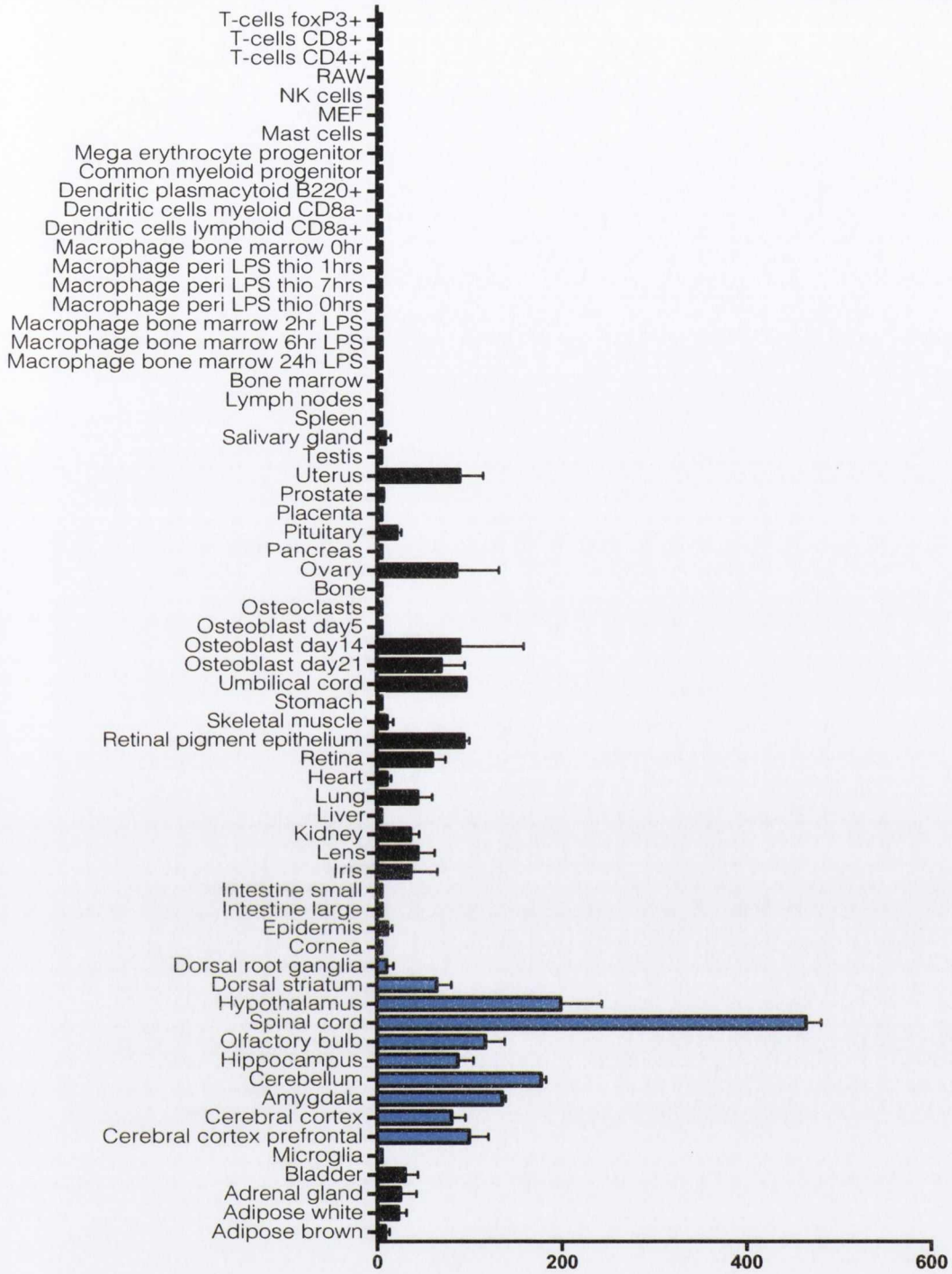

Figure 4.2 TRIL is predominantly expressed within the central nervous system (CNS)

Data available from BioGPS (http://biogps.org). Measurements were obtained for 61 normal mouse tissues and cells hybridized against MG-U74B. The Affymetrix MAS5 algorithm was used for array processing and probe sets were averaged per gene.

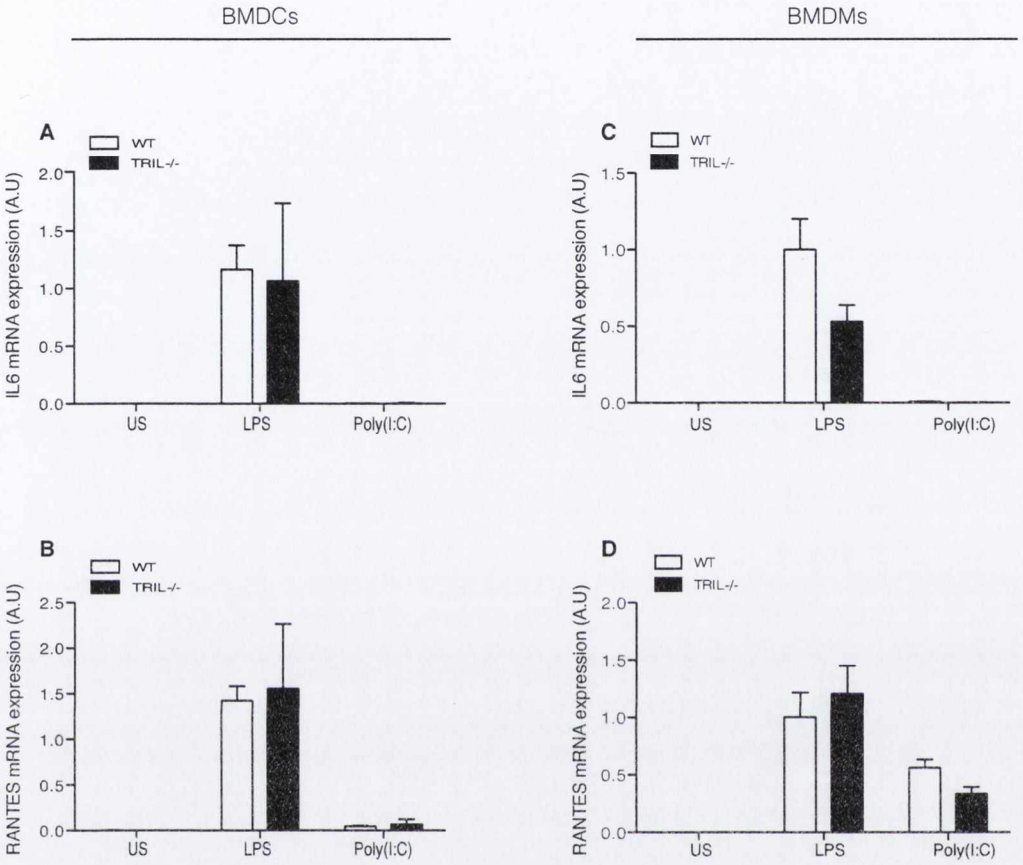

Figure 4.3 TRIL does not impact on IL6 and RANTES expression in primary bone marrow derived macrophages (BMDMs) and dendritic cells (BMDCs)

Following differentiation primary BMDMs and BMDCs derived from TRIL$^{-/-}$ and corresponding WT mice were set up for an experiment. Cells were plated at a concentration of 1 x 10^6 cells/ml in 6 well plates. Following 24 h incubation, cells were left untreated or stimulated with 100 ng/ml of LPS or 25 μg/ml of Poly(I:C) for 5 h prior to lysis and the RNA extraction. Following the reverse transcription reaction, the expression of IL6 (**A** and **C**), and RANTES (**B** and **D**) was examined by QPCR. Obtained mRNA levels were normalised against β-actin and expressed in arbitrary units (A.U). Data are presented as the mean ± SEM of two independent experiments, each carried out in triplicate.

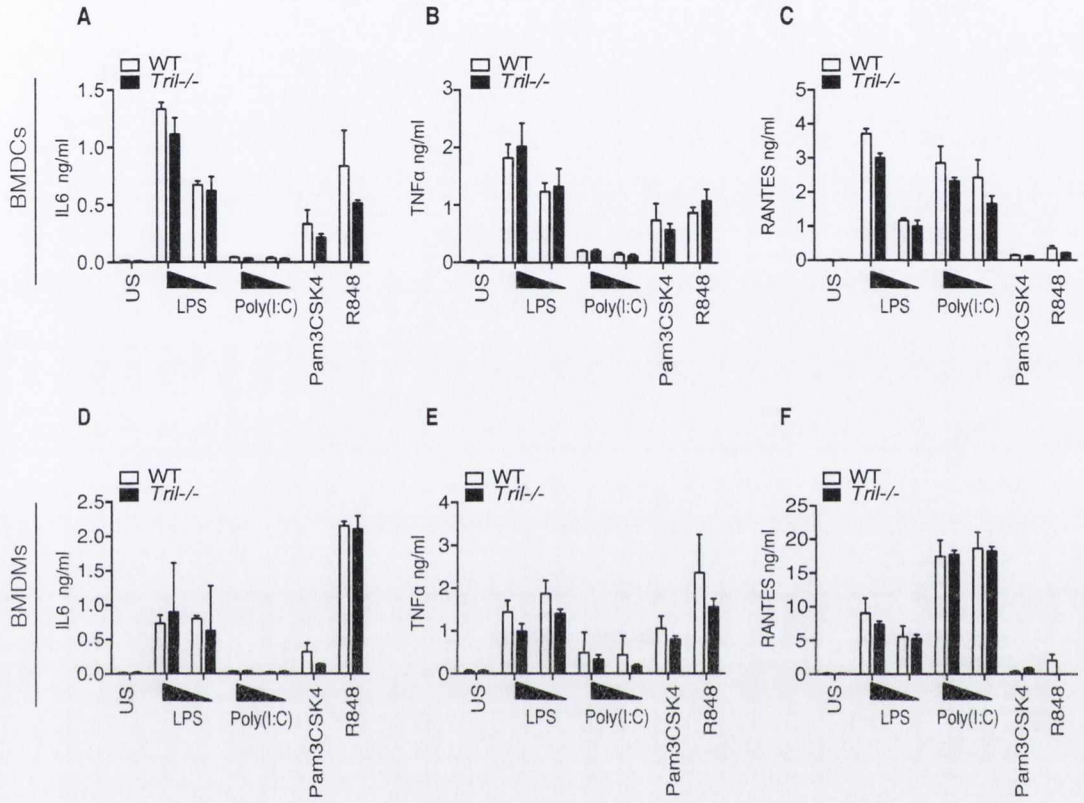

Figure 4.4 TRIL does not impact on TLR mediated responses in bone marrow-derived macrophages (BMDMs) and dendritic cells (BMDCs)

Following differentiation primary BMDMs and BMDCs derived from WT and TRIL$^{-/-}$ mice were set up for an experiment. Cells were plated at a concentration of 0.1 x 10^6 cells/ml in 96 well plates and left to rest for 24 h. Following incubation, cells were left untreated or stimulated with LPS (10 and 100 ng/ml), Poly(I:C) (25 and 50 μg/ml), R848 (1 μg/ml) or Pam3CSK4 (100 nM) for 24 h. Supernatants were collected and assayed for IL6 (**A** and **C**), TNFα (**B** and **D**) and RANTES (**C** and **E**) production. Results are presented as the mean ± SEM of three independent experiments, each carried out in triplicates.

4.2.3 TRIL is highly expressed in glial cells, most predominantly in astrocytes and neurons

In order to examine the expression of TRIL across different murine brain cell populations, specific TRIL primers were designed. QPCR analysis carried out using RNA isolated from cultured murine microglia, astrocytes and neurons demonstrated high levels of TRIL primarily in astrocytes and neurons, compared to microglia (Fig. 4.5), which is in agreement with previous findings on TRIL expression. Interestingly, the expression profile of TRIL within glial cells mirrors that of TLR3, which was also found highly expressed primarily in astrocytes and neurons, but not microglia (Fig. 4.6 A). In contrast, TLR4 was found to be highly expressed in microglia compared to moderate levels detected in astrocytes and neurons (Fig. 4.6 B).

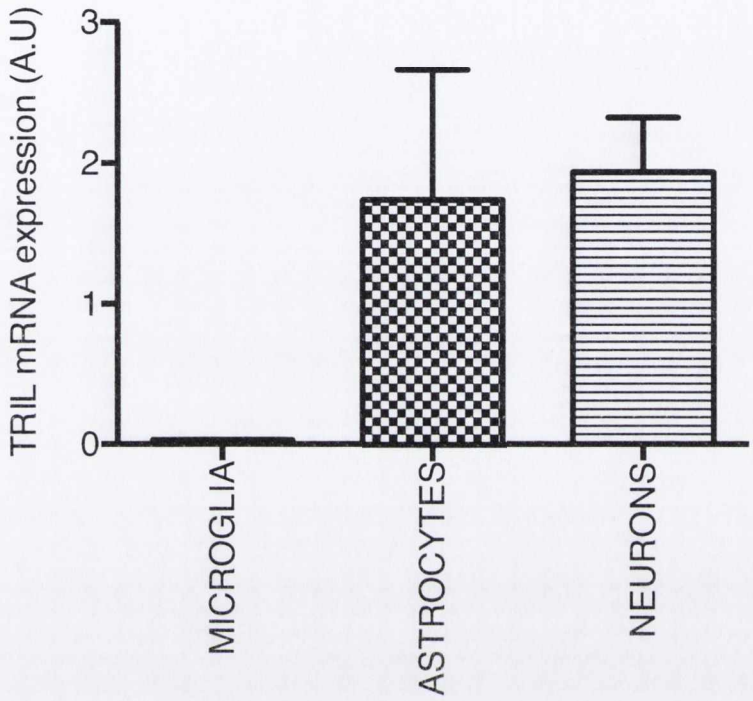

Figure 4.5 TRIL expression profile across glial cell populations

Cultured mouse microglia, astrocytes and neurons were set up at 1 x 10^6 cells/ml in 6 well plates and left to rest for 24 h. Following incubation cells were lysed and RNA was extracted. Following the reverse transcription reaction, expression of TRIL was examined. Obtained mRNA levels were normalised against β-actin and expressed in arbitrary units (A.U). Data are presented as the mean ± SEM of two independent experiments, each carried out in triplicates.

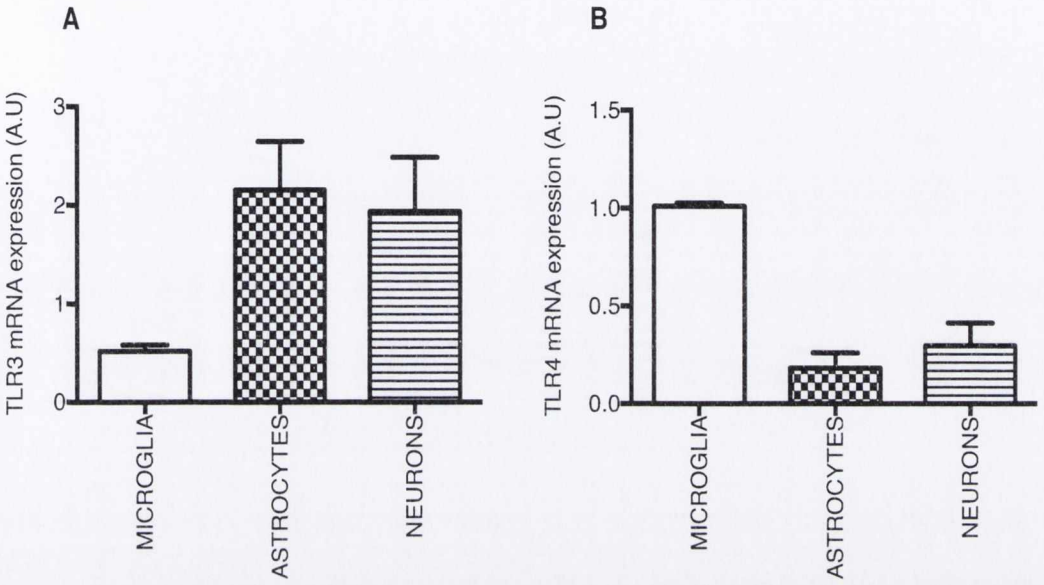

Figure 4.6 TLR3 and TLR4 expression profile across glial cell populations

Cultured mouse microglia, astrocytes and neurons were set up at 1 x 10^6 cells/ml in 6 well plates and left to rest for 24 h. Following incubation cells were lysed and RNA was extracted. Following the reverse transcription reaction, expression of TLR3 (**A**) and TLR4 (**B**) was examined by QPCR. Obtained mRNA levels were normalised against β-actin and expressed in arbitrary units (A.U). Data are presented as the mean ± SEM of two independent experiments, each carried out in triplicates.

4.2.4 Studying the function of TRIL in primary murine mixed glial cells

Having established high expression of TRIL within glial cell populations, notably astrocytes and neurons, I next decided to investigate in more detail the function of TRIL in primary mixed glial cells, consisting largely of astrocytes (approximately 70% astrocytes and 30% microglia) derived from WT and TRIL$^{-/-}$ mice.

As seen from the Figure 4.7 TRIL deficient cells are indeed devoid of TRIL expression as expected, while high basal levels of TRIL mRNA in the untreated WT mixed glial cells were further boosted following 5 h of stimulation with both LPS and Poly(I:C). In agreement with the previous data implicating TRIL in the regulation of TLR3 and TLR4 signalling, the absence of TRIL led to a decrease in IL6 and RANTES expression following both LPS and Poly(I:C) stimulation (Fig. 4.8 A and B).

I next analysed the mRNA levels of 50 murine genes in WT and TRIL$^{-/-}$ primary mixed glial cells (Fig. 4.9) using a non-enzymatic RNA profiling technology that employs bar-coded fluorescent probes to simultaneously analyse mRNA expression levels of differentially regulated genes (nCounter, Nanostring). This further, more comprehensive QPCR analysis revealed reduced expression of a number of proinflammatory cytokines and chemokines in TRIL deficient cells in response to LPS and Poly(I:C) (Fig. 4.9). The mRNA levels of IL6, RANTES (Ccl5), TNFα, IL1α, IL1β and IFNβ were all decreased in TRIL deficient cells. Additionally, the expression levels of chemokines such as the Cxcl2 and Ccl4 were also reduced in TRIL deficient cells upon ligand activation (Fig. 4.9).

In agreement with the gene expression data, following 24 h treatment with two different doses of LPS (10 and 100 ng/ml) and Poly(I:C) (25 and 50 μg/ml) a statistically significant decrease in the IL6 and RANTES protein production was observed in primary mixed glial cells derived from TRIL$^{-/-}$ mice compared to WT controls (Fig. 4.10 A and B). In addition, lack of TRIL affected TNFα protein level in response to LPS and production of IFNβ upon induction with Poly(I:C) (Fig. 4.10 C and D). No major differences in the responses of TRIL deficient and WT cells were seen following treatment with the TLR2 agonist Pam3CSK4, and TLR7/8 ligand R848 (Fig. 4.10 A-D).

These data clearly demonstrated the involvement of TRIL in the modulation of TLR3 and TLR4 but not TLR2 and TLR7/8 responses in the primary mixed glial cells.

In addition, I also confirmed the specificity of LPS and Poly(I:C) in mixed glial cells by examining cells from TLR4, TLR3 and TRIF deficient mice ($TLR4^{-/-}$, $TLR3^{-/-}$, $TRIF^{-/-}$, respectively). Examination of primary mixed glial cells derived from $TLR4^{-/-}$ mice revealed significantly reduced levels of IL6 and RANTES expression as well as IL6 and TNFα production following LPS stimulation, compared to WT controls (Fig. 4.11 A-D). As expected, cytokine expression and production triggered by stimulation with other TLR agonists such as Poly(I:C), Pam3CSK4 and R848, was not affected by the absence of TLR4 (Fig. 4.11 A-D). In the study using WT and $TLR3^{-/-}$ primary mixed glial cells, differences in IL6 and RANTES expression and/or production were observed exclusively upon treatment with TLR3 ligand Poly(I:C) (Fig. 4.12 A-D), whereas responses to LPS, Pam3CSK4 and R848 stimulation were the same for WT and TLR3 deficient cells. In the case of primary mixed glial cells derived from WT and $TRIF^{-/-}$ mice, decreased expression and production of IL6 and RANTES was detected following both LPS and Poly(I:C) challenge (Fig. 4.13 A-D), consistent with the role for TRIF in the TLR3 and endosomal TLR4 signalling pathways.

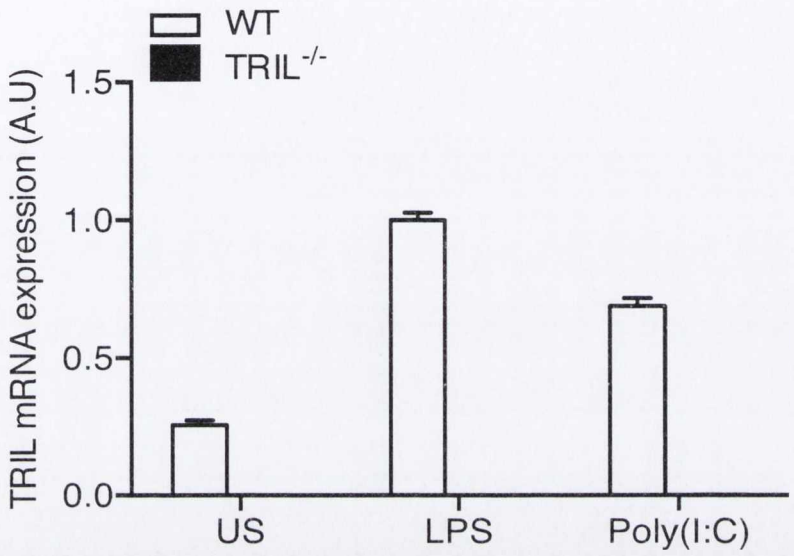

Figure 4.7 The expression of TRIL is enhanced following LPS and Poly(I:C) stimulation in primary murine mixed glial cells

On day 8 post isolation, primary murine mixed glial cells deriver from TRIL deficient and corresponding wild-type control mice were set up for an experiment. Cells were plated at a concentration of 1 x 10^6 cells/ml in 6 well plates. Following incubation, cells were left untreated or stimulated with LPS (100 ng/ml) or Poly(I:C) (25 μg/ml) for 5 h, prior to lysis and the RNA extraction. Next, the QPCR analysis was carried out in order to examine the level of TRIL expression. The mRNA levels of TRIL were normalised to β-actin and expressed in arbitrary units (A.U). Data are represented as the mean ± SD of one experiment representative of three independent experiments, each carried out in triplicates.

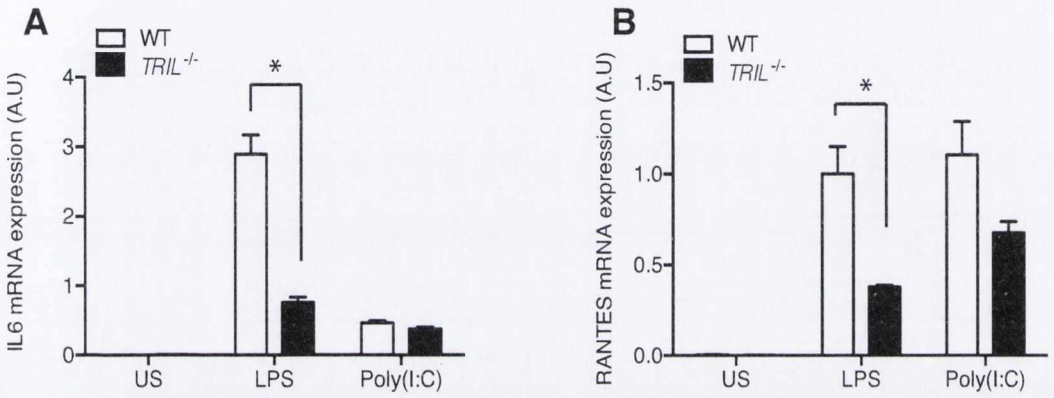

Figure 4.8 Lack of TRIL affects expression of both IL6 and RANTES in primary murine mixed glial cells following stimulation with LPS and RANTES upon induction with Poly(I:C)

On day 8 post-isolation, primary murine mixed glial cells and corresponding wild-type controls, were set up for an experiment. Cells were plated at a concentration of 1 x 10^6 cells/ml in 6 well plates and left over night to rest. Following incubation, cells were left untreated or stimulated for 5 h with LPS (100 ng/ml) or Poly(I:C) (25 μg/ml), prior to lysis and the RNA extraction. Following the reverse transcription reaction, the expression of IL6 **A** and RANTES **B** and was examined by QPCR. Obtained mRNA levels were normalised to β-actin and expressed in arbitrary units (A.U). Data are represented as the mean ± SD of one experiment representative of three independent experiments, each carried out in triplicates. *, $p < 0.05$.

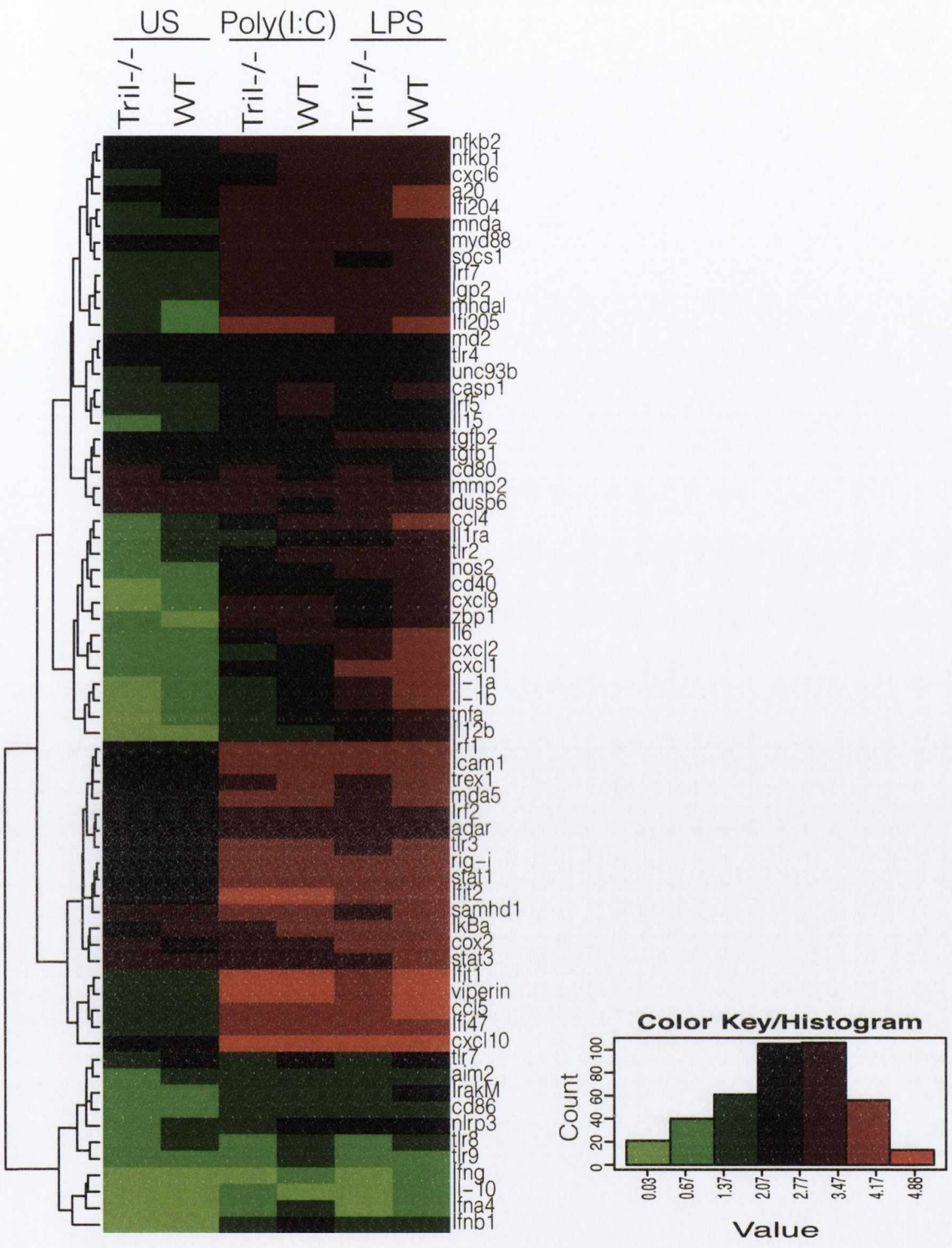

Figure 4.9 Gene expression profile in primary murine mixed glial cells derived from WT and TRIL deficient mice at the basal level and following stimulation with LPS and Poly(I:C)

Figure 4.9 Gene expression profile in primary murine mixed glial cells derived from WT and TRIL deficient mice at the basal level and following stimulation with LPS and Poly(I:C)

On day 8 post-isolation, primary murine mixed glial cells and age/sex matched wild-type controls, were set up for an experiment. Cells were plated at a concentration of 1 x 10^6 cells/ml in 6 well plates and left over night to rest. Following incubation, cells were left untreated or stimulated for 5 h with LPS (100 ng/ml) or Poly(I:C) (25 μg/ml), prior to lysis and RNA extraction. Total RNA was next hybridised to a custom gene expression CodeSet and analysed on an nCounter Digital Analyser. Counts were normalised to endogenous controls per Nanostring Technologies' specifications. Gene expression profiles are displayed as a heat map (log10 transformed) with hierarchical clustering indicated by dendrogram. Up-regulated genes are shown in red, down regulated genes are represented in green.

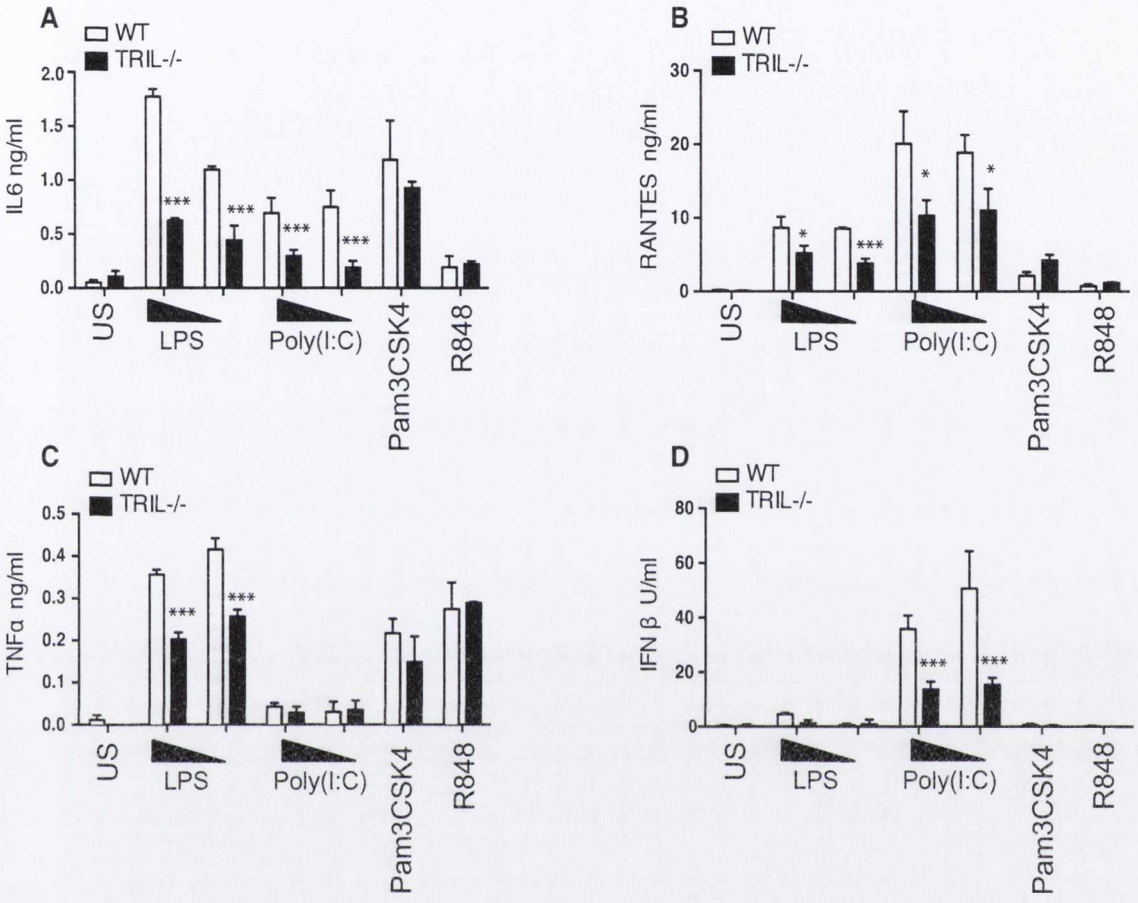

Figure 4.10 Lack of TRIL affects TLR3 and TLR4 but not TLR2 and TLR7 mediated signalling pathways in primary murine mixed glial cells

On day 8 post-isolation, primary murine mixed glial cells derived form TRIL deficient and sex/aged matched WT mice were plated at 0.1 x 10^6 cells/ml in 96-well plates. Following over night incubation cells were stimulated with LPS (100 ng/ml), Poly(I:C) (25 μg/ml), R848 (1μg/ml), Pam3CSK4 (100nM) for 24h. Supernatants were collected and assayed by ELISA for IL6 **A**, RANTES **B**, TNFα **C**, and IFNβ **D** production. Results are presented as the mean ± SEM of three independent experiments, each carried out in triplicates. ***, $p < 0.001$; **, $p < 0.01$, *, $p < 0.05$.

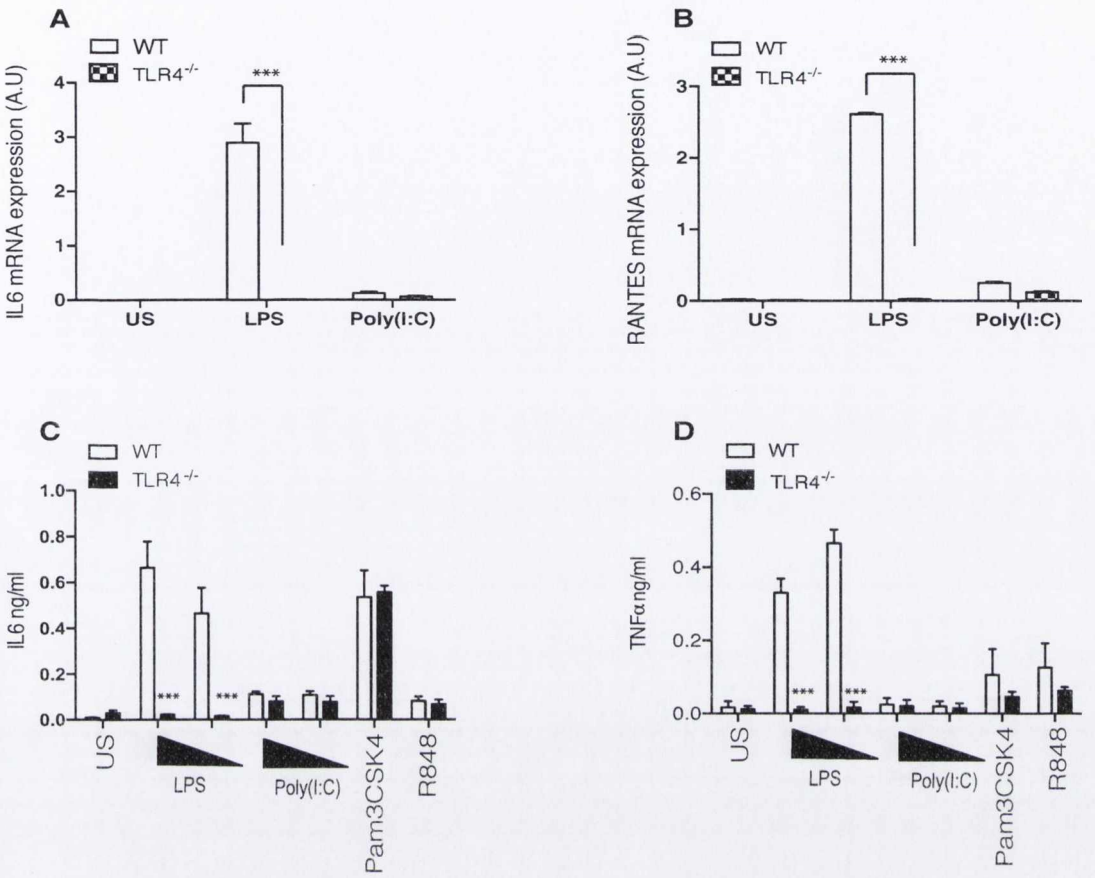

Figure 4.11 Analysis of TLR mediated responses primary murine mixed glial cells derived from WT and TLR4 deficient mice

On day 8 post-isolation, primary murine mixed glial cells derived form TRIL deficient and sex/aged matched WT mice were set up for an experiments. **A** and **B**, Cells were plated at a concentration of 1 x 10^6 cells/ml in 6 well plates and left over night to rest. Following incubation, cells were left untreated or stimulated for 5 h with LPS (100 ng/ml) or Poly(I:C) (25 μg/ml), prior to lysis and RNA extraction. Following reverse transcription reaction, expression of IL6 **A** and RANTES **B**, was examined by QPCR. Obtained mRNA levels were normalised to β-actin and expressed in arbitrary units (A.U). Results are expressed as mean ± SD for triplicate determinations and are representative of three independent experiments, each carried out in triplicates. **C** and **D,** Cells were plated at 0.1 x 10^6 cells/ml in 96-well plates. Following over-night incubation cells were stimulated with LPS (100 ng/ml), Poly(I:C) (25 μg/ml), R848 (1μg/ml), Pam3CSK4 (100 nM) for 24h. Supernatants were collected and IL6 **C** and RANTES **D**, production was examined by ELISA. Data are represented as mean ± SD for triplicate determinations and are representative of three independent experiments each carried out in triplicate. ***, $p < 0.001$; **, $p < 0.01$, *, $p < 0.05$.

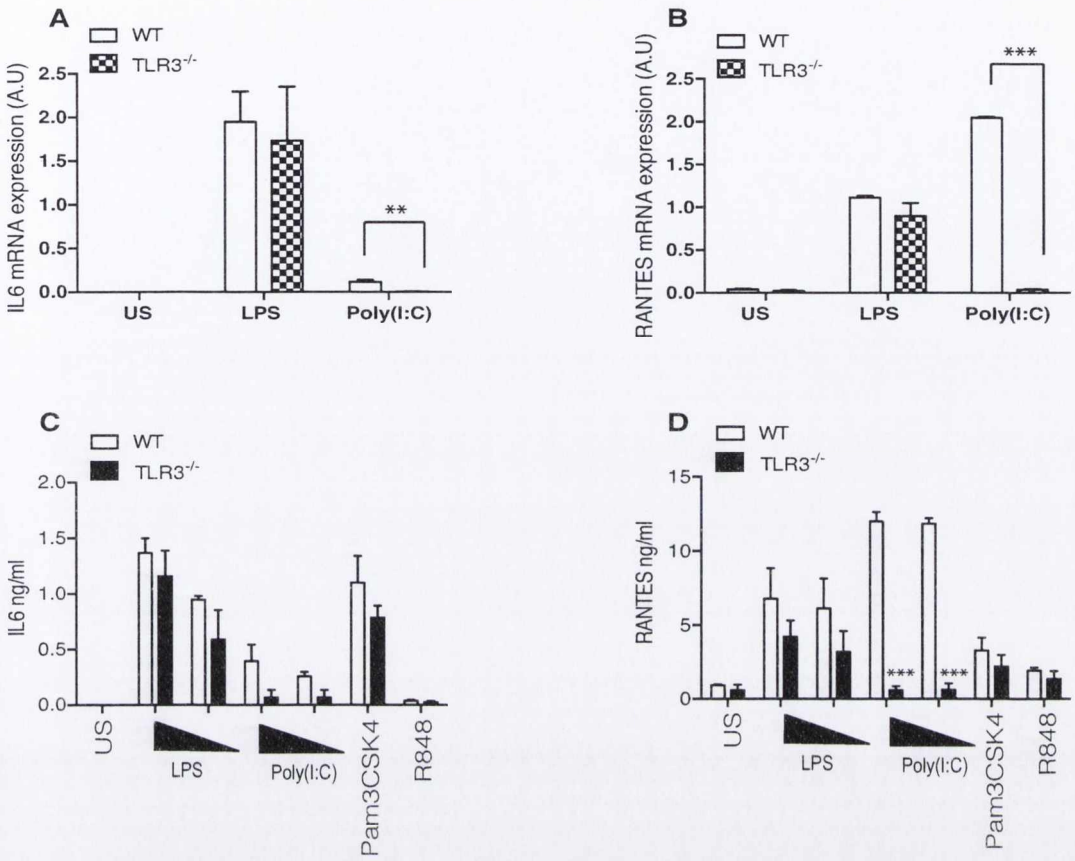

Figure 4.12 Analysis of TLR responses primary murine mixed glial cells derived from WT and TLR3 deficient mice

On day 8 post-isolation, primary murine mixed glial cells derived form TRIL deficient and sex/aged matched WT mice were set up for an experiments. **A** and **B**, Cells were plated at a concentration of 1 x 10^6 cells/ml in 6 well plates and left over night to rest. Following incubation, cells were left untreated or stimulated for 5 h with LPS (100 ng/ml) or Poly(I:C) (25 μg/ml), prior to lysis and the RNA extraction. Following the reverse transcription reaction, the expression of IL6 **A** and RANTES **B**, was examined by the QPCR. Obtained mRNA levels were normalised to β-actin and expressed in arbitrary units (A.U). Results are expressed as mean ± SD for triplicate determinations and are representative of three independent experiments, each carried out in triplicates. **C** and **D,** Cells were plated at 0.1 x 10^6 cells/ml in 96-well plates. Following over-night incubation cells were stimulated with LPS (100 ng/ml), Poly(I:C) (25 μg/ml), R848 (1 μg/ml), Pam3CSK4 (100 nM) for 24h. Supernatants were collected and IL6 **C** and RANTES **D**, production was examined by ELISA. Data are represented as mean ± SD for triplicate determinations and are representative of three independent experiments each carried out in triplicate. ***, $p < 0.001$; **, $p < 0.01$.

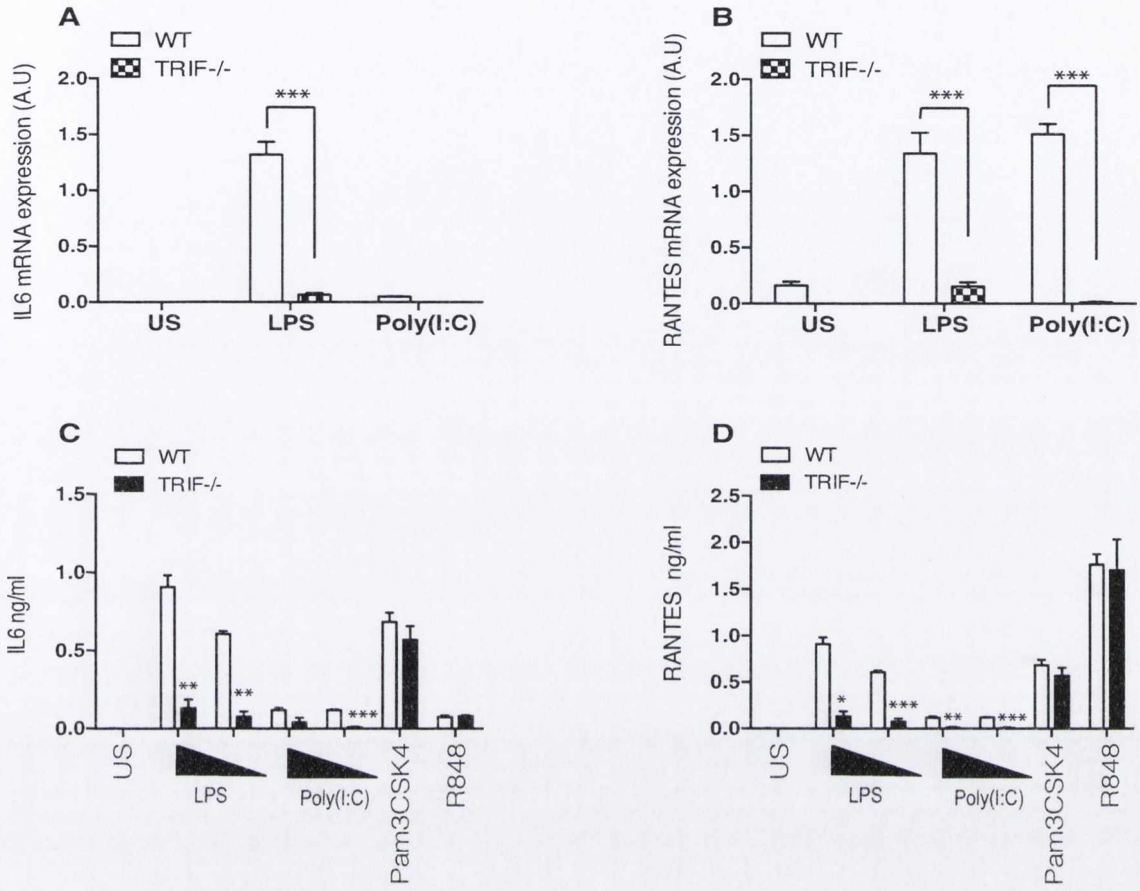

Figure 4.13 Analysis of TLR mediated responses primary murine mixed glial cells derived from WT and TRIF deficient mice

On day 8 post-isolation, primary murine mixed glial cells derived form TRIL deficient and sex/aged matched WT mice were set up for an experiments. **A** and **B**, Cells were plated at a concentration of 1 x 10^6 cells/ml in 6 well plates and left over night to rest. Following incubation, cells were left untreated or stimulated for 5 h with LPS (100 ng/ml) or Poly(I:C) (25 μg/ml), prior to lysis and the RNA extraction. Following the reverse transcription reaction, the expression of IL6 **A** and RANTES **B**, was examined by the QPCR. Obtained mRNA levels were normalised to β-actin and expressed in arbitrary units (A.U). Results are expressed as mean ± SD for triplicate determinations and are representative of three independent experiments each carried out in triplicates. **C** and **D,** Cells were plated at 0.1 x 10^6 cells/ml in 96-well plates. Following over-night incubation cells were stimulated with LPS (100 ng/ml), Poly(I:C) (25 μg/ml), R848 (1 μg/ml), Pam3CSK4 (100 nM) for 24h. Supernatants were collected and IL6 **C** and RANTES **D**, production was examined by ELISA. Data are represented as mean ± SD for triplicate determinations and are representative of three independent experiments each carried out in triplicates. ***, $p < 0.001$; **, $p < 0.01$, *, $p < 0.05$.

4.2.5 Studies into the *in vivo* role of TRIL in *E.coli*-induced acute peritonitis model

Infections with the Gram-negative bacteria such as *E.coli* are well known to induce TLR4-driven signal through LPS. Accessory molecules LBP, MD2 and CD14 all participate in binding and delivery of LPS to TLR4. Due to the essential role of accessory molecules in LPS recognition and activation of TLR4, CD14, MD2 and LBP actively contribute to lethal Gram-negative bacterial infections.

TRIL was shown to play a role in modulation of TLR4 responses and was found to interact with both TLR4 and its ligand LPS (Carpenter et al, 2009). However the function of TRIL *in vivo* has not been examined TRIL deficient mice. I therefore next tested a Gram-negative *E.coli* induced acute peritonitis infection model using TRIL deficient mice.

4.2.5.1 Intraperitoneal *E.coli* infection leads to increased TRIL expression in brain

Following the intraperitoneal *E.coli*, observed basal expression of TRIL was significantly higher in the brain compared to the spleen of WT mice and it was even further enhanced upon *E.coli* challenge (Fig. 4.14). TRIL expression within the spleen was rather low and clearly was not increased following bacterial infection (Fig. 4.14).

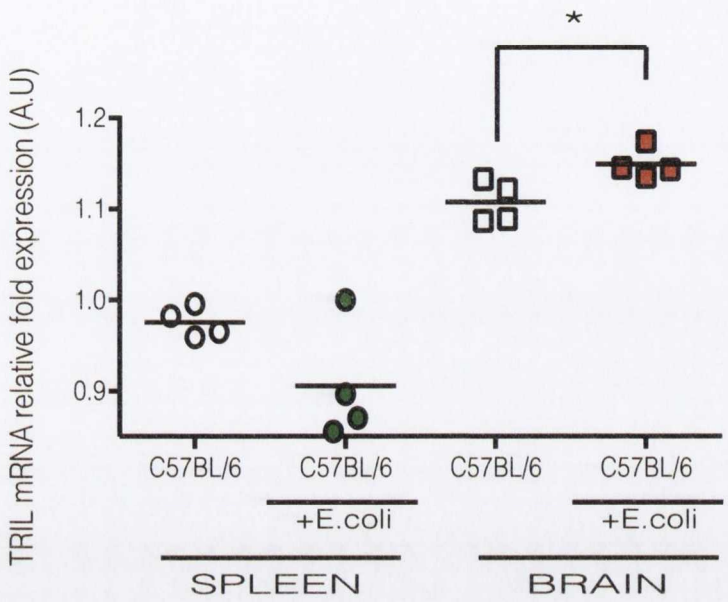

Figure 4.14 TRIL expression increases within the brain but not spleen of WT (C57BL/6) mice following the *E.coli* challenge

The *E.coli* strain BL21 (10^9 CFU) or corresponding amount of PBS, were administrated into the C57BL/6 mice (n=4), via the intraperitoneal (IP) route. Following 6h of incubation, mice were sacrificed and both spleen and brain were isolated. Organs were homogenised, followed by RNA extraction. Samples were next analysed by QPCR for TRIL expression. mRNA levels of TRIL were normalised against β-actin control and expressed in arbitrary units (A.U). Data are presented as mean ± SEM of two independent experiments, both carried out in triplicates. *, $p<0.05$.

4.2.5.2 Bacteria can be detected in brain following intraperitoneal *E.coli* infection

As the expression of TRIL was significantly enhanced following the intraperitoneal *E.coli* challenge within the brain but not the spleen, I decided to evaluate if the detected differences in TRIL expression were triggered directly by bacteria present in the brain. Bacterial load measured in the spleen and brain of WT mice revealed that both tissues contain comparable amounts of bacteria ranging from 10^8 to 10^4 CFU/ml in the spleen and brain, respectively (Fig. 4.15). This data demonstrated that *E.coli* entered the brain following the intraperitoneal *E.coli* challenge, most probably through the compromised BBB. Therefore an increase in the expression of TRIL in the brain following *E.coli* challenge was presumably induced directly by the bacteria present in the brain.

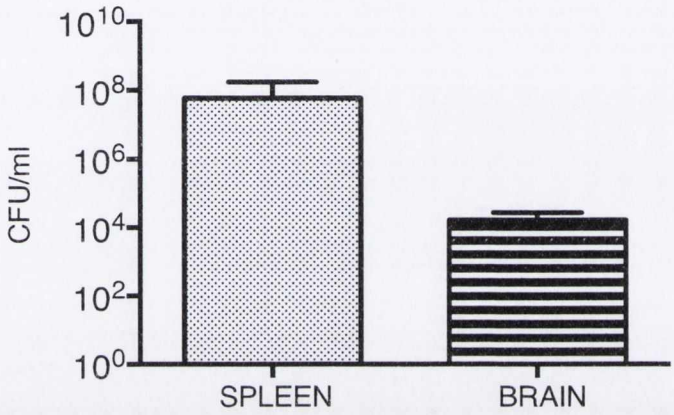

Figure 4.15 Bacterial load within the spleen and brain of WT mice following *E.coli* infection

WT mice were infected with the *E.coli* (10^9 CFU) via the IP route. 6h post infection mice (n=8) were sacrificed and both spleen and brain were isolated. Organs were homogenized and lysates were plated on agar plates. Following 24 h incubation number of bacteria in the spleen and brain was calculated. Data are expressed as mean ± SEM of three independent experiments, each carried out in triplicates.

4.2.5.3 TRIL modulates cytokine expression in the brain following intraperitoneal *E.coli* challenge

Following on from the initial observation demonstrating increased expression of TRIL in the brain following *E.coli* challenge, I decided to next examine the importance of TRIL in response to *E.coli* infection in spleen, brain and periphery using WT and TRIL$^{-/-}$ mice. mRNA levels of IL6 and RANTES were significantly decreased following *E.coli* challenge exclusively in the brain but not spleen samples derived from mice lacking TRIL, compared to WT controls (Fig. 4.16 A and B). When the QPCR was conducted using cDNA generated from the spleen of WT and TRIL deficient mice, the mRNA levels of both IL6 and RANTES did not show a significant decrease (Fig. 4.16 C and D).

An additional, extensive analysis of the mRNA levels of 50 murine genes in the brain samples of WT and TRIL deficient mice following *E.coli* challenge, revealed reduced expression levels of numerous proinflammatory cytokines such as IL6, TNFα, IL1α, IL1β as well as chemokines Ccl4 and Cxcl2, in the TRIL$^{-/-}$ mice compared to WT controls (Fig. 4.17). Interestingly, a number of genes implicated in the antiviral response, such as VIPERIN and RIG-I were also dramatically reduced in the absence of TRIL (Fig. 4.17).

Overall these data demonstrated the involvement of TRIL in the regulation of proinflammatory gene expression during *E.coli*-induced acute peritonitis. The effect of TRIL was apparent in the brain and less marked in the spleen, which correlates with the expression pattern of brain-enriched TRIL.

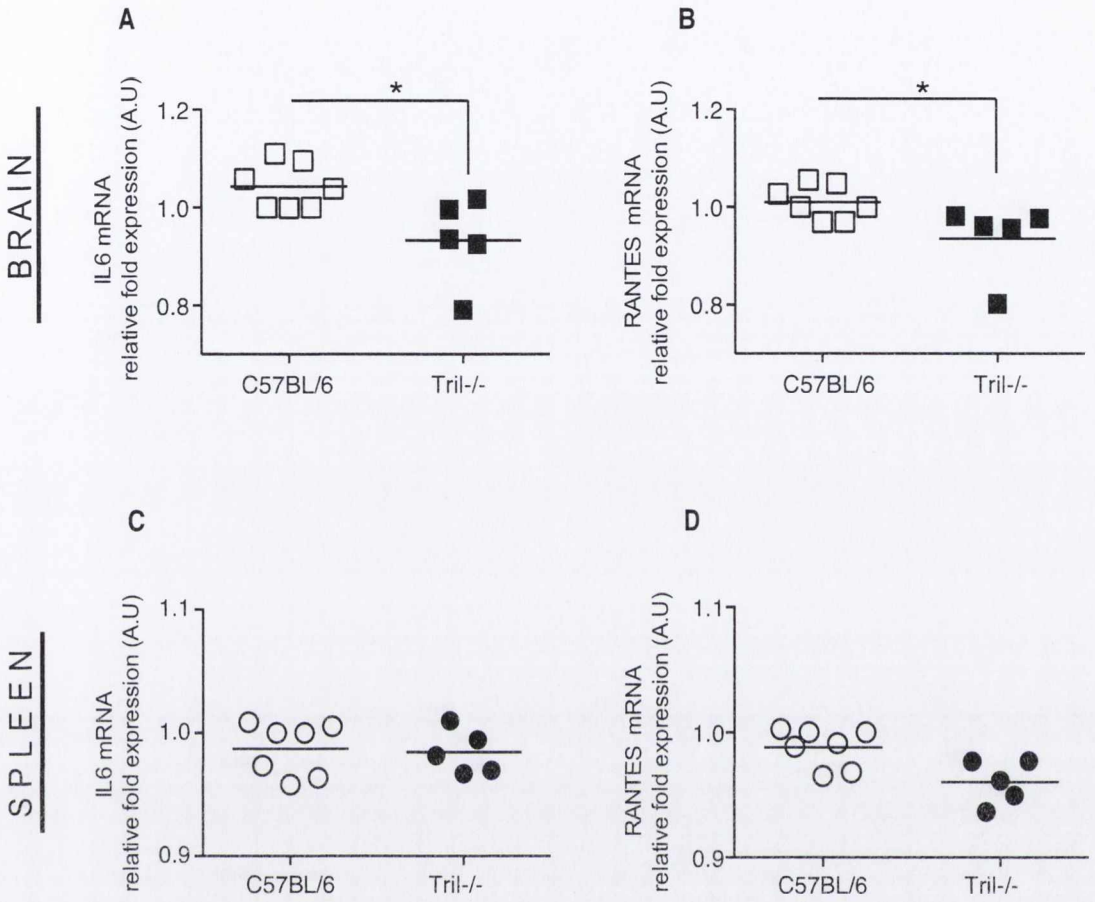

Figure 4.16 Expression of proinflammatory cytokines in the brain and spleen of WT and TRIL$^{-/-}$ mice following *E.coli* challenge

TRIL deficient mice (TRIL$^{-/-}$) and sex/age matched C57BL/6 mice (n=5-7), were infected with the *E.coli* strain BL21 (10^9 CFU) via the IP route. 6h post infection mice were sacrificed and both spleen and brain were isolated. Organs were homogenised, followed by the RNA extraction. Both brain (**A** and **B)** spleen (**C** and **D**) derived samples were next analysed by the QPCR for IL6 and RANTES expression. The mRNA levels were normalised to β-actin and expressed as relative to WT mice (C57BL/6) in arbitrary units (A.U). Data are presented as a mean ± SEM of three independent experiments, each carried out in triplicates. *, $p<0.05$.

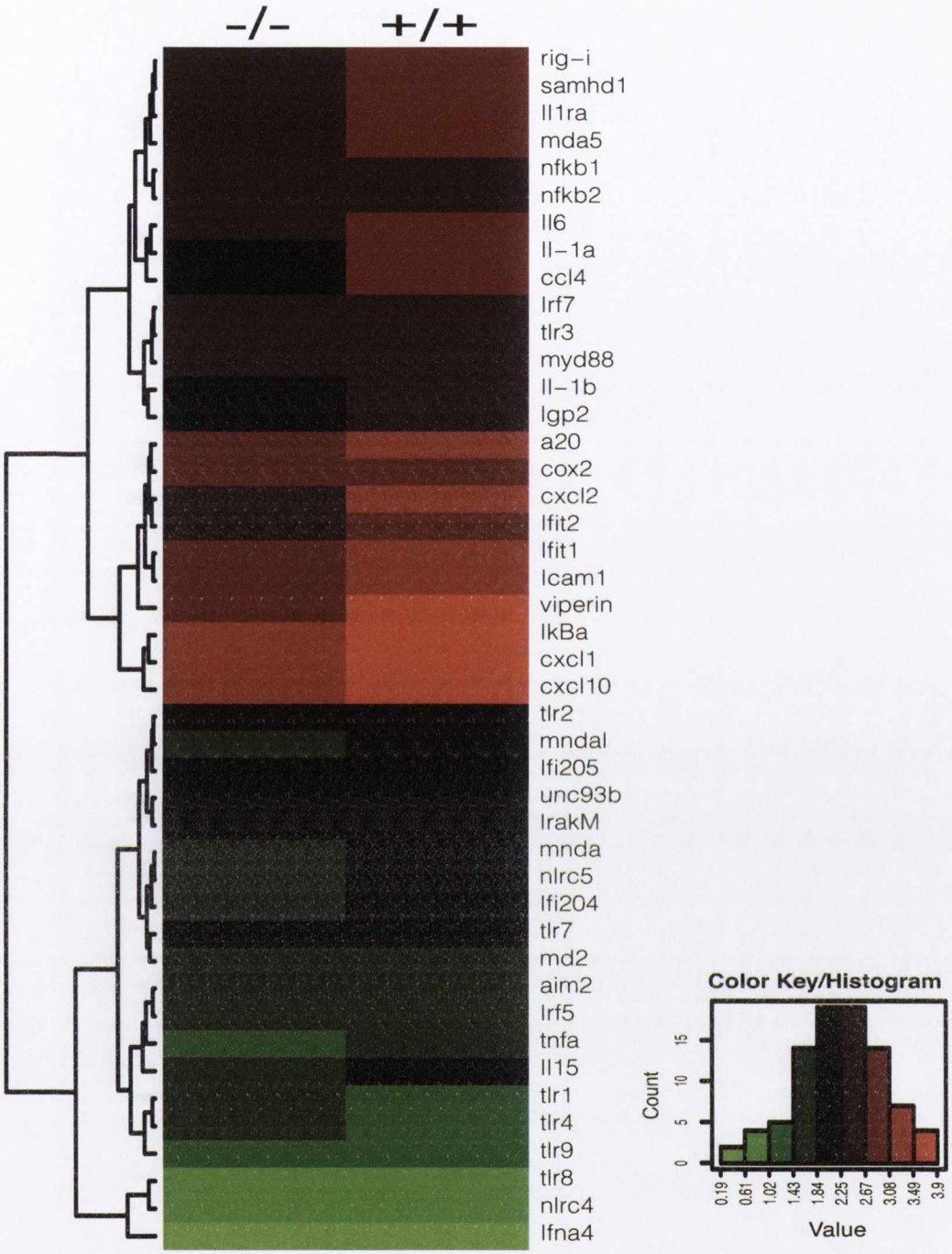

Figure 4.17 Gene expression profile in the brain of WT and TRIL$^{-/-}$ mice following *E.coli* challenge

Figure 4.17 Gene expression profile in the brain of WT and TRIL$^{-/-}$ mice prior and following *E.coli* challenge

TRIL deficient mice (TRIL$^{-/-}$) and sex/age matched C57BL/6 mice (n=5-8), were infected with the *E.coli* strain BL21 (10^9 CFU) via the IP route. 6h post infection mice were sacrificed and brain tissue was isolated. Organs were homogenised, followed by the RNA extraction. Total RNA was next hybridized to a custom gene expression CodeSet and analysed on an nCounter Digital Analyser. Counts were normalised to endogenous controls per Nanostring Technologies specifications. Gene expression profiles are displayed as a heat map (log10 transformed) with hierarchical clustering indicated by dendrogram. Upregulated genes are shown in red, down regulated genes are represented in green.

4.2.5.4 IL6 is dramatically reduced in serum and peritoneal lavage of TRIL deficient mice upon *E.coli* challenge

Carrying on from the expression studies, I next investigated the impact of TRIL on production of proinflammatory cytokines during the intraperitoneal *E.coli* infection. TRIL-deficiency led to a significant decrease in IL6 (Fig. 4.18 A and B) production within the serum and peritoneal lavage of $TRIL^{-/-}$ mice compared to WT controls. Differences observed for RANTES production were very moderate and did not reach statistical significance (Fig. 4.18 C and D).

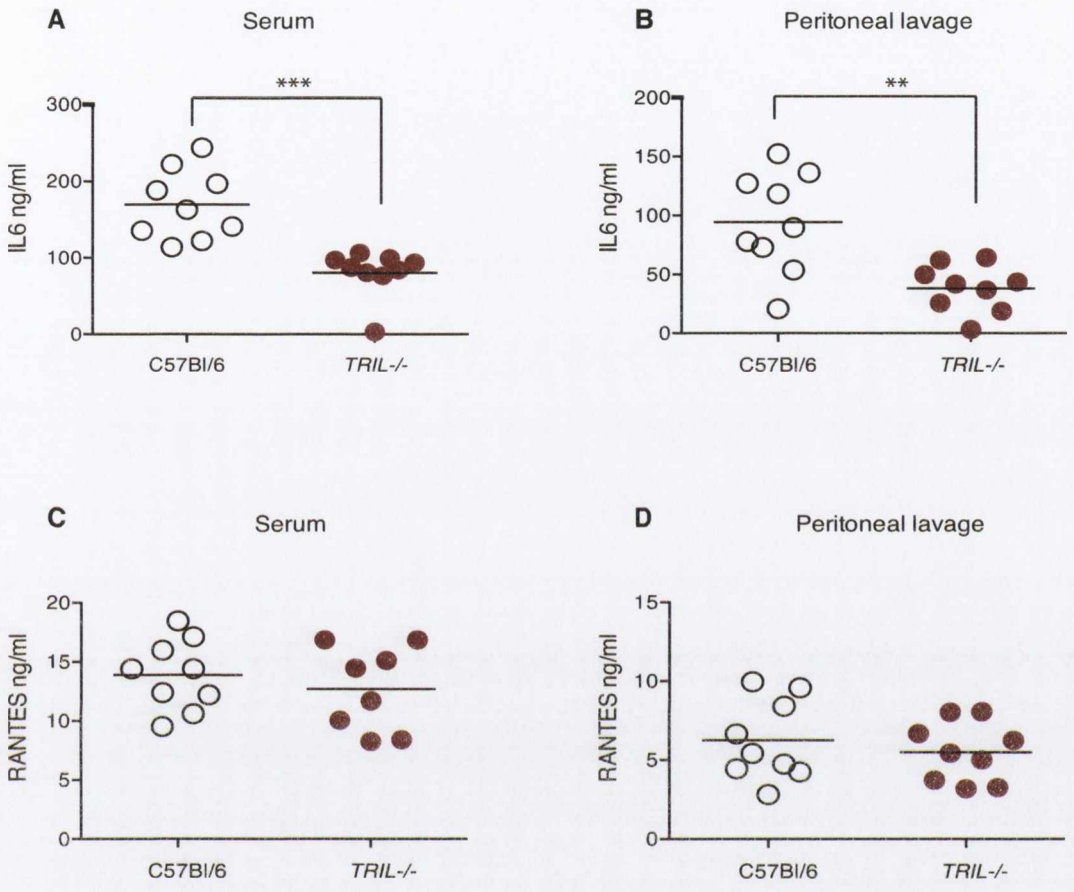

Figure 4.18 Proinflammatory cytokine production in the serum and peritoneum of C57BL/6 and TRIL deficient mice following *E.coli* infection

The *E.coli* strain BL21 (10^9 CFU) was IP injected into the sex/age matched TRIL deficient ($TRIL^{-/-}$) and corresponding C57BL/6 control mice (n=9). Following 6h stimulation mice were sacrificed followed by the peritoneal lavage and serum collection. Samples were processed according to protocol described earlier and assayed by ELISA for IL6 and RANTES production in the serum (**A** and **C**) and peritoneum (**B** and **D**). Data are presented as a mean ± SEM of three independent experiments, each carried out in triplicates ***, $p < 0.001$; **, $p < 0.01$.

4.2.5.5 Enhanced expression of TRIL in the cell population infiltrating peritoneal cavity following *E.coli* challenge compared to peritoneal resident cells

TRIL was found to be poorly expressed in primary BMDMs, therefore macrophages could not be responsible for the observed reduction in IL6 production in the peritoneal lavage isolated from TRIL deficient mice. I hypothesized that the cells infiltrating the peritoneal cavity following *E.coli* infection might be responsible for the observed effect. In order to test this hypothesis I examined the expression of TRIL within the peritoneal cells of WT mice prior to and following the *E.coli* challenge. Figure 4.19 demonstrates a low expression of TRIL in the resident peritoneal cells isolated from the uninfected WT mice and significantly higher levels of TRIL expression in the cells infiltrating the peritoneal cavity following the *E.coli* infection (Fig. 4.19).

These data demonstrated enhanced TRIL expression in the population of peritoneal infiltrating cells upon intraperitoneal *E.coli* infection compared to the resident cell population in the uninfected animals. This could partially explain the detrimental effect of TRIL on IL6 production in the peritoneal lavage upon the *E.coli* challenge observed in the previous experiment (Fig. 4.18).

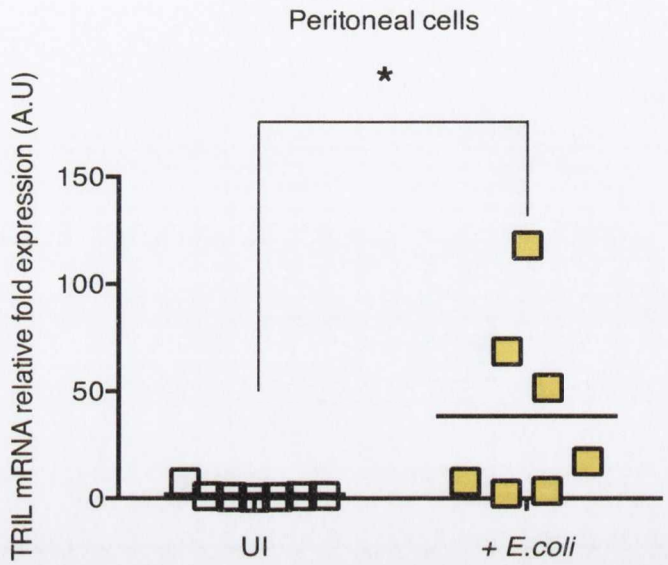

Figure 4.19 TRIL expression in peritoneal cells population derived from C57BL/6 mice prior and following infection with *E.coli*

C57BL/6 mice (n=7) were IP injected with *E.coli* or equivalent amount of PBS. Following 6h of incubation, mice were sacrificed followed by the peritoneal lavage collection. Peritoneal cells were isolated according to the protocol described earlier and used to extract the RNA. Samples were next analysed by QPCR for TRIL expression. The mRNA levels were normalised against β-actin control and expressed in arbitrary units (A.U). Data are presented as mean ± SEM of three independent experiments, all carried out in triplicates. *, $p<0.05$.

4.2.5.6 TLR4/TRIF signalling pathway mediates cytokine expression and production during the peritoneal *E.coli* challenge

Following on from studies on TRIL$^{-/-}$ mice I next examined responses of WT, TLR4$^{-/-}$ and TRIF$^{-/-}$ mice subjected to *E.coli* acute peritonitis model.

First, I set out to test the level of TRIL expression within the spleen and brain of WT, TLR4$^{-/-}$ and TRIF$^{-/-}$ mice following *E.coli* challenge. Consistent with the previous data, TRIL expression was significantly higher in the brain of WT mice, compared to low levels of TRIL expression observed in the spleen (Fig. 4.20 A and B). TLR4 deficiency (Fig. 4.20 A) as well as the absence of TRIF (Fig. 4.20 B), did not impact on TRIL expression levels in both spleen and brain suggesting that TRIL functions upstream of TLR3 and TLR4.

Following on from the TRIL expression analysis, I next examined the expression and production of proinflammatory cytokines in the WT and TLR4$^{-/-}$ mice following *E.coli* infection. As anticipated, the mRNA level of IL6, RANTES and IFNβ were significantly reduced in the spleen (Fig. 4.21 A-C) and brain (Fig. 4.21 D-F) of TLR4$^{-/-}$ mice when compared to WT controls (Fig. 4.21 A-F). Similarly, production of RANTES and IL6 in the serum, peritoneal lavage and spleen was also largely affected by the absence of TLR4 upon intraperitoneal *E.coli* challenge (Fig. 4.22 A-F).

I next confirmed that endosomal TRIF-dependent TLR4 signalling was involved in the response to *E.coli*-induced acute peritonitis. Analysis of the expression and production of proinflammatory cytokines in WT and TRIF$^{-/-}$ mice subjected to *E.coli*-induced acute peritonitis model demonstrates clearly that TRIF participates in the TLR4-mediated response to intraperitoneal *E.coli* infection (Fig. 4.23 and 4.24). The expression levels of IL6, RANTES and TNFα were strongly reduced in the spleen and brains derived from TRIF$^{-/-}$ mice when compared to WT controls (Fig. 4.23 A-F). Additionally, production of IL6 and RANTES were also reduced in the serum, peritoneal lavage and spleen of TRIF deficient but not WT mice (Fig. 4.24 A-F), further supporting the involvement of TRIF-dependent TLR4-mediated response to intraperitoneal *E.coli* challenge.

Overall these data confirmed the implication of TLR4/TRIF-mediated signalling pathway in response to the intraperitoneal *E.coli* infection. This is in agreement with the earlier study by Biswas *et al.* who also demonstrated an evidence for a role of TRIF-dependent TLR4 signalling in the endotoxin shock (Biswas et al, 2011).

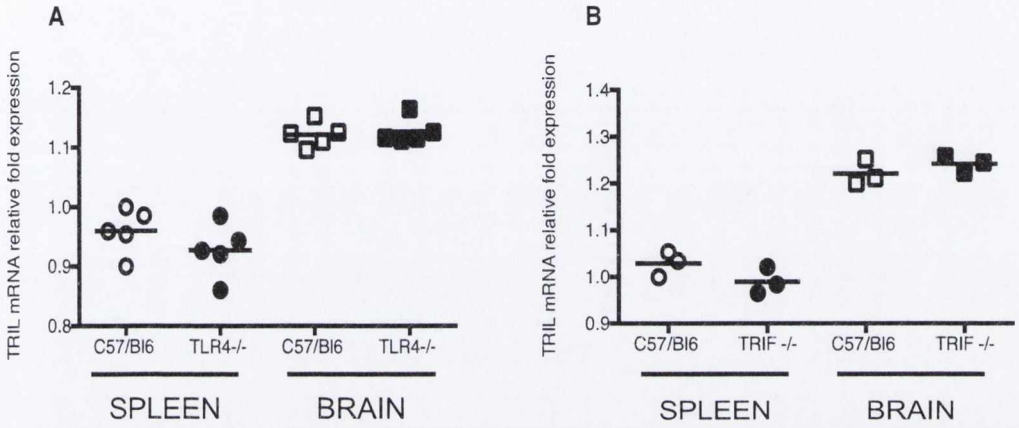

Figure 4.20 Expression of TRIL within the brain and spleen of WT, TLR4$^{-/-}$ and TRIF$^{-/-}$ mice following an *E.coli* challenge

A, TLR4 deficient mice and corresponding C57BL/6 control mice (n=5) were challenge with *E.coli* (10^9 CFU) **B**, The *E.coli* (10^9 CFU) was administrated into the C57BL/6 and TRIF deficient mice (n=3), via the intraperitoneal (IP) route. Following 6h of incubation, mice were sacrificed and both spleen and brain were isolated. Organs were homogenised, followed by the RNA extraction. Samples were next analysed by QPCR for TRIL expression. mRNA levels were normalised against β-actin control and expressed in arbitrary units (A.U). Data are presented as mean ± SEM of two independent experiments, all carried out in triplicates.

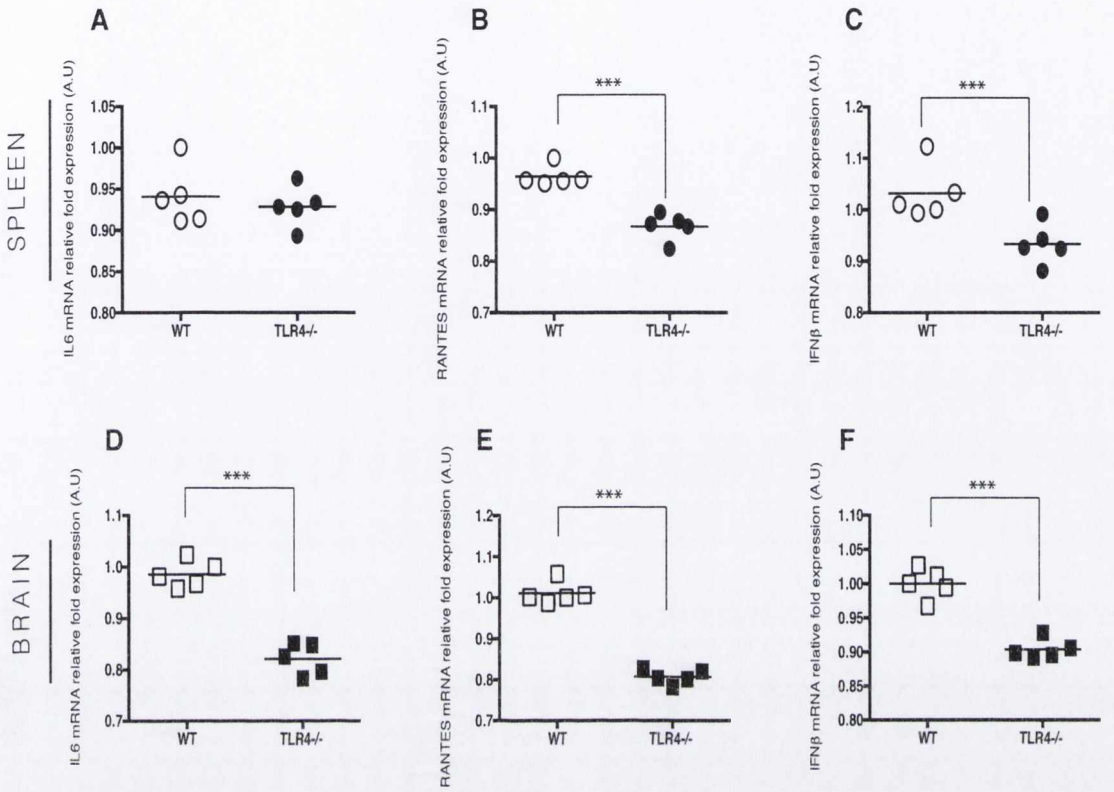

Figure 4.21 Expression of proinflammatory cytokines in the brain and spleen of WT and TLR4$^{-/-}$ mice following *E.coli* challenge

TLR4$^{-/-}$ mice and corresponding C57BL/6 mice (n=5), were infected with the *E.coli* (10^9 CFU) via the IP route. 6 hours post infection mice were sacrificed and both spleen and brain were isolated. Organs were homogenised, followed by RNA extraction. Both spleen (top panel) and brain (bottom panel) derived samples were next analysed by QPCR for IL6 (**A** and **D**), RANTES (**B** and **E**), and IFNβ (**C** and **F**) expression. The mRNA levels were normalised to β-actin and expressed as relative to C57BL/6 mice in arbitrary units (A.U). Data are presented as a mean ± SEM of three independent experiments, each carried out in triplicates. *, $p<0.05$.

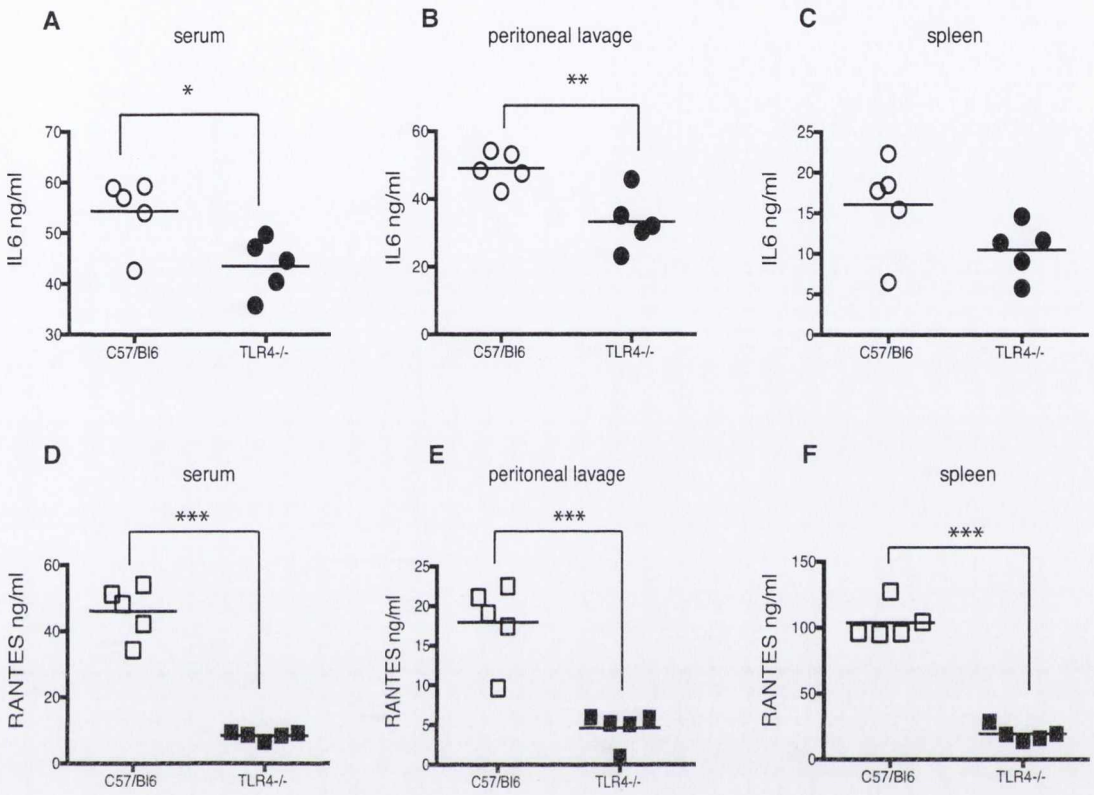

Figure 4.22 Proinflammatory cytokine production in the serum, peritoneum and spleen of C57BL/6 and TLR4$^{-/-}$ mice following *E.coli* infection

TLR4$^{-/-}$ and corresponding C57BL/6 mice (n=5), were infected with the *E.coli* (10^9 CFU) via the IP route. 6 hours post infection mice were sacrificed followed by the peritoneal lavage, serum and spleen collection. Samples were processed according to protocol described earlier and the IL6 (top panel) and RANTES (bottom panel) production in the serum (**A** and **D**), peritoneal cavity (**B** and **E**) and spleen (**C** and **F**) were measured by ELISA. Data are presented as a mean ± SEM of two independent experiments, each carried out in triplicates ***, $p < 0.001$; **, $p < 0.01$, *, $p < 0.05$.

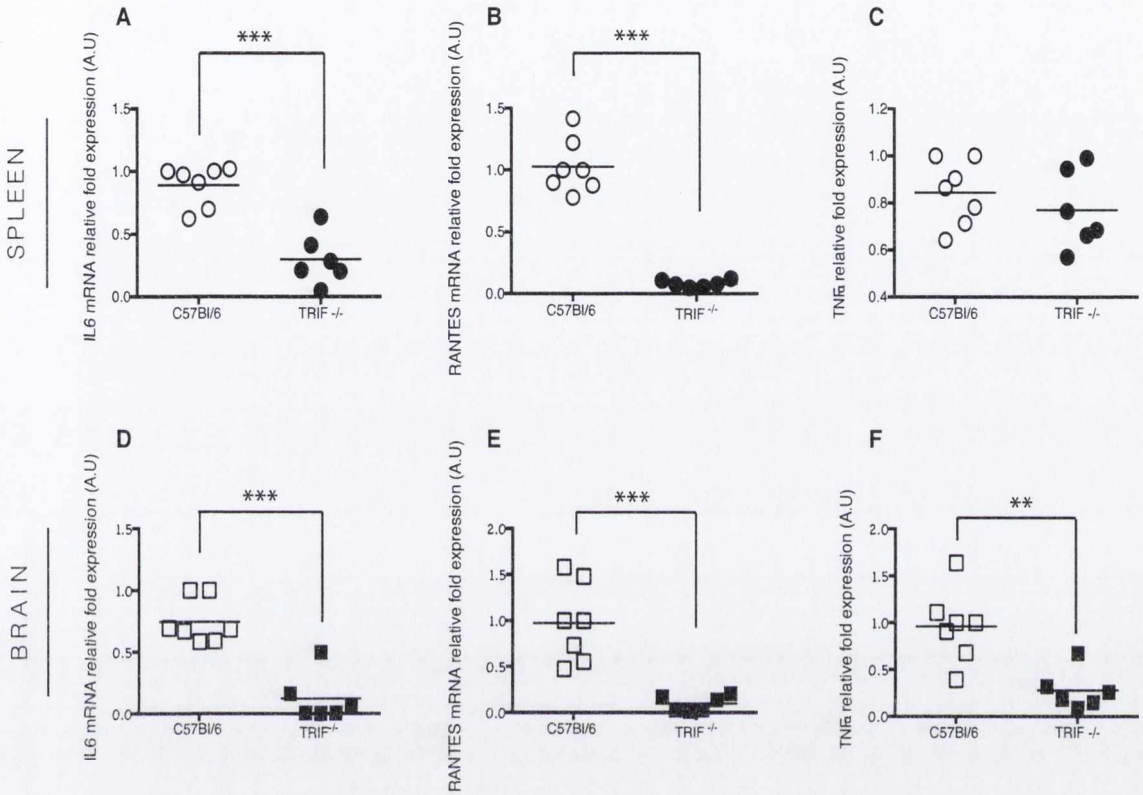

Figure 4.23 Expression of proinflammatory cytokines in the brain and spleen of WT and TRIF$^{-/-}$ mice following *E.coli* challenge

TRIF$^{-/-}$ and corresponding C57BL/6 control mice (n=6-7), were infected with the *E.coli* (10^9 CFU) via the IP route. 6 hours post infection mice were sacrificed and both spleen and brain were isolated. Organs were homogenized, followed by the RNA extraction. Both brain (top panel) and spleen (bottom panel) derived samples were next analysed by the QPCR for IL6 (**A** and **D**), RANTES (**B** and **E**), and TNFα (**C** and **F**) expression. The mRNA levels were normalised to β-actin and expressed as relative to C57BL/6 mice in arbitrary units (A.U). Data are presented as a mean ± SEM of three independent experiments, each carried out in triplicates. ***, $p < 0.001$; **, $p < 0.01$.

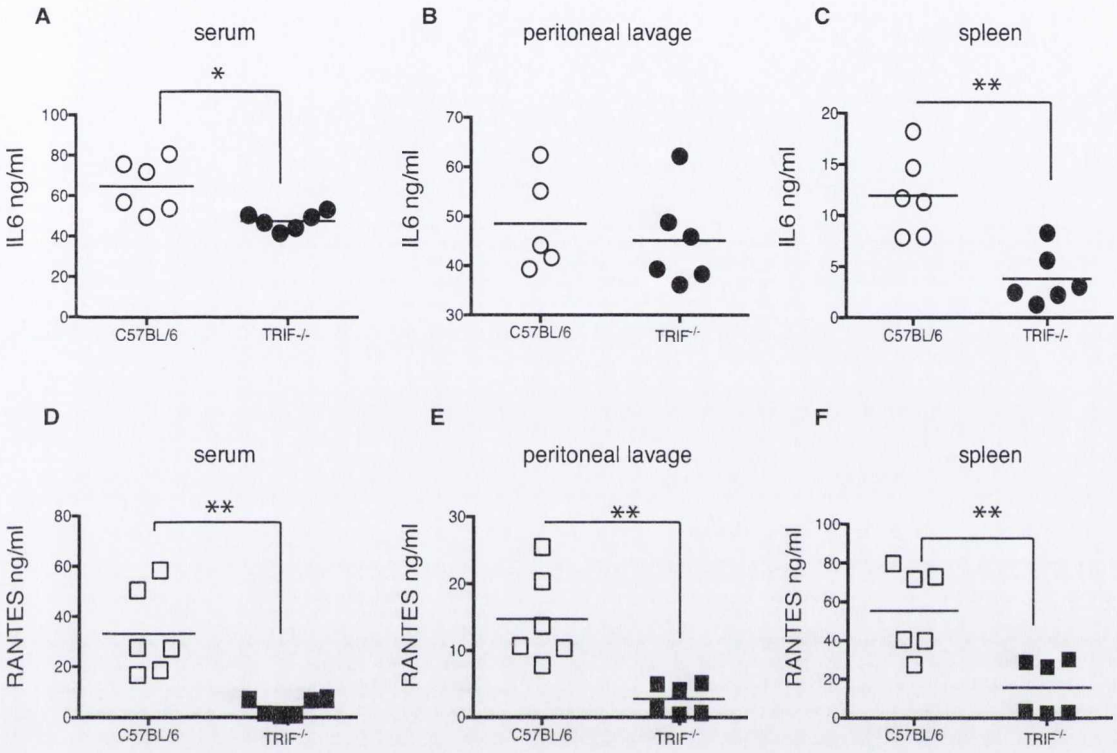

Figure 4.24 Proinflammatory cytokine production in the serum, peritoneum and spleen of C57BL/6 and TRIF deficient mice following *E.coli* infection

$TRIF^{-/-}$ and corresponding C57BL/6 control mice (n=6) were infected with the *E.coli* (10^9 CFU) via the IP route. Following 6h stimulation mice were sacrificed followed by the peritoneal lavage, serum and spleen collection. Samples were processed according to protocol described earlier and the IL6 (top panel) and RANTES (bottom panel) production in the serum (**A** and **D**), peritoneal cavity (**B** and **E**) and spleen (**C** and **F**) were measured by ELISA. Data are presented as a mean ± SEM of two independent experiments, each carried out in triplicates ***, $p < 0.001$; **, $p < 0.01$, *, $p < 0.05$.

4.2.6 The *in vivo* role of TRIL in the antiviral response to vesicular stomatitis virus infection

The *in vivo* studies using WT and TRIL$^{-/-}$ mice subjected to a bacterial model of infection clearly demonstrated a role for TRIL in the regulation of the immune response following intraperitoneal *E.coli* challenge. As I observed reduced expression levels of specific antiviral mediators such as VIPERIN and RIG-I within the brain of TRIL$^{-/-}$ mice, I next decided to examine the role for TRIL in the neurotropic viral infection.

VSV is a neurotropic ssRNA virus triggering brain inflammation associated with acute encephalitis and breakdown of the BBB. Responses to VSV in the brain are T-cell independent and mediated primarily by the resident glial cells (Huneycutt et al, 1993). VSV has been shown to activate TLR4/TRIF-dependent response in macrophages and DCs, resulting in the IRF3 activation and production of type I IFNs (Georgel et al, 2007). Additionally, VSV activates an alternative TLR4 signalling pathway leading to phosphorylation of PI3K and IRF7-dependent type I IFN production, which has been shown to be mediated by CD14 in macrophages (Schabbauer et al, 2008).

4.2.6.1 Examination of TRIL's function in the immune response to VSV in primary mixed glial cells

I examined the expression and function of TRIL during VSV infection *in vitro,* using primary murine mixed glial cells derived from WT and TRIL$^{-/-}$ mice. As can be seen from Figure 4.25 A, the expression of TRIL is significantly enhanced following the VSV infection in the WT cells. In additional, I also examined the mRNA levels of IL6 and RANTES in the unstimulated and VSV treated WT and TRIL deficient primary mixed glial cells. As anticipated stimulation with VSV led to an increase in IL6 and RANTES expression in primary mixed glial cells. TRIL-deficiency affected the expression of IL6 and RANTES, which were reduced in TRIL deficient mixed glial cells compared to WT controls following stimulation with VSV (Fig. 4.25 B and C, respectively).

These studies demonstrated the involvement of TRIL in mediating immune response to VSV infection *in vitro* in the primary mixed glial cells. However the

observed effect was somehow marginal due to a limited number of aminals used in the study. Therefore further analysis is required in order to fully confirm these data.

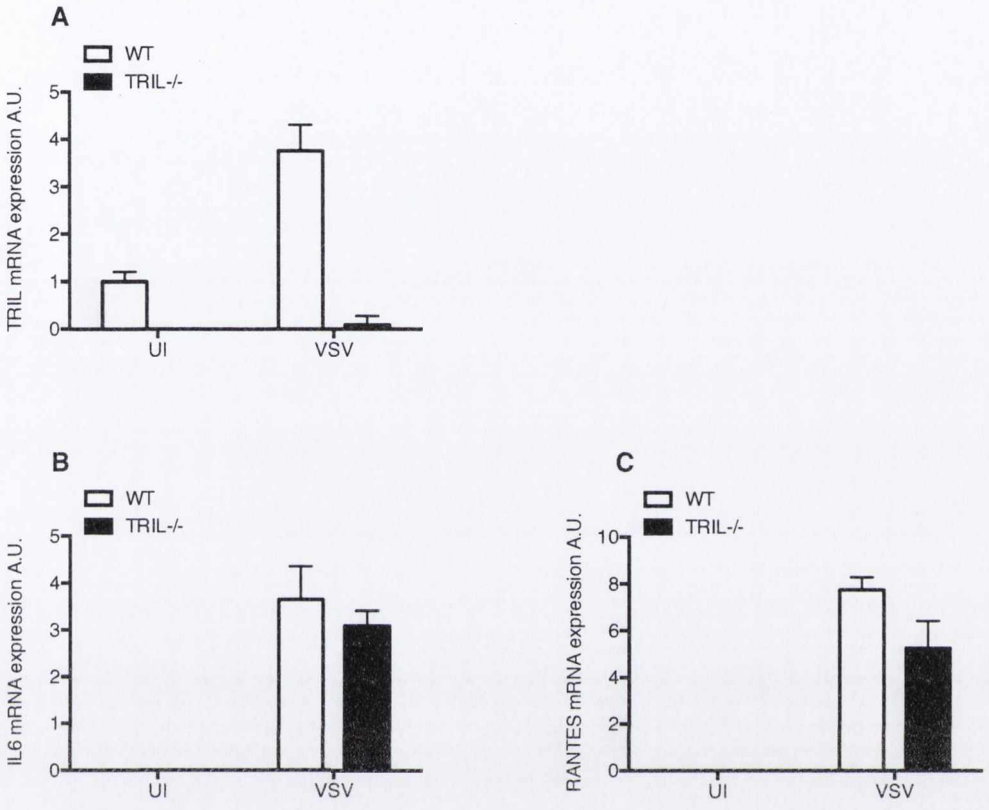

Figure 4.25 Expression of TRIL and proinflammatory cytokines in primary mixed glial cells derived from WT and TRIL$^{-/-}$ mice

A-C, Primary murine mixed glial cells isolated from wild-type (WT) and TRIL$^{-/-}$ mice were left untreated or stimulated for 5h with VSV. Following stimulation mRNA levels of TRIL (**A**), IL6 (**B**) and RANTES (**C**) were measured by QPCR. mRNA levels were normalised to β-actin and represented in arbitrary units (A.U). Results are presented as a mean ± SD for triplicate determinations. Data are representative of one experiment out of three experiments, all carried out in triplicates.

4.2.6.2 TRIL expression increases following VSV infection in spleen and brain of WT mice

Having established the involvement of TRIL in modulating the immune response to VSV infection *in vitro,* I subsequently investigated the importance of TRIL in VSV infection *in vivo* using WT and TRIL deficient mice. First, I examined the expression of TRIL in the spleen and brain of WT (C57BL/6) mice, prior to and following infection with VSV. As can be seen from the Fig. 4.26, infection with VSV leads to only moderate increase in TRIL expression both in the spleen and brain compared to the uninfected controls (Fig. 4.26). The lack of significant differences was most likely a result of reduced number of animals used in this study due to limited resources.

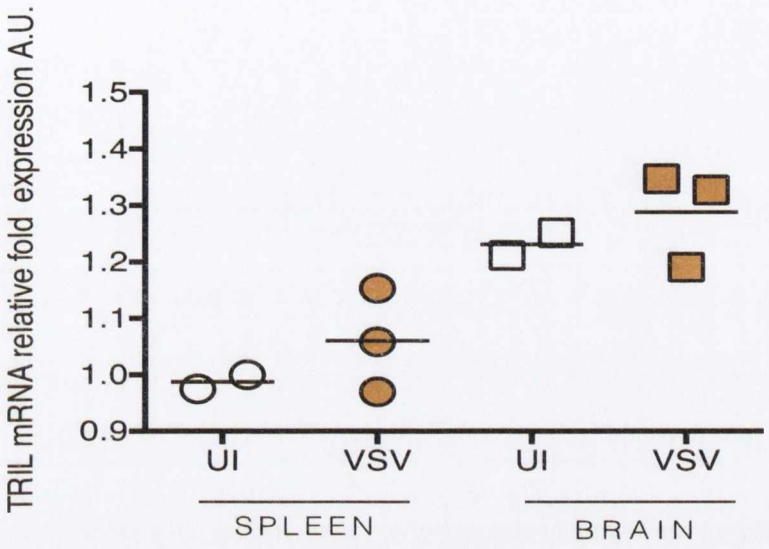

Figure 4.26 Expression of TRIL within the spleen and brain of C57BL/6 WT mice uninfected and following 48h of infection with VSV

C57BL/6 WT mice (n=2-3) were intranasally infected with VSV ($5x10^5$ PFU) or an equal amount of PBS. 48 h following infection mice were sacrificed and both spleen and brain were isolated. Organs were homogenised, followed by the RNA extraction. Samples were next analysed by QPCR for TRIL expression. The mRNA levels were normalised against β-actin control and expressed in arbitrary units (A.U). Data are presented as mean ± SEM of two independent experiments, each carried out in triplicate.

4.2.6.3 TRIL regulates the antiviral response to VSV infection *in vivo*

Aiming to establish the impact of TRIL on the immune response to VSV infection, I next investigated expression of proinflammatory cytokines and antiviral mediators in the WT and TRIL$^{-/-}$ following intranasal VSV inoculation.

QPCR analysis of spleen and brain tissue demonstrated reduced levels of RANTES, VIPERIN and IL6 expression following VSV infection in TRIL$^{-/-}$ mice compared to WT controls. Of note, in the case of VIPERIN and RANTES the differences were found to be statistically significant at the time of 24 h and 48 h post infection, respectively (Fig. 4.27 D-F). In contrast, the mRNA levels of RANTES, VIPERIN and IL6 were not significantly affected by the lack of TRIL within analysed spleen samples (Fig. 4.27 A-C).

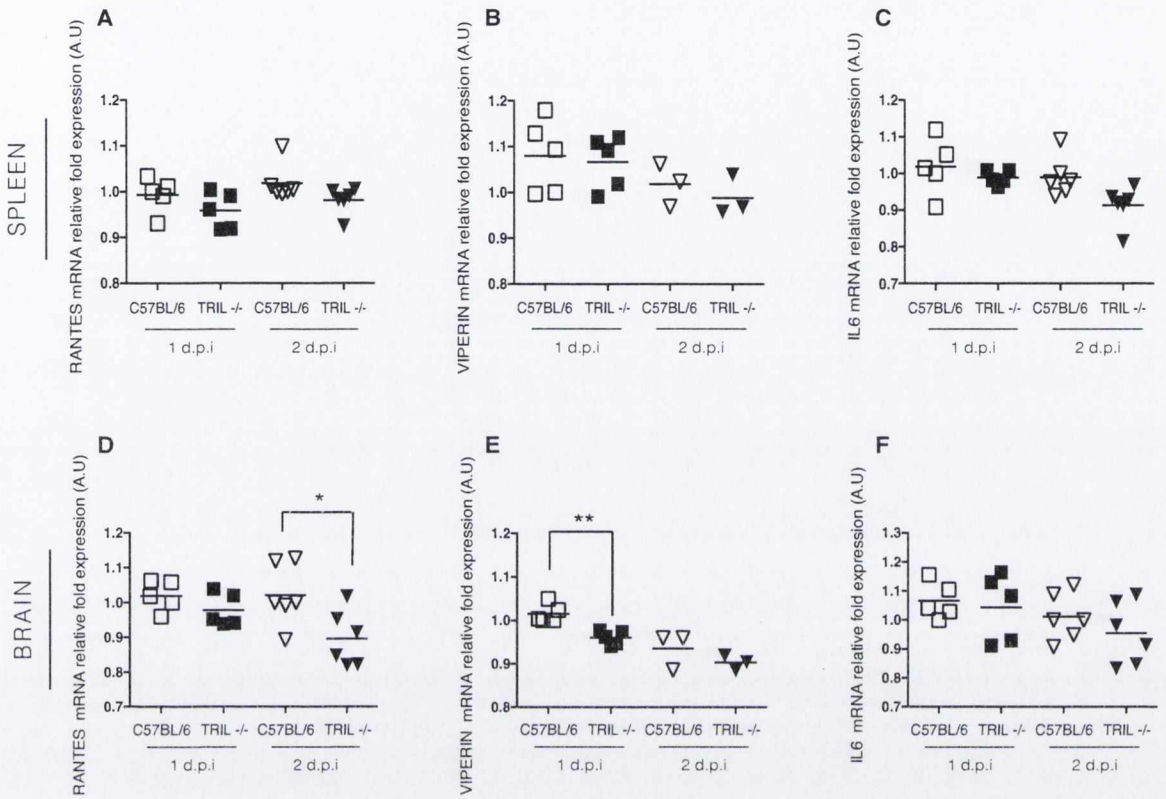

Figure 4.27 Expression of proinflammatory cytokines in the brain and spleen of WT and TRIL deficient mice following 24 h and 48 h of VSV infection

TRIL deficient mice ($TRIL^{-/-}$) and sex/age matched C57BL/6 mice (n=3-5), were intranasally infected with VSV ($5x10^5$ PFU). 24 h and 48 h post infection mice were sacrificed and both spleen and brain were isolated. Organs were homogenised, followed by the RNA extraction. Both spleen (top panel) and brain (bottom panel) derived samples were next analysed by QPCR for RANTES (**A** and **D**), VIPERIN (**B** and **E**) and IL6 (**C** and **F**) expression. The mRNA levels were normalised to β-actin and expressed relative to C57BL/6 mice in arbitrary units (A.U). Data are presented as a mean ± SEM of three independent experiments, each carried out in triplicates. **, $p < 0.01$; *, $p < 0.05$.

4.2.6.4 TLR3-deficiency impacts on antiviral gene expression in brain following intranasal VSV infection

As previously mentined, VSV was shown to trigger the TLR4/TRIF-dependent IRF3 activation as well as the TLR4/CD14-dependent PI3K phosphorylation resulting in type I IFN production (Georgel et al, 2007; Jiang et al, 2005; Schabbauer et al, 2008). TLR3 recognises dsRNA and it is capable of sensing RNA viruses, such as neurotropic WNV (Wang et al, 2004) or HSV (Zhang et al, 2007). Although VSV has been shown to produce the dsRNA in infected cells (Kato et al, 2006), the role of TLR3 in the antiviral response to VSV infection remains controversial. Study by Edelmann *et al.* demonstrated normal reponse to VSV infection in the TLR3 deficient mice (Edelmann et al, 2004), however the tested model of infection utilised the systemic and not the intranasal VSV infection, which is a natural way of entry for the VSV.

Therefore, I decided to evaluate whether TLR3 mediates the antiviral response to intranasal VSV infection *in vivo,* as this had not been previously studied. In order to address this, I first examined the expression of antiviral genes in the WT and $TLR3^{-/-}$ mice following 48 h of VSV infection. QCPR analysis of spleen and brain tissue revealed significant decrease in the expression of RANTES and VIPERIN and less marked change in the IL6 mRNA level in the brain but not spleen of $TLR3^{-/-}$ mice compared to WT controls (Fig. 4.28 D-F and A-C, respectively). Interestingly, the effect observed in the $TLR3^{-/-}$ mice was highly similar to one detected earlier using TRIL deficient mice. Absence of TRIL also had a more significant impact on the cytokine expression within brain compared to spleen.

These data demonstrated that TLR3 contributes to the antiviral response following the intranasal infection with VSV. However, TLR3 was found to be redundant for this response as the production of antiviral mediators was only reduced and not totally abolished in mice lacking TLR3 compared to WT controls. This would suggest that other receptors participate in the response to VSV infection, which is in agreement with the literature.

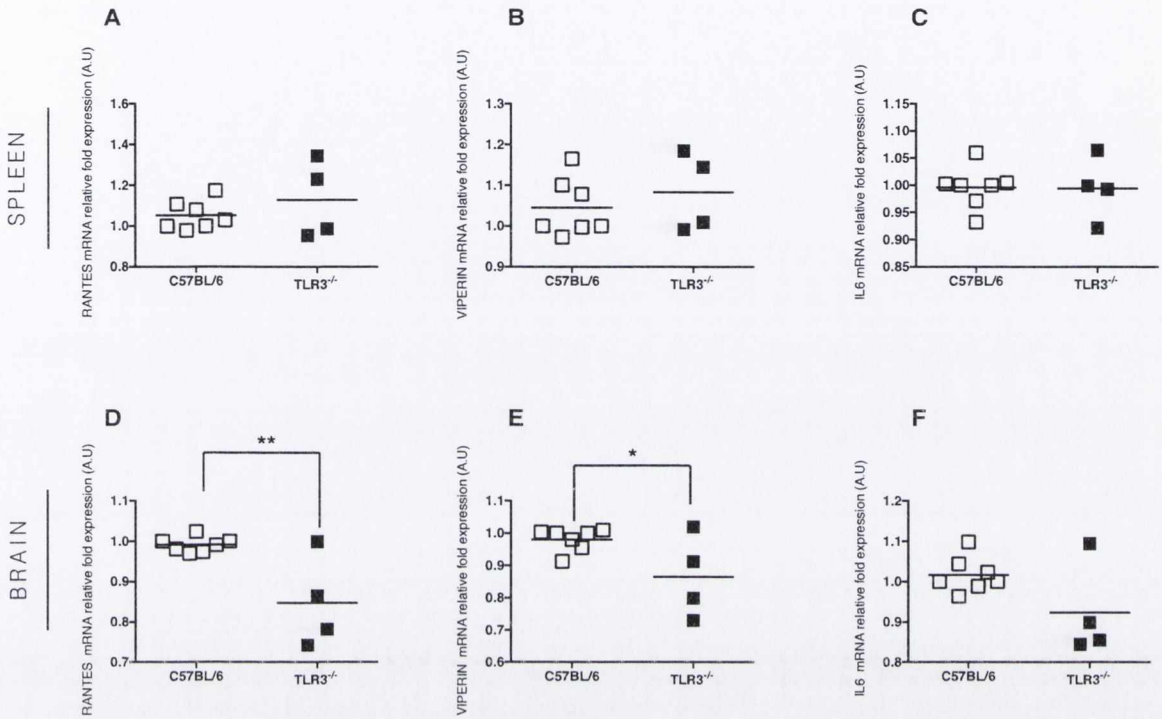

Figure 4.28 Expression of proinflammatory cytokines in the brain and spleen of WT and TLR3 deficient mice following 48 h of VSV infection

TLR3 deficient mice ($TLR3^{-/-}$) and sex/age matched C57BL/6 mice (n=4-7), were intranasally infected with VSV ($5x10^5$ PFU). 48 h post infection mice were sacrificed and both spleen and brain were isolated. Organs were homogenized, followed by the RNA extraction. Both spleen (top panel) and brain (bottom panel) derived samples were next analysed by the QPCR for RANTES (**A** and **D**), VIPERIN (**B** and **E**) and IL6 (**C** and **F**) expression. The mRNA levels were normalised to β-actin and expressed as relative to C57BL/6 mice in arbitrary units (A.U). Data are presented as a mean ± SEM of three independent experiments, each carried out in triplicate. **, $p < 0.01$; *, $p < 0.05$.

4.3 Discussion

The CNS has been considered in the past as an immune privileged site, sequestered from the immune system by the BBB, lacking a lymphatic system and essentially devoid of MHC expression (Galea et al, 2007). Numerous data have challenged this concept by demonstrating immune responses within the CNS. CNS infection or injury triggers immune responses mediated by resident glial cells and a compromised BBB leads to peripheral immune cell infiltration, resulting in either neuroprotective or neurodesctructive events.

A number of bacteria and viruses are capable of triggering the immune response within the brain mediated primarily by the brain resident glial cells, microglia and astrocytes expressing a wide range of TLRs (Bsibsi et al, 2006; Bsibsi et al, 2002; Jack et al, 2005). As mentioned previously myeloid-derived microglia express nearly all TLRs (Bsibsi et al, 2002; Lehnardt, 2010; Olson & Miller, 2004), whereas a more restricted array of TLRs is expressed in astrocytes (Bsibsi et al, 2006; Bsibsi et al, 2002; Jack et al, 2005). Additionally, some of the TLRs, like TLR2, TLR3 and TLR4 are also expressed in neuronal cells (Hoffmann et al, 2007; Kim et al, 2007b; Lafon et al, 2006; Lehnardt et al, 2003). TLRs expressed in the brain have also been associated with neuronal damage caused by excessive production of proinflammatory mediators during brain inflammation (Schachtele et al, 2010). The precise regulation of TLRs within the brain is therefore critical for preventing deleterious neurodegeneration during CNS infection.

Accessory molecules are key modulators of TLR-mediated responses. They have been implicated in in the ligand delivery, signalling and modulation of TLRs. Nearly all known TLRs associate with one or more accessory molecule. Several accessory proteins function as regulators of multiple TLRs. One such example is CD14, which acts as a modulator of multiple TLRs, primarily TLR4, but also TLR2 (Lee et al, 2012; Miyake, 2006; Raby et al, 2013) and endosomal TLR3 (Lee et al, 2006), TLR7 and TLR8 (Baumann et al, 2010). CD14 facilitates ligand binding and delivery as well as trafficking of TLRs. It has been shown to play a role in both MyD88 and TRIF-dependent response of TLR4 (Jiang et al, 2005; Zanoni et al, 2011). CD14 transfers LPS from LBP to the

plasma membrane receptor complex MD2-TLR4, which in turn initiate MyD88 signalling at the cell surface and triggers endosomal trafficking of TLR4 and subsequent TRIF-dependent responses. In addition, CD14 modulates responses of endosomal TLR3, TLR7, TLR8 and TLR9 by promoting a general internalisation of Poly(I:C), imiquimod and CpG DNA (Baumann et al, 2010; Lee et al, 2006). Interestingly, CD14 appears dispensable for TLRs to signal, suggesting involvement of other accessory molecule that can fulfill its role.

TRIL and CD14 share many common features, from similar structures to functional implications in the modulation of TLR3 and TLR4. Thus, it has been speculated before that TRIL might act as a substitute for CD14 in cells where the latter is expressed at low levels. CD14 is abundantly expressed in myeloid cells, including the 'macrophage like' microglia, while astrocytes and neurons both lack its expression. In contrast TRIL has been found to be highly expressed primarily in the astrocytes and neurons compared to myeloid cells BMDMs and BMDCs and microglia. Examination of TLR-mediated responses in primary BMDMs and BMDCs derived from WT and TRIL deficient mice confirm that TRIL does not play a role in the regulation of TLR mediated responses in BMDMs and BMDCs, which is in agreement with the low expression of TRIL in these cells.

As TRIL was found to be primarily expressed in astrocytes, I next investigated the impact of TRIL on TLR-mediated response in primary murine mixed glial cells, consisting largely of astrocytes, derived from WT and TRIL deficient mice. As anticipated the expression of TRIL in the WT cells was enhanced following stimulation with LPS and Poly(I:C), further emphasizing the role for TRIL in the regulation of TLR4 and TLR3-mediated responses. Subsequent gene expression analysis revealed that mRNA levels of various proinflammatory cytokines are strongly reduced in primary mixed glial cells lacking TRIL upon LPS and Poly(I:C) stimulation, compared to WT controls. Similarly to reduced mRNA levels, production of proinflammatory cytokines assayed by ELISA was also affected by the absence of TRIL. Additionally, no difference was seen in response to Pam3CSK4 or R848, consistent with the lack of a role for TRIL in signalling mediated by TLR2 and TLR7. As in mouse model R848 activates exclusively

TLR7 but not TLR8 mediated response, and due to the lack of the activation of human U373 cells upon R848 stimulation in the previous experiment (Figure 3.30) the impact of TRIL on human TLR8 signalling pathway remains elusive. These results further emphasize the positive role of TRIL in the regulation of TLR3 and TLR4 responses, primarily in mixed glial cells. They also support the hypothesis that TRIL might compensate for the low expression of CD14 in these cells.

In order to confirm that LPS and Poly(I:C) were acting via TLR4 and TLR3 respectively in mixed glial cells, I also examined the TLR mediated responses in cells from TLR4, TLR3 and TRIF deficient mice, both at the mRNA and the protein level and observed attenuated responses to LPS in TLR4 and TRIF deficient cells, and to Poly(I:C) in cells lacking TRIF and TLR3. This anticipated result suggested that TRIL regulates the endosomal TLR4 and TLR3 signalling pathway acting via the adaptor protein TRIF in the primary mixed glial cells. Interestingly, the gene expression studies revealed also that TRIL deficiency notably impacted the levels of potent antiviral mediators such as type I IFNs (α and β) as well as RANTES (CCL5) and viral inhibitory protein VIPERIN in response to LPS and/or Poly(I:C) stimulation. This data is consistent with the role of TRIL in modulating the TRIF-dependent TLR4 signalling pathway. It also suggests possible implication of TRIL in the antiviral response mediated by mixed glial cells.

In the previous chapter TRIL was shown to directly interact with the TLR adaptor SARM. SARM was initially implicated in modulation of TRIF dependent TLR signalling pathway (Carty et al, 2006; Peng et al, 2010). It was also demonstrated to be highly expressed in the brain, particularly in neurons where it was shown to play a role in the antiviral response within the brain. SARM deficient mice infected with WNV demonstrated decreased levels of cytokine production correlated with increased susceptibility to lethal WNV infection. Additionally, recent study by Hou *et al.,* revealed a protective role for SARM in the brain following VSV infection. SARM deficient mice demonstrated dramatically reduced cytokine production in the brain following VSV challenge and were also protected from viral induced neurodegeneration. Investigation into the expression of TRIL within various subpopulations of cultured murine glial cells revealed enhanced TRIL expression in the astrocytes and neurons but

not microglia. The elevated level of TRIL mRNA in the neuronal cells together with previously identified TRIL-SARM interaction, suggested that TRIL might execute a similar role to SARM, acting in synergy during the viral infection within the brain.

Overall *in vitro* studies using primary mixed glial cells derived from WT and $TRIL^{-/-}$ mice demonstrated a function for TRIL in the regulation of TLR3 and TLR4, but not TLR2 and not TLR7/8 signalling pathways within primary mixed glial cells, where TRIL most likely compensated for the low expression of CD14. Additionally, they also uncovered a possible role for TRIL in the regulation of antiviral responses in glial cells.

I next sought to investigate the *in vivo* role for TRIL in bacterial and viral models of infection using WT and TRIL deficient mice. TRIL participates in the regulation of TLR4 signalling where it has been found to directly interact with TLR4 and LPS (Carpenter et al, 2009). The TLR accessory molecules LBP and CD14 are both implicated in the regulation of immune response during bacterial infection. LBP and CD14 have been shown to potentiate TLR4 activation by LPS, contributing to lethal Gram-negative sepsis (Le Roy et al, 2001). A Study by Carpenter *et al*, has demonstrated that TRIL positively regulates TLR4 response, which has been further validated in this study using primary mixed glial cells. The *E.coli* induced-acute peritonitis septic shock model has therefore been selected to study the *in vivo* role of TRIL in TLR-mediated immune response.

Examination of TRIL expression within the brain and spleen of WT mice demonstrated its higher basal expression in the brain compared to spleen, which was even further boosted upon the *E.coli* challenge. Further analysis of the cytokine expression profile in the brain following the *E.coli* challenge revealed reduced levels of proinflammatory cytokines and chemokines in samples derived from $TRIL^{-/-}$ mice. Similar to the earlier observation in the *in vitro* studies using primary mixed glial cells, levels of many inflammatory cytokines such as IL6, TNFα, IL1α and IL1β and chemokines CCL4, CXCL2, CXCL10, were all reduced in the TRIL deficient mice upon bacterial infection. Analysis of gene expression panels also revealed a dramatic difference in some of the genes involved in viral recognition and the antiviral response,

such as MDA5, RIG-I and VIPERIN respectively, once again pointing towards a possible role for TRIL in the regulation of immune responses to viral infection in the brain.

The *in vivo E.coli* peritonitis shock model revealed a role for TRIL in modulation of TLR4-mediated responses primarily in the brain and not spleen, despite the intraperitoneal administration of the *E.coli*. As previously mentioned, high levels of TLR4 can be found in the meninges, choroid plexus and circumventricular organs (CVOs) of the brain (Laflamme & Rivest, 2001). Constitutive expression of TLR4 and CD14 in the CVO and meninges, sites of the brain with direct access to the circulation provide for the possibility of direct TLR4-mediated LPS action in the CNS, which would also require TRIL (Chakravarty & Herkenham, 2005; Laflamme & Rivest, 2001). Alternatively, brain inflammation can also be triggered by direct sensing of bacteria mediated by the resident glial cells, microglia and astrocytes within the brain parenchyma following disruption of the BBB. Observed high levels of bacteria in the brain of WT mice following infection with *E.coli* suggest that the integrity of BBB was breached allowing for bacteria to disseminate throughout the brain. Thus, the function of TRIL would be mediating immune response within brain resident cells. It is also possible that TRIL impacts on the BBB permeability. TNFα is one of the mediators implicated in BBB permeability and its increased levels are correlated with the degree of the BBB breakdown, disease severity and induction of brain inflammation (Sharief et al., 1992). TRIL positively impacted on the expression of TNFα within the brain following the *E.coli* infection, thus it is possible that TRIL also plays also a key role in the modulation of BBB permeability, preventing dissemination of bacteria through the brain and induction of brain inflammation. However, further studies are needed to clarify this.

Expression of proinflammatory cytokines following the intraperitoneal *E.coli* challenge within the spleen was unaffected by the absence of TRIL, most likely due to the low expression level of TRIL in this tissue. In contrast, levels of IL6 but not RANTES were dramatically reduced in serum and peritoneal lavage of $TRIL^{-/-}$ mice compared to WT controls. Peritoneal macrophages are the main resident cells and key producers of proinflammatory cytokines within peritoneal cavity. In the course of acute peritonitis,

peritoneal resident cell populations are enriched and/or replaced by the peripheral infiltrating cells such as neutrophils and macrophages. Interestingly, migration of neutrophils from the periphery is strictly regulated by the levels of IL6, which prevents the detrimental accumulation of neutrophils at the site of infection. Additionally, IL6 is also responsible for the regulation of lymphocyte and B-cells recruitment in the later phase of infection (Hurst et al, 2001). Since TRIL was not expressed in primary macrophages I speculated that the peritoneal infiltrating cells might be responsible for the reduced IL6 production detected in the peritoneal lavage of TRIL deficient mice. Examination of TRIL expression in the cells infiltrating the peritoneal cavity following the *E.coli* challenge confirmed significantly higher levels of TRIL in these cells compared to resident peritoneal cells. This observation could partially explain the detrimental effect of TRIL on the IL6 production in the peritoneal lavage upon the *E.coli* challenge. It would certainly be interesting to investigate this further and examine exactly which cell types among the infiltrating cells population is responsible for an increased expression of TRIL.

An additional examination of WT, TLR4 and TRIF deficient mice subjected to an intraperitoneal *E.coli*-induced septic shock model demonstrated involvement of TLR4 and TRIF-mediated signalling in response to *E.coli* infection. This study also confirmed that TRIL acts upstream of TLR4 and TRIF as the expression of TRIL following the *E.coli* challenge was unaffected by the absence of TLR4 and TRIF.

Taken together these data clearly demonstrated a key role for TRIL in TLR4 responses in the brain, providing *in vivo* evidence that TRIL regulates TLR4-mediated cytokine production in response to *E.coli* infection, primarily in the brain. A number of studies have investigated novel potential therapeutic targets in Gram-negative endotoxic shock. However, the most satisfactory results were obtained in the TLR4-targeted therapy of Gram-negative sepsis (Roger et al, 2009). Given the fact that TRIL deficient mice demonstrated abolished TLR4 responses to the *E.coli* induced peritonitis shock, TRIL may represent a new therapeutic target to limit severity of sepsis acting primarily in the brain.

I also observed that deficiency of TRIL in primary mixed glia cells strongly affected the expression of antiviral mediators such as RANTES, type I IFN and VIPERIN, suggesting a potential role for TRIL in the modulation of antiviral response. Carrying on from this observation I next addressed the role for TRIL in the antiviral response *in vivo* using WT and TRIL deficient mice.

Infection of primary mixed glial cells with neurotropic VSV led to increased TRIL expression in WT cells and simultaneously reduced levels of IL6 and RANTES in $TRIL^{-/-}$ cells compared to WT controls. VSV was shown to trigger the TLR4/TRIF and CD14 mediated immune response in macrophages (Georgel et al, 2007; Jiang et al, 2005; Schabbauer et al, 2008). In primary mixed glial cells, which were reported to be permissive to VSV infection (Huneycutt et al, 1993), this response was most likely dependent in part on TRIL.

Intranasal infection of mice with VSV results in breakdown of the BBB, viral dissemination and subsequent induction of brain resident cells (Huneycutt et al, 1993). The expression of TRIL was slightly increased within both the spleen and brain following 48 h of VSV infection, suggesting a role for TRIL in the antiviral response to VSV. However in both spleen and brain the difference was not statistically significant, most likely due to a limited number of animals tested. Similar to the *E.coli* model, it would be extremely intresting to examine the impact of TRIL on the permeability of the BBB following VSV infection.

I next examined the expression of proinflammatory cytokines and antiviral mediators in WT and $TRIL^{-/-}$ mice during the VSV infection. QPCR analysis revealed that mRNA levels of antiviral mediators such as RANTES and VIPERIN were significantly reduced following 24 or 48 h post intranasal VSV infection, specifically in the brain but not spleen of TRIL deficient mice. VIPERIN and RANTES can efficiently abrogate viral replication, therefore reduced levels of these antiviral mediators in TRIL deficient mice suggests the role for TRIL in the antiviral response, once again largely within the brain.

VIPERIN is a potent viral inhibitory protein residing in the ER and involved in the regulation of viral replication (Fitzgerald, 2011; Seo & Cresswell, 2013). The expression of VIPERIN is primarily induced by IFN, the production of which in turn depends on

multiple signalling pathways induced downstream of TLR3 and TLR4, cytosolic viral receptors RIG-I and MDA-5 as well as cytosolic dsDNA sensors. Interestingly, VIPERIN can be also induced in an IFN-independent manner upon viral infection. VSV is capable of direct, IFN-independent induction of VIPERIN, mediated by a pathway involving antiviral adaptor protein MAVS, localised to mitochondria and peroxisomes. Following viral infection peroxisomal MAVS initiate rapid and transient IFN-independent VIPERIN expression limiting viral replication. This is followed by the activation of mitochondrial MAVS, which mediate more robust antiviral response and IFN-dependent activation of VIPERIN expression (Dixit et al, 2010).

It is possible that the reduced levels of VIPERIN in the brain of TRIL$^{-/-}$ mice observed following VSV infection resulted from the limited activation of TLR4 and/or TLR3 signalling pathways as both RANTES and VIPERIN expression were also reduced in TLR3 deficient mice upon VSV infection. In addition, TRIL deficient primary mixed glial cells also demonstrated decreased expression of VIPERIN following stimulation with LPS and Poly(I:C), further emphasizing an impact of TRIL on IFN-mediated VIPERIN production. However it is also possible that TRIL modulates other signalling pathways leading to type I IFN production and subsequent VIPERIN induction such as one mediated by cytosolic receptors MDA5 and RIG-I. Of note RIG-I has been shown to participate in the antiviral response to VSV in primary human astrocytes (Furr et al, 2008). Upon VSV recognition RIG-I initiates the signalling cascade mediated by the ER and mitochondria associated stimulator of IFN genes, STING, which is crucial for RIG-I dependent type I IFN production (Barber, 2011; Ishikawa & Barber, 2008). It is possible that localised within the ER TRIL is also implicated in the modulation of RIG-I dependent signaling pathway following VSV infection, either directly, or via the interaction with STING. Further work is however required to test this hypothesis and evaluate the potential involvement of TRIL in the signaling of RIG-I.

The *in vivo* studies uncovered a role for TRIL in regulation of antibacterial and antiviral response primarily in the brain. However the impact of TRIL on the immune response was somewhat marginal, especially compared to TLR3, TLR4 and/or TRIF. While the lack of TRIL led to only a moderate decrease in the expression and

production of proinflammatory cytokines and antiviral mediators upon bacterial and/or viral infection, the deficiency of specific TLRs totally abolished antibacterial and/or antiviral response. Thus TRIL is important but not essential for TLR3 and TLR4 mediated response, which is in agreement with its regulatory function.

In summary this study identified a role for TRIL in TLR3 and TLR4-mediated responses in the brain. It also provided *in vivo* evidence that TRIL in the brain mediates cytokine production in response to *E.coli* infection and impacts on the antiviral response to neurotropic VSV infection.

CHAPTER FIVE

Final discussion and future perspectives

5.1 Final discussion and future perspectives

TLRs play a central role in the innate immune response to invading pathogens and endogenous danger signals. In order to execute their function TLRs require a number of accessory molecules implicated in ligand recognition and binding, signalling and modulation of TLR responses. Similar to TLRs these accessory molecules localise at the plasma membrane (MD2, RP105) and within endosomal compartments (gp96, UNC93B, PRAT4A). Some are also capable of direct interaction with TLRs and/or their ligands (CD14, LBP, CD36). The primary role of accessory molecules lies in the fine-tuning of TLR responses, however some like MD2 are indispensable for TLRs to function (Nagai et al, 2002a).

This study set out to further characterise TRIL, a novel accessory molecule of the TLR4 receptor complex and a positive modulator of the TLR4 response. The work presented herein has provided valuable insights into the expression and function of TRIL and uncovered its new role in the modulation of TLR3-dependent signalling. The study revealed intracellular localisation of TRIL in the human astrocytoma U373 and monocytic THP-1 cell lines, and its plasma membrane expression in HEK-293T cells. Localised within the early endosome TRIL modulates TLR3 and endosomal TLR4 signalling pathways. In particular TRIL appears to participate in endosomal ligand delivery. Additionally the study revealed that TRIL does not modulate TLR2, mediated response. Unfortunatelly due to unresponsiveness of U373 cells to human TLR7/8 agoinst R848, impact of TRIL on human TLR8 signalling pathway remains evasive and its implication in the modulation of both murine and human TLR7 response requires further investigation. This project also aimed to determine the role of TRIL *in vivo* using mouse models of bacterial and viral infection. Studies using TRIL deficient mice further confirmed the function of TRIL in TLR3 and TLR4-mediated response. TRIL regulates the TLR4 response during systemic *E.coli* infection. It also participates in the regulation of the antiviral response to neurotropic vesicular stomatitis virus infection (VSV), where its function is largely in the brain. Thus, TRIL can be defined as a positive modulator of TLR3 and TLR4 response both *in vitro* and *in vivo*.

Interestingly, recent studies by Petrietti *et al.* identified a Teleost fish homolog of TRIL. Zebrafish TRIL possesses high structural resemblance and a similar expression pattern to mammalian TRIL. However in contrast to the mammalian counterpart, zebrafish TRIL was not induced by LPS, Poly(I:C) or bacterial infection (Pietretti et al, 2013).

Zebrafish have recently emerged as a powerful tool and an excellent model for studying vertebrate innate and adaptive immunity that can complement research in mouse models and human cell lines. The biggest advantage of the zebrafish model lies in its unique temporal separation of the innate and adaptive immune systems during zebrafish development, which allows studying of the innate and adaptive immune responses independently. An additional benefit of the zebrafish model is the ease of introducing genetic modifications and high-throughput *in vivo* screening of potential therapeutic agents. Moreover, transparency of the zebrafish in the early life stages allows for a real-time visualisation of processes like microbe host-interaction or demonstrated recently by live imaging of microglial-mediated neuronal degeneration (Peri & Nusslein-Volhard, 2008).

The innate immune system machinery of humans and zebrafish are highly conserved. A number of orthologs of mammalian TLRs have been identified in zebrafish and demonstrated to mirror the function of their mammalian forms. However some of them seem to be dramatically different, for example zebrafish TLR4, which is unable to sense bacterial LPS, or TLR3 which is replaced by a fish-specific TLR22 (van der Vaart et al, 2012). A number of accessory molecules have been recently identified in zebrafish. Among them gp96 which is a master chaperone for TLRs (Yang et al, 2007) and PRAT4A acting as a regulator of fibroblast growth factor (FGF) in the fish brain (Hirate & Okamoto, 2006). Intriguingly, CD14 a central accessory molecule of multiple TLRs including TLR3 and TLR4, and MD2 which is critical for TLR4 signalling, are both absent in the zebrafish (van der Vaart et al, 2012). Zebrafish and mammalian TRIL demonstrate similar expression patterns and both have been found to be highly expressed in the brain. It will be of interest to further investigate the function of TRIL

using this animal model. TRIL may be involved in the regulation of other TLRs in zebrafish. It could also point towards a different, yet unidentified function of TRIL.

Interestingly, some of the TLR adaptor molecules such as MyD88, Mal, TRIF, and SARM are also conserved in mammals and fish. This study uncovered direct interaction of TRIL and SARM. However the exact outcome of this interaction has not been thoroughly investigated. Like TRIL, mammalian SARM plays a role in the regulation of TLR signalling pathways. Notably, SARM has also been associated with the regulation of various mechanisms of neuronal survival and cell death. Studies by Kim *et al.,* demonstrated that neurons derived from SARM deficient mice are protected from death after oxygen and glucose deprivation (Kim et al, 2007b). Additionally SARM was also found to play a critical role in the regulation of an active form of neuronal death akin to apoptosis, called Wallerian degeneration (Osterloh et al, 2012a). After injury to axons, neurons undergo degradation distal to the injury site followed by the clearance of the necrotic debris, degeneration and subsequent regeneration. In SARM deficient neurons, axons are preserved from Wallerian degeneration, suggesting a role for SARM in the regulation of the injury-induced axon death pathway (Osterloh et al, 2012a). Given the functional similarity between TRIL and SARM and the direct association of these two proteins, it is interesting to speculate that TRIL's role is far more complex and not exclusive to modulation of the immune response. Of note, this study provided evidence of enhanced expression of TRIL in the cultured murine neurons. It will therefore be exciting to examine whether similar to SARM, TRIL impacts on neuronal survival and degeneration first using the zebrafish and later the mouse animal model.

This study provided *in vivo* evidence of the role for TRIL in the antiviral response to VSV in the brain. The immune response in the brain is usually associated with a positive outcome as it leads to pathogen clearance and infection resolution, however an excessive or prolonged response can also cause deleterious neurodegeneration. Infections with neurotropic HSV-1 or WNV are known to induce neuronal cell death, mediated by an excessive immune response and cytokine production. This process can be mediated by both innate immunity mediated by brain

resident glial cells, as well as the later response governed by the infiltration of peripheral immune cells due to a compromised BBB. This study revealed a role for TRIL in the modulation of the immune response to viral infection dependent on glial cells in the brain. However, the impact of TRIL on BBB permeability and migration of peripheral immune cells into the brain remains ill defined. Similarly the implication of TRIL in the regulation of viral induced neurodegeneration is undetermined. It would be exciting to expand our knowledge of TRIL by examining its function in the zebrafish, which could provide not only further insights into the role of TRIL in the regulation of TLR-mediated signalling but also uncover novel functions of TRIL within the CNS.

A number of studies demonstrated a link between the brain inflammation and pathogenecity of neurodegenerative disorders such as Alzheimer's disease (AD), Parkinson's disease (PD) and MS. In the previous studies Carpenter *et al.* reported enhanced TRIL expression in the brain samples from patients with AD (Carpenter et al, 2009). In an additional, independent study Rabin *et al.* found increased levels of TRIL in patients suffering from a neurodegenerative amyotrophic lateral sclerosis ALS. This study revealed high leves of TRIL in the brain resident cells, most predominantly in astrocytes and neurons, where TRIL impacts on the innate immune response to bacterial and viral infection. It is possible that TRIL, which is highly expressed in neurons, will have an additional role in modulation of neuronal survival and degeneration, thus contributing to neuronal cell death common to neurodegenerative disorders. A further investigation is required in order to establish the exact correlation of TRIL with neurodegenerative diseases such as AD, PD, and MS.

Further studies into TRIL will provide a better understanding of the mechanisms whereby TRIL contributes to anti-bacterial and anti-viral responses within the brain. These studies are also likely to provide exciting and valuable new insights into the function of TRIL in the regulation of neuronal survival and degeneration

CHAPTER SIX

References

6.1 References

Abe T, Shimamura M, Jackman K, Kurinami H, Anrather J, Zhou P, Iadecola C (2010) Key role of CD36 in Toll-like receptor 2 signaling in cerebral ischemia. *Stroke* **41:** 898-904

Ablasser A, Bauernfeind F, Hartmann G, Latz E, Fitzgerald KA, Hornung V (2009) RIG-I-dependent sensing of poly(dA:dT) through the induction of an RNA polymerase III-transcribed RNA intermediate. *Nature immunology* **10:** 1065-1072

Akashi-Takamura S, Miyake K (2008) TLR accessory molecules. *Current opinion in immunology* **20:** 420-425

Akira S, Uematsu S, Takeuchi O (2006) Pathogen recognition and innate immunity. *Cell* **124:** 783-801

Alexopoulou A, Michael A, Dourakis SP (2001a) Acute thrombocytopenic purpura in a patient treated with chlordiazepoxide and clidinium. *Arch Intern Med* **161:** 1778

Alexopoulou L, Holt AC, Medzhitov R, Flavell RA (2001b) Recognition of double-stranded RNA and activation of NF-kappaB by Toll-like receptor 3. *Nature* **413:** 732-738

Asea A, Rehli M, Kabingu E, Boch JA, Bare O, Auron PE, Stevenson MA, Calderwood SK (2002) Novel signal transduction pathway utilized by extracellular HSP70: role of toll-like receptor (TLR) 2 and TLR4. *The Journal of biological chemistry* **277:** 15028-15034

Atianand MK, Fitzgerald KA (2013) Molecular basis of DNA recognition in the immune system. *Journal of immunology* **190:** 1911-1918

Bafica A, Santiago HC, Goldszmid R, Ropert C, Gazzinelli RT, Sher A (2006) Cutting edge: TLR9 and TLR2 signaling together account for MyD88-dependent control of parasitemia in Trypanosoma cruzi infection. *Journal of immunology* **177:** 3515-3519

Barbalat R, Lau L, Locksley RM, Barton GM (2009) Toll-like receptor 2 on inflammatory monocytes induces type I interferon in response to viral but not bacterial ligands. *Nature immunology* **10:** 1200-1207

Barber GN (2011) STING-dependent signaling. *Nat Immunol* **12:** 929-930

Baumann CL, Aspalter IM, Sharif O, Pichlmair A, Bluml S, Grebien F, Bruckner M, Pasierbek P, Aumayr K, Planyavsky M, Bennett KL, Colinge J, Knapp S, Superti-Furga G (2010) CD14 is a coreceptor of Toll-like receptors 7 and 9. *The Journal of experimental medicine* **207:** 2689-2701

Belinda LW, Wei WX, Hanh BT, Lei LX, Bow H, Ling DJ (2008) SARM: a novel Toll-like receptor adaptor, is functionally conserved from arthropod to human. *Molecular immunology* **45:** 1732-1742

Beraud D, Twomey M, Bloom B, Mittereder A, Ton V, Neitzke K, Chasovskikh S, Mhyre TR, Maguire-Zeiss KA (2011) alpha-Synuclein Alters Toll-Like Receptor Expression. *Frontiers in neuroscience* **5:** 80

Bernard JJ, Cowing-Zitron C, Nakatsuji T, Muehleisen B, Muto J, Borkowski AW, Martinez L, Greidinger EL, Yu BD, Gallo RL (2012) Ultraviolet radiation damages self noncoding RNA and is detected by TLR3. *Nature medicine* **18:** 1286-1290

Bhoj VG, Chen ZJ (2009) Ubiquitylation in innate and adaptive immunity. *Nature* **458:** 430-437

Bianchi ME (2007) DAMPs, PAMPs and alarmins: all we need to know about danger. *Journal of leukocyte biology* **81:** 1-5

Bieback K, Lien E, Klagge IM, Avota E, Schneider-Schaulies J, Duprex WP, Wagner H, Kirschning CJ, Ter Meulen V, Schneider-Schaulies S (2002) Hemagglutinin protein of wild-type measles virus activates toll-like receptor 2 signaling. *Journal of virology* **76:** 8729-8736

Biswas N, Liu S, Ronni T, Aussenberg SE, Liu W, Fujita T, Wang T (2011) The ubiquitin-like protein PLIC-1 or ubiquilin 1 inhibits TLR3-Trif signaling. *PloS one* **6:** e21153

Bloor S, Maelfait J, Krumbach R, Beyaert R, Randow F (2010) Endoplasmic reticulum chaperone gp96 is essential for infection with vesicular stomatitis virus. *Proc Natl Acad Sci U S A* **107:** 6970-6975

Blum ES, Abraham MC, Yoshimura S, Lu Y, Shaham S (2012) Control of nonapoptotic developmental cell death in Caenorhabditis elegans by a polyglutamine-repeat protein. *Science* **335:** 970-973

Bowie AG, Fitzgerald KA (2007) RIG-I: tri-ing to discriminate between self and non-self RNA. *Trends Immunol* **28:** 147-150

Brinkmann MM, Spooner E, Hoebe K, Beutler B, Ploegh HL, Kim YM (2007) The interaction between the ER membrane protein UNC93B and TLR3, 7, and 9 is crucial for TLR signaling. *The Journal of cell biology* **177:** 265-275

Brown KL, Poon GF, Birkenhead D, Pena OM, Falsafi R, Dahlgren C, Karlsson A, Bylund J, Hancock RE, Johnson P (2011) Host defense peptide LL-37 selectively reduces proinflammatory macrophage responses. *Journal of immunology* **186:** 5497-5505

Bsibsi M, Persoon-Deen C, Verwer RW, Meeuwsen S, Ravid R, Van Noort JM (2006) Toll-like receptor 3 on adult human astrocytes triggers production of neuroprotective mediators. *Glia* **53:** 688-695

Bsibsi M, Ravid R, Gveric D, van Noort JM (2002) Broad expression of Toll-like receptors in the human central nervous system. *Journal of neuropathology and experimental neurology* **61:** 1013-1021

Cabanes D, Sousa S, Cebria A, Lecuit M, Garcia-del Portillo F, Cossart P (2005) Gp96 is a receptor for a novel Listeria monocytogenes virulence factor, Vip, a surface protein. *EMBO J* **24:** 2827-2838

Calvo D, Dopazo J, Vega MA (1995) The CD36, CLA-1 (CD36L1), and LIMPII (CD36L2) gene family: cellular distribution, chromosomal location, and genetic evolution. *Genomics* **25:** 100-106

Carpenter S, Carlson T, Dellacasagrande J, Garcia A, Gibbons S, Hertzog P, Lyons A, Lin LL, Lynch M, Monie T, Murphy C, Seidl KJ, Wells C, Dunne A, O'Neill LA (2009) TRIL, a functional component of the TLR4 signaling complex, highly expressed in brain. *Journal of immunology* **183:** 3989-3995

Carpenter S, Wochal P, Dunne A, O'Neill LA (2011) Toll-like receptor 3 (TLR3) signaling requires TLR4 Interactor with leucine-rich REPeats (TRIL). *The Journal of biological chemistry* **286:** 38795-38804

Carpentier PA, Begolka WS, Olson JK, Elhofy A, Karpus WJ, Miller SD (2005) Differential activation of astrocytes by innate and adaptive immune stimuli. *Glia* **49:** 360-374

Carpentier PA, Duncan DS, Miller SD (2008) Glial toll-like receptor signaling in central nervous system infection and autoimmunity. *Brain, behavior, and immunity* **22:** 140-147

Carty M, Goodbody R, Schroder M, Stack J, Moynagh PN, Bowie AG (2006) The human adaptor SARM negatively regulates adaptor protein TRIF-dependent Toll-like receptor signaling. *Nature immunology* **7:** 1074-1081

Casrouge A, Zhang SY, Eidenschenk C, Jouanguy E, Puel A, Yang K, Alcais A, Picard C, Mahfoufi N, Nicolas N, Lorenzo L, Plancoulaine S, Senechal B, Geissmann F, Tabeta K, Hoebe K, Du X, Miller RL, Heron B, Mignot C, de Villemeur TB, Lebon P, Dulac O, Rozenberg F, Beutler B, Tardieu M, Abel L, Casanova JL (2006) Herpes simplex virus encephalitis in human UNC-93B deficiency. *Science* **314:** 308-312

Casula M, Iyer AM, Spliet WG, Anink JJ, Steentjes K, Sta M, Troost D, Aronica E (2011) Toll-like receptor signaling in amyotrophic lateral sclerosis spinal cord tissue. *Neuroscience* **179:** 233-243

Cervantes JL, Weinerman B, Basole C, Salazar JC (2012) TLR8: the forgotten relative revindicated. *Cellular & molecular immunology* **9:** 434-438

Chakravarty S, Herkenham M (2005) Toll-like receptor 4 on nonhematopoietic cells sustains CNS inflammation during endotoxemia, independent of systemic cytokines. *J Neurosci* **25:** 1788-1796

Chang C, Hsieh YW, Lesch BJ, Bargmann CI, Chuang CF (2011) Microtubule-based localization of a synaptic calcium-signaling complex is required for left-right neuronal asymmetry in C. elegans. *Development* **138:** 3509-3518

Chang M, Jin W, Sun SC (2009) Peli1 facilitates TRIF-dependent Toll-like receptor signaling and proinflammatory cytokine production. *Nature immunology* **10:** 1089-1095

Chen CY, Lin CW, Chang CY, Jiang ST, Hsueh YP (2011) Sarm1, a negative regulator of innate immunity, interacts with syndecan-2 and regulates neuronal morphology. *J Cell Biol* **193:** 769-784

Chen ZJ (2005) Ubiquitin signalling in the NF-kappaB pathway. *Nature cell biology* **7:** 758-765

Civril F, Deimling T, de Oliveira Mann CC, Ablasser A, Moldt M, Witte G, Hornung V, Hopfner KP (2013) Structural mechanism of cytosolic DNA sensing by cGAS. *Nature* **498:** 332-337

Coban C, Ishii KJ, Kawai T, Hemmi H, Sato S, Uematsu S, Yamamoto M, Takeuchi O, Itagaki S, Kumar N, Horii T, Akira S (2005) Toll-like receptor 9 mediates innate immune activation by the malaria pigment hemozoin. *The Journal of experimental medicine* **201:** 19-25

Compton T, Kurt-Jones EA, Boehme KW, Belko J, Latz E, Golenbock DT, Finberg RW (2003) Human cytomegalovirus activates inflammatory cytokine responses via CD14 and Toll-like receptor 2. *J Virol* **77:** 4588-4596

Cooney R, Baker J, Brain O, Danis B, Pichulik T, Allan P, Ferguson DJ, Campbell BJ, Jewell D, Simmons A (2010) NOD2 stimulation induces autophagy in dendritic cells influencing bacterial handling and antigen presentation. *Nature medicine* **16:** 90-97

Couillault C, Pujol N, Reboul J, Sabatier L, Guichou JF, Kohara Y, Ewbank JJ (2004) TLR-independent control of innate immunity in Caenorhabditis elegans by the TIR domain adaptor protein TIR-1, an ortholog of human SARM. *Nature immunology* **5:** 488-494

Daffis S, Samuel MA, Suthar MS, Gale M, Jr., Diamond MS (2008) Toll-like receptor 3 has a protective role against West Nile virus infection. *Journal of virology* **82:** 10349-10358

de Bouteiller O, Merck E, Hasan UA, Hubac S, Benguigui B, Trinchieri G, Bates EE, Caux C (2005) Recognition of double-stranded RNA by human toll-like receptor 3 and downstream receptor signaling requires multimerization and an acidic pH. *The Journal of biological chemistry* **280:** 38133-38145

Deane JA, Pisitkun P, Barrett RS, Feigenbaum L, Town T, Ward JM, Flavell RA, Bolland S (2007) Control of toll-like receptor 7 expression is essential to restrict autoimmunity and dendritic cell proliferation. *Immunity* **27:** 801-810

Diebold SS, Kaisho T, Hemmi H, Akira S, Reis e Sousa C (2004) Innate antiviral responses by means of TLR7-mediated recognition of single-stranded RNA. *Science* **303:** 1529-1531

Divanovic S, Trompette A, Atabani SF, Madan R, Golenbock DT, Visintin A, Finberg RW, Tarakhovsky A, Vogel SN, Belkaid Y, Kurt-Jones EA, Karp CL (2005a) Inhibition of TLR-4/MD-2 signaling by RP105/MD-1. *J Endotoxin Res* **11:** 363-368

Divanovic S, Trompette A, Atabani SF, Madan R, Golenbock DT, Visintin A, Finberg RW, Tarakhovsky A, Vogel SN, Belkaid Y, Kurt-Jones EA, Karp CL (2005b) Negative regulation of Toll-like receptor 4 signaling by the Toll-like receptor homolog RP105. *Nature immunology* **6:** 571-578

Dixit E, Boulant S, Zhang Y, Lee AS, Odendall C, Shum B, Hacohen N, Chen ZJ, Whelan SP, Fransen M, Nibert ML, Superti-Furga G, Kagan JC (2010) Peroxisomes are signaling platforms for antiviral innate immunity. *Cell* **141:** 668-681

Doyle SL, Husebye H, Connolly DJ, Espevik T, O'Neill LA, McGettrick AF (2012) The GOLD domain-containing protein TMED7 inhibits TLR4 signalling from the endosome upon LPS stimulation. *Nature communications* **3:** 707

Dziarski R, Tapping RI, Tobias PS (1998) Binding of bacterial peptidoglycan to CD14. *The Journal of biological chemistry* **273:** 8680-8690

Dziarski R, Ulmer AJ, Gupta D (2000) Interactions of CD14 with components of gram-positive bacteria. *Chem Immunol* **74:** 83-107

Edelmann KH, Richardson-Burns S, Alexopoulou L, Tyler KL, Flavell RA, Oldstone MB (2004) Does Toll-like receptor 3 play a biological role in virus infections? *Virology* **322:** 231-238

Ermolaeva MA, Michallet MC, Papadopoulou N, Utermohlen O, Kranidioti K, Kollias G, Tschopp J, Pasparakis M (2008) Function of TRADD in tumor necrosis factor receptor 1 signaling and in TRIF-dependent inflammatory responses. *Nature immunology* **9:** 1037-1046

Esen N, Tanga FY, DeLeo JA, Kielian T (2004) Toll-like receptor 2 (TLR2) mediates astrocyte activation in response to the Gram-positive bacterium Staphylococcus aureus. *Journal of neurochemistry* **88:** 746-758

Ewald SE, Engel A, Lee J, Wang M, Bogyo M, Barton GM (2011) Nucleic acid recognition by Toll-like receptors is coupled to stepwise processing by cathepsins and asparagine endopeptidase. *The Journal of experimental medicine* **208:** 643-651

Ewald SE, Lee BL, Lau L, Wickliffe KE, Shi GP, Chapman HA, Barton GM (2008) The ectodomain of Toll-like receptor 9 is cleaved to generate a functional receptor. *Nature* **456:** 658-662

Farina C, Aloisi F, Meinl E (2007) Astrocytes are active players in cerebral innate immunity. *Trends in immunology* **28:** 138-145

Farina C, Krumbholz M, Giese T, Hartmann G, Aloisi F, Meinl E (2005) Preferential expression and function of Toll-like receptor 3 in human astrocytes. *Journal of neuroimmunology* **159:** 12-19

Fassbender K, Walter S, Kuhl S, Landmann R, Ishii K, Bertsch T, Stalder AK, Muehlhauser F, Liu Y, Ulmer AJ, Rivest S, Lentschat A, Gulbins E, Jucker M, Staufenbiel M, Brechtel K, Walter J, Multhaup G, Penke B, Adachi Y, Hartmann T, Beyreuther K (2004) The LPS receptor (CD14) links innate immunity with Alzheimer's disease. *FASEB J* **18:** 203-205

Filewod NC, Pistolic J, Hancock RE (2009) Low concentrations of LL-37 alter IL-8 production by keratinocytes and bronchial epithelial cells in response to proinflammatory stimuli. *FEMS Immunol Med Microbiol* **56:** 233-240

Fitzgerald KA (2011) The interferon inducible gene: Viperin. *Journal of interferon & cytokine research : the official journal of the International Society for Interferon and Cytokine Research* **31:** 131-135

Fitzgerald KA, Palsson-McDermott EM, Bowie AG, Jefferies CA, Mansell AS, Brady G, Brint E, Dunne A, Gray P, Harte MT, McMurray D, Smith DE, Sims JE, Bird TA, O'Neill LA (2001) Mal (MyD88-adapter-like) is required for Toll-like receptor-4 signal transduction. *Nature* **413:** 78-83

Fitzgerald KA, Rowe DC, Barnes BJ, Caffrey DR, Visintin A, Latz E, Monks B, Pitha PM, Golenbock DT (2003) LPS-TLR4 signaling to IRF-3/7 and NF-kappaB involves the toll adapters TRAM and TRIF. *The Journal of experimental medicine* **198:** 1043-1055

Franchi L, Munoz-Planillo R, Nunez G (2012) Sensing and reacting to microbes through the inflammasomes. *Nature immunology* **13:** 325-332

Fukui R, Saitoh S, Kanno A, Onji M, Shibata T, Ito A, Matsumoto M, Akira S, Yoshida N, Miyake K (2011a) Unc93B1 restricts systemic lethal inflammation by orchestrating Toll-like receptor 7 and 9 trafficking. *Immunity* **35:** 69-81

Fukui R, Saitoh S, Kanno A, Onji M, Shibata T, Ito A, Onji M, Matsumoto M, Akira S, Yoshida N, Miyake K (2011b) Unc93B1 restricts systemic lethal inflammation by orchestrating Toll-like receptor 7 and 9 trafficking. *Immunity* **35:** 69-81

Fukui R, Saitoh S, Matsumoto F, Kozuka-Hata H, Oyama M, Tabeta K, Beutler B, Miyake K (2009) Unc93B1 biases Toll-like receptor responses to nucleic acid in dendritic cells toward DNA- but against RNA-sensing. *J Exp Med* **206:** 1339-1350

Furr SR, Chauhan VS, Sterka D, Jr., Grdzelishvili V, Marriott I (2008) Characterization of retinoic acid-inducible gene-I expression in primary murine glia following exposure to vesicular stomatitis virus. *Journal of neurovirology* **14:** 503-513

Galea I, Bechmann I, Perry VH (2007) What is immune privilege (not)? *Trends in immunology* **28:** 12-18

Ganguly D, Chamilos G, Lande R, Gregorio J, Meller S, Facchinetti V, Homey B, Barrat FJ, Zal T, Gilliet M (2009) Self-RNA-antimicrobial peptide complexes activate human dendritic cells through TLR7 and TLR8. *J Exp Med* **206:** 1983-1994

Garcia-Cattaneo A, Gobert FX, Muller M, Toscano F, Flores M, Lescure A, Del Nery E, Benaroch P (2012) Cleavage of Toll-like receptor 3 by cathepsins B and H is essential for signaling. *Proceedings of the National Academy of Sciences of the United States of America* **109:** 9053-9058

Geijtenbeek TB, Gringhuis SI (2009) Signalling through C-type lectin receptors: shaping immune responses. *Nature reviews Immunology* **9:** 465-479

Georgel P, Jiang Z, Kunz S, Janssen E, Mols J, Hoebe K, Bahram S, Oldstone MB, Beutler B (2007) Vesicular stomatitis virus glycoprotein G activates a specific antiviral Toll-like receptor 4-dependent pathway. *Virology* **362:** 304-313

Gewirtz AT, Navas TA, Lyons S, Godowski PJ, Madara JL (2001) Cutting edge: bacterial flagellin activates basolaterally expressed TLR5 to induce epithelial proinflammatory gene expression. *Journal of immunology* **167:** 1882-1885

Gilliet M, Lande R (2008) Antimicrobial peptides and self-DNA in autoimmune skin inflammation. *Curr Opin Immunol* **20:** 401-407

Goodridge HS, Underhill DM (2008) Fungal Recognition by TLR2 and Dectin-1. *Handbook of experimental pharmacology*: 87-109

Gorden KK, Qiu X, Battiste JJ, Wightman PP, Vasilakos JP, Alkan SS (2006a) Oligodeoxynucleotides differentially modulate activation of TLR7 and TLR8 by imidazoquinolines. *Journal of immunology* **177:** 8164-8170

Gorden KK, Qiu XX, Binsfeld CC, Vasilakos JP, Alkan SS (2006b) Cutting edge: activation of murine TLR8 by a combination of imidazoquinoline immune response modifiers and polyT oligodeoxynucleotides. *Journal of immunology* **177:** 6584-6587

Guo Y, Audry M, Ciancanelli M, Alsina L, Azevedo J, Herman M, Anguiano E, Sancho-Shimizu V, Lorenzo L, Pauwels E, Philippe PB, Perez de Diego R, Cardon A, Vogt G, Picard C, Andrianirina ZZ, Rozenberg F, Lebon P, Plancoulaine S, Tardieu M, Valerie D, Jouanguy E, Chaussabel D, Geissmann F, Abel L, Casanova JL, Zhang SY (2011) Herpes simplex virus encephalitis in a patient with complete TLR3 deficiency: TLR3 is otherwise redundant in protective immunity. *The Journal of experimental medicine* **208:** 2083-2098

Haas T, Metzger J, Schmitz F, Heit A, Muller T, Latz E, Wagner H (2008) The DNA sugar backbone 2' deoxyribose determines toll-like receptor 9 activation. *Immunity* **28:** 315-323

Hanke ML, Kielian T (2011) Toll-like receptors in health and disease in the brain: mechanisms and therapeutic potential. *Clinical science* **121:** 367-387

Hardison SE, Brown GD (2012) C-type lectin receptors orchestrate antifungal immunity. *Nature immunology* **13:** 817-822

Hashimoto C, Hudson KL, Anderson KV (1988) The Toll gene of Drosophila, required for dorsal-ventral embryonic polarity, appears to encode a transmembrane protein. *Cell* **52:** 269-279

Hayashi F, Smith KD, Ozinsky A, Hawn TR, Yi EC, Goodlett DR, Eng JK, Akira S, Underhill DM, Aderem A (2001) The innate immune response to bacterial flagellin is mediated by Toll-like receptor 5. *Nature* **410:** 1099-1103

Haziot A, Ferrero E, Kontgen F, Hijiya N, Yamamoto S, Silver J, Stewart CL, Goyert SM (1996) Resistance to endotoxin shock and reduced dissemination of gram-negative bacteria in CD14-deficient mice. *Immunity* **4:** 407-414

Heil F, Ahmad-Nejad P, Hemmi H, Hochrein H, Ampenberger F, Gellert T, Dietrich H, Lipford G, Takeda K, Akira S, Wagner H, Bauer S (2003) The Toll-like receptor 7

(TLR7)-specific stimulus loxoribine uncovers a strong relationship within the TLR7, 8 and 9 subfamily. *European journal of immunology* **33:** 2987-2997

Heil F, Hemmi H, Hochrein H, Ampenberger F, Kirschning C, Akira S, Lipford G, Wagner H, Bauer S (2004) Species-specific recognition of single-stranded RNA via toll-like receptor 7 and 8. *Science* **303:** 1526-1529

Hemmi H, Kaisho T, Takeuchi O, Sato S, Sanjo H, Hoshino K, Horiuchi T, Tomizawa H, Takeda K, Akira S (2002) Small anti-viral compounds activate immune cells via the TLR7 MyD88-dependent signaling pathway. *Nature immunology* **3:** 196-200

Hemmi H, Takeuchi O, Kawai T, Kaisho T, Sato S, Sanjo H, Matsumoto M, Hoshino K, Wagner H, Takeda K, Akira S (2000) A Toll-like receptor recognizes bacterial DNA. *Nature* **408:** 740-745

Hirate Y, Okamoto H (2006) Canopy1, a novel regulator of FGF signaling around the midbrain-hindbrain boundary in zebrafish. *Current biology : CB* **16:** 421-427

Hoebe K, Du X, Georgel P, Janssen E, Tabeta K, Kim SO, Goode J, Lin P, Mann N, Mudd S, Crozat K, Sovath S, Han J, Beutler B (2003) Identification of Lps2 as a key transducer of MyD88-independent TIR signalling. *Nature* **424:** 743-748

Hoebe K, Georgel P, Rutschmann S, Du X, Mudd S, Crozat K, Sovath S, Shamel L, Hartung T, Zahringer U, Beutler B (2005) CD36 is a sensor of diacylglycerides. *Nature* **433:** 523-527

Hoffmann O, Braun JS, Becker D, Halle A, Freyer D, Dagand E, Lehnardt S, Weber JR (2007) TLR2 mediates neuroinflammation and neuronal damage. *Journal of immunology* **178:** 6476-6481

Honda K, Yanai H, Negishi H, Asagiri M, Sato M, Mizutani T, Shimada N, Ohba Y, Takaoka A, Yoshida N, Taniguchi T (2005) IRF-7 is the master regulator of type-I interferon-dependent immune responses. *Nature* **434:** 772-777

Horng T, Barton GM, Medzhitov R (2001) TIRAP: an adapter molecule in the Toll signaling pathway. *Nat Immunol* **2:** 835-841

Hornung V, Guenthner-Biller M, Bourquin C, Ablasser A, Schlee M, Uematsu S, Noronha A, Manoharan M, Akira S, de Fougerolles A, Endres S, Hartmann G (2005) Sequence-specific potent induction of IFN-alpha by short interfering RNA in plasmacytoid dendritic cells through TLR7. *Nature medicine* **11:** 263-270

Hou YJ, Banerjee R, Thomas B, Nathan C, Garcia-Sastre A, Ding A, Uccellini MB (2013) SARM is required for neuronal injury and cytokine production in response to central nervous system viral infection. *Journal of immunology* **191:** 875-883

Huneycutt BS, Bi Z, Aoki CJ, Reiss CS (1993) Central neuropathogenesis of vesicular stomatitis virus infection of immunodeficient mice. *Journal of virology* **67:** 6698-6706

Hurst SM, Wilkinson TS, McLoughlin RM, Jones S, Horiuchi S, Yamamoto N, Rose-John S, Fuller GM, Topley N, Jones SA (2001) Il-6 and its soluble receptor orchestrate a temporal switch in the pattern of leukocyte recruitment seen during acute inflammation. *Immunity* **14:** 705-714

Husebye H, Halaas O, Stenmark H, Tunheim G, Sandanger O, Bogen B, Brech A, Latz E, Espevik T (2006) Endocytic pathways regulate Toll-like receptor 4 signaling and link innate and adaptive immunity. *EMBO J* **25:** 683-692

Ishikawa H, Barber GN (2008) STING is an endoplasmic reticulum adaptor that facilitates innate immune signalling. *Nature* **455:** 674-678

Itoh H, Tatematsu M, Watanabe A, Iwano K, Funami K, Seya T, Matsumoto M (2011) UNC93B1 physically associates with human TLR8 and regulates TLR8-mediated signaling. *PloS one* **6:** e28500

Ivanov S, Dragoi AM, Wang X, Dallacosta C, Louten J, Musco G, Sitia G, Yap GS, Wan Y, Biron CA, Bianchi ME, Wang H, Chu WM (2007) A novel role for HMGB1 in TLR9-mediated inflammatory responses to CpG-DNA. *Blood* **110:** 1970-1981

Jack CS, Arbour N, Manusow J, Montgrain V, Blain M, McCrea E, Shapiro A, Antel JP (2005) TLR signaling tailors innate immune responses in human microglia and astrocytes. *Journal of immunology* **175:** 4320-4330

Jack RS, Fan X, Bernheiden M, Rune G, Ehlers M, Weber A, Kirsch G, Mentel R, Furll B, Freudenberg M, Schmitz G, Stelter F, Schutt C (1997) Lipopolysaccharide-binding protein is required to combat a murine gram-negative bacterial infection. *Nature* **389:** 742-745

Janeway CA, Jr. (1992) The immune system evolved to discriminate infectious nonself from noninfectious self. *Immunology today* **13:** 11-16

Jiang Z, Georgel P, Du X, Shamel L, Sovath S, Mudd S, Huber M, Kalis C, Keck S, Galanos C, Freudenberg M, Beutler B (2005) CD14 is required for MyD88-independent LPS signaling. *Nature immunology* **6:** 565-570

Jin MS, Kim SE, Heo JY, Lee ME, Kim HM, Paik SG, Lee H, Lee JO (2007) Crystal structure of the TLR1-TLR2 heterodimer induced by binding of a tri-acylated lipopeptide. *Cell* **130:** 1071-1082

Johnson GB, Brunn GJ, Kodaira Y, Platt JL (2002) Receptor-mediated monitoring of tissue well-being via detection of soluble heparan sulfate by Toll-like receptor 4. *Journal of immunology* **168:** 5233-5239

Jorgenson RL, Young SL, Lesmeister MJ, Lyddon TD, Misfeldt ML (2005) Human endometrial epithelial cells cyclically express Toll-like receptor 3 (TLR3) and exhibit TLR3-dependent responses to dsRNA. *Human immunology* **66:** 469-482

Jurk M, Heil F, Vollmer J, Schetter C, Krieg AM, Wagner H, Lipford G, Bauer S (2002) Human TLR7 or TLR8 independently confer responsiveness to the antiviral compound R-848. *Nature immunology* **3:** 499

Kaech S, Banker G (2006) Culturing hippocampal neurons. *Nature protocols* **1:** 2406-2415

Kagan JC, Medzhitov R (2006) Phosphoinositide-mediated adaptor recruitment controls Toll-like receptor signaling. *Cell* **125:** 943-955

Kagan JC, Su T, Horng T, Chow A, Akira S, Medzhitov R (2008) TRAM couples endocytosis of Toll-like receptor 4 to the induction of interferon-beta. *Nature immunology* **9:** 361-368

Kaiser WJ, Offermann MK (2005) Apoptosis induced by the toll-like receptor adaptor TRIF is dependent on its receptor interacting protein homotypic interaction motif. *Journal of immunology* **174:** 4942-4952

Kang JY, Nan X, Jin MS, Youn SJ, Ryu YH, Mah S, Han SH, Lee H, Paik SG, Lee JO (2009) Recognition of lipopeptide patterns by Toll-like receptor 2-Toll-like receptor 6 heterodimer. *Immunity* **31:** 873-884

Kanneganti TD (2010) Central roles of NLRs and inflammasomes in viral infection. *Nature reviews Immunology* **10:** 688-698

Kariko K, Buckstein M, Ni H, Weissman D (2005) Suppression of RNA recognition by Toll-like receptors: the impact of nucleoside modification and the evolutionary origin of RNA. *Immunity* **23:** 165-175

Kato H, Takeuchi O, Sato S, Yoneyama M, Yamamoto M, Matsui K, Uematsu S, Jung A, Kawai T, Ishii KJ, Yamaguchi O, Otsu K, Tsujimura T, Koh CS, Reis e Sousa C, Matsuura Y, Fujita T, Akira S (2006) Differential roles of MDA5 and RIG-I helicases in the recognition of RNA viruses. *Nature* **441:** 101-105

Kawagoe T, Sato S, Matsushita K, Kato H, Matsui K, Kumagai Y, Saitoh T, Kawai T, Takeuchi O, Akira S (2008) Sequential control of Toll-like receptor-dependent responses by IRAK1 and IRAK2. *Nature immunology* **9:** 684-691

Kawai T, Adachi O, Ogawa T, Takeda K, Akira S (1999) Unresponsiveness of MyD88-deficient mice to endotoxin. *Immunity* **11:** 115-122

Kawai T, Akira S (2006) TLR signaling. *Cell death and differentiation* **13:** 816-825

Kawai T, Akira S (2007) Antiviral signaling through pattern recognition receptors. *Journal of biochemistry* **141:** 137-145

Kawai T, Akira S (2008) Toll-like receptor and RIG-I-like receptor signaling. *Annals of the New York Academy of Sciences* **1143:** 1-20

Kawai T, Akira S (2010) The role of pattern-recognition receptors in innate immunity: update on Toll-like receptors. *Nature immunology* **11:** 373-384

Kawai T, Akira S (2011) Toll-like receptors and their crosstalk with other innate receptors in infection and immunity. *Immunity* **34:** 637-650

Kawai T, Takahashi K, Sato S, Coban C, Kumar H, Kato H, Ishii KJ, Takeuchi O, Akira S (2005) IPS-1, an adaptor triggering RIG-I- and Mda5-mediated type I interferon induction. *Nat Immunol* **6:** 981-988

Kawai T, Takeuchi O, Fujita T, Inoue J, Muhlradt PF, Sato S, Hoshino K, Akira S (2001) Lipopolysaccharide stimulates the MyD88-independent pathway and results in activation of IFN-regulatory factor 3 and the expression of a subset of lipopolysaccharide-inducible genes. *Journal of immunology* **167:** 5887-5894

Kenny EF, Talbot S, Gong M, Golenbock DT, Bryant CE, O'Neill LA (2009) MyD88 adaptor-like is not essential for TLR2 signaling and inhibits signaling by TLR3. *J Immunol* **183:** 3642-3651

Kielian T (2009) Overview of toll-like receptors in the CNS. *Current topics in microbiology and immunology* **336:** 1-14

Kielian T, Esen N, Bearden ED (2005a) Toll-like receptor 2 (TLR2) is pivotal for recognition of S. aureus peptidoglycan but not intact bacteria by microglia. *Glia* **49:** 567-576

Kielian T, Haney A, Mayes PM, Garg S, Esen N (2005b) Toll-like receptor 2 modulates the proinflammatory milieu in Staphylococcus aureus-induced brain abscess. *Infection and immunity* **73:** 7428-7435

Kigerl KA, Lai W, Rivest S, Hart RP, Satoskar AR, Popovich PG (2007) Toll-like receptor (TLR)-2 and TLR-4 regulate inflammation, gliosis, and myelin sparing after spinal cord injury. *J Neurochem* **102:** 37-50

Kim C, Ho DH, Suk JE, You S, Michael S, Kang J, Joong Lee S, Masliah E, Hwang D, Lee HJ, Lee SJ (2013) Neuron-released oligomeric alpha-synuclein is an endogenous agonist of TLR2 for paracrine activation of microglia. *Nature communications* **4:** 1562

Kim HM, Park BS, Kim JI, Kim SE, Lee J, Oh SC, Enkhbayar P, Matsushima N, Lee H, Yoo OJ, Lee JO (2007a) Crystal structure of the TLR4-MD-2 complex with bound endotoxin antagonist Eritoran. *Cell* **130:** 906-917

Kim JI, Lee CJ, Jin MS, Lee CH, Paik SG, Lee H, Lee JO (2005) Crystal structure of CD14 and its implications for lipopolysaccharide signaling. *The Journal of biological chemistry* **280:** 11347-11351

Kim S, Takahashi H, Lin WW, Descargues P, Grivennikov S, Kim Y, Luo JL, Karin M (2009) Carcinoma-produced factors activate myeloid cells through TLR2 to stimulate metastasis. *Nature* **457:** 102-106

Kim T, Pazhoor S, Bao M, Zhang Z, Hanabuchi S, Facchinetti V, Bover L, Plumas J, Chaperot L, Qin J, Liu YJ (2010) Aspartate-glutamate-alanine-histidine box motif (DEAH)/RNA helicase A helicases sense microbial DNA in human plasmacytoid dendritic cells. *Proceedings of the National Academy of Sciences of the United States of America* **107:** 15181-15186

Kim Y, Zhou P, Qian L, Chuang JZ, Lee J, Li C, Iadecola C, Nathan C, Ding A (2007b) MyD88-5 links mitochondria, microtubules, and JNK3 in neurons and regulates neuronal survival. *The Journal of experimental medicine* **204:** 2063-2074

Kim YM, Brinkmann MM, Paquet ME, Ploegh HL (2008) UNC93B1 delivers nucleotide-sensing toll-like receptors to endolysosomes. *Nature* **452:** 234-238

Koarada S, Ide M, Haruta Y, Tada Y, Ushiyama O, Morito F, Ohta A, Nagasawa K (2005) Two cases of antinuclear antibody negative lupus showing increased proportion of B cells lacking RP105. *J Rheumatol* **32:** 562-564

Koarada S, Tada Y (2012) RP105-negative B cells in systemic lupus erythematosus. *Clin Dev Immunol* **2012:** 259186

Kobayashi K, Inohara N, Hernandez LD, Galan JE, Nunez G, Janeway CA, Medzhitov R, Flavell RA (2002) RICK/Rip2/CARDIAK mediates signalling for receptors of the innate and adaptive immune systems. *Nature* **416:** 194-199

Koblansky AA, Jankovic D, Oh H, Hieny S, Sungnak W, Mathur R, Hayden MS, Akira S, Sher A, Ghosh S (2013) Recognition of profilin by Toll-like receptor 12 is critical for host resistance to Toxoplasma gondii. *Immunity* **38:** 119-130

Koch GL, Macer DR, Wooding FB (1988) Endoplasmin is a reticuloplasmin. *J Cell Sci* **90 (Pt 3):** 485-491

Koedel U, Angele B, Rupprecht T, Wagner H, Roggenkamp A, Pfister HW, Kirschning CJ (2003) Toll-like receptor 2 participates in mediation of immune response in experimental pneumococcal meningitis. *Journal of immunology* **170:** 438-444

Kofoed EM, Vance RE (2011) Innate immune recognition of bacterial ligands by NAIPs determines inflammasome specificity. *Nature* **477:** 592-595

Kroemer G, Galluzzi L, Vandenabeele P, Abrams J, Alnemri ES, Baehrecke EH, Blagosklonny MV, El-Deiry WS, Golstein P, Green DR, Hengartner M, Knight RA, Kumar S, Lipton SA, Malorni W, Nunez G, Peter ME, Tschopp J, Yuan J, Piacentini M, Zhivotovsky B, Melino G (2009) Classification of cell death: recommendations of the Nomenclature Committee on Cell Death 2009. *Cell death and differentiation* **16:** 3-11

Krug A, French AR, Barchet W, Fischer JA, Dzionek A, Pingel JT, Orihuela MM, Akira S, Yokoyama WM, Colonna M (2004) TLR9-dependent recognition of MCMV

by IPC and DC generates coordinated cytokine responses that activate antiviral NK cell function. *Immunity* **21:** 107-119

Kurt-Jones EA, Chan M, Zhou S, Wang J, Reed G, Bronson R, Arnold MM, Knipe DM, Finberg RW (2004) Herpes simplex virus 1 interaction with Toll-like receptor 2 contributes to lethal encephalitis. *Proceedings of the National Academy of Sciences of the United States of America* **101:** 1315-1320

Kurt-Jones EA, Popova L, Kwinn L, Haynes LM, Jones LP, Tripp RA, Walsh EE, Freeman MW, Golenbock DT, Anderson LJ, Finberg RW (2000) Pattern recognition receptors TLR4 and CD14 mediate response to respiratory syncytial virus. *Nature immunology* **1:** 398-401

Laflamme N, Echchannaoui H, Landmann R, Rivest S (2003) Cooperation between toll-like receptor 2 and 4 in the brain of mice challenged with cell wall components derived from gram-negative and gram-positive bacteria. *Eur J Immunol* **33:** 1127-1138

Laflamme N, Rivest S (2001) Toll-like receptor 4: the missing link of the cerebral innate immune response triggered by circulating gram-negative bacterial cell wall components. *FASEB journal : official publication of the Federation of American Societies for Experimental Biology* **15:** 155-163

Laflamme N, Soucy G, Rivest S (2001) Circulating cell wall components derived from gram-negative, not gram-positive, bacteria cause a profound induction of the gene-encoding Toll-like receptor 2 in the CNS. *Journal of neurochemistry* **79:** 648-657

Lafon M, Megret F, Lafage M, Prehaud C (2006) The innate immune facet of brain: human neurons express TLR-3 and sense viral dsRNA. *Journal of molecular neuroscience : MN* **29:** 185-194

Lai Y, Adhikarakunnathu S, Bhardwaj K, Ranjith-Kumar CT, Wen Y, Jordan JL, Wu LH, Dragnea B, San Mateo L, Kao CC (2011) LL37 and cationic peptides enhance TLR3 signaling by viral double-stranded RNAs. *PLoS One* **6:** e26632

Lande R, Gregorio J, Facchinetti V, Chatterjee B, Wang YH, Homey B, Cao W, Su B, Nestle FO, Zal T, Mellman I, Schroder JM, Liu YJ, Gilliet M (2007) Plasmacytoid dendritic cells sense self-DNA coupled with antimicrobial peptide. *Nature* **449:** 564-569

Latz E, Visintin A, Lien E, Fitzgerald KA, Monks BG, Kurt-Jones EA, Golenbock DT, Espevik T (2002) Lipopolysaccharide rapidly traffics to and from the Golgi apparatus

with the toll-like receptor 4-MD-2-CD14 complex in a process that is distinct from the initiation of signal transduction. *The Journal of biological chemistry* **277:** 47834-47843

Le Roy D, Di Padova F, Adachi Y, Glauser MP, Calandra T, Heumann D (2001) Critical role of lipopolysaccharide-binding protein and CD14 in immune responses against gram-negative bacteria. *Journal of immunology* **167:** 2759-2765

Lee BL, Moon JE, Shu JH, Yuan L, Newman ZR, Schekman R, Barton GM (2013) UNC93B1 mediates differential trafficking of endosomal TLRs. *eLife* **2:** e00291

Lee CC, Avalos AM, Ploegh HL (2012) Accessory molecules for Toll-like receptors and their function. *Nature reviews Immunology* **12:** 168-179

Lee HK, Dunzendorfer S, Soldau K, Tobias PS (2006) Double-stranded RNA-mediated TLR3 activation is enhanced by CD14. *Immunity* **24:** 153-163

Lee J, Chuang TH, Redecke V, She L, Pitha PM, Carson DA, Raz E, Cottam HB (2003) Molecular basis for the immunostimulatory activity of guanine nucleoside analogs: activation of Toll-like receptor 7. *Proceedings of the National Academy of Sciences of the United States of America* **100:** 6646-6651

Lehmann SM, Rosenberger K, Kruger C, Habbel P, Derkow K, Kaul D, Rybak A, Brandt C, Schott E, Wulczyn FG, Lehnardt S (2012) Extracellularly delivered single-stranded viral RNA causes neurodegeneration dependent on TLR7. *Journal of immunology* **189:** 1448-1458

Lehnardt S (2010) Innate immunity and neuroinflammation in the CNS: the role of microglia in Toll-like receptor-mediated neuronal injury. *Glia* **58:** 253-263

Lehnardt S, Henneke P, Lien E, Kasper DL, Volpe JJ, Bechmann I, Nitsch R, Weber JR, Golenbock DT, Vartanian T (2006) A mechanism for neurodegeneration induced by group B streptococci through activation of the TLR2/MyD88 pathway in microglia. *J Immunol* **177:** 583-592

Lehnardt S, Massillon L, Follett P, Jensen FE, Ratan R, Rosenberg PA, Volpe JJ, Vartanian T (2003) Activation of innate immunity in the CNS triggers neurodegeneration through a Toll-like receptor 4-dependent pathway. *Proceedings of the National Academy of Sciences of the United States of America* **100:** 8514-8519

Lemaitre B, Nicolas E, Michaut L, Reichhart JM, Hoffmann JA (1996) The dorsoventral regulatory gene cassette spatzle/Toll/cactus controls the potent antifungal response in Drosophila adults. *Cell* **86:** 973-983

Leonard JN, Ghirlando R, Askins J, Bell JK, Margulies DH, Davies DR, Segal DM (2008) The TLR3 signaling complex forms by cooperative receptor dimerization. *Proceedings of the National Academy of Sciences of the United States of America* **105:** 258-263

Li S, Strelow A, Fontana EJ, Wesche H (2002) IRAK-4: a novel member of the IRAK family with the properties of an IRAK-kinase. *Proceedings of the National Academy of Sciences of the United States of America* **99:** 5567-5572

Lien E, Sellati TJ, Yoshimura A, Flo TH, Rawadi G, Finberg RW, Carroll JD, Espevik T, Ingalls RR, Radolf JD, Golenbock DT (1999) Toll-like receptor 2 functions as a pattern recognition receptor for diverse bacterial products. *The Journal of biological chemistry* **274:** 33419-33425

Lima GK, Zolini GP, Mansur DS, Freire Lima BH, Wischhoff U, Astigarraga RG, Dias MF, das Gracas Almeida Silva M, Bela SR, do Valle Antonelli LR, Arantes RM, Gazzinelli RT, Bafica A, Kroon EG, Campos MA (2010) Toll-like receptor (TLR) 2 and TLR9 expressed in trigeminal ganglia are critical to viral control during herpes simplex virus 1 infection. *The American journal of pathology* **177:** 2433-2445

Liu B, Li Z (2008) Endoplasmic reticulum HSP90b1 (gp96, grp94) optimizes B-cell function via chaperoning integrin and TLR but not immunoglobulin. *Blood* **112:** 1223-1230

Liu B, Yang Y, Qiu Z, Staron M, Hong F, Li Y, Wu S, Hao B, Bona R, Han D, Li Z (2010a) Folding of Toll-like receptors by the HSP90 paralogue gp96 requires a substrate-specific cochaperone. *Nat Commun* **1:** 79

Liu B, Yang Y, Qiu Z, Staron M, Hong F, Li Y, Wu S, Li Y, Hao B, Bona R, Han D, Li Z (2010b) Folding of Toll-like receptors by the HSP90 paralogue gp96 requires a substrate-specific cochaperone. *Nature communications* **1:** 79

Liu B, Zhang N, Liu Z, Fu Y, Feng S, Wang S, Cao Y, Li D, Liang D, Li F, Song X, Yang Z (2013) RP105 involved in activation of mouse macrophages via TLR2 and TLR4 signaling. *Molecular and cellular biochemistry* **378:** 183-193

Liu L, Botos I, Wang Y, Leonard JN, Shiloach J, Segal DM, Davies DR (2008) Structural basis of toll-like receptor 3 signaling with double-stranded RNA. *Science* **320:** 379-381

Liu Y, Walter S, Stagi M, Cherny D, Letiembre M, Schulz-Schaeffer W, Heine H, Penke B, Neumann H, Fassbender K (2005) LPS receptor (CD14): a receptor for phagocytosis of Alzheimer's amyloid peptide. *Brain* **128:** 1778-1789

Lomen-Hoerth C (2008) Amyotrophic lateral sclerosis from bench to bedside. *Seminars in neurology* **28:** 205-211

Loo YM, Fornek J, Crochet N, Bajwa G, Perwitasari O, Martinez-Sobrido L, Akira S, Gill MA, Garcia-Sastre A, Katze MG, Gale M, Jr. (2008) Distinct RIG-I and MDA5 signaling by RNA viruses in innate immunity. *Journal of virology* **82:** 335-345

Lotze MT, Tracey KJ (2005) High-mobility group box 1 protein (HMGB1): nuclear weapon in the immune arsenal. *Nature reviews Immunology* **5:** 331-342

Lu YC, Yeh WC, Ohashi PS (2008) LPS/TLR4 signal transduction pathway. *Cytokine* **42:** 145-151

Lund J, Sato A, Akira S, Medzhitov R, Iwasaki A (2003) Toll-like receptor 9-mediated recognition of Herpes simplex virus-2 by plasmacytoid dendritic cells. *The Journal of experimental medicine* **198:** 513-520

Lund JM, Alexopoulou L, Sato A, Karow M, Adams NC, Gale NW, Iwasaki A, Flavell RA (2004) Recognition of single-stranded RNA viruses by Toll-like receptor 7. *Proceedings of the National Academy of Sciences of the United States of America* **101:** 5598-5603

Lundberg AM, Drexler SK, Monaco C, Williams LM, Sacre SM, Feldmann M, Foxwell BM (2007) Key differences in TLR3/poly I:C signaling and cytokine induction by human primary cells: a phenomenon absent from murine cell systems. *Blood* **110:** 3245-3252

Ma Y, Haynes RL, Sidman RL, Vartanian T (2007) TLR8: an innate immune receptor in brain, neurons and axons. *Cell cycle* **6:** 2859-2868

Ma Y, Li J, Chiu I, Wang Y, Sloane JA, Lu J, Kosaras B, Sidman RL, Volpe JJ, Vartanian T (2006) Toll-like receptor 8 functions as a negative regulator of neurite outgrowth and inducer of neuronal apoptosis. *The Journal of cell biology* **175:** 209-215

Malley R, Henneke P, Morse SC, Cieslewicz MJ, Lipsitch M, Thompson CM, Kurt-Jones E, Paton JC, Wessels MR, Golenbock DT (2003) Recognition of pneumolysin by Toll-like receptor 4 confers resistance to pneumococcal infection. *Proceedings of the National Academy of Sciences of the United States of America* **100:** 1966-1971

Mancuso G, Gambuzza M, Midiri A, Biondo C, Papasergi S, Akira S, Teti G, Beninati C (2009) Bacterial recognition by TLR7 in the lysosomes of conventional dendritic cells. *Nature immunology* **10:** 587-594

Mathur R, Oh H, Zhang D, Park SG, Seo J, Koblansky A, Hayden MS, Ghosh S (2012) A mouse model of Salmonella typhi infection. *Cell* **151:** 590-602

Matsumoto M, Funami K, Tanabe M, Oshiumi H, Shingai M, Seto Y, Yamamoto A, Seya T (2003) Subcellular localization of Toll-like receptor 3 in human dendritic cells. *Journal of immunology* **171:** 3154-3162

Matsumoto M, Kikkawa S, Kohase M, Miyake K, Seya T (2002) Establishment of a monoclonal antibody against human Toll-like receptor 3 that blocks double-stranded RNA-mediated signaling. *Biochemical and biophysical research communications* **293:** 1364-1369

McGettrick AF, O'Neill LA (2010) Localisation and trafficking of Toll-like receptors: an important mode of regulation. *Current opinion in immunology* **22:** 20-27

McKimmie CS, Fazakerley JK (2005) In response to pathogens, glial cells dynamically and differentially regulate Toll-like receptor gene expression. *Journal of neuroimmunology* **169:** 116-125

McKimmie CS, Johnson N, Fooks AR, Fazakerley JK (2005) Viruses selectively upregulate Toll-like receptors in the central nervous system. *Biochemical and biophysical research communications* **336:** 925-933

Medzhitov R, Janeway CA, Jr. (1997) Innate immunity: the virtues of a nonclonal system of recognition. *Cell* **91:** 295-298

Medzhitov R, Preston-Hurlburt P, Janeway CA, Jr. (1997) A human homologue of the Drosophila Toll protein signals activation of adaptive immunity. *Nature* **388:** 394-397

Medzhitov R, Preston-Hurlburt P, Kopp E, Stadlen A, Chen C, Ghosh S, Janeway CA, Jr. (1998) MyD88 is an adaptor protein in the hToll/IL-1 receptor family signaling pathways. *Mol Cell* **2:** 253-258

Meijer AH, Gabby Krens SF, Medina Rodriguez IA, He S, Bitter W, Ewa Snaar-Jagalska B, Spaink HP (2004) Expression analysis of the Toll-like receptor and TIR domain adaptor families of zebrafish. *Mol Immunol* **40:** 773-783

Meylan E, Burns K, Hofmann K, Blancheteau V, Martinon F, Kelliher M, Tschopp J (2004) RIP1 is an essential mediator of Toll-like receptor 3-induced NF-kappa B activation. *Nature immunology* **5:** 503-507

Meylan E, Curran J, Hofmann K, Moradpour D, Binder M, Bartenschlager R, Tschopp J (2005) Cardif is an adaptor protein in the RIG-I antiviral pathway and is targeted by hepatitis C virus. *Nature* **437:** 1167-1172

Midwood K, Sacre S, Piccinini AM, Inglis J, Trebaul A, Chan E, Drexler S, Sofat N, Kashiwagi M, Orend G, Brennan F, Foxwell B (2009) Tenascin-C is an endogenous activator of Toll-like receptor 4 that is essential for maintaining inflammation in arthritic joint disease. *Nature medicine* **15:** 774-780

Miller YI, Viriyakosol S, Binder CJ, Feramisco JR, Kirkland TN, Witztum JL (2003) Minimally modified LDL binds to CD14, induces macrophage spreading via TLR4/MD-2, and inhibits phagocytosis of apoptotic cells. *The Journal of biological chemistry* **278:** 1561-1568

Mink M, Fogelgren B, Olszewski K, Maroy P, Csiszar K (2001) A novel human gene (SARM) at chromosome 17q11 encodes a protein with a SAM motif and structural similarity to Armadillo/beta-catenin that is conserved in mouse, Drosophila, and Caenorhabditis elegans. *Genomics* **74:** 234-244

Miyake K (2006) Roles for accessory molecules in microbial recognition by Toll-like receptors. *Journal of endotoxin research* **12:** 195-204

Mogensen TH, Paludan SR, Kilian M, Ostergaard L (2006) Live Streptococcus pneumoniae, Haemophilus influenzae, and Neisseria meningitidis activate the inflammatory response through Toll-like receptors 2, 4, and 9 in species-specific patterns. *Journal of leukocyte biology* **80:** 267-277

Moynagh PN (2009) The Pellino family: IRAK E3 ligases with emerging roles in innate immune signalling. *Trends in immunology* **30:** 33-42

Mukherjee P, Woods TA, Moore RA, Peterson KE (2013) Activation of the innate signaling molecule MAVS by bunyavirus infection upregulates the adaptor protein SARM1, leading to neuronal death. *Immunity* **38:** 705-716

Nagai Y, Akashi S, Nagafuku M, Ogata M, Iwakura Y, Akira S, Kitamura T, Kosugi A, Kimoto M, Miyake K (2002a) Essential role of MD-2 in LPS responsiveness and TLR4 distribution. *Nature immunology* **3:** 667-672

Nagai Y, Kobayashi T, Motoi Y, Ishiguro K, Akashi S, Saitoh S, Kusumoto Y, Kaisho T, Akira S, Matsumoto M, Takatsu K, Miyake K (2005) The radioprotective 105/MD-1 complex links TLR2 and TLR4/MD-2 in antibody response to microbial membranes. *Journal of immunology* **174:** 7043-7049

Nagai Y, Shimazu R, Ogata H, Akashi S, Sudo K, Yamasaki H, Hayashi S, Iwakura Y, Kimoto M, Miyake K (2002b) Requirement for MD-1 in cell surface expression of RP105/CD180 and B-cell responsiveness to lipopolysaccharide. *Blood* **99:** 1699-1705

Negishi H, Fujita Y, Yanai H, Sakaguchi S, Ouyang X, Shinohara M, Takayanagi H, Ohba Y, Taniguchi T, Honda K (2006) Evidence for licensing of IFN-gamma-induced IFN regulatory factor 1 transcription factor by MyD88 in Toll-like receptor-dependent gene induction program. *Proceedings of the National Academy of Sciences of the United States of America* **103:** 15136-15141

Netea MG, Van Der Graaf CA, Vonk AG, Verschueren I, Van Der Meer JW, Kullberg BJ (2002) The role of toll-like receptor (TLR) 2 and TLR4 in the host defense against disseminated candidiasis. *The Journal of infectious diseases* **185:** 1483-1489

Ni M, MacFarlane AWt, Toft M, Lowell CA, Campbell KS, Hamerman JA (2012) B-cell adaptor for PI3K (BCAP) negatively regulates Toll-like receptor signaling through activation of PI3K. *Proc Natl Acad Sci U S A* **109:** 267-272

Nishiya T, DeFranco AL (2004) Ligand-regulated chimeric receptor approach reveals distinctive subcellular localization and signaling properties of the Toll-like receptors. *The Journal of biological chemistry* **279:** 19008-19017

O'Neill LA, Bowie AG (2007) The family of five: TIR-domain-containing adaptors in Toll-like receptor signalling. *Nature reviews Immunology* **7:** 353-364

Ohashi K, Burkart V, Flohe S, Kolb H (2000) Cutting edge: heat shock protein 60 is a putative endogenous ligand of the toll-like receptor-4 complex. *Journal of immunology* **164:** 558-561

Ohto U, Fukase K, Miyake K, Satow Y (2007) Crystal structures of human MD-2 and its complex with antiendotoxic lipid IVa. *Science* **316:** 1632-1634

Okada T, Maeda A, Iwamatsu A, Gotoh K, Kurosaki T (2000) BCAP: the tyrosine kinase substrate that connects B cell receptor to phosphoinositide 3-kinase activation. *Immunity* **13:** 817-827

Oldenburg M, Kruger A, Ferstl R, Kaufmann A, Nees G, Sigmund A, Bathke B, Lauterbach H, Suter M, Dreher S, Koedel U, Akira S, Kawai T, Buer J, Wagner H, Bauer S, Hochrein H, Kirschning CJ (2012) TLR13 recognizes bacterial 23S rRNA devoid of erythromycin resistance-forming modification. *Science* **337:** 1111-1115

Olson JK, Miller SD (2004) Microglia initiate central nervous system innate and adaptive immune responses through multiple TLRs. *Journal of immunology* **173:** 3916-3924

Onji M, Kanno A, Saitoh S, Fukui R, Motoi Y, Shibata T, Matsumoto F, Lamichhane A, Sato S, Kiyono H, Yamamoto K, Miyake K (2013) An essential role for the N-terminal fragment of Toll-like receptor 9 in DNA sensing. *Nature communications* **4:** 1949

Oshiumi H, Matsumoto M, Funami K, Akazawa T, Seya T (2003a) TICAM-1, an adaptor molecule that participates in Toll-like receptor 3-mediated interferon-beta induction. *Nat Immunol* **4:** 161-167

Oshiumi H, Okamoto M, Fujii K, Kawanishi T, Matsumoto M, Koike S, Seya T (2011) The TLR3/TICAM-1 pathway is mandatory for innate immune responses to poliovirus infection. *Journal of immunology* **187:** 5320-5327

Oshiumi H, Sasai M, Shida K, Fujita T, Matsumoto M, Seya T (2003b) TIR-containing adapter molecule (TICAM)-2, a bridging adapter recruiting to toll-like receptor 4 TICAM-1 that induces interferon-beta. *J Biol Chem* **278:** 49751-49762

Osorio F, Reis e Sousa C (2011) Myeloid C-type lectin receptors in pathogen recognition and host defense. *Immunity* **34:** 651-664

Osterloh JM, Yang J, Rooney TM, Fox AN, Adalbert R, Powell EH, Sheehan AE, Avery MA, Hackett R, Logan MA, MacDonald JM, Ziegenfuss JS, Milde S, Hou YJ, Nathan C, Ding A, Brown RH, Jr., Conforti L, Coleman M, Tessier-Lavigne M, Zuchner S, Freeman MR (2012a) dSarm/Sarm1 is required for activation of an injury-induced axon death pathway. *Science* **337:** 481-484

Osterloh JM, Yang J, Rooney TM, Fox AN, Adalbert R, Powell EH, Sheehan AE, Avery MA, Hackett R, Logan MA, Macdonald JM, Ziegenfuss JS, Milde S, Hou YJ, Nathan C, Ding A, Brown RH, Jr., Conforti L, Coleman M, Tessier-Lavigne M, Zuchner S, Freeman MR (2012b) dSarm/Sarm1 Is Required for Activation of an Injury-Induced Axon Death Pathway. *Science*

Ozinsky A, Underhill DM, Fontenot JD, Hajjar AM, Smith KD, Wilson CB, Schroeder L, Aderem A (2000) The repertoire for pattern recognition of pathogens by the innate immune system is defined by cooperation between toll-like receptors. *Proceedings of the National Academy of Sciences of the United States of America* **97:** 13766-13771

Palaniyar N, Nadesalingam J, Reid KB (2002) Pulmonary innate immune proteins and receptors that interact with gram-positive bacterial ligands. *Immunobiology* **205:** 575-594

Palsson-McDermott EM, Doyle SL, McGettrick AF, Hardy M, Husebye H, Banahan K, Gong M, Golenbock D, Espevik T, O'Neill LA (2009) TAG, a splice variant of the adaptor TRAM, negatively regulates the adaptor MyD88-independent TLR4 pathway. *Nat Immunol* **10:** 579-586

Palsson-McDermott EM, O'Neill LA (2007) Building an immune system from nine domains. *Biochemical Society transactions* **35:** 1437-1444

Paludan SR, Bowie AG (2013) Immune sensing of DNA. *Immunity* **38:** 870-880

Panaro MA, Lofrumento DD, Saponaro C, De Nuccio F, Cianciulli A, Mitolo V, Nicolardi G (2008) Expression of TLR4 and CD14 in the central nervous system (CNS) in a MPTP mouse model of Parkinson's-like disease. *Immunopharmacology and immunotoxicology* **30:** 729-740

Park BS, Song DH, Kim HM, Choi BS, Lee H, Lee JO (2009) The structural basis of lipopolysaccharide recognition by the TLR4-MD-2 complex. *Nature* **458:** 1191-1195

Park JS, Gamboni-Robertson F, He Q, Svetkauskaite D, Kim JY, Strassheim D, Sohn JW, Yamada S, Maruyama I, Banerjee A, Ishizaka A, Abraham E (2006) High mobility

group box 1 protein interacts with multiple Toll-like receptors. *American journal of physiology Cell physiology* **290:** C917-924

Park JS, Svetkauskaite D, He Q, Kim JY, Strassheim D, Ishizaka A, Abraham E (2004) Involvement of toll-like receptors 2 and 4 in cellular activation by high mobility group box 1 protein. *The Journal of biological chemistry* **279:** 7370-7377

Parvatiyar K, Zhang Z, Teles RM, Ouyang S, Jiang Y, Iyer SS, Zaver SA, Schenk M, Zeng S, Zhong W, Liu ZJ, Modlin RL, Liu YJ, Cheng G (2012) The helicase DDX41 recognizes the bacterial secondary messengers cyclic di-GMP and cyclic di-AMP to activate a type I interferon immune response. *Nature immunology* **13:** 1155-1161

Peng J, Yuan Q, Lin B, Panneerselvam P, Wang X, Luan XL, Lim SK, Leung BP, Ho B, Ding JL (2010) SARM inhibits both TRIF- and MyD88-mediated AP-1 activation. *European journal of immunology* **40:** 1738-1747

Peri F, Nusslein-Volhard C (2008) Live imaging of neuronal degradation by microglia reveals a role for v0-ATPase a1 in phagosomal fusion in vivo. *Cell* **133:** 916-927

Phulwani NK, Esen N, Syed MM, Kielian T (2008) TLR2 expression in astrocytes is induced by TNF-alpha- and NF-kappa B-dependent pathways. *Journal of immunology* **181:** 3841-3849

Piccinini AM, Midwood KS (2010) DAMPening inflammation by modulating TLR signalling. *Mediators of inflammation* **2010**

Piccinini AM, Midwood KS (2012) Endogenous control of immunity against infection: tenascin-C regulates TLR4-mediated inflammation via microRNA-155. *Cell reports* **2:** 914-926

Pietretti D, Spaink HP, Falco A, Forlenza M, Wiegertjes GF (2013) Accessory molecules for Toll-like receptors in Teleost fish. Identification of TLR4 interactor with leucine-rich repeats (TRIL). *Molecular immunology* **56:** 745-756

Poltorak A, He X, Smirnova I, Liu MY, Van Huffel C, Du X, Birdwell D, Alejos E, Silva M, Galanos C, Freudenberg M, Ricciardi-Castagnoli P, Layton B, Beutler B (1998) Defective LPS signaling in C3H/HeJ and C57BL/10ScCr mice: mutations in Tlr4 gene. *Science* **282:** 2085-2088

Qi R, Singh D, Kao CC (2012) Proteolytic processing regulates Toll-like receptor 3 stability and endosomal localization. *The Journal of biological chemistry* **287:** 32617-32629

Qin H, Wilson CA, Lee SJ, Zhao X, Benveniste EN (2005) LPS induces CD40 gene expression through the activation of NF-kappaB and STAT-1alpha in macrophages and microglia. *Blood* **106:** 3114-3122

Qiu J, Xu J, Zheng Y, Wei Y, Zhu X, Lo EH, Moskowitz MA, Sims JR (2010) High-mobility group box 1 promotes metalloproteinase-9 upregulation through Toll-like receptor 4 after cerebral ischemia. *Stroke* **41:** 2077-2082

Rabin SJ, Kim JM, Baughn M, Libby RT, Kim YJ, Fan Y, La Spada A, Stone B, Ravits J (2010) Sporadic ALS has compartment-specific aberrant exon splicing and altered cell-matrix adhesion biology. *Hum Mol Genet* **19:** 313-328

Raby AC, Holst B, Le Bouder E, Diaz C, Ferran E, Conraux L, Guillemot JC, Coles B, Kift-Morgan A, Colmont CS, Szakmany T, Ferrara P, Hall JE, Topley N, Labeta MO (2013) Targeting the TLR co-receptor CD14 with TLR2-derived peptides modulates immune responses to pathogens. *Science translational medicine* **5:** 185ra164

Randow F, Seed B (2001) Endoplasmic reticulum chaperone gp96 is required for innate immunity but not cell viability. *Nature cell biology* **3:** 891-896

Rassa JC, Meyers JL, Zhang Y, Kudaravalli R, Ross SR (2002) Murine retroviruses activate B cells via interaction with toll-like receptor 4. *Proceedings of the National Academy of Sciences of the United States of America* **99:** 2281-2286

Rathinam VA, Vanaja SK, Waggoner L, Sokolovska A, Becker C, Stuart LM, Leong JM, Fitzgerald KA (2012) TRIF licenses caspase-11-dependent NLRP3 inflammasome activation by gram-negative bacteria. *Cell* **150:** 606-619

Reed-Geaghan EG, Savage JC, Hise AG, Landreth GE (2009) CD14 and toll-like receptors 2 and 4 are required for fibrillar A{beta}-stimulated microglial activation. *J Neurosci* **29:** 11982-11992

Reynolds A, Anderson EM, Vermeulen A, Fedorov Y, Robinson K, Leake D, Karpilow J, Marshall WS, Khvorova A (2006) Induction of the interferon response by siRNA is cell type- and duplex length-dependent. *RNA* **12:** 988-993

Richard KL, Filali M, Prefontaine P, Rivest S (2008) Toll-like receptor 2 acts as a natural innate immune receptor to clear amyloid beta 1-42 and delay the cognitive decline in a mouse model of Alzheimer's disease. *J Neurosci* **28:** 5784-5793

Roberts ZJ, Goutagny N, Perera PY, Kato H, Kumar H, Kawai T, Akira S, Savan R, van Echo D, Fitzgerald KA, Young HA, Ching LM, Vogel SN (2007) The chemotherapeutic agent DMXAA potently and specifically activates the TBK1-IRF-3 signaling axis. *The Journal of experimental medicine* **204:** 1559-1569

Robinson MJ, Sancho D, Slack EC, LeibundGut-Landmann S, Reis e Sousa C (2006) Myeloid C-type lectins in innate immunity. *Nature immunology* **7:** 1258-1265

Roelofs MF, Boelens WC, Joosten LA, Abdollahi-Roodsaz S, Geurts J, Wunderink LU, Schreurs BW, van den Berg WB, Radstake TR (2006) Identification of small heat shock protein B8 (HSP22) as a novel TLR4 ligand and potential involvement in the pathogenesis of rheumatoid arthritis. *Journal of immunology* **176:** 7021-7027

Roger T, Froidevaux C, Le Roy D, Reymond MK, Chanson AL, Mauri D, Burns K, Riederer BM, Akira S, Calandra T (2009) Protection from lethal gram-negative bacterial sepsis by targeting Toll-like receptor 4. *Proceedings of the National Academy of Sciences of the United States of America* **106:** 2348-2352

Sabbah A, Chang TH, Harnack R, Frohlich V, Tominaga K, Dube PH, Xiang Y, Bose S (2009) Activation of innate immune antiviral responses by Nod2. *Nature immunology* **10:** 1073-1080

Saitoh S (2009) Chaperones and transport proteins regulate TLR4 trafficking and activation. *Immunobiology* **214:** 594-600

Sato M, Sano H, Iwaki D, Kudo K, Konishi M, Takahashi H, Takahashi T, Imaizumi H, Asai Y, Kuroki Y (2003a) Direct binding of Toll-like receptor 2 to zymosan, and zymosan-induced NF-kappa B activation and TNF-alpha secretion are down-regulated by lung collectin surfactant protein A. *Journal of immunology* **171:** 417-425

Sato S, Sanjo H, Takeda K, Ninomiya-Tsuji J, Yamamoto M, Kawai T, Matsumoto K, Takeuchi O, Akira S (2005) Essential function for the kinase TAK1 in innate and adaptive immune responses. *Nature immunology* **6:** 1087-1095

Sato S, Sugiyama M, Yamamoto M, Watanabe Y, Kawai T, Takeda K, Akira S (2003b) Toll/IL-1 receptor domain-containing adaptor inducing IFN-beta (TRIF) associates with TNF receptor-associated factor 6 and TANK-binding kinase 1, and activates two

distinct transcription factors, NF-kappa B and IFN-regulatory factor-3, in the Toll-like receptor signaling. *Journal of immunology* **171:** 4304-4310

Schabbauer G, Luyendyk J, Crozat K, Jiang Z, Mackman N, Bahram S, Georgel P (2008) TLR4/CD14-mediated PI3K activation is an essential component of interferon-dependent VSV resistance in macrophages. *Molecular immunology* **45:** 2790-2796

Schachtele SJ, Hu S, Little MR, Lokensgard JR (2010) Herpes simplex virus induces neural oxidative damage via microglial cell Toll-like receptor-2. *Journal of neuroinflammation* **7:** 35

Schaefer L, Babelova A, Kiss E, Hausser HJ, Baliova M, Krzyzankova M, Marsche G, Young MF, Mihalik D, Gotte M, Malle E, Schaefer RM, Grone HJ (2005) The matrix component biglycan is proinflammatory and signals through Toll-like receptors 4 and 2 in macrophages. *The Journal of clinical investigation* **115:** 2223-2233

Schlee M, Roth A, Hornung V, Hagmann CA, Wimmenauer V, Barchet W, Coch C, Janke M, Mihailovic A, Wardle G, Juranek S, Kato H, Kawai T, Poeck H, Fitzgerald KA, Takeuchi O, Akira S, Tuschl T, Latz E, Ludwig J, Hartmann G (2009) Recognition of 5' triphosphate by RIG-I helicase requires short blunt double-stranded RNA as contained in panhandle of negative-strand virus. *Immunity* **31:** 25-34

Schroder K, Tschopp J (2010) The inflammasomes. *Cell* **140:** 821-832

Schroder NW, Heine H, Alexander C, Manukyan M, Eckert J, Hamann L, Gobel UB, Schumann RR (2004) Lipopolysaccharide binding protein binds to triacylated and diacylated lipopeptides and mediates innate immune responses. *J Immunol* **173:** 2683-2691

Schroder NW, Morath S, Alexander C, Hamann L, Hartung T, Zahringer U, Gobel UB, Weber JR, Schumann RR (2003) Lipoteichoic acid (LTA) of Streptococcus pneumoniae and Staphylococcus aureus activates immune cells via Toll-like receptor (TLR)-2, lipopolysaccharide-binding protein (LBP), and CD14, whereas TLR-4 and MD-2 are not involved. *The Journal of biological chemistry* **278:** 15587-15594

Schumann RR, Leong SR, Flaggs GW, Gray PW, Wright SD, Mathison JC, Tobias PS, Ulevitch RJ (1990) Structure and function of lipopolysaccharide binding protein. *Science* **249:** 1429-1431

Scumpia PO, Kelly KM, Reeves WH, Stevens BR (2005) Double-stranded RNA signals antiviral and inflammatory programs and dysfunctional glutamate transport in TLR3-expressing astrocytes. *Glia* **52:** 153-162

Seo JY, Cresswell P (2013) Viperin Regulates Cellular Lipid Metabolism during Human Cytomegalovirus Infection. *PLoS pathogens* **9:** e1003497

Sharma S, Fitzgerald KA (2011) Innate immune sensing of DNA. *PLoS pathogens* **7:** e1001310

Sharma S, tenOever BR, Grandvaux N, Zhou GP, Lin R, Hiscott J (2003) Triggering the interferon antiviral response through an IKK-related pathway. *Science* **300:** 1148-1151

Sheedy FJ, Grebe A, Rayner KJ, Kalantari P, Ramkhelawon B, Carpenter SB, Becker CE, Ediriweera HN, Mullick AE, Golenbock DT, Stuart LM, Latz E, Fitzgerald KA, Moore KJ (2013) CD36 coordinates NLRP3 inflammasome activation by facilitating intracellular nucleation of soluble ligands into particulate ligands in sterile inflammation. *Nature immunology* **14:** 812-820

Shi H, Kokoeva MV, Inouye K, Tzameli I, Yin H, Flier JS (2006) TLR4 links innate immunity and fatty acid-induced insulin resistance. *The Journal of clinical investigation* **116:** 3015-3025

Shibata T, Takemura N, Motoi Y, Goto Y, Karuppuchamy T, Izawa K, Li X, Akashi-Takamura S, Tanimura N, Kunisawa J, Kiyono H, Akira S, Kitamura T, Kitaura J, Uematsu S, Miyake K (2012) PRAT4A-dependent expression of cell surface TLR5 on neutrophils, classical monocytes and dendritic cells. *International immunology* **24:** 613-623

Shimazu R, Akashi S, Ogata H, Nagai Y, Fukudome K, Miyake K, Kimoto M (1999) MD-2, a molecule that confers lipopolysaccharide responsiveness on Toll-like receptor 4. *The Journal of experimental medicine* **189:** 1777-1782

Smiley ST, King JA, Hancock WW (2001) Fibrinogen stimulates macrophage chemokine secretion through toll-like receptor 4. *Journal of immunology* **167:** 2887-2894

Spillantini MG, Crowther RA, Jakes R, Hasegawa M, Goedert M (1998) alpha-Synuclein in filamentous inclusions of Lewy bodies from Parkinson's disease and

dementia with lewy bodies. *Proceedings of the National Academy of Sciences of the United States of America* **95:** 6469-6473

Staron M, Wu S, Hong F, Stojanovic A, Du X, Bona R, Liu B, Li Z (2011) Heat-shock protein gp96/grp94 is an essential chaperone for the platelet glycoprotein Ib-IX-V complex. *Blood* **117:** 7136-7144

Stefanova N, Reindl M, Neumann M, Kahle PJ, Poewe W, Wenning GK (2007) Microglial activation mediates neurodegeneration related to oligodendroglial alpha-synucleinopathy: implications for multiple system atrophy. *Movement disorders : official journal of the Movement Disorder Society* **22:** 2196-2203

Stewart CR, Stuart LM, Wilkinson K, van Gils JM, Deng J, Halle A, Rayner KJ, Boyer L, Zhong R, Frazier WA, Lacy-Hulbert A, El Khoury J, Golenbock DT, Moore KJ (2010) CD36 ligands promote sterile inflammation through assembly of a Toll-like receptor 4 and 6 heterodimer. *Nature immunology* **11:** 155-161

Sun L, Wu J, Du F, Chen X, Chen ZJ (2013) Cyclic GMP-AMP synthase is a cytosolic DNA sensor that activates the type I interferon pathway. *Science* **339:** 786-791

Suzuki N, Suzuki S, Yeh WC (2002) IRAK-4 as the central TIR signaling mediator in innate immunity. *Trends in immunology* **23:** 503-506

Szretter KJ, Samuel MA, Gilfillan S, Fuchs A, Colonna M, Diamond MS (2009) The immune adaptor molecule SARM modulates tumor necrosis factor alpha production and microglia activation in the brainstem and restricts West Nile Virus pathogenesis. *Journal of virology* **83:** 9329-9338

Tabeta K, Georgel P, Janssen E, Du X, Hoebe K, Crozat K, Mudd S, Shamel L, Sovath S, Goode J, Alexopoulou L, Flavell RA, Beutler B (2004) Toll-like receptors 9 and 3 as essential components of innate immune defense against mouse cytomegalovirus infection. *Proceedings of the National Academy of Sciences of the United States of America* **101:** 3516-3521

Tabeta K, Hoebe K, Janssen EM, Du X, Georgel P, Crozat K, Mudd S, Mann N, Sovath S, Goode J, Shamel L, Herskovits AA, Portnoy DA, Cooke M, Tarantino LM, Wiltshire T, Steinberg BE, Grinstein S, Beutler B (2006) The Unc93b1 mutation 3d disrupts exogenous antigen presentation and signaling via Toll-like receptors 3, 7 and 9. *Nature immunology* **7:** 156-164

Tada H, Nemoto E, Shimauchi H, Watanabe T, Mikami T, Matsumoto T, Ohno N, Tamura H, Shibata K, Akashi S, Miyake K, Sugawara S, Takada H (2002) Saccharomyces cerevisiae- and Candida albicans-derived mannan induced production of tumor necrosis factor alpha by human monocytes in a CD14- and Toll-like receptor 4-dependent manner. *Microbiology and immunology* **46:** 503-512

Tadie JM, Bae HB, Banerjee S, Zmijewski JW, Abraham E (2012) Differential activation of RAGE by HMGB1 modulates neutrophil-associated NADPH oxidase activity and bacterial killing. *American journal of physiology Cell physiology* **302:** C249-256

Takahashi K, Shibata T, Akashi-Takamura S, Kiyokawa T, Wakabayashi Y, Tanimura N, Kobayashi T, Matsumoto F, Fukui R, Kouro T, Nagai Y, Takatsu K, Saitoh S, Miyake K (2007) A protein associated with Toll-like receptor (TLR) 4 (PRAT4A) is required for TLR-dependent immune responses. *The Journal of experimental medicine* **204:** 2963-2976

Takaoka A, Wang Z, Choi MK, Yanai H, Negishi H, Ban T, Lu Y, Miyagishi M, Kodama T, Honda K, Ohba Y, Taniguchi T (2007) DAI (DLM-1/ZBP1) is a cytosolic DNA sensor and an activator of innate immune response. *Nature* **448:** 501-505

Takaoka A, Yanai H, Kondo S, Duncan G, Negishi H, Mizutani T, Kano S, Honda K, Ohba Y, Mak TW, Taniguchi T (2005) Integral role of IRF-5 in the gene induction programme activated by Toll-like receptors. *Nature* **434:** 243-249

Takeda K (2005) [Toll-like receptor]. *Nihon Rinsho Meneki Gakkai Kaishi* **28:** 309-317

Takeda K, Akira S (2005) Toll-like receptors in innate immunity. *International immunology* **17:** 1-14

Takeda K, Takeuchi O, Akira S (2002) Recognition of lipopeptides by Toll-like receptors. *Journal of endotoxin research* **8:** 459-463

Takeuchi O, Akira S (2010) Pattern recognition receptors and inflammation. *Cell* **140:** 805-820

Takeuchi O, Hoshino K, Kawai T, Sanjo H, Takada H, Ogawa T, Takeda K, Akira S (1999) Differential roles of TLR2 and TLR4 in recognition of gram-negative and gram-positive bacterial cell wall components. *Immunity* **11:** 443-451

Tanimura N, Saitoh S, Matsumoto F, Akashi-Takamura S, Miyake K (2008) Roles for LPS-dependent interaction and relocation of TLR4 and TRAM in TRIF-signaling. *Biochem Biophys Res Commun* **368:** 94-99

Tatematsu M, Nishikawa F, Seya T, Matsumoto M (2013) Toll-like receptor 3 recognizes incomplete stem structures in single-stranded viral RNA. *Nature communications* **4:** 1833

Taylor KR, Trowbridge JM, Rudisill JA, Termeer CC, Simon JC, Gallo RL (2004) Hyaluronan fragments stimulate endothelial recognition of injury through TLR4. *The Journal of biological chemistry* **279:** 17079-17084

Taylor KR, Yamasaki K, Radek KA, Di Nardo A, Goodarzi H, Golenbock D, Beutler B, Gallo RL (2007) Recognition of hyaluronan released in sterile injury involves a unique receptor complex dependent on Toll-like receptor 4, CD44, and MD-2. *The Journal of biological chemistry* **282:** 18265-18275

Termeer C, Benedix F, Sleeman J, Fieber C, Voith U, Ahrens T, Miyake K, Freudenberg M, Galanos C, Simon JC (2002) Oligosaccharides of Hyaluronan activate dendritic cells via toll-like receptor 4. *The Journal of experimental medicine* **195:** 99-111

Thieblemont N, Wright SD (1999) Transport of bacterial lipopolysaccharide to the golgi apparatus. *J Exp Med* **190:** 523-534

Thompson MR, Kaminski JJ, Kurt-Jones EA, Fitzgerald KA (2011) Pattern recognition receptors and the innate immune response to viral infection. *Viruses* **3:** 920-940

Tian J, Avalos AM, Mao SY, Chen B, Senthil K, Wu H, Parroche P, Drabic S, Golenbock D, Sirois C, Hua J, An LL, Audoly L, La Rosa G, Bierhaus A, Naworth P, Marshak-Rothstein A, Crow MK, Fitzgerald KA, Latz E, Kiener PA, Coyle AJ (2007) Toll-like receptor 9-dependent activation by DNA-containing immune complexes is mediated by HMGB1 and RAGE. *Nat Immunol* **8:** 487-496

Toshchakov V, Jones BW, Perera PY, Thomas K, Cody MJ, Zhang S, Williams BR, Major J, Hamilton TA, Fenton MJ, Vogel SN (2002) TLR4, but not TLR2, mediates IFN-beta-induced STAT1alpha/beta-dependent gene expression in macrophages. *Nature immunology* **3:** 392-398

Town T, Jeng D, Alexopoulou L, Tan J, Flavell RA (2006) Microglia recognize double-stranded RNA via TLR3. *Journal of immunology* **176:** 3804-3812

Triantafilou M, Gamper FG, Haston RM, Mouratis MA, Morath S, Hartung T, Triantafilou K (2006) Membrane sorting of toll-like receptor (TLR)-2/6 and TLR2/1 heterodimers at the cell surface determines heterotypic associations with CD36 and intracellular targeting. *J Biol Chem* **281:** 31002-31011

Troutman TD, Hu W, Fulenchek S, Yamazaki T, Kurosaki T, Bazan JF, Pasare C (2012) Role for B-cell adapter for PI3K (BCAP) as a signaling adapter linking Toll-like receptors (TLRs) to serine/threonine kinases PI3K/Akt. *Proceedings of the National Academy of Sciences of the United States of America* **109:** 273-278

Trudler D, Farfara D, Frenkel D (2010) Toll-like receptors expression and signaling in glia cells in neuro-amyloidogenic diseases: towards future therapeutic application. *Mediators of inflammation* **2010**

Tsujimoto H, Ono S, Majima T, Kawarabayashi N, Takayama E, Kinoshita M, Seki S, Hiraide H, Moldawer LL, Mochizuki H (2005) Neutrophil elastase, MIP-2, and TLR-4 expression during human and experimental sepsis. *Shock* **23:** 39-44

Unterholzner L, Keating SE, Baran M, Horan KA, Jensen SB, Sharma S, Sirois CM, Jin T, Latz E, Xiao TS, Fitzgerald KA, Paludan SR, Bowie AG (2010) IFI16 is an innate immune sensor for intracellular DNA. *Nat Immunol* **11:** 997-1004

Uronen-Hansson H, Allen J, Osman M, Squires G, Klein N, Callard RE (2004) Toll-like receptor 2 (TLR2) and TLR4 are present inside human dendritic cells, associated with microtubules and the Golgi apparatus but are not detectable on the cell surface: integrity of microtubules is required for interleukin-12 production in response to internalized bacteria. *Immunology* **111:** 173-178

Vabulas RM, Braedel S, Hilf N, Singh-Jasuja H, Herter S, Ahmad-Nejad P, Kirschning CJ, Da Costa C, Rammensee HG, Wagner H, Schild H (2002) The endoplasmic reticulum-resident heat shock protein Gp96 activates dendritic cells via the Toll-like receptor 2/4 pathway. *The Journal of biological chemistry* **277:** 20847-20853

van der Vaart M, Spaink HP, Meijer AH (2012) Pathogen recognition and activation of the innate immune response in zebrafish. *Advances in hematology* **2012:** 159807

van Noort JM, Bsibsi M (2009) Toll-like receptors in the CNS: implications for neurodegeneration and repair. *Progress in brain research* **175:** 139-148

Wakabayashi Y, Kobayashi M, Akashi-Takamura S, Tanimura N, Konno K, Takahashi K, Ishii T, Mizutani T, Iba H, Kouro T, Takaki S, Takatsu K, Oda Y, Ishihama Y, Saitoh S, Miyake K (2006) A protein associated with toll-like receptor 4 (PRAT4A) regulates cell surface expression of TLR4. *Journal of immunology* **177:** 1772-1779

Walter P, Johnson AE (1994) Signal sequence recognition and protein targeting to the endoplasmic reticulum membrane. *Annu Rev Cell Biol* **10:** 87-119

Walter S, Letiembre M, Liu Y, Heine H, Penke B, Hao W, Bode B, Manietta N, Walter J, Schulz-Schuffer W, Fassbender K (2007) Role of the toll-like receptor 4 in neuroinflammation in Alzheimer's disease. *Cell Physiol Biochem* **20:** 947-956

Wang C, Deng L, Hong M, Akkaraju GR, Inoue J, Chen ZJ (2001) TAK1 is a ubiquitin-dependent kinase of MKK and IKK. *Nature* **412:** 346-351

Wang T, Town T, Alexopoulou L, Anderson JF, Fikrig E, Flavell RA (2004) Toll-like receptor 3 mediates West Nile virus entry into the brain causing lethal encephalitis. *Nature medicine* **10:** 1366-1373

Wang Y, Liu L, Davies DR, Segal DM (2010) Dimerization of Toll-like receptor 3 (TLR3) is required for ligand binding. *The Journal of biological chemistry* **285:** 36836-36841

Weber F, Wagner V, Rasmussen SB, Hartmann R, Paludan SR (2006) Double-stranded RNA is produced by positive-strand RNA viruses and DNA viruses but not in detectable amounts by negative-strand RNA viruses. *Journal of virology* **80:** 5059-5064

Weber JR, Freyer D, Alexander C, Schroder NW, Reiss A, Kuster C, Pfeil D, Tuomanen EI, Schumann RR (2003) Recognition of pneumococcal peptidoglycan: an expanded, pivotal role for LPS binding protein. *Immunity* **19:** 269-279

Wesche H, Henzel WJ, Shillinglaw W, Li S, Cao Z (1997) MyD88: an adapter that recruits IRAK to the IL-1 receptor complex. *Immunity* **7:** 837-847

Wilson JR, de Sessions PF, Leon MA, Scholle F (2008) West Nile virus nonstructural protein 1 inhibits TLR3 signal transduction. *Journal of virology* **82:** 8262-8271

Wright SD, Ramos RA, Tobias PS, Ulevitch RJ, Mathison JC (1990) CD14, a receptor for complexes of lipopolysaccharide (LPS) and LPS binding protein. *Science* **249:** 1431-1433

Wu J, Sun L, Chen X, Du F, Shi H, Chen C, Chen ZJ (2013) Cyclic GMP-AMP is an endogenous second messenger in innate immune signaling by cytosolic DNA. *Science* **339:** 826-830

Yamamoto M, Okamoto T, Takeda K, Sato S, Sanjo H, Uematsu S, Saitoh T, Yamamoto N, Sakurai H, Ishii KJ, Yamaoka S, Kawai T, Matsuura Y, Takeuchi O, Akira S (2006) Key function for the Ubc13 E2 ubiquitin-conjugating enzyme in immune receptor signaling. *Nature immunology* **7:** 962-970

Yamamoto M, Sato S, Hemmi H, Hoshino K, Kaisho T, Sanjo H, Takeuchi O, Sugiyama M, Okabe M, Takeda K, Akira S (2003a) Role of adaptor TRIF in the MyD88-independent toll-like receptor signaling pathway. *Science* **301:** 640-643

Yamamoto M, Sato S, Hemmi H, Sanjo H, Uematsu S, Kaisho T, Hoshino K, Takeuchi O, Kobayashi M, Fujita T, Takeda K, Akira S (2002) Essential role for TIRAP in activation of the signalling cascade shared by TLR2 and TLR4. *Nature* **420:** 324-329

Yamamoto M, Sato S, Hemmi H, Uematsu S, Hoshino K, Kaisho T, Takeuchi O, Takeda K, Akira S (2003b) TRAM is specifically involved in the Toll-like receptor 4-mediated MyD88-independent signaling pathway. *Nature immunology* **4:** 1144-1150

Yamamoto M, Takeda K (2010) Current views of toll-like receptor signaling pathways. *Gastroenterology research and practice* **2010:** 240365

Yamashita M, Chattopadhyay S, Fensterl V, Zhang Y, Sen GC (2012) A TRIF-independent branch of TLR3 signaling. *Journal of immunology* **188:** 2825-2833

Yanai H, Ban T, Wang Z, Choi MK, Kawamura T, Negishi H, Nakasato M, Lu Y, Hangai S, Koshiba R, Savitsky D, Ronfani L, Akira S, Bianchi ME, Honda K, Tamura T, Kodama T, Taniguchi T (2009) HMGB proteins function as universal sentinels for nucleic-acid-mediated innate immune responses. *Nature* **462:** 99-103

Yang H, Hreggvidsdottir HS, Palmblad K, Wang H, Ochani M, Li J, Lu B, Chavan S, Rosas-Ballina M, Al-Abed Y, Akira S, Bierhaus A, Erlandsson-Harris H, Andersson U, Tracey KJ (2010a) A critical cysteine is required for HMGB1 binding to Toll-like receptor 4 and activation of macrophage cytokine release. *Proceedings of the National Academy of Sciences of the United States of America* **107:** 11942-11947

Yang P, An H, Liu X, Wen M, Zheng Y, Rui Y, Cao X (2010b) The cytosolic nucleic acid sensor LRRFIP1 mediates the production of type I interferon via a beta-catenin-dependent pathway. *Nature immunology* **11:** 487-494

Yang Y, Liu B, Dai J, Srivastava PK, Zammit DJ, Lefrancois L, Li Z (2007) Heat shock protein gp96 is a master chaperone for toll-like receptors and is important in the innate function of macrophages. *Immunity* **26:** 215-226

Yarovinsky F, Zhang D, Andersen JF, Bannenberg GL, Serhan CN, Hayden MS, Hieny S, Sutterwala FS, Flavell RA, Ghosh S, Sher A (2005) TLR11 activation of dendritic cells by a protozoan profilin-like protein. *Science* **308:** 1626-1629

Yoshimura A, Lien E, Ingalls RR, Tuomanen E, Dziarski R, Golenbock D (1999) Cutting edge: recognition of Gram-positive bacterial cell wall components by the innate immune system occurs via Toll-like receptor 2. *Journal of immunology* **163:** 1-5

Zanoni I, Bodio C, Broggi A, Ostuni R, Caccia M, Collini M, Venkatesh A, Spreafico R, Capuano G, Granucci F (2012) Similarities and differences of innate immune responses elicited by smooth and rough LPS. *Immunol Lett* **142:** 41-47

Zanoni I, Ostuni R, Marek LR, Barresi S, Barbalat R, Barton GM, Granucci F, Kagan JC (2011) CD14 controls the LPS-induced endocytosis of Toll-like receptor 4. *Cell* **147:** 868-880

Zekki H, Feinstein DL, Rivest S (2002) The clinical course of experimental autoimmune encephalomyelitis is associated with a profound and sustained transcriptional activation of the genes encoding toll-like receptor 2 and CD14 in the mouse CNS. *Brain pathology* **12:** 308-319

Zhang D, Zhang G, Hayden MS, Greenblatt MB, Bussey C, Flavell RA, Ghosh S (2004) A toll-like receptor that prevents infection by uropathogenic bacteria. *Science* **303:** 1522-1526

Zhang SY, Jouanguy E, Ugolini S, Smahi A, Elain G, Romero P, Segal D, Sancho-Shimizu V, Lorenzo L, Puel A, Picard C, Chapgier A, Plancoulaine S, Titeux M, Cognet C, von Bernuth H, Ku CL, Casrouge A, Zhang XX, Barreiro L, Leonard J, Hamilton C, Lebon P, Heron B, Vallee L, Quintana-Murci L, Hovnanian A, Rozenberg F, Vivier E, Geissmann F, Tardieu M, Abel L, Casanova JL (2007) TLR3 deficiency in patients with herpes simplex encephalitis. *Science* **317:** 1522-1527

Zhang X, Brann TW, Zhou M, Yang J, Oguariri RM, Lidie KB, Imamichi H, Huang DW, Lempicki RA, Baseler MW, Veenstra TD, Young HA, Lane HC, Imamichi T (2011a) Cutting edge: Ku70 is a novel cytosolic DNA sensor that induces type III rather than type I IFN. *Journal of immunology* **186:** 4541-4545

Zhang Z, Yuan B, Bao M, Lu N, Kim T, Liu YJ (2011b) The helicase DDX41 senses intracellular DNA mediated by the adaptor STING in dendritic cells. *Nature immunology* **12:** 959-965

Zhou X, Jiang T, Du X, Zhou P, Jiang Z, Michal JJ, Liu B (2012) Molecular characterization of porcine SARM1 and its role in regulating TLRs signaling during highly pathogenic porcine reproductive and respiratory syndrome virus infection in vivo. *Dev Comp Immunol*

Zhu J, van Drunen Littel-van den Hurk S, Brownlie R, Babiuk LA, Potter A, Mutwiri GK (2009) Multiple molecular regions confer intracellular localization of bovine Toll-like receptor 8. *Molecular immunology* **46:** 884-892

CHAPTER SEVEN

Appendices

7.1 Record of publications

Paulina Wochal, Susan Carpenter, Aisling Dunne, Luke A.J O'Neill (2012). TRIL: a novel component of TLR4 complex is also required for TLR3 signalling and interacts with SARM. *Keystone Symposia 'Sensing the Microbes and Damage Signals'* 2012.

Carpenter S, **Wochal P**, Dunne A, O'Neill LA (2011) Toll-like receptor 3 (TLR3) signaling requires TLR4 Interactor with leucine-rich Repeats (TRIL). *The Journal of biological chemistry* 286: 38795-38804

Wochal P, Carpenter S, Rathinam VAK, Dunne A, Carlson T, Kuang W, Seidl KJ, Hall JP, Lin LL, Collins M, Fitzgerald KA and O'Neill LA TRIL is involved in cytokine production in the brain following *Escherichia coli* infection. (Manuscript accepted for publication in the *Journal of Immunology* with minor revision)

TRIL: a novel component of TLR4 complex is also required for TLR3 signalling and interacts with SARM.

Paulina Wochal, Susan Carpenter, Aisling Dunne, Luke A.J O'Neill.
School of Biochemistry and Immunology, Trinity College Dublin, Dublin 2, Ireland.

Toll-like receptors (TLRs) are a family of pattern recognition receptors involved in the innate immune response to a wide range of pathogen-associated molecules and endogenous danger signals. Studies revealed that these key receptors mediating host defence against invading pathogens also play a major role in neuroinflammation and have been linked to autoimmune neuropathy and neurodegenerative disorders.

The aim of this study was to examine in more detail the function of the novel protein we recently identified as TLR4 interactor with leucine-rich repeats (TRIL). We previously found that TRIL is a functional component of TLR4 complex and is highly expressed in the brain. Our recent work now reveals that TRIL is also requried for TLR3 signaling. In human astrocytoma cell line (U373) TRIL is expressed intracellularly and it colocalises with the endosomal compartments. TRIL interacts with TLR3 and is induced by the TLR3 ligand Poly(I:C). Overexpression of TRIL leads to increased cytokine production and ISRE activation in response to Poly(I:C) stimulation. Transient and stable knockdown of TRIL using specific siRNA or shRNA respectively attenuates TLR3 signalling in U373 by reducing ISRE luciferase, RANTES and type I interferon production. Knockdown of TRIL does not affect TLR2 signalling suggesting that TRILs functions are specific to TLR2 and TLR3.

The TLR adaptor protein sterile α and HEAT/Armadillo motif containing protein (SARM) has been identified as a negative regulator of adaptor protein TRIF that acts downstream of TLR3 and TLR4 mediated signalling. Here we show that TRIL is capable of interacting with SARM. Interestingly SARM has recently been shown to be almost exclusively expressed in neurons. This provides us with the intriguing possibility that TRIL and SARM are somehow functioning to alter TLR signalling within the CNS. Perhaps these proteins are somehow competing to fine-tune the innate immune response within the CNS in order to maintain homeostatis.